UNIVERSITY OF BIRMINGHAM

EMULSION DESIGN FOR REDUCED FAT BAKING MARGARINE

ROSS STUART MORRISON

A THESIS SUBMITTED TO THE UNIVERSITY OF BIRMINGHAM FOR THE DEGREE OF

DOCTOR OF PHILOSOPHY

DEPARTMENT OF CHEMICAL ENGINEERING
COLLEGE OF PHYSICAL AND ENGINEERING SCIENCES

SEPTEMBER 2015

UNIVERSITY^{OF} BIRMINGHAM

University of Birmingham Research Archive

e-theses repository

Abstract

Water-in-Oil emulsions present a potential strategy for fat reduction in conventional baking margarine (and thereupon bakery products), by replacing a portion of the fat with a water-based fat mimetic.

Using hydrocolloids, polymers, and stabilisers, this aqueous phase may be structured in such a way as to emulate the physical and mechanical behaviour of the fat, but with almost none of the associated energy contribution – presenting potential for a realistic, marketable solution towards weight management and calorie control. This work has adopted a holistic strategy in order to characterise and understand the various structural components and processes consolidating to form a final, optimized, baking margarine emulsion structure.

The relationship between the microstructure and the physicomechanical properties of standalone structured aqueous hydrocolloid phases is studied, and modelled for more complex systems. Emulsification processing parameters were optimized for production of water in palm oil baking margarine emulsions, before then applying these learnings for successful formulation of reduced fat palm oil emulsions incorporating the structured aqueous phase.

A conventional margarine process is optimised for a contemporary role of emulsification to successfully create fully emulsified 30% reduced fat baking margarine emulsions, with potential for considerably higher aqueous phase fractions depending upon particular baking application.

Acknowledgements

To Mum and Dad,

You have always supported me.

Thank You.

And to Grandma Firth - n°1 fan.

Hope this fits the bill.

I

INTRODUCTION

1 Introduction

The demands of modern society upon the food industry are higher than ever before, and continue to progress at exponentially [1]. Public consumer taste now assumes variety, flavour, satiety, appearance and organoleptic quality, whilst simultaneously demanding longevity, affordability, and in more recent times an alignment towards nutritional value and 'clean labelling' [2] - in itself presenting considerable challenges. Such consumer trends have been the primary stimulus for dramatic advancement of food science and engineering in the last century [1, 3] and the continued pursuit of new and innovative processes, techniques and materials.

1.1. Call for a Change in Diet

One prominent consumer-led driving force for such culinary technological advancements which has accelerated to the fore in recent decades is that of the obesity epidemic. In a UK government report published in March 2015 [4] it was announced that 26.0% and 41.1% of males in England were either obese or overweight, respectively. Woman were marginally lower at 23.8% and 33.4% respectively, whilst perhaps most alarmingly 19.1% of children aged 10-11 were defined medically obese (BMI of $25kg.m^{-2}$ to $29.9kg.m^{-2}$ being considered overweight, whilst a BMI of $30kg.m^{-2}$ or above is considered obese [5]).

Whilst direct medical implications of overweight and obesity are well appreciated, repercussions of increasing overweight and obesity are not exclusive to morbidity figures; it is calculated [6] that the cost to the NHS in 2007 exceeded £4.2 billion for direct treatment of overweight and obesity cases, with an additional £15.8 billion in indirect costs to the economy.

This non-communicable epidemic is not a localised case specific to the United Kingdom; as shown in Fig. 1.
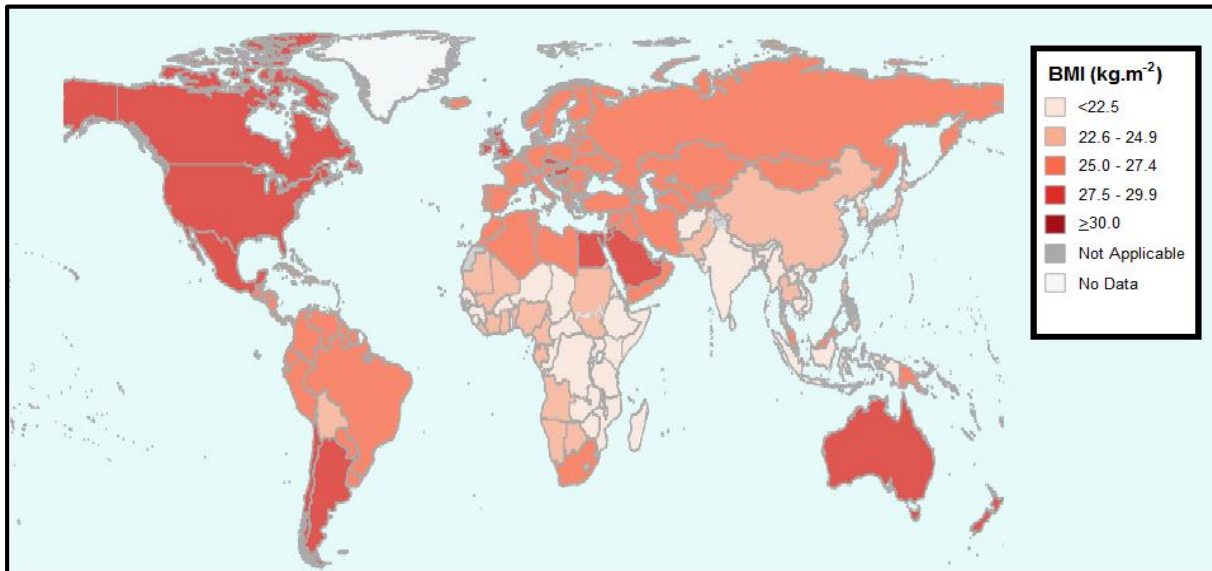
Fig. 1: Worldwide Mean Body Mass Index in males aged 18 and above, 2010-2014 (age standardised estimate) as reported by Global Health Observatory, WHO [7].

In 2004 the World Health Assembly adopted the WHO Global Strategy on Diet, Physical Activity and Health [7] stipulating the increasing prevalence of overweight and obesity globally, and responsive action(s) necessary in order to combat it. These recognised the requirement to promote an improved diet on a number of platforms in order for successful implementation, namely; at the individual (e.g. reduce / eliminate consumption), on a societal platform (e.g. government obligation to facilitate opportunity for healthier eating), and at the food industry level (e.g. presenting accessible and affordable healthier foods, and actively reducing fat, sugar, and salt in products). To this end, the food science industry has turned its attention towards the development of new and/or evolved processes and materials in an attempt to mimic the textures, functionality, and organoleptic signatures of those foodstuffs with which consumers have become accustomed, whilst promoting nutritional value and/or satiety [8] [9].

1.2. Targeting Reduction in Dietary Fats

Fat is a particularly attractive target component in developing healthier food alternatives and reducing over energy consumption, on the basis that:

a) Fat is of low nutritional value (broadly speaking); those essential nutritional requirements cumulating to only $18.6g.day^{-1}$ and $13.1g.day^{-1}$ in adult males and females respectively, and less in children [10].

b) Fat represents more than twice the mean energy weight concentration of carbohydrates and proteins ($9kcal.g^{-1}$ compared to $4kcal.g^{-1}$) [11].

c) Satiation power and response time from fat compared to that of proteins and carbohydrates does not reflect its increased energy density [12], and subsequently this inherently leads to passive overconsumption and excessive energy intake [13, 14] unless eating habits are actively checked, subsequently contributing towards overweight and obesity.

It should be specified at this point that fats are not entirely devoid of nutritional benefit, in particular fatty acids Omega 3 alpha linolenic acid and Omega 6 linoleic acid are essential for growth and repair of cell membranes [15]. Vitamins A, D, E and K are also fat soluble [16] and subsequently require fat for delivery. It is therefore important to specify which fats in particular within the macronutrient category 'fat' are of less nutritional value, by looking more closely at their structural variants and associated functionality.

To the chemist, fats are known as triglycerides (TAGs); that is tri-esters formed from the triple esterification of the triol glycerol with three fatty acids (Fig. 2). The critical variable within this structure is the fatty acid chain, specifically the chain length, chain saturation (number of carbon-carbon double bonds), and double bond conformation (i.e. cis or trans).

Of the different fatty acid chains, there are two distinct groups, those with an unsaturated chain (one double bond equates to 'mono-unsaturated', whilst multiple double bonds equate to 'poly-unsaturated'), and those with a saturated chain (no double bonds).
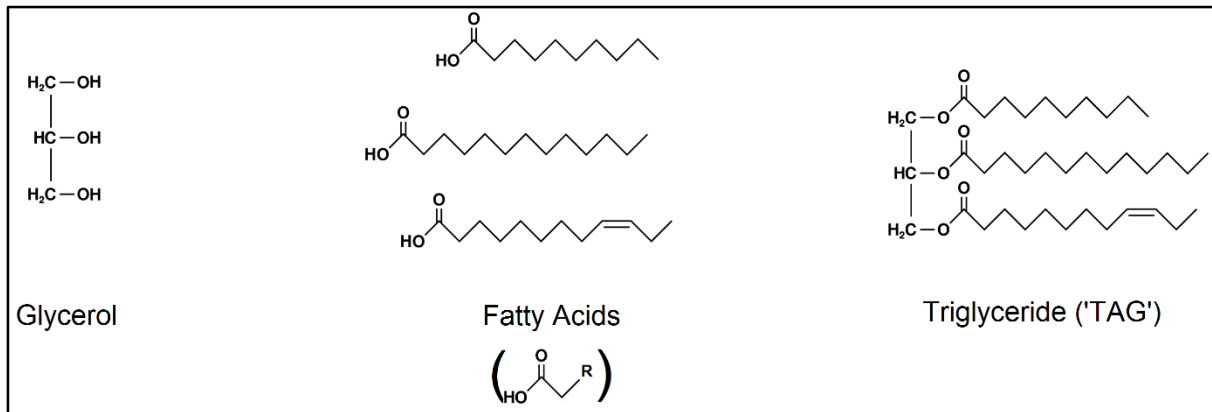
Fig. 2: Chemical structure of triglyceride and the glycerol and fatty acid components. Three example fatty acids have been used to demonstrate chain length and saturation variability. Generalised fatty acid structure indicated in brackets.
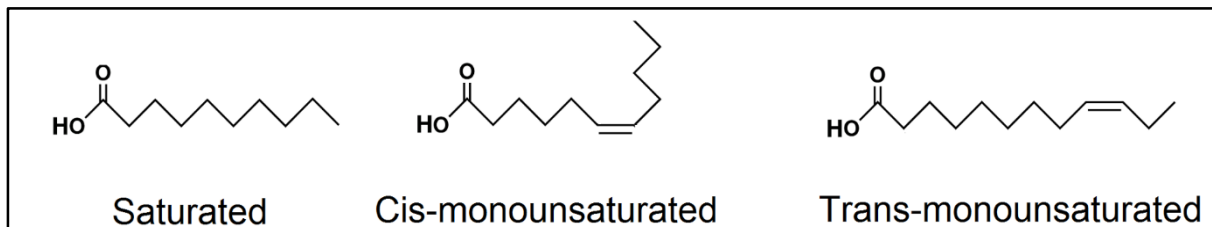
Fig. 3: Conformation variability in fatty acid chains.

The unsaturated fatty acids in themselves may be divided into two sub-variants. Within human body, all natural fatty acids are unsaturated cis fatty acids [15]; that is, the carbon chain groups sit adjacent to one another across the carbon-carbon double bond (Fig. 3). Subsequently the body's enzyme active sites are designed to break down and facilitate the metabolising of cis fatty acids, and as a result they are comparatively less efficient in the breakdown of saturated

and trans-unsaturated fatty acids (carbon chain groups on either side of the carbon-carbon double bond are situated across from one another), which will slow the conversion of these particular fatty acids into energy, allowing fat levels to accumulate, potentially resulting in fat storage. Saturated and trans-unsaturated fatty acids present no specific essential nutritional value to the body, and owing to the linearity of the chain structures they are able to pack relatively well, usually existing in solid form with high nutritional energy density and low satiety benefit. Saturated and trans-unsaturated fatty acids therefore present excellent potential targets for reduction, in engineering towards healthier foods.

One food category which is particularly notorious for its lack of nutritional value and elevated saturated and trans-unsaturated fat contents is that of bakery - the primary contributor towards this being conventional baking margarine used in the recipe [17].

Baking margarine or 'shortening' is a hard blend of fats both natural and processed, extracted from plant sources (typically soybean, cottonseed, palm, or palm kernel) used in baking applications for biscuits, cakes and pastries [18]. It should not be confused with table top margarine spread, which is softer, and contains less saturated and trans-unsaturated fats. Margarine for specific baking applications also does not include water; whilst standard margarine spread will typically incorporate a 15-20% aqueous phase [18].

Initial indications would therefore highlight baking margarine as the ideal candidate for reformulation in efforts to try and reduce dietary fat. However, prior to contemplation of strategies by which fat in baking margarine may be reduced, it is imperative that the role(s) which fat has to play in bakery products is considered, such that the experimental design may be modelled around replicating the key functions of fats in bakery applications as best possible.

1.3. The Roles of Fat in Baking

In order to systematically consider the number of roles which fat plays in the baking process and the final product it is useful to distinguish between the various process stages of its application, specifically; mixing, baking, and consumption.

The alias 'shortening' is often found useful in distinguishing between baking margarine and its spreadable affiliate; the name itself referring to the action of the fat in physically inhibiting development of a gluten structure during mixing. Fat smothers the flour particles, the baking margarine ('shortening') fat blend is hydrophobic and incorporates no aqueous phase itself, and subsequently hydration of the proteins in the flour is impeded, they are therefore unable to fully uncoil and form an extended gluten network, i.e. 'shortening' the structure.

In actual fact, baking margarine is used in creating both short and long dough. Finely cut margarine fat will create a coarse granular short dough when mixed with dry ingredients (flour etc.) producing a crumbly texture once baked, for preparation of tarts, biscuits and cakes, whilst larger cuts of the fat will create a lumpy, long dough, resulting in a flakier crumb such as that used in pastries, as the fat smothering will be less absolute, and subsequently some small gluten networks are able to develop creating the 'flakes' observed.

Alternatively laminate dough may be prepared, whereby the fat is applied in alternating layers with the dough, so that the inhibitory effect of the fat on the formation of the gluten structure exists only in one plane, resulting in a sheeted pastry, such as puff pastry.

If we therefore consider the functional requirements which a reduced fat baking margarine is to fulfil, it is imperative that any fat reduction must not prevent the necessary gluten network inhibition during the mixing step, and that it may not incorporate any readily available water which may hydrate proteins in the flour. The characteristic crumbly/flaky baked textures are produced as the gluten network is restricted from extending, and therefore gluten networks are

only able to accumulate to crumb/flake size depending on the mixing method, with these microstructures being held together by the fat to create the macrostructure. Any means of fat reduction must therefore also maintain the hard, solid state under ambient temperature and pressure, whilst still melting as required. In order to mix well and effectively smother flour particles, the mechanical response to applied stress and precursors in order to initiate flow should also emulate those of conventional baking margarine. Finally, it goes without saying that any alterations to facilitate a reduced fat content be stable during manipulation which might be experienced during the mixing stage.

Post-mixing, consideration must be given toward the chemical and/or physical transformations undergone within the baking step, and any adverse consequences this may have during baking (e.g. lift, burning, and separation) and also upon the organoleptic and aesthetic delivery (e.g. appearance, texture, flavour profile and delivery, and mouth feel). Chemical stability is critical throughout, specifically fat oxidation mechanisms, and water activity, both in ingredient storage and in the final product [19].

The particulars of mixing of the fat into the dough, the baking conditions; the physical and chemical processes undergone, and the final desired sensory delivery will ultimately vary with product and application. The aim here therefore is not to design a reduced fat margarine product tailored towards one specific bakery application, but rather to develop an understanding of the strategic parameters and controls involved in designing a reduced fat baking margarine, and how these may be defined in order to achieve specific qualities relative to any given application. Inherently therefore, the experimental design must remain non-specific to any one baking application, and as a consequence these studies shall focus upon emulating the physical and mechanical (i.e. 'physicomechanical') properties and behaviour of baking margarine. By this approach, a reduced fat alternative to baking margarine may be

developed and fully characterised, and a reasoned hypothesis for a suitable baking application(s) be made corresponding with the specifications and understanding drawn throughout the study.

1.4. Strategies for Fat Reduction

It is clear that within a baking application fat cannot simply be removed from the recipe as a means of fat reduction. Subsequently, a strategy for replacing the fat removed must be established. As has already been highlighted, the breadth in particular functionality requirements across the spectrum of baking applications is vast, and therefore a 'one shoe fits all' silver bullet approach - whilst attractive in theory, is improbable in practise.

Consequently, a holistic approach must be adopted; just as fat is involved within a range of functions and processes, so too should a range of ingredients and technologies be used in order to attempt to replace them, which would change depending on specific application. The significance of the chosen experimental design targeted at understanding the mechanisms and effects of ingredients and parameters of processes involved (as opposed to designing a product for a specific application) is therefore highly pertinent.

Following growing consumer demands for dietary fat reduction, a great number of replacement strategies have already been adopted and developed by the food industry, to varying degrees of success [20] [19] [21] [14]. In order to identify a particular strategy which is best suited to this application in reducing fat within baking margarine, a series of questions must first be considered: firstly, do we chose to replace the fat in its entirety, or only partially? In this instance partial replacement appears the clear preference, on the basis that: (i) fat represents a substantial portion of the recipe (typically a third by weight in short dough), (ii) that partial replacement would facilitate a systematic approach in subsequent investigations increasing the fat replacer portion, and that (iii) any fat replacer will be subjected to intense treatment in

application, i.e. high temperatures for a prolonged amount of time during baking, during which it is exceptionally unlikely that the entirety of the physical and chemical behaviours of the fat can be unequivocally reciprocated. Rather, it is considered whether by diluting the actual fat with a fat replacer which may be partially substituted into the baking margarine at no cost to its overall chemical and physicomechanical behaviour at the mixing stage, the actual fat may be applied more efficiently.

A useful analogy in order to appreciate this line of thought is that of dermatological medicine applications, whereby the active ingredient in a skin cream may only represent a small fraction of the overall cream weight, but an inactive bulking ingredient has been added for practicality in application as the small volume of active agent required may struggle to physically spread over the target area, and subsequently a greater volume than is actually physiologically needed may inevitably be applied simply in order to ensure full coverage. Correspondingly if we consider fat in baking, it is suggested that the fat replacer may act as a fat extender during the mixing stage, improving efficiency and efficacy in delivery of the fat through the dough during mixing, allowing it to go further [22].

The next consideration to be made is whether the substitute should be a modified, 'low calorie' fat, or a mimetic – that is, non-fat ingredient or ingredients capable of imitating the functional properties of fat.

Low calorie fats have been developed commercially as a regular fat alternative, e.g. Olestra, Caprenin, Salatrim, however they have traditionally been met by stiff resistance in securing FDA and consumer approval [23] [24] [20] [25] amid concerns for gastrointestinal side effects and, in the case of Olestra, binding to fat soluble vitamins A, D, E, & K, carrying them out of the body. From a technological perspective, the addition of alternative fats in an effort to replace conventional baking fat poses further problems when considering ingredient

interactions; those ingredients which would typically interact physically and chemically with fat in the dough mixture similarly can be expected to do so with the alternative fat replacing it, the outcome(s) of which could be extremely difficult evaluate completely. In particular, one recurring limitation in the development of medium chain triglycerides as a low calorie alternative is the tendency for the free fatty acids produced upon hydrolysis to release an unpleasant odour and flavour [26] [19]. Finally, it should be highlighted that many of the low calorie fat alternatives provided by industry are not yet priced competitively to the full fat alternatives, and therefore industry is slow to accept these alternatives.

Fat mimetics are therefore considered as a more viable strategy for partial replacement of baking margarine. Mimetics may be assembled of any number of proteins and/or carbohydrates, on their own or in combination.

In accordance with the holistic approach adopted, this investigation shall focus upon exploring the potential for multiple non-fat ingredients in replacing part of the fat in baking margarine; that by studying the physicomechanical attributes of the ingredients and the associated control parameters, an understanding of the fat mimetic blend formulation may be developed so that it might be tailored to match those of regular baking margarine (and hypothetically any alternative fat texture thereafter outside of this study).

1.5. Fat Mimetics & Emulsions

Fat mimetics typically share one universal theme, in that they are water based [27] [28]. The reasoning for this is quite simple; water is cheap, and calorie free, and offers the potential to act as a carrier solvent for a wide variety of miscible carbohydrates, proteins, and ionic salts as may be required; which critically cannot be reciprocated by alternative strategies achieving fat reduction via aeration. The incorporation of a polar aqueous phase into a non-polar lipid phase in the context of food process manufacture presents a plethora of challenges however [27], not least due to the thermodynamic instability of the immiscible pairing, but also in application; where physical, chemical and sensory attributes will all be significantly affected [29]. The contingency of being able to incorporate additional ingredients within either phase and the composition subsequently selected is therefore critical in tackling these challenges.

A mixture of two (or more) immiscible solutions such as that of water and oil (fat) is referred to as an emulsion. The incompatibility of oil and water originates from the polar structure of water, which will seek to stabilize itself by associating with other polar (i.e. water) molecules, therefore excluding non-polar (oil/fat) molecules in the process. The cumulative effect of this is that straightforward mixtures of the two are not thermodynamically stable and tend towards separation [27]; the thermodynamic incompatibility between the two phases driving this separation is referred to as the interfacial tension – the 'interface' being the name given to the surface formed between the two phases. The science and understanding of emulsion formulation and the interface will be discussed and explored later on in these studies, but for now it is useful to inaugurate an appreciation of the basic ideals and affiliated nomenclature.

In order to stabilise these mixtures and reduce the interfacial tension, molecules of specific amphiphilic structure are used, called emulsifiers. The adjacent polar and non-polar regions in their amphiphilic structure allow them to situate at the interface and interact with both water and oil respectively, adding to the stability of the emulsion, and the particulars of their structure

and polarity distribution will affect their efficacy in doing so [30] [31]. Of the two immiscible phases, one is considered dispersed within the other one, correspondingly referred to as the 'discrete' or 'dispersed' phase, and the 'continuous' phase. Which phase constitutes as which is the subject of some debate [27] but Bancroft's Rule may be used as a useful empirical reference, stipulating the continuous phase as that which the emulsifier is most readily soluble.

1.6. Perceived Challenges & Proposed Solutions

1.6.1. Stabilisation

Having chosen a strategy by which to approach fat reduction in baking margarine, it is important to consider the critical challenges presented towards incorporation of a water based mimetic within a fat system to form an emulsion.

The first has already been highlighted, in that the two phases are thermodynamically incompatible and require additional stabilisation. This may be achievable by a number of mechanisms [27], particularly the action(s) of emulsifiers in reducing the thermodynamic driving force for destabilisation, and subsequently these studies shall investigate the impact of emulsifier type and concentration on stability of an aqueous fat mimetic incorporated within a baking margarine fat system. Analogously, the stabilisation required will be affected by the amount of aqueous fat mimetic present [32], and the effects of aqueous phase concentration shall therefore be investigated accordingly.

In addition to changes in conformation, instability mechanisms within w/o emulsions may also be countered by altering formulation parameters [30, 33-35] controlling the forces distributing the aqueous phase, and the fat crystal formation which will define structuring of the fat continuous phase and association at the interface [30]. In order to understand and quantitatively

define formulation parameters control upon baking margarine emulsion properties a systematic investigation of each key variable processing parameter shall be carried out.

1.6.2. *Water Activity*

Another principle challenge is that of water activity; defined as the ratio of water vapour within the food against that of pure distilled water at the same temperature, and used to specify the amount of water readily available. Earlier it was highlighted that it is imperative that any fat reduction must uphold the application of baking margarine inhibition of the gluten network formation during the mixing step, preventing water from hydrating proteins in the flour. Addition of a water based fat mimetic might appear counter intuitive therefore, however it is critical in this instance to differentiate between water concentration and water activity; whilst a specified portion of the fat may be replaced by an aqueous fat mimetic, successful encapsulation and complete emulsification of this aqueous phase would imply none of this aqueous phase was available for external interaction e.g. with flour particles, and therefore the functionality is maintained, so long as emulsification / encapsulation is complete.

This hypothesis extends further to those ubiquitous problems both physical and chemical presented by water inclusion in foods. Elevated water activity has been demonstrated to exhibit an inhibitory effect upon the Maillard reaction mechanism between reducing sugars and amino compounds, which are principle within baking [36]. Of particular relevance within a w/o emulsion application is the effect of free water upon the mechanisms of fat autoxidation. This is not a straightforward implication and depends critically upon the saturation point of the monolayer [37], below which water will have an antioxidant effect reacting preferentially with hydroperoxides and radicals, whilst if water activity is allowed to exceed this value it can act as a pro-oxidant; facilitating mobilisation of reactants [38].

Unbound water in food also facilitates the growth of bacteria, fungi, and yeasts [39, 40] which individually will require a specific water activity environment in order for uninhibited growth specific to the particular culture species, labelled the limiting water activity [40]. Generally speaking, processed food and food ingredients are preserved via a combined approach of microbe elimination (during initial formulation), and deterrence via either free water removal or treatment.

Therefore, in summary, it is clear that any aqueous phase incorporated within the baking margarine fat must therefore be made unavailable to any of these mechanisms, by achievement of complete emulsification.

Recent studies [32, 35, 41-44] using a conventional margarine line rotor / stator device incorporating a scraped surface heat exchanger followed by a pin stirrer have been successful in creating stable w/o emulsions, although no investigations have been performed thus far upon formulation of baking margarine emulsions. In particular, it has been demonstrated that using the high shear and rapid cooling, close temperature control capability of this technique it is possible to create complete sintered fat 'shells' about droplets; entirely encapsulating them even under applied osmotic pressure [41]; subsequently this experimental design is seen to offer a viable solution for water droplet emulsification and encapsulation, and subsequently water activity reduction in baking margarine emulsion formulation.

This technique is therefore proposed as the chosen method for emulsion formulation in these studies, targeting complete emulsification and encapsulation of the aqueous phase, whilst supporting emulsification via rapid crystallisation of the fat phase, as shall be discussed in depth later. Successful emulsification shall therefore be facilitated by both process and formulation parameter control, and both shall be studied systematically in order to develop an understanding of how either accredits successful emulsion formation.

At this point it is valuable to specify the terms of emulsification 'success' other than a simple empirical measure. Here, success has been defined as a free water value of 0%; free water having been defined as all water bodies greater than 50μm in diameter in accordance with the limitations of the equipment used in the study, although this has been deemed by the Author as a fair standard. Micrographs have also been included for a close visual interpretation of interfacial coverage, and efficacy in fat crystal shells sintering about droplets, as was used in those previous studies [41]. Similarly, mean droplet size shall be targeted at 5μm.

1.6.3. *Physicomechanical Properties*

In addition to problems presented by undesirable activity with both ingredients and deterioration mechanisms, the effects of fat replacement upon the material behaviour properties of the fat system must be considered. Specifications for a successful baking margarine replacement earlier outlined that the resulting reduced fat emulsion must adhere as closely to the physicomechanical behaviour and shear response of conventional baking margarine as possible, that it might minimize any behaviour change within the mixing process.

The effects of emulsification of a water phase within a solid fat upon the overall material properties are well established; reducing hardness, resistance to mechanical deformation, and altering flow behaviour and viscosity [32] [43, 45] as a consequence of water's comparatively viscous physical state. Indeed formulation of reduced fat spreads, where hardness and a high yield stress are generally considered undesirable and impractical, has seen numerous advancements in recent times [46, 47], and whilst carbohydrate and protein structuring agents have been incorporated within the aqueous phase [48], intention has typically been to stabilise the aqueous phase at high aqueous phase fractions achieved and mimic organoleptic delivery. Subsequently, the addition of structuring agents to the aqueous phase targeting the

comparatively high manipulative force resistance and yield stresses associated with baking margarine present an entirely novel challenge.

The principle difficulty associated with this challenge lies in the juxtaposed requirements of an aqueous phase structure that is both sufficient to preserve the mechanical response behaviour of conventional baking margarine, whilst synonymously not being too structured so as to inhibit the accomplished distribution of the aqueous phase as spherical, fully encapsulated droplets. The use of hydrocolloids - that is, a colloidal structuring system wherein the colloid particles are hydrophilic polymers dispersed in water, therefore demands a novel approach in keeping with the challenge presented to facilitate both of these requirements. In order to attempt to achieve this, it is proposed that a particular sensitivity in the gelation and structural aggregation of the polymers be exploited.

Approaching the turn of the 19th century, Franz Hofmeister carried out a series of investigations which first recognised the direct impact of simple ionic salts upon the dissolution of proteins in solution [49]. Since this revolutionary work, many studies and interpretations have been provided on proteins and polysaccharides, further details of which shall be visited later in this study. Critically however, the aggregate (i.e. gel, in this context) material and thermo-transitional properties may be controlled not only by salt concentration but also the specific ions present, and a series has been developed in order to systematically rank ions on their wide range of 'lyotropic' effects on polymers, proteins and colloidal suspensions; appropriately coined the Hofmeister series [50].

Subsequently, it is proposed that this control be utilised in preparing an aggregating hydrocolloid aqueous phase with a specific setting temperature onset which facilitates complete aqueous phase distribution and emulsification of the aqueous phase (and fat crystal nucleation),

whilst allowing aggregate development once brought to ambient conditions in order preserve the mechanical response behaviour of conventional baking margarine.

One hydrocolloid forming polysaccharide in particular with physical properties aligned to the requirements of this study is that of K-carrageenan. This repeating sulphated disaccharide unit polymer is widely used in food applications, particularly as a thickener and stabilising agent in desserts and spreads [51] [52], and is already approved for a substantial range of food applications including (but not limited to) in organic foods [53], as a vegan alternative, and in infant formulae [54]. Specifically, K-carrageenan is capable of forming strong, rigid thermo reversible gels in the particular presence of potassium cations, even at low concentrations. Moreover, the ionic sensitivity of aggregate formation and aggregation onset/melting hysteresis is understood to extend to anions [55], presenting the potential for additional control.

Subsequently, the K-carrageenan polysaccharide is proposed as a focal point for these studies in the capacity of an aqueous phase structuring agent. In order to sufficiently understand the material and structural transformation behaviour of the K-carrageenan aggregates and the control exhibited by anionic presence, methodical studies shall be performed on the standalone hydrocolloid systems prior to inclusion within an emulsion, under a wide range of anionic environments. The systematic investigation of the anionic dependency of K-carrageenan aggregates and their mechanical properties upon anionic Hofmeister values over such a prolific range is a novel approach, and accompanied with the more conventional microstructure analysis it is hoped that a full picture may be created of the aqueous phase material characteristics prior to incorporation within the continuous fat phase.

The anions selected for investigation, as suggested, shall be simple monovalent anions of suitably varied Hofmeister number in order to attain as extensive an interpretation of the lyotropic control as possible. Two anions of specific interest should be given particular

mention however; sorbate, and citrate (monobasic), both presented as monovalent potassium salt forms. The particular interest of these anions and their salts stems from their roles as popular food additives; potassium citrate is widely used as an acidity regulator given its alkaline salt nature [56], whilst potassium sorbate is used universally as a preservative and microorganism growth inhibitor [57]. It may come as surprising therefore that very little attention has been given towards these organic salts in the perspective of their lyotropic effects; in particular K(sorbate) – which does not even carry an officialised Hofmeister valuation. The effects of both of these salts shall therefore form a core theme to these anionic lyotropy studies, and subsequent studies in emulsion formulation, as the preservative effects of K(sorbate) in particular will conveniently lend itself to contravening those challenges earlier raised regarding microbe growth associated with elevated water availability.

1.6.4. Syneresis

Finally, on a continuing note the use of hydrocolloid aggregate systems (including K-carrageenan), will inherently be accompanied by syneresis [51]. Syneresis is the expulsion of water from the aggregate over time, via a combination of aggregate tightening (specifically helical tightening in K-carrageenan) and gravitational drainage. To put this into an analogy, if you wring out a soaked sponge, the water will be expelled, similarly if you leave a soaked sponge on the floor, it is likely to form a puddle around it if left for a short period of time; as while it will be capable of holding on to a certain degree of the water, some will eventually escape; the consequences of freely available water having already been outlined.

A number of applications within the food industry have sought to address this problem, one solution exhibiting particular degrees of success is the chemical modification of native starches, to form cross-linked starches [58] [59]. These modified cross linked starches are designed

specifically to retain some of their structure upon heating and re-cooling; and have been proven to exhibit reduced retrogradation and syneresis behaviour to those of their corresponding unmodified starches [60] [61]. Addition of modified cross-linked waxy maize starch to a K-carrageenan solution aqueous phase within these reduced fat baking margarine emulsion systems is therefore presented as a potential solution toward syneresis elimination.

In doing so, the physicomechanical properties and thermal behaviour of the gelled aqueous phase cannot be expected to remain unaffected, nor can it even be expected to simply equate to an empirical total of the physicomechanical properties of the two phases [62], and consequently a novel systematic study of individual K-carrageenan and cross linked waxy maize starch solutions, and their subsequent mixed solutions, shall be performed and used to develop a model for the standalone mixed polymer system prior to formulation into the baking margarine emulsion system.

1.7. Objectives Summary

The key objective statements for these studies is therefore to investigate the capability for emulsion formulation as a strategy for baking margarine fat reduction, by systematically defining parameters in turn and identifying:

- Optimum composition to support a w/o baking margarine emulsion.

- Optimum processing conditions to support a w/o baking margarine emulsion.

- Organisation of the microstructure and accumulated macrostructure of the different components and their physicomechanical properties, and establish the relationship between the two.

- Optimum composition and formulation of the salt / polymer solutions for aqueous phase structuring.

The aqueous phase of emulsions shall be structured using K-carrageenan (with various potassium salts and salt concentrations), modified cross linked waxy maize starch, and combinations of the two, and therefore analogous microstructure and physicomechanical studies shall initially be performed upon polymer standalone solutions and their mixtures prior to emulsion formulation in order to develop a complete understanding of the components in the final emulsion system. Structuring of the aqueous phase is primarily targeted at mimicking the baking margarine fat physicomechanical behaviour and limiting water availability, and therefore emulsions shall be benchmarked against those respective properties of the original shortening. Before proceeding, it should be clarified that the central focus of this study does not extend to practical investigations into mixing with other ingredients nor baking, however as has already been demonstrated in the planned research strategy these process applications remain relevant and shall be taken into consideration for experimental planning and structuring conclusions.

A number of novel studies are presented in this work, both in terms of composition structure, processing formulation, and mechanical characterisation. Of particular interest is the investigation into lyotropic properties of common food additives; potassium sorbate and potassium citrate, and inclusion within a broader study of a particularly wide range of anion effects upon K-carrageenan domain structure and mechanical behaviour. Another novel focus is the modelling of the physicomechanical properties of K-carrageenan / XLWM mixed polymer systems within the presence of salt. Finally (and most critically) emulsion formulation, and the incorporation of post-processing quiescent gelling aqueous phase, is an unprecedented approach to fat reduction in baking margarine.

1.8. Thesis Layout

In order to guide the reader, it is helpful to briefly explain the structure in which the study is presented. The core structure of this work comprises of an introduction, four results chapters, and concluding remarks including considerations for further work (Fig. 4). Broadly speaking, the four results chapters are arranged in an order of increasing microstructure design complexity. The first two chapters focus upon hydrocolloids and mixed polymer solutions respectively, with a view to distributing this structured aqueous phase within baking margarine emulsions later in the final results chapter. The third chapter focusses upon the control of processing parameters upon emulsion formulation for w/o baking margarine emulsions, and the fourth results chapter then takes the learnings from the w/o emulsion formulation studies and the polymer studies and uses them to formulate emulsions with a structured aqueous phase.
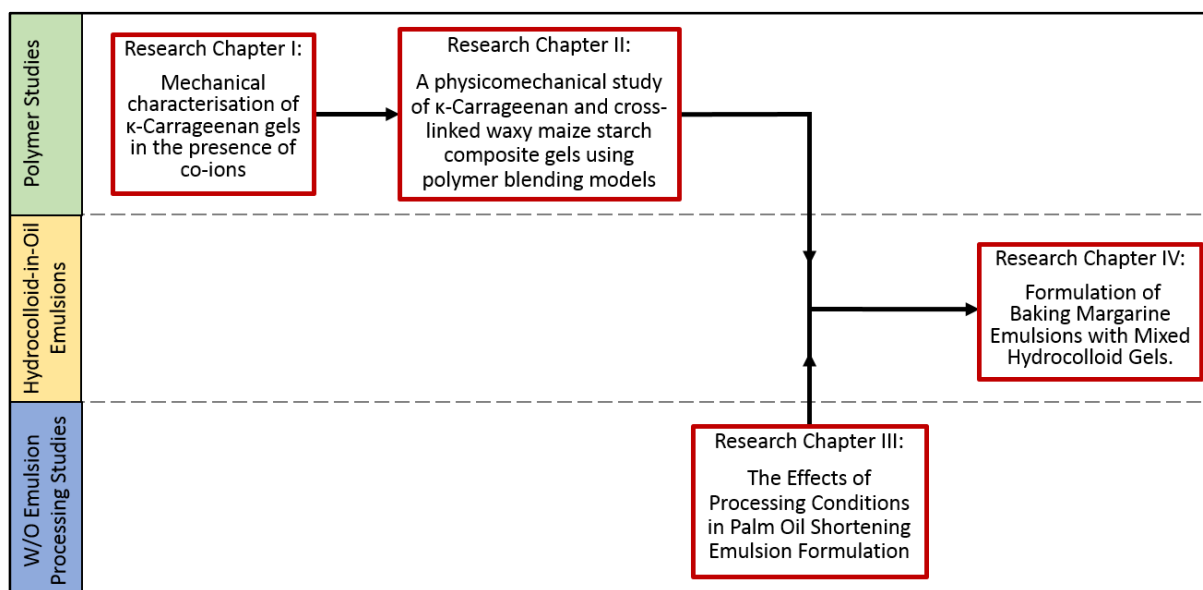

Fig. 4: Illustrative plan mapping the order of work as reported here, and how the various themes run parallel to one another, to later cumulate into the formulation of combined baking margarine emulsions with a gelled aqueous phase.

Each of the four individual results chapters has been styled as an semi-individual piece, and subsequently includes an introduction, discussion and conclusions particular to the material

within that chapter, the reasoning for this format being firstly that it allowed a smoother progression through the various different themes of materials science within this study, e.g. hydrocolloids, polymer blending, processing formulation, interface and emulsion science, and secondly that it simply suited the preferred writing style of the Author. Finally, the main findings of the study are drawn together in Chapter 6, and recommendations for future work are discussed. Figures have been numbered continuously throughout the whole of the text; tabulated in the list of figures (1.11), whilst equations have been numbered within each chapter, symbols described in text are also collected in the list of nomenclatures (1.10).

1.9. Presentation of Findings

Findings from this work have been presented as follows:

1. Morrison, R. S., Sullo, A., Spyropoulus, F., Norton, I. T: *The effect of potassium salts on K-carrageenan & cross-linked waxy maize starch composite gels: solvent partitioning and mechanical properties.* **12th International Hydrocolloids Conference**, Taipei, Taiwan, May 2014.

2. Morrison, R. S., Sullo, A., Spyropoulus, F., Norton, I. T: *Physicomechanical properties of K-carrageenan in the presence of varying Potassium Salts.* **Gums and Stabilisers for the Food Industry Conference***,* Glyndwr University, Wrexham, Wales, June 2013.

1.10. Nomenclature

1.10.1. Salts, Ions, Polymers & Hydrocolloids

κ-C	*κ-carrageenan*
XLWM	*Cross Link Waxy Maize (Starch)*
KCl	*Potassium Chloride*
KF	*Potassium Fluoride*
KBr	*Potassium Bromide*
KI	*Potassium Iodide*
KNO3	*Potassium Nitrate*
K(sorbate)	*Potassium Sorbate*
K(citrate)	*Potassium Citrate (monobasic)*
K^+	*Potassium Cation*
Cl^-	*Chloride*
F^-	*Fluoride*
Br^-	*Bromide*
I^-	*Iodide*
$NO3^-$	*Nitrate*
$(sorbate)^-$	*Sorbate*
$(citrate)^-$	*Citrate (monobasic)*
Kosmotrop(e)ic	*Solvents which contribute towards the ordering of water in the bulk (water) phase.*
Chaotrop(e)ic	*Solvents which contribute towards the disruption of water molecules' structuring in the bulk (water) phase.*
Bulk Water	*Also referred to as 'free' water (in polymer solvation context) 3 hydration sphere diameters of separation (from polymer).*

1.10.2. Uniaxial Compression to Failure

ε_H	*True Strain*
σ_T	*True Stress*
ε_E	*Engineering Strain*
σ_E	*Engineering Stress*
H_0	*Initial Height (of sample)*
A_0	*Sample Cross Sectional Contact Area (at time = 0)*
F	*Force (applied)*
h	*Height (at time = t)*
P	*Mechanical Property Value*
a	*Dependency Coefficient (linear)*
b	*Polymer Aggregation Coefficient (non-linear)*

1.10.3. Uniaxial Compression: Stress Relaxation

F_0	*Initial Force (at time=0)*
F_t	*Force (at time=t)*
k_1	*Initial Relaxation Rate Constant*
$1/k_1$	*Initial Relaxation Rate*
k_2	*Resting Strain Relaxation Constant*
E_A	*Asymptotic Residual Modulus*
A_ε	*Sample Cross Sectional Contact Area (at strain = ε)*

1.10.4. Uniaxial Compression: Recoverable Work Done

n	*Compression Cycle Number*

1.10.5. UV Transmission Spectroscopy

T%	*Percentage Transmission*
UVT_{sample}	*Transmission Reading of Sample*
UVT_0	*Transmission Reading of Deionised Water Reference*
λ_n	*Light Wavelength (in nanometres; n)*

1.10.6. Centrifugation

Φ	*Phase Volume Fraction*
Φ_{mXLWM}	*Starch Phase Water Mass Fraction*
Φ_{XLWM}	*Starch Phase Water Volume Fraction*
Φ_{K-C}	*κ-carrageenan Phase Water Volume Fraction*
m_{sample}	*Mass of Sample*
m_{XLWM}	*Mass of XLWM Starch Dissolved in Solution*
$m_{supern.}$	*Mass of Supernatant Tipped Off Following Centrifuging*
ρ_{water}	*Density of Water*
$m_{water\ in\ granules}$	*Mass of Water Remaining in Granules after Centrifuging*
$m_{water\ p.\ mass\ XLWM}$	*Mass of Water Remaining per gram of XLWM Starch*
$V_{water\ p.\ mass\ XLWM}$	*Volume of Water Remaining per gram of XLWM Starch*
$c_{K-Ceff.}$	*Effective concentration of κ-carrageenan*

1.10.7. Polarimetry

$[\alpha]_T$	*Optical Rotation Angle (at temperature; T)*

1.10.8. Oscillatory Rheology

G'	*Shear Storage Modulus*
G''	*Shear Loss Modulus*
a	*Power Law Constant (linear aspect)*
b	*Power Law Constant (non-linear aspect)*
$G'_{composite}$	*Shear Storage Modulus of the Composite*
G'_{K-C}	*Shear Storage Modulus of the κ-carrageenan Phase*
G'_{XLWM}	*Shear Storage Modulus of the XLWM Starch Phase*

1.10.9. Micro Differential Scanning Calorimetry

T_{K-C}	*κ-carrageenan Gel Melting Temperature*
T_{gel}	*κ-carrageenan Gelling Temperature*
T_{XLWM}	*XLWM Starch Granule Gelatinization Temperature*
T_{peak}	*Peak Temperature*
T_{onset}	*Onset Temperature*
T_{offset}	*Offset Temperature*

1.10.10.   Emulsification Process

SSHE	*Scraped Surface Heat Exchanger*
PS	*Pin Stirrer*
T_{SSHE}	*Scraped Surface Heat Exchanger Jacket Temperature*
T_{PS}	*Pin Stirrer Jacket Temperature*
$T_{SSHE\ Enter}$	*Mix Temperature Entering Scraped Surface Heat Exchanger*
$T_{SSHE\ Exit}$	*Mix Temperature Exiting Scraped Surface Heat Exchanger*
$T_{PS\ Enter}$	*Mix Temperature Entering Pin Stirrer*
$T_{PS\ Exit}$	*Mix Temperature Exiting Pin Stirrer*
ω_{SSHE}	*Scraped Surface Heat Exchanger Rotation Speed*
ω_{PS}	*Pin Stirrer Rotation Speed*
Q	*Flow Rate*

1.10.11.   Fat Morphology

PO	*Palm Oil*
TAG	*Triacylglyceride*
DAG	*Diacylglyceride*
MAG	*Monoacylglyceride*
α	*Alpha (crystal polymorph)*
β	*Beta (crystal polymorph)*
β'	*Beta Prime (crystal polymorph)*
H	*Hexagonal*
O_T	*Orthorhombic Perpendicular*
T_{II}	*Triclinic Parallel*

1.10.12.   Emulsions, Fats & Stabilizers

W/O	*Water-in-Oil (Emulsion)*
HMMG(E)	*High Melting Monoglyceride Emulsifier*
LMMG(E)	*Low Melting Monoglyceride Emulsifier*
MG2643	*Product Code (High Melting Monoglyceride Emulsifier)*
P-100 NH	*Product Code (Non-Hydrogenated Palm Oil)*
DFPO	*Double Fraction Palm Oil*
CB	*Cocoa Butter*

1.10.13.   Fractal Network Model

F	*Force to Overcome Microstructure Association*
m	*Number of Adjacent Identical Pairs Elements*
d_0	*Equilibrium Distance Between the Element Pairing*
A	*Hamaker's Constant*
σ	*Diameter of Element (assumed spherical)*
ε	*Deformation Strain*

1.10.14.   Squeeze Flow

σ_y	*Apparent Extensional Yield Stress*
F	*Force Applied*
R_0	*Initial Radius of the Cylindrical Sample*
H_0	*Initial Height*
H_L	*Limiting Height*

1.10.15.   Droplet Analysis

NMR	*Nuclear Magnetic Resonance*
$d_{3.3}$	*Volume-Weighted Mean Diameter*
$d_{3.2}$	*Surface-Weighted Mean Diameter*
σ	*Standard Deviation of Water Droplet Diameter*

1.10.16.   Solid Fat Content Analysis

SFC	*Solid Fat Content*
$SFC\%_{20°C}$	*Percentage of Fat in Solid State at 20˚C*
$FC_{50°C}$	*Liquid Fat at 50˚C (assumed all fat)*
$LFC_{20°C}$	*Percentage of Fat in Liquid State at 20˚C*
C	*Correction Factor*

1.10.17.   Microscopy

Cryo-SEM	*Cryogenic Scanning Electron Microscopy*

1.11. Contents

1.12. Figures

II

MECHANICAL CHARACTERISATION OF K-CARRAGEENAN GELS IN THE PRESENCE OF CO-IONS

2 Mechanical characterisation of κ-carrageenan gels in the presence of co-ions

2.1. Abstract

The physicomechanical and textural properties of thermo-reversible κ-carrageenan gels in the presence of a wide range of potassium salts with different monovalent anions of varying Hofmeister number has been investigated using uniaxial compression and small strain oscillatory rheometry. Decreasing anionic Hofmeister number was observed to increase the strength and elastic properties of 0.4% κ-carrageenan gel structure. Gel strength was assessed by Young's modulus, bulk modulus, yield stress and work done to achieve failure; interpreted from uniaxial compression data, and elastic storage and loss moduli taken from rheometry studies. Stress relaxation and work recoverability studies also highlighted increased brittle character of gels in the presence of anions of lower Hofmeister number (kosmotropes), compared to those of higher Hofmeister number (chaotropes). Polarimetry and transmission spectroscopy studies were performed in order to evaluate the degree of conformational ordering and aggregation respectively.

Citrate and sorbate monobasic anions were specifically involved in this study due to their relevance to the food industry as preservatives [1]. The sorbate anion does not as yet carry an officially assigned Hofmeister number, and was therefore fitted to each analysis trend based on the experimental data, and a final Hofmeister number valuation of 10.4±0.15 was suggested, indicating a similar lyotropic behaviour to that of chloride (Hofmeister number 10).

2.2. Introduction

Carrageenan is a naturally occurring polysaccharide extracted from numerous genera of Red Seaweed, *Rhodophyceae* [51]. Chemically, Carrageenan is a high molecular weight, linear, anionic polysaccharide composed of alternating copolymers of 1,3-linked β-D-galactose 4-sulphate and 1,4-linked 3,6-anhydro-α-D-galactose [63-65] (Fig. 5).

Further categorization of these polymers is possible by defining the degree of 2-sulphation on the anhydro ring; in the case of κ-carrageenan this is measured to be zero; giving a sulphate: monosaccharide unit ratio of 0.5. In contrast, ι-Carrageenan is measured to be fully 2-sulphated; and thus gives a sulphate: monosaccharide unit ratio of 1 [66].

Of particular interest regarding κ-carrageenan is its ability to form thermo-reversible gels under appropriate conditions (temperature, concentration, ionic presence, pH etc.) [67-69] via an aggregated double helices domain model [66, 70-72].

Carrageenan	R	R'
Iota	SO_3^-	SO_3^-
Kappa	H	SO_3^-
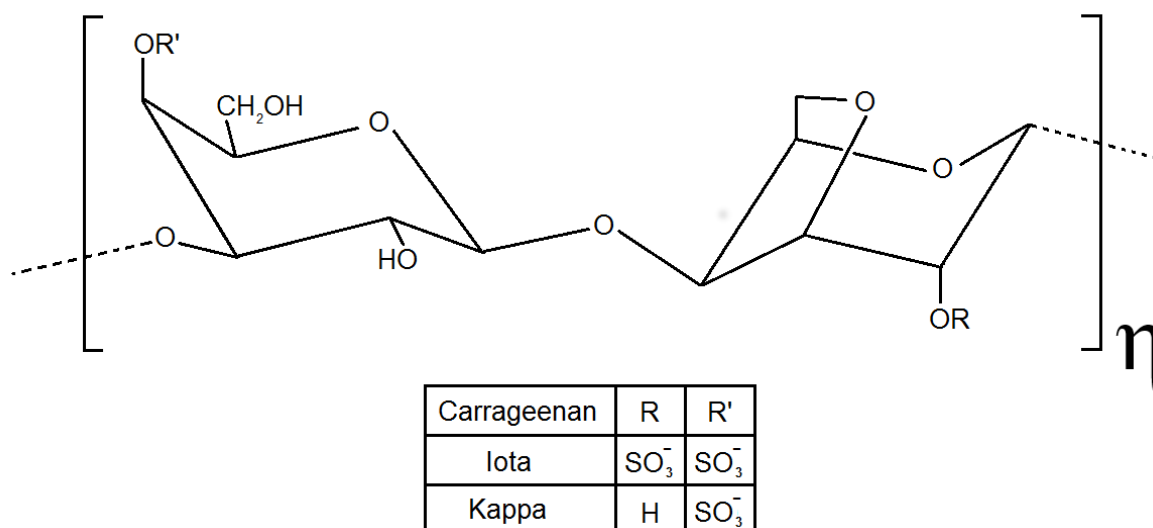
Fig. 5: Structure of repeating disaccharide unit in ι- and κ-carrageenan, reproduced from [66].

The κ-carrageenan chains associate firstly via direct intermolecular association to give a secondary structure of conformational ordered three-fold right handed double helices (Fig. 6), whose presence has been established via single wavelength optical rotation studies owing to the optical activity of the helices [66, 67, 69, 73, 74]. A number of these helices may then randomly associate and accumulate to form tertiary structures of small ordered "domains" (Fig. 6). In the case of κ-carrageenan in particular compared to other carrageenan, these intermediate secondary and tertiary structural stages are thermodynamically unstable [66, 69], and the system interchanges reversibly between the double helix (secondary) and ordered domain (tertiary) structures.

In the presence of cations, these ordered tertiary structure double helix "domains" are able to form cation bridges or "junction zones" by association of negative regions on the K-Carrageenan double helices to the positive cation, to form a thermo-dependent, quaternary network, which is stable under ambient conditions, with Potassium cations facilitating the highest degrees of aggregation [66, 71, 74-76] (Fig. 6), increasingly with higher cation concentrations up to a critical salt concentration [77].
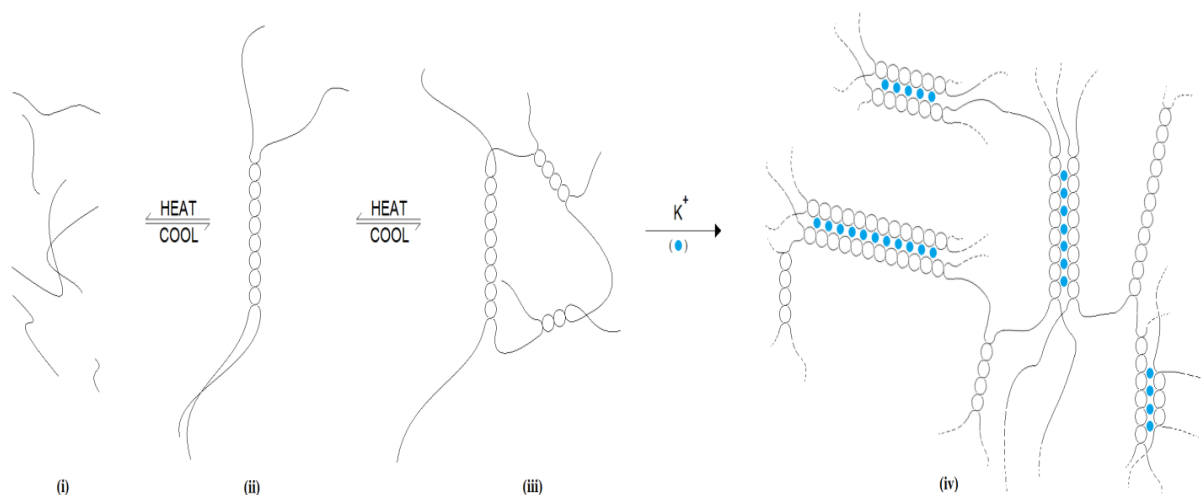
Fig. 6: Domain Model for κ-carrageenan Gelation. (i) Random coil primary structure. (ii) Double helices secondary structure. (iii) Ordered domains tertiary structure. (iv) Aggregated domain quaternary structure, reproduced from Morris, Rees [67].

Potassium cations are known to give the strongest aggregates in the group I metal cation order $Li^+>Na^+>Cs^+>K^+$ [75] however whilst multiple hypothesis have been explored [70, 75, 76, 78] no definitive proof of a particular cation-polymer interaction mechanism has been established.

The most probable and widely accepted mechanism at present is considered to involve the ionic association between the potassium monovalent cation and electron donor atoms on the κ-carrageenan disaccharide chain; namely oxygen atoms and/or sulphate group (Fig. 5). Nilsson et al. [78] suggested that one oxygen atom from either κ-carrageenan chain coordinates to the potassium cation, replacing some of its hydration shell. Sulphate groups are not considered as good ligands for alkali cations, whilst oxygen typically associates well according to Pearson's Hard Soft Acid Base theory [79], thus these appear the more likely donors. The rigid structure of the double helix is believed to lock oxygen donor atoms on adjacent κ-carrageenan disaccharide chains in place so that essentially a macrocyclic ligand is formed, which are renowned as being highly selective due to conflicting steric restrictions and ionic bonding distances [80], thus explaining the high selectivity for a particular cation (potassium) observed.

Studies regarding the effects of cations on κ-carrageenan are extensive, however the effects of the anions of a potassium (or any metal) salt added to a solution of κ-carrageenan have received less attention by comparison. Early studies [73] suggested that anions had no effect on the gel melting and cooling temperature profiles as assessed via optical rotation and conductivity. ^{127}I NMR studies [81] later observed that Iodide anions appeared to show exception, and suggested that Iodide anions are involved in specific site binding with the κ-carrageenan (proposed single helix) chains. This proposed mechanism would appear fundamentally unlikely however given the negative charge on the disaccharide chain (Fig. 5). Studies over a wider range of anions performed by Norton et al. [55] then revealed that κ-carrageenan gelling structure exhibits a dependency on co-ion Hofmeister number through the lyotropic series [49], [82] [83] [84] whilst salt concentration and cation are held constant.

The Hofmeister (or lyotropic) series is an empirical assignment of numbers used to quantitatively compare simple ions' promotion or suppression of polymer (or protein) ordering, with zero equating to the ion instigating no effect either way on polymer order; ionic presence and aggregate formation being independent of one another. Subsequently, Hofmeister numbers are unitless, and independent of temperature and pressure.

Norton et al. [55] observed temperature of conformational ordering of the double helices to be highest (as studied by optical rotation) in those chaotropic anions such as SCN^-; systematically decreasing through the lyotropic series whilst degree of aggregation followed the inverse trend; greatest in kosmotropic anions such as SO_4^{2-}.

Anion	Hofmeister No.		
F^-	4.8		Greater aggregation, poorer conformational ordering
citrate$^-$	7.2	Kosmotropic	
Cl^-	10.0		
Br^-	11.3		
NO_3^-	11.6		
I^-	12.5	Chaotropic	Less aggregation, greater conformational ordering
SCN^-	13.3		

Table 1: Lyotropic series ordering of anion effects on conformational ordering and mid-point setting temperature.

As the anionic effects appeared to follow a trend of anion charge density, it was suggested that anions do not site-bind to the polyelectrolyte as previously suggested [81], but instead alter the charge density of the polymer charge cloud and the water structuring (solvent quality), affecting the stability of the polymer, and therefore the conformation / aggregating behaviour. Austen et al. [85] later showed that rate of aggregation was inversely dependent upon lyotropic number (Table 1), in a reaction of second order kinetics: a 'fast phase' of double helix

nucleation, followed by a 'slow phase' of aggregation and annealing. Light scattering studies [86] confirmed the conformational ordering dependency on anion type, however the precise mechanism of the anion effects on κ-carrageenan remained elusive [87], concluding that whilst anion charge density influenced aggregation, the effects observed remained insufficient for consistent behaviour interpretation.

Finally, attention was turned towards the material behaviour and properties of κ-carrageenan gels in the presence of different counter-ions [88] [89] [90] [91] [92] and co-ions. Rheological studies [93] [94] observed that the dynamic Young's modulus of κ-carrageenan gels exhibited a dependency on anions present to the same trend as that of gel aggregation (i.e. inverse dependence to Hofmeister number), with the presence of iodide anions giving weaker mechanical properties than those gels with bromide anions present, which in turn gave weaker mechanical properties than those gels with chloride anions present. This would appear reasonable as increasing aggregation would assume both a greater number and / or size of the junction zones, and therefore greater association between ordered domains (Fig. 6). A greater number of junction zones would imply more intermolecular bridging to spread an applied load across a cross section; reducing stress concentration which cumulates in plastic deformation, whilst increased junction zone size would indicate stronger connections between ordered domains, and therefore higher yield stresses.

Whilst rheology imparts highly sensitive and useful information regarding the mechanical properties of viscous systems, its applications to gel systems presents a fundamental problem with regards to slippage between the sample and the plate, particularly in systems such as κ-carrageenan which are renowned for syneresis effects [51] [95] which may result in experimental data suggesting elastic properties below their actual values [96]. An alternative to rheology as a means of measuring mechanical response is therefore attractive.

Large scale deformation studies using a texture analyser in modern times are typically less precise in measurement than rheometry, however rather than slippage of gel systems presenting a problem it may actually be considered advantageous here, as slippage will lubricate the interface between the gel sample and the plates and ensure no barrelling occurs and force perpendicular to the vector of the compression plates is uniformed, implying a more accurate analysis of gel mechanical properties.

Assessment of the mechanical strength of κ-carrageenan gels via uniaxial compression remains scarce in the literature; previous work [97] has characterised the mechanical properties (Young's modulus, hardness, compressibility, cohesiveness and adhesiveness) of κ-carrageenan gels with KCl and $CaCl_2$, however no such study exists regarding the dependency of mechanical properties on a wide range of anions such that initially investigated by Norton et al. [55]. Moreover, there is an absence of studies considering the mechanical behaviour of gels leading to and at the point of failure compared to those studies within the elastic limits.

The present study therefore aims to investigate the mechanical properties of κ-carrageenan gels. Studies shall be carried out alongside and related to rheological small strain oscillatory studies, ultraviolet transmission, and polarised light studies in order to gain information on material behaviour under lower degrees of shear during and after gelling, aggregate development, and conformational ordering of the gel structures respectively – that it might be possible to gain as complete an understanding as possible of the gel aggregate microstructure in order to explain the material trends under (high strain uniaxial) compression. The anionic dependency of the mechanical properties shall be investigated for an exceptionally extensive number of potassium salts in order to distinguish any trends which may arise, including (but not limited to) citrate monobasic and sorbate potassium salts with a mind towards food grade application.

The sorbate anion has not been assigned an official Hofmeister number. This shall therefore be fitted to each of the attribute lyotropic dependency trends using the experimental data. This, along with a substantial investigation into the effects of a wide range of anionic Hofmeister number on the high strain uniaxial compression of κ-carrageenan, are the two central areas of novel research presented here by the author which are previously unexplored.

2.3. Materials & Methods

2.3.1. Materials

K-carrageenan (*Eucheuma Cottonii*, M_W 600-700 kDa, E407A EU specification processed, propan-2-ol washed, cat no.22048) and silicon oil was purchased from Sigma Aldrich (Gillingham, UK). All κ-carrageenan solutions were prepared with deionised and distilled water from an Aquatron A4000D (Stuart, Staffordshire, UK). Chloride, fluoride, iodide, nitrate, citrate, thiocyanate bromide and sorbate potassium salts were of analytical grade and also purchased from Sigma Aldrich (Gillingham, UK). Materials were given no further purification or modification of their properties. Molar quantities of salts were kept the same throughout.

2.3.2. Sample Preparation

K-carrageenan solutions (400ml at a time, 0.4% concentration by mass) in the presence of different (see above) potassium salts (0.0269M) were prepared by firstly dissolving the κ-carrageenan powder in deionised water at 80˚C under continued mixing using a hot plate stirrer (Stuart, Staffordshire, UK) before adding potassium salt. Mixtures were then sealed and held for 30 minutes in a water bath at 80°C with gentle stirring using a magnetic stirrer.

2.3.3. Rheology

Oscillatory tests were performed using a Kinexus rheometer (Malvern, UK) fitted with a Ø60mm roughened parallel plate geometry. K-carrageenan hot solutions were loaded onto the rheometer at 60˚C and a silicon oil water trap applied to the periphery to reduce water loss via evaporation. Gap was set at 1mm. Samples were then cooled to 5˚C at 1.0 K.min^{-1}, under a constant shear strain of 0.5% at 1.592 Hz, where they were held for 5 minutes before taking

final G' values. Measurements of shear storage modulus (G') and shear loss modulus (G")
were taken throughout. Experiments were performed in triplicate.

2.3.4. Uniaxial Compression

K-carrageenan hot solutions were prepared as above and poured into Ø20mm x 20mm moulds
and stored at 5˚C for 24 hours. Cylindrical gelled samples were then loaded onto a
TA.XT.plus® Texture Analyser (Stable Micro Systems, UK) with a 5kg load cell and a
cylindrical head geometry (Ø40mm). Samples were then compressed at a probe cross head
speed of 0.2 mm.s^{-1} to a distance of 5mm from the plate (75% strain). A force trigger of
0.04903N was used. Force/distance data was converted into true strain ε_H and true stress σ_T
using Equation1-4, as employed by Moresi et al. and adapted by Norton et al. [98, 99], where
ε_E and σ_E are the engineering strain and stress respectively, H_0 and A_0 are the initial height and
cross sectional area of the sample, and F and h are the force applied and the height of the sample.

$$\varepsilon_E = \frac{(H_0 - h)}{H_0} \tag{1}$$

$$\varepsilon_H = -\ln(1 + \varepsilon_E) \tag{2}$$

$$\sigma_E = \frac{F}{A_0} \tag{3}$$

$$\sigma_T = \sigma_E(1 + \varepsilon_E) \tag{4}$$

Young's modulus, work done up to total failure and bulk modulus were determined from the true stress / true strain plots in accordance with Smidsrod et al. [100], Kaletunc et al. [101], and Nussinovitch [102] respectively. Stress at total failure was also recorded. No barrelling occurred (Fig. 7) indicating an absence of frictional forces perpendicular to compression between the gel and the plate, and subsequently lubrication was not required. Experiments were performed to 10 repeats and averaged.
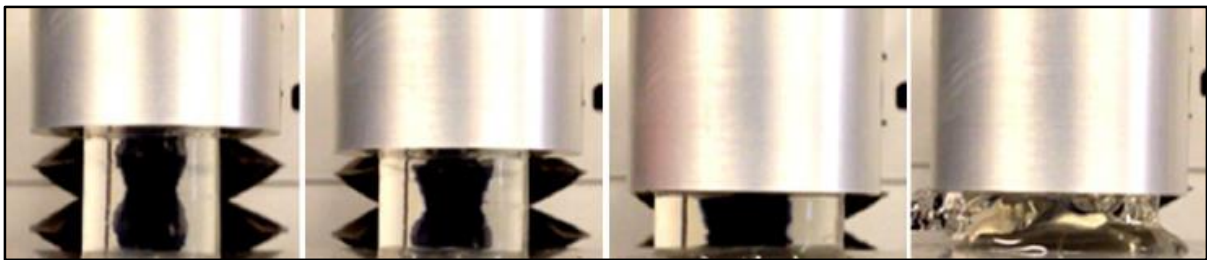
Fig. 7: Typical κ-carrageenan gelled sample undergoing compression up to and including failure.

2.3.5. Stress Relaxation Studies

Sample preparation, equipment set up, cross head speed and force trigger parameters were identical to those employed for uniaxial compression to fracture studies. This time however samples were compressed by 20% (4mm depth), as implemented by Koliandris et al. [103], and held for 600s to ensure a good indication of the residual value was obtained.

The force / time relaxation data was normalized and linearized using Equation 5 as originally proposed by Peleg [104], where is the initial force at, is the force at, and and are relaxation constants which may define the bulk properties of the gels.

$$\frac{F_0 \cdot t}{F_0 - F_t} = k_1 + k_2 \cdot t \tag{5}$$

$$E_A = \frac{F_0}{A_{(\varepsilon)} \cdot \varepsilon} \cdot \left[1 - \frac{1}{k_2} \right] \tag{6}$$

$$A_\varepsilon = \frac{A_0 H_0}{H_0 - \Delta H} \tag{7}$$

Relaxation constant was then converted into the asymptotic residual modulus, E_A which serves as a quantitative measure of gel solidity [105] [106] [107] using Equation 6 where is the strain applied (i.e. 0.2 in these studies) and is the corresponding calculated cross section area of the relaxing gel sample, defined by Equation 7. Tests were performed at 20°C and studies repeated (n=5).

2.3.6. Recoverable Work Done Studies

Sample preparation, equipment set up, cross head speed and force trigger parameters were identical to those employed for uniaxial compression to fracture and stress relaxation studies. Samples were loaded to achieve a 20% Strain (4mm decrease in H_0) and then immediately unloaded, monitoring the work done upon loading by determining the area beneath the stress vs. strain data. Probe cross head speed of 0.2 mm.s^{-1} both compressing and decompressing was used. Cycles were repeated on the same sample an additional 3 times with 1 minute intervals, comparing the work input required on each instance of loading. The work done recovered by the gel system on time of loading was then determined using Equation 8. Tests were performed at 20˚C and repeated (n=5).

$$Recoverable\ Work\ Done = \frac{Work\ done\ to\ compress\ sample_n}{Work\ done\ on\ initial\ compression} \times 100\% \qquad (8)$$

2.3.7. Polarimetry

Polarimetry studies were performed using an Anton Paar GmbH Gyromat polarimeter (Graz, Austria) with a jacketed cell of 50mm path length, at a wavelength of 365nm. Hot 0.4% κ-carrageenan 0.0269M potassium salt solutions were injected into the cell via syringe at 80˚C and then held at 60˚C whilst a background reference was recorded. Silicon Oil water traps were used throughout in order to eliminate water loss via evaporation whilst bearing no impact on the pressure within the cell. Temperature of the polymer solution was measured directly throughout using thermocouple wires submerged in solution, taking care not to interrupt the light path (thermocouple accuracy ±0.1⁰C).

Three cooling and heating cycles were performed between 60 °C and 15°C at 0.5K.min^{-1}, holding for 20 minutes at 15°C and 60°C to allow for helical structuring and de-structuring respectively. Temperature was controlled via thermostatically regulated circulating water bath (Julabo, UK). Temperature was recorded using a HH309/309A Datalogger thermometer (Omega®, UK). Temperature and optical activity was logged using an Anton Paar custom excel software Gyromat add-on. Helix onset and dissociation midpoint temperatures were taken from sharp increase in optical rotation on cooling and heating respectively. Optical rotation of plane polarised light for κ-carrageenan gels with 0.0269M potassium salts was recorded upon each cycle, after 20 minutes holding at 15°C, allowing for helical structuring to develop, and therefore maximum distinction between any anion effects in conformational ordering.

2.3.8. UV Transmission Spectroscopy

UV transmission spectroscopy was performed using a Libra S12 Visible & UV Spectrophotometer (Biochrom, UK), at a wavelength of 365nm; well within the UV range, as used for polarimetry studies. Hot 0.4% κ-carrageenan 0.0269M potassium salt solutions were injected into the cuvettes (10×4×45mm) at 80°C, covered and stored at 5°C. Tests were performed at 20°C in quintuplet against a deionised water background reference using Equation 9, where T% is the percentage transmission, UVT_{sample} is the transmission reading of the sample, and UVT_0 is the transmission reading of the reference cell with deionised water.

$$T\% = \frac{UVT_{sample} - UVT_0}{UVT_0} \times 100\% \qquad (9)$$

2.4. Results & Discussion

2.4.1. Plain Polarised Light Polarimetry Studies

Due to the optical activity of the κ-carrageenan double helix the conformational ordering may be conveniently studied using a plane polarised light polarimeter [67] [69] [66] [73] [74], the degree of which is understood to be dependent (in part) upon anionic presence [55]. By measuring optical activity through a temperature cycle, the temperatures of helix to coil transition are identified. Aggregation of these ordered domains (assuming sufficient potassium ion concentration) will immediately succeed ordering (Fig. 6) as the ordered conformation is in fact not stable for κ-carrageenan solutions and therefore the temperature at onset of conformational ordering is indicative of aggregation initiation.

Intermediate conformation stability is increased [55] by the presence of anions of a higher Hofmeister number due to their structure breaking properties on water in the bulk phase. Chaotropes' low charge density disrupts hydrogen bonding between water molecules in the bulk phase, facilitating availability to move to the charged polysaccharide chain intermediate and stabilise it [108]. Subsequently these polysaccharide solutions would be expected to show increased optical activity. Systems containing kosmotropic anions will aggregate from the (more) unstable intermediate faster, thus conformational ordering will be poorer than in those systems with chaotropes which allow a greater time window for more conformational ordering prior to aggregation.

The effect of anionic Hofmeister number in 0.0269M potassium monovalent salts upon the helix-coil transition temperature of 0.4% κ-carrageenan solutions are shown in Fig. 8a. Dissociation temperature is observed to demonstrate no dependence on anion Hofmeister number outside of one degree of standard deviation as indicated by the error bars (Fig. 8a).

Association temperature displayed a far greater dependency, which increased with increasing Hofmeister number in a non-linear dependency as observed in work by Norton et al [55].

The temperature of association transition of κ-carrageenan chains to helices is dependent upon stabilisation of the intermediate (Fig. 6). Chaotropic anions of higher Hofmeister number disrupt hydrogen bond water structuring interactions in the free water phase (free defined as 3 or more hydration spheres away [108]), due to their low charge density, and subsequently reduce the escape energy required for water molecules to leave the bulk water phase and associate to the polysaccharide chain and stabilise it. Increased stabilisation of the polysaccharide chains will reduce the energy, and subsequently facilitate organisation of polysaccharide chains into the (higher order) intermediate helical conformations at higher temperatures. Citrate monobasic anion solutions – which were not included in previous studies [55] [85] [93] [94]) –fit the trend well, whilst sorbate anion effects on the association / dissociation effects of double helix conformation in κ-carrageenan solutions fitted a Hofmeister number valuation of 10.4 and optical rotation a value of 11.3.

Hysteresis between temperatures of conformational ordering and dissociation (Fig. 8a) displayed an inverse dependence on potassium salt anion Hofmeister number; decreasing with increasing anionic Hofmeister number – in agreement with reports in literature [55] [90]. Hysteresis varied from approximately 12˚C (F$^-$), to 7˚C (SCN$^-$).
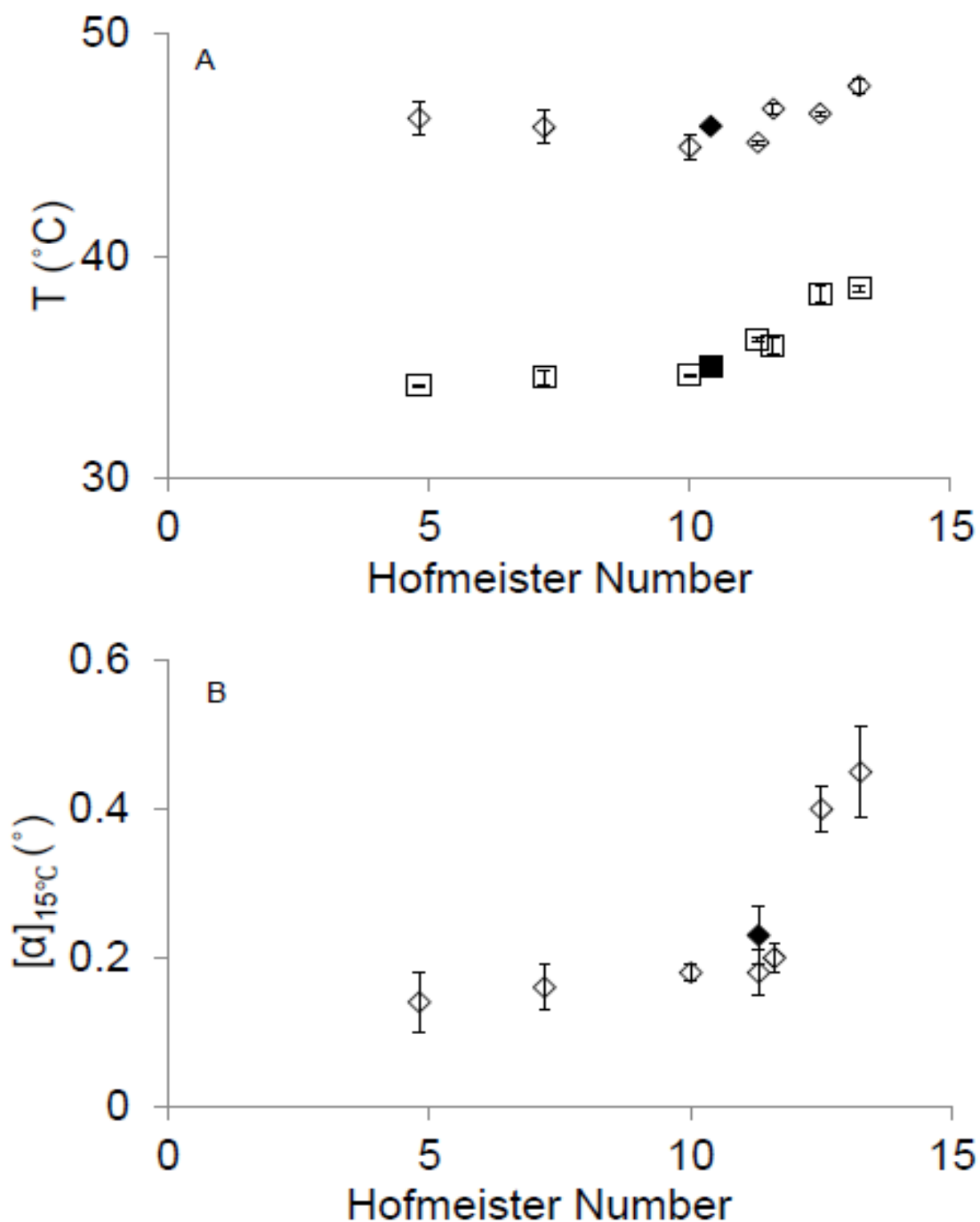
Fig. 8: (a) conformation association (□) and disassociation (◊) transition midpoint temperatures for 0.4% κ-carrageenan solutions with 0.0269M potassium salts, as a function of anionic Hofmeister number. Data for K(sorbate) (■ and ♦ respectively) has been fitted. (b) Optical rotation of plane polarised light after 20 minutes held at 15℃ , as a function of anionic Hofmeister number. Data for K(sorbate) (♦) has been fitted.

Hysteresis is attributed to the second order kinetics of gelation [85]; aggregation of the helices and helical domains stabilising the conformation to temperatures above those stable if the helices were in isolation [69]. Subsequently the dissociation temperature of the aggregate structure is well above that of the helices on their own, and exhibits significantly less dependency upon anionic Hofmeister compared to association temperature. Subsequently, the anionic Hofmeister number dependency of the association temperature defined by the stabilisation of the helical coil intermediate will similarly define the hysteresis between association and dissociation temperatures, as observed here.

Optical rotation for conformers at 15 (Fig. 8b) was positive in all systems: indicative of a right hand helix. Optical activity increased with increasing anion Hofmeister number – attributed to higher levels of conformational ordering, indicating greater stabilisation of the conformer intermediate in the presence of these anions.

2.4.2. *Ultraviolet Light Scattering Studies*

Transmission of UV light (λ_{365}) through aggregated networks allows the turbidity and aggregation within a polymer system to be determined and compared. A densely structured and complex aggregate network will scatter light passed through it more, giving a lower transmission percentage.

The UV transmission of 0.4% κ-carrageenan solutions after 24 hours was observed to increase with increasing potassium salt anion Hofmeister number outside of the boundaries of one standard deviation as indicated by the error bars (Fig. 9a). Transmission varied between approximately 60% and 72%. Increase was, again, non-linear; displaying an increasing dependency on anion presence with increasing anion Hofmeister number, as was observed in the conformational ordering temperature, in concurrence with previous reports made by Norton

et al. [55]. This observed trend in UV transmission would indicate more light scattering in with the presence of kosmotropic anions such as F^- and citrate$^-$, suggesting these anions encourage the number and size of aggregates. Inversely chaotropic anions such as I^- and SCN^- allow higher UV transmission, implying reduced aggregate development. The degree of aggregation and network formation is directly related to hardness and strength of the textural properties [51] [109], and this shall be explored later. Sorbate monobasic anion effects on UV transmission of κ-carrageenan solutions fitted the trend with a Hofmeister number valuation of 10.8.

The same samples were again studied after 48 hours in order to assess the progression of aggregation over time. Aggregates with kosmotropic anions showed almost no change in transmission, whilst systems with increasingly chaotropic anions showed a small but progressive loss in transmission up to 4%. This would suggest that κ-carrageenan aggregates of more conformationally ordered helices (formed in the presence of anions of higher Hofmeister number) are able to reorganise locally, more so than those in the presence of anions of low Hofmeister number which are less regularly ordered in organisation and therefore have less capability to re-orientate locally. The reason for this is understood to result from the relative stability of the conformer intermediate: kosmotropic anions with a higher charge cloud density will exhibit greater affinity towards polar water molecules in the bulk phase – demanding preferential hydration of surfaces towards them and away from the polymer chain inhibiting any charge stabilization effects the polar water molecules might have there [108]. Inversely chaotropic anions will interrupt the water intermolecular bulk phase structure and free water molecules up for migration to the polymer charged regions; stabilizing the polymer chain intermediate. The more stabilized the charged intermediate is, the lower the thermodynamic driving force behind the reaction and therefore the slower the rate of aggregation and the more organised the structure will be.
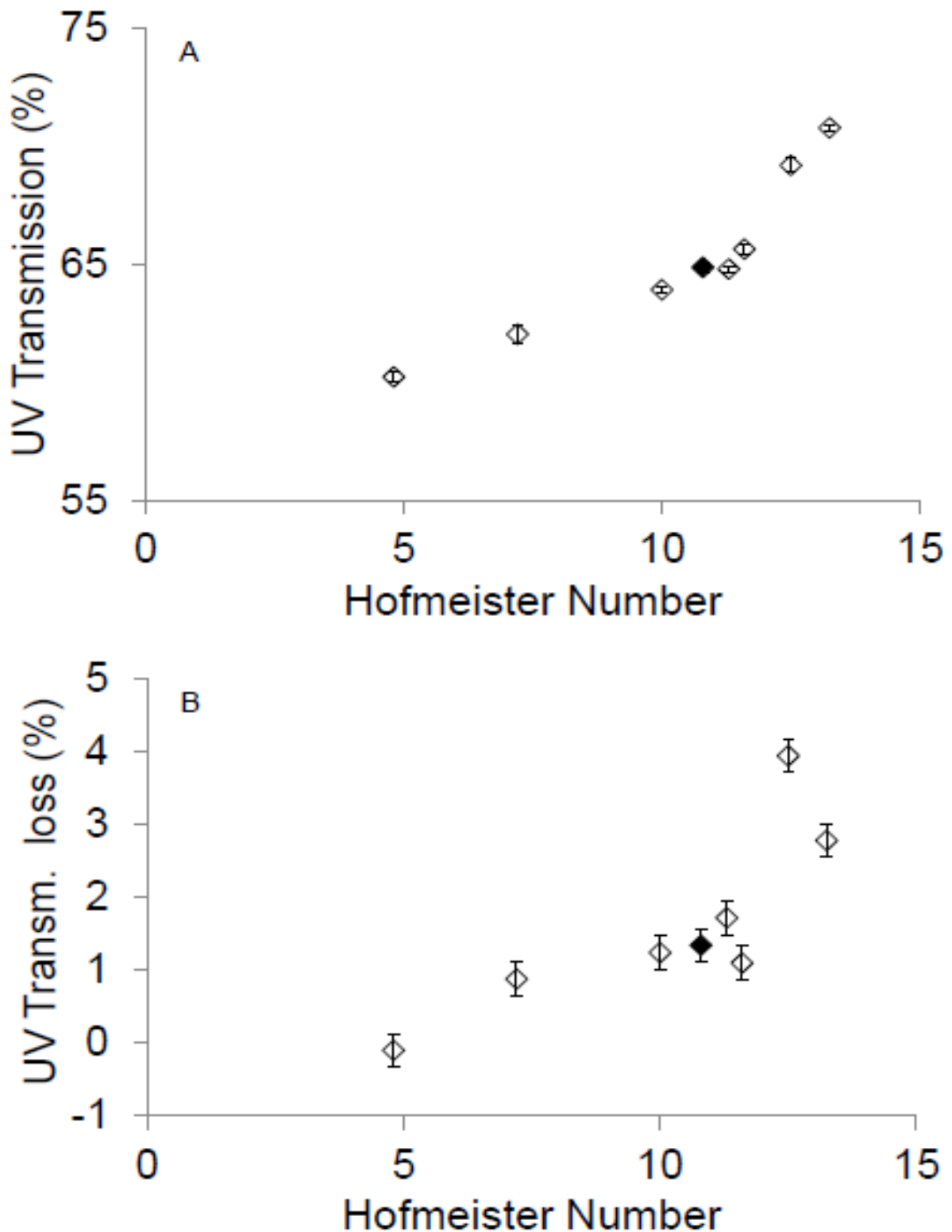
Fig. 9: (a) UV transmission (λ365) for 0.4% κ-carrageenan gels with 0.0269M potassium salts 24 hours after preparation stored at 5°C, as a function of anionic Hofmeister number. Data for K(sorbate) (♦) has been fitted. (b) Further loss in UV transmission between 24 and 48 hours as a function of anionic Hofmeister number. Data for K(sorbate) (♦) has been fitted.

2.4.3. Oscillatory Rheology

By applying low level shear oscillation to κ-carrageenan gel systems it is possible to ascertain the network development and degree of junction zone formation present, by quantifying the recoverability of the aggregate from shear displacement; i.e. the elastic shear storage modulus G'. Inversely, shear which is not recovered by the system is referred to as the shear loss modulus; G". The greater the aggregate network development, the greater the number of junction zone connections in a cross sectional area of the system, and therefore the greater distribution of an applied load, reducing stress concentration and increasing the recoverability and elastic character in the material: this may be observed experimentally in the developing prominence of G' over G". Allowing stress to concentrate in a specific region (i.e. poor connectivity and aggregate network development, leading to inefficient stress transfer) will mean stress accumulation at this position will be heightened for a given strain, subsequently elastic potential energy storage (G') will decrease and plastic potential energy loss (G") will increase.

G' of κ-carrageenan gels was studied as a function of the Hofmeister number of the potassium salt anions added (Fig. 10a) taken after having been held at 5 for 5 minutes in order to achieve an acceptable level of equilibrated network development (±2.5% over 5 minutes) and ensure any pronounced initial peak which might give a false reading was avoided [96], [88]. G' decreased linearly with Hofmeister number from approximately 600 Pa (F⁻) to 100 Pa (SCN⁻). Sorbate monobasic anion effects on elastic shear modulus and elastic loss modulus of κ-carrageenan solutions fitted the trend with a Hofmeister number valuation of 10.4. [93] reported that the elastic response of κ-carrageenan gels with alkali metal salts decreased with increasing Hofmeister number of the salt anion: for Cl⁻, Br⁻, and I⁻ salts tested. These studies here would appear to agree with those findings, and present evidence that the trend continues over a much wider Hofmeister number range (Fig. 10a).
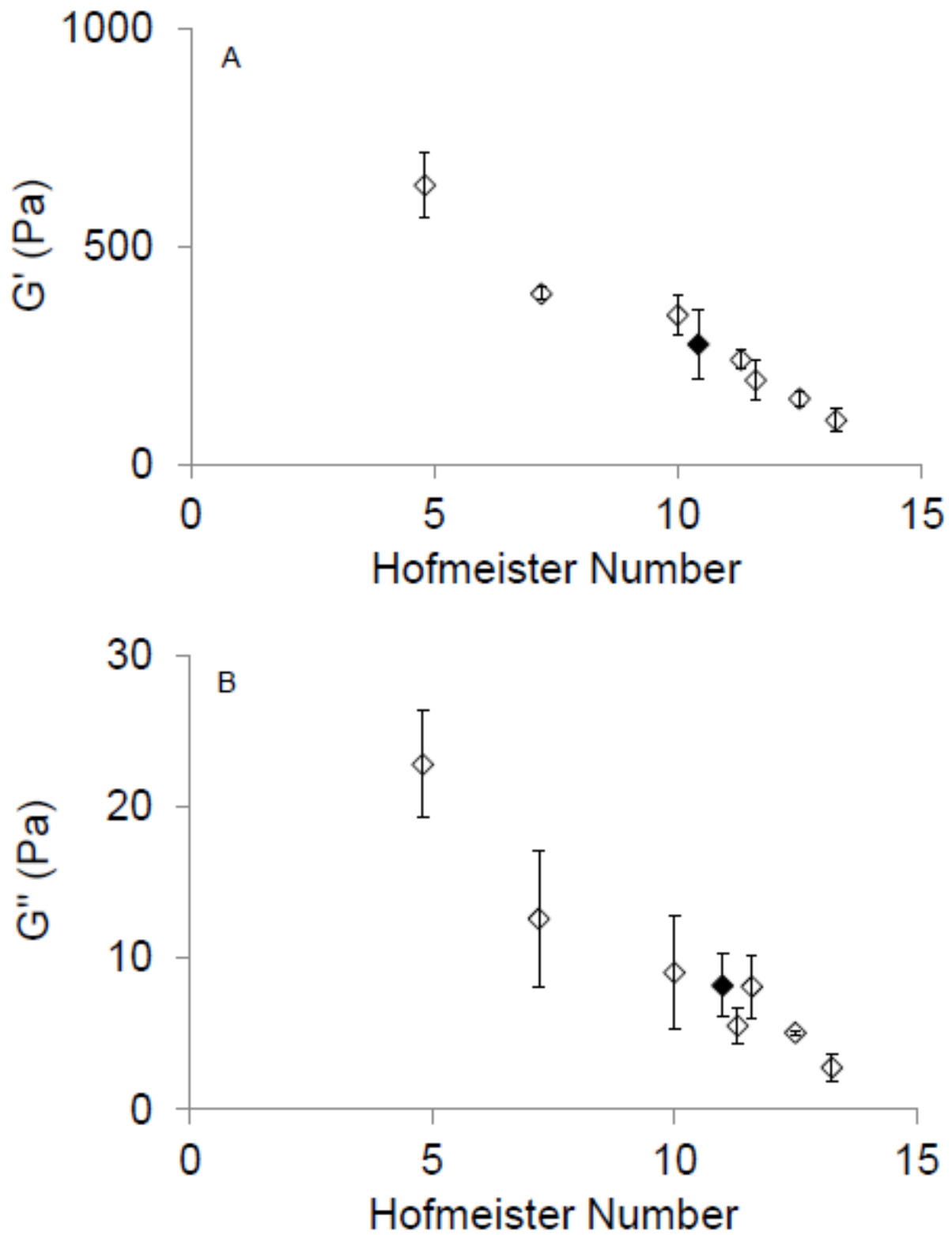
Fig. 10: (a) Shear storage modulus and (b) Shear loss modulus for 0.4% κ-carrageenan gels with 0.0269M potassium salts, as a function of anionic Hofmeister number. Data for K(sorbate) (♦) has been fitted.

Observed increase in elastic shear response of κ-carrageenan quiescent gels in the presence of kosmotropic anions arises due to increasing aggregation promotion; kosmotropic anions are 'hard' anions with a high charge density, as such they are able to interact with highly polar water molecules amongst the bulk phase (on or above 3 hydration spheres) away from the κ-carrageenan double helix charge cloud, contributing towards the structuring of water molecules in that bulk phase. Thus the κ-carrageenan double helix unstable intermediate receives reduced stabilisation, and thermodynamic preference towards aggregation and intermolecular bridging (junction zone formation with K^+ cations) is increased, subsequently increasing network aggregation (Fig. 10a) at a faster rate (Fig. 10b). More aggregation and intermolecular bridging means a greater spread of applied shear stress across a cross section, and therefore less shear stress concentration and greater overall elastic shear tolerance. Inversely, large singly charged ions with low charge density (i.e. chaotropic anions such as I^- and SCN^-) exhibit weaker interactions with water than water with itself (water is reasonably charge dense and therefore prefers interaction with similarly 'hard' ions), and thus interfere little in the hydrogen bonding of the surrounding water. This very weak degree of interaction between water molecules in the bulk phase and chaotropic anions means the water molecules are available to move toward and stabilise the polysaccharide chains - stabilising the intermediate double helix conformation. Consequently, because the precursor for aggregate formation (Fig. 6) is now more stable, thermodynamic drive towards aggregation will be decreased – resulting in slower, less extensive κ-carrageenan network development and junction zone connectivity as greater conformational ordering of the double helices assists in stabilisation of the negative regions on the polymer chains. Subsequently any applied stress in oscillation (rheology) studies will be dispributed across fewer junction zones in those aggregate structures in the presence of chaotropic anions, resulting in greater shear stress concentration, and a lower elastic shear tolerance (Fig. 10a).

G" of κ-carrageenan gels was studied as a function of the Hofmeister number of the potassium salt anions added (Fig. 10b). This was observed to decrease with increasing Hofmeister number. It is believed this is a result of relative structural formation in the samples: more aggregate material in a sample will inherently result in a slightly elevated G", as more material is being displaced and friction between displacing microstructure planes is increasing. The observations and hypotheses from these studies may now be compared directly to mechanical response of 0.4% κ-carrageenan gel systems with 0.0269M potassium salts subject to high (75%) strain uniaxial compression.

2.4.4. Uniaxial Compression

Analysis of resistance behaviour when subjected to uniaxial compression between parallel plates is a fast and simple means of analysing the elastic and inelastic properties of a quiescent polymer gel macrostructure [97], and any changes the microstructure may have upon this. Elastic Young's modulus may be predicted from the elastic shear behaviour [110], whereas other properties associated with plastic deformation and fracture generally show no trend in correlation to the elastic shear behaviour [111].

Young's modulus has been taken as the gradient of the initial linear region of the true stress strain curve [100], and is understood to represent the load range over which the aggregate network and the intermolecular binding (junction zones) may be elastically deformed and displaced from their equilibrium position at resting; returning to their prior equilibrium position after unloading.

Fig. 11 shows the effect of the Hofmeister number of the potassium salt anions (0.0269M) on the Young's modulus of 0.4% κ-carrageenan gels. As with G' studies (Fig. 10a), Young's modulus was observed to display an inverse dependency upon anionic Hofmeister number.

Furthermore, both G' and Young's modulus of 0.4% κ-carrageenan gels exhibit the same linear

trend of increasing elastic character with decreasing anionic Hofmeister number.
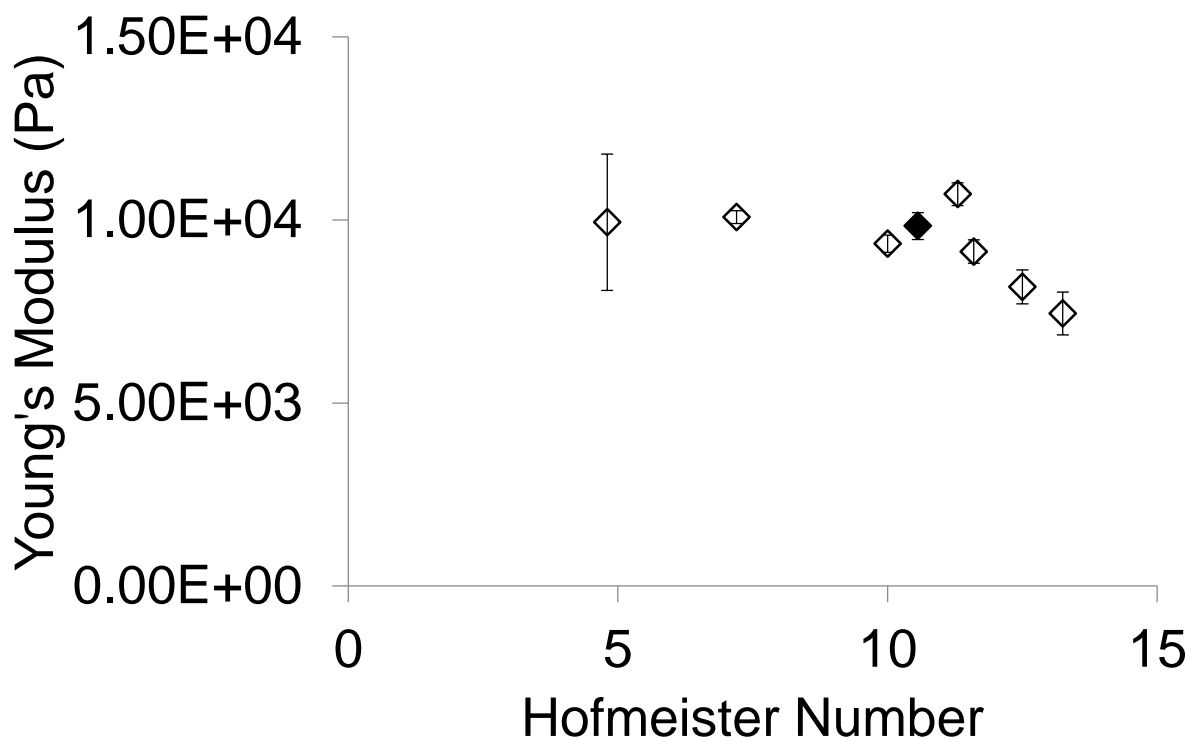
Fig. 11: **Elastic Young's modulus for 0.4% κ-carrageenan gels with 0.0269M potassium salts, as a function of anionic Hofmeister number. Data for K(sorbate) (♦) has been fitted.**

Systems with kosmotropic anions of lower Hofmeister number will promote greater levels of

intermolecular binding, and therefore applied load will be spread over a greater number of

junction zones and stress concentration will be decreased.

As a result of this the elastic properties of the material will be greater. Here, two systems of

equal polymer concentration and salt molar concentration, subjected to an applied force

(such as is being used in these studies) are displayed in a simplified representation (Fig. 12);

the system on the left includes potassium salt of a chaotropic anion, whilst the system on the

right includes a potassium salt of a kosmotropic anion. Chaotropic/Kosmotropic anions will drive aggregate formation as discussed, with chaotropic systems of less developed aggregate structure distributing the applied stress less effectively than those of kosmotropic anion aggregates which exhibit greater junction zone formation, and subsequently distribute applied stress more.
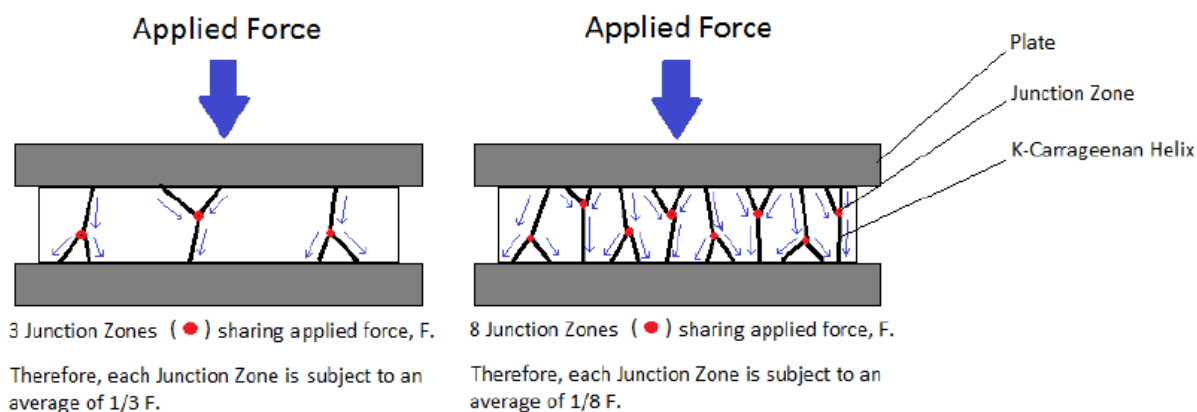
Fig. 12: **Simplified model demonstrating how κ- Carrageenan gelled systems of increased aggregation and further developed network structure (right) dissipate applied force better than those of lower aggregation and less developed network structure (left), resulting in smaller forces localising on each junction (on average). Note ratios are purely hypothetical, and bear no exact numerical correlation to these results observed.**

Despite both representing a quantification of elastic character, and exhibiting analogous trends, Young's modulus of elasticity taken from uniaxial compression (Fig. 11) and the elastic shear storage modulus taken from rheology (Fig. 10a) do not exhibit quite the same relative dependency factor upon Hofmeister number, with G' displaying a reduced sensitivity to anionic Hofmeister number. Whilst rheological studies operated at a 0.5% shear strain, Young's elastic modulus as determined from textural studies (Fig. 11) was taken up until approximately ≤10% uniaxial compressive strain, however both were derived from the respective linear regions of elastic deformation. It should also be noted that samples for rheological analysis were submitted as hot solutions and gelled in the rheometer over a time course of 60 minutes, whilst

samples for compression studies were prepared 24 hours in advance, allowing for additional network development and organisation (chain conformer optimization). Even once gelled, quiescent κ-Carrageenan systems will continue to restructure over time as conformations reorganise and helical coils tighten. Even this, however, is only marginal – especially over the relatively short timescale of 24 hours. Another suggestion for the discrepancy is slippage at the plates, which persistently a primary concern in hydrocolloid rheology studies. Minor slippage at the plate (which if we recall is actually beneficial in texture analysis to prevent barrelling) could therefore result in G' displaying a reduced sensitivity to anionic Hofmeister number compared to Young's modulus. It is hypothesised therefore, that the increased anionic Hofmeister number sensitivity of 0.4% κ-carrageenan gel elastic material properties seen in uniaxial compression studies (Fig. 11) compared to rheology studies (Fig. 10a) is a result Of a combination of these three factors.

Bulk modulus under uniaxial compression (not to be confused with the bulk modulus under uniformed compression [98]) has been taken as the gradient of the linear region approaching the point of failure [102] [99], and represents the non-elastic resistance to compaction, or rigidity, of the aggregate network. It is indicative of the ability of the macrostructure to undergo localised failure: i.e. irreversible displacement/breaking of intermolecular binding sites and compacting of the aggregate network, prior to complete bulk failure of the material.

Bulk modulus of 0.4% κ-carrageenan gels is presented (Fig. 13) as a function of the anion Hofmeister number for the 0.0269M potassium salt added. Bulk modulus is observed to exhibit an inverse dependency on anion Hofmeister number, showing an approximate 60% decrease from F^- (Hofmeister number 4.8) to SCN^- (Hofmeister number 13.3).
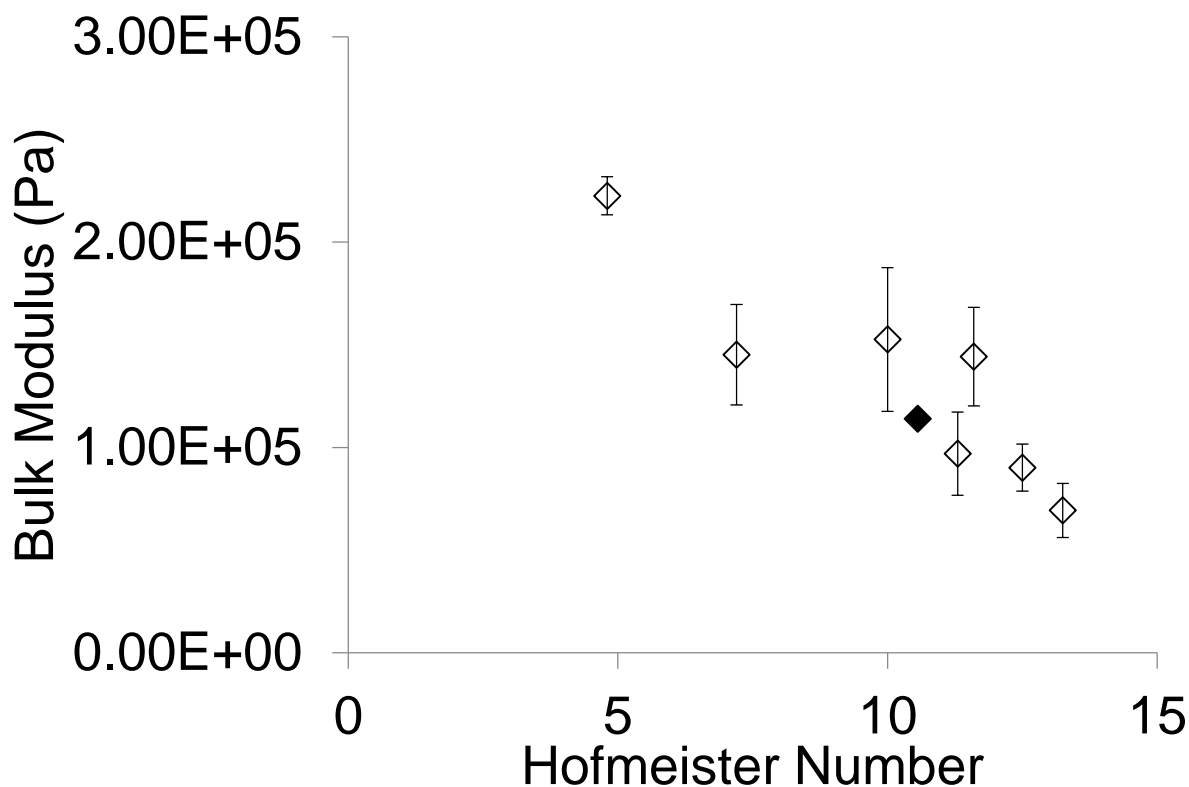
Fig. 13: **Bulk modulus for 0.4% κ-carrageenan gels with 0.0269M potassium salts, as a function of anionic Hofmeister number. Data for K(sorbate) (♦) has been fitted.**

The hypothesis for this observed inverse trend is thus: the degree to which intermolecular binding between ordered domains (Fig. 6) can be irreversibly deformed and broken on a micro scale without causing macroscopic failure of the structure is directly dependent on the extent of intermolecular binding in the network. Microscopic failure; i.e. failure on a particle level [112] will divert stress concentration on the surrounding junction zones, and the number of immediate junction zones will determine how this stress is apportioned; lower levels of intermolecular binding in a system will result in greater stress concentration on the fewer surrounding junction zones and therefore greater chance of failure in these neighbouring junction zones, upon where the sequence may then repeat and ultimately accumulate in crack tip propagation, this will then accumulate and ultimately result in macroscopic failure of the bulk structure, i.e. failure on a 'strand' level [112].

Therefore anions of lower Hofmeister number which promote junction zone formation and aggregation (see Fig. 9a) in κ-carrageenan gels should withstand more accumulated microscopic localised failure prior to failure. Inversely, chaotropic anions of higher Hofmeister number will hinder junction zone formation and aggregation, subsequently resistance to microstructure compaction will decrease, and localised failure will accumulate in macroscopic failure under lower stress conditions.

Finally, at the point of complete failure, the accumulative work and the stress up to macroscopic failure has been determined. Stress was observed to fall away sharply upon bulk failure in all studies, as is typical for brittle systems such as κ-carrageenan gels [51]. In trends analogous to that of the bulk modulus, failure work (Fig. 14a) and failure stress (Fig. 14b) show a strong inverse relationship to the anion Hofmeister number. Similarly, it is hypothesised (as for the bulk modulus) that the more intermolecular binding in a network the greater the work input required to overcome the accumulative strength of the aggregated domain associations and cause fracture resulting in failure.

Stress (i.e. force per unit area) required for bulk failure will depend on the extent of intermolecular bonding in the sample, as the number of junction zones will result in higher stress concentration at these points in the network, and thus failure is likely to occur sooner (under lower applied stress). As such the presence of those kosmotropic anions of lower Hofmeister number which promote aggregation will increase the bulk strength properties of κ-carrageenan gels, whilst those chaotropic anions of higher Hofmeister number which favour conformer intermediate stabilisation will decrease the bulk strength properties of κ-carrageenan gels, as displayed here, represented by the resistance to compression (Fig. 13) and macroscopic failure (Fig. 14a-b).
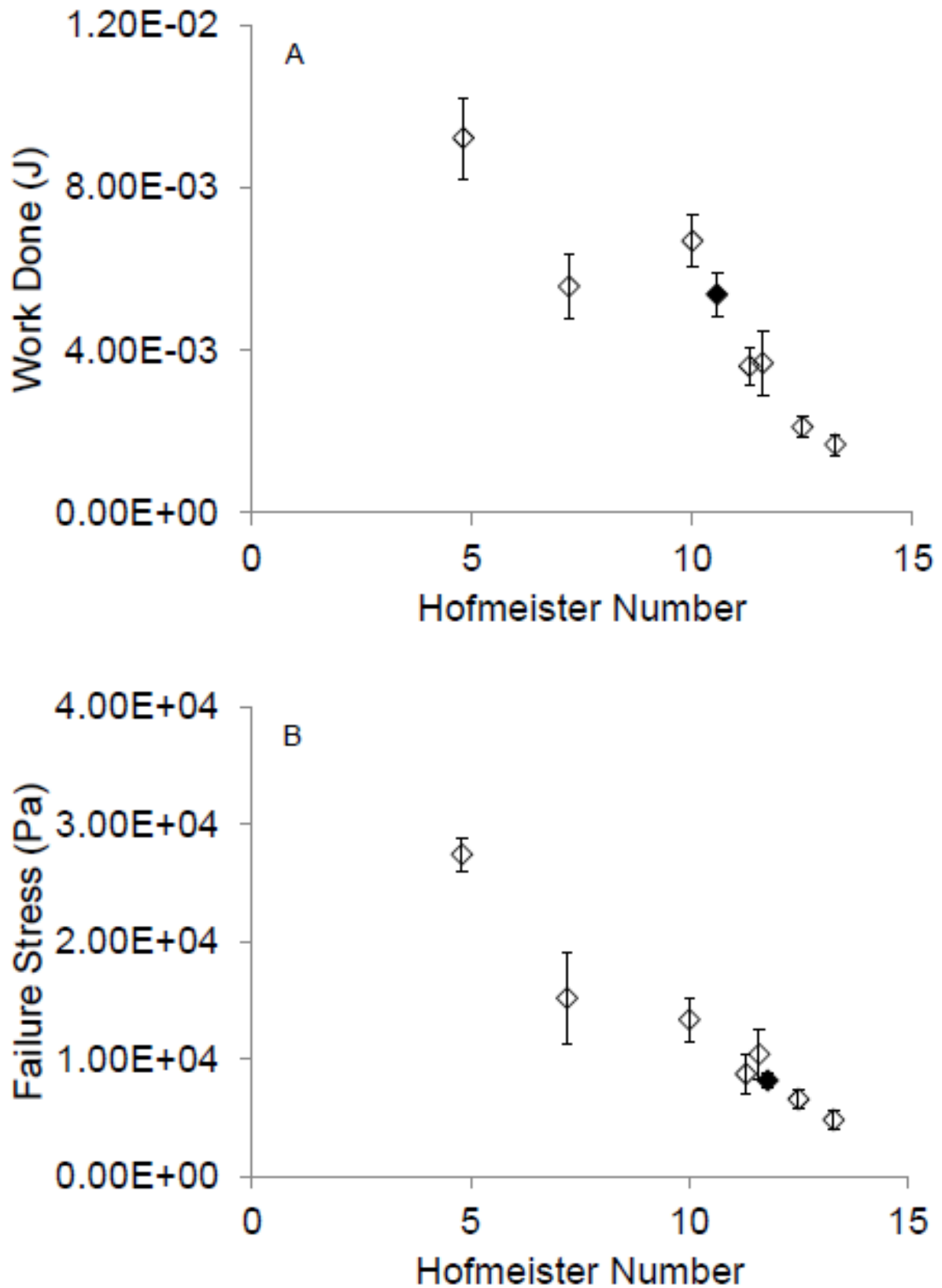
Fig. 14: (a) Failure work, and (b) failure stress for 0.4% κ-carrageenan gels with 0.0269M potassium salts, as a function of anionic Hofmeister number. Data for K(sorbate) (♦) has been fitted.

Sorbate monobasic anion effects on the Young's modulus, bulk modulus, and failure work of κ-carrageenan gels fitted with an average Hofmeister number valuation of 10.6. Stress at failure fitted the trend with a Hofmeister number valuation of 11.8. Standard deviation as indicated by error bars was small throughout indicating a high level of reproducibility.

2.4.5. Stress Relaxation Studies

By applying a constant strain to a hydrocolloid quiescent gel system and recording the gel response over time (i.e. the stress required to hold strain) it is possible to assess the resilience (that is – storage of potential energy through elastic character) of the aggregate structure, and how it relaxes with time (how potential energy stored is gradually dissipated as irreversible structure deformation). The rate at which this gel initially relaxes, and how far it ultimately allows itself to relax, are both quantifiable via Equation 5 and 6, and impart useful information regarding the textural properties of the system.

Initial gel relaxation rate may be represented by $\frac{1}{k_1}$ and for a fixed strain this may be directly related to brittleness [104], which subsequently will provide information on the relative extent of aggregates structuring. The final 'resting' strain is defined by the second constant and this may be converted into an asymptotic residual modulus E_A that serves as a definition of bulk resilience, directly related to the solid character and strength of the gel network (note: brittleness and strength are not the same) [113] [105] [106] [114] [107].

The stress relaxation of 0.4% κ-carrageenan gel systems in the presence of different 0.0269M potassium salts was studied, and results presented as a function of anionic Hofmeister number. The initial stress relaxation rate, as represented by $\frac{1}{k_1}$ is observed to decrease with increasing Hofmeister number (Fig. 15a).
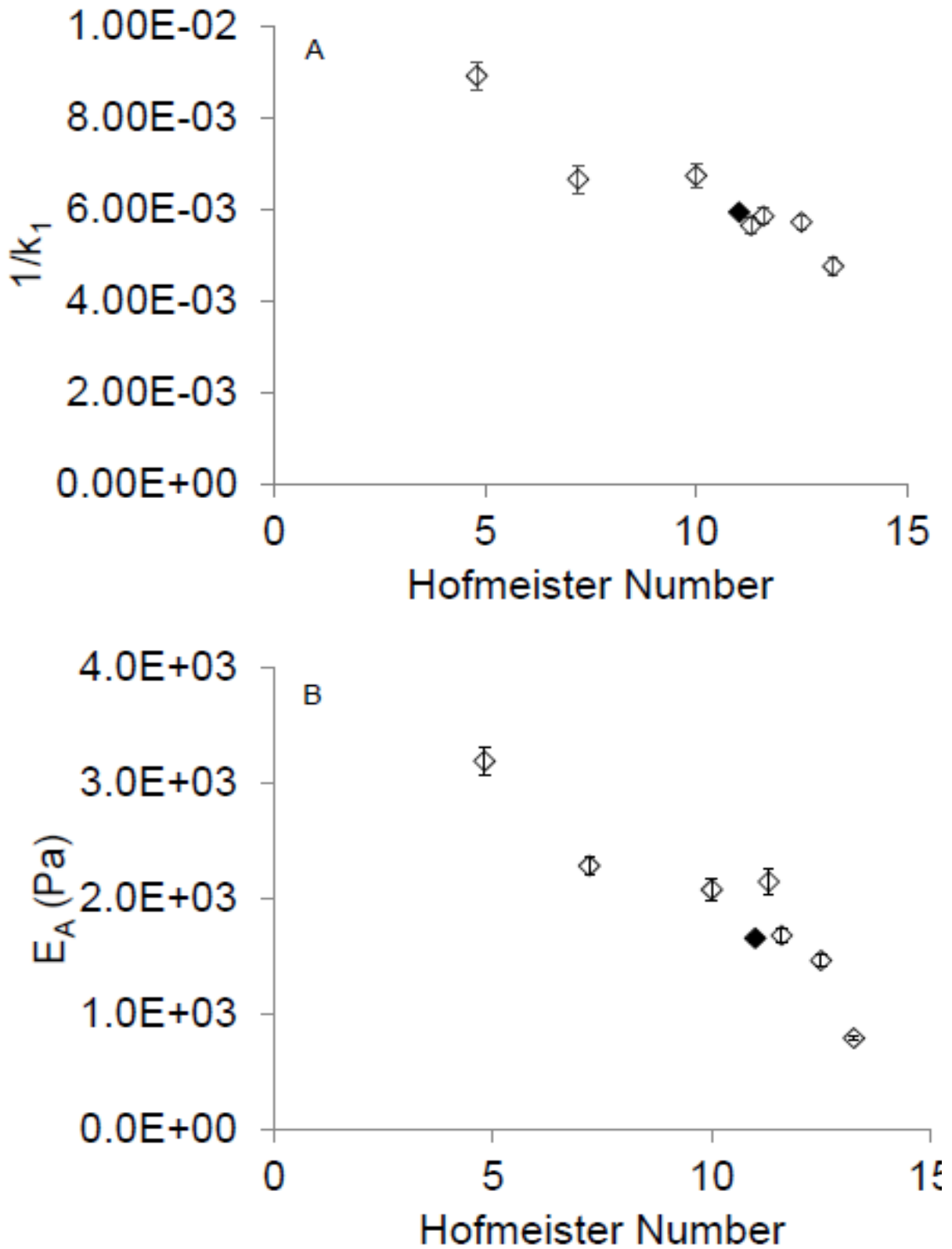
Fig. 15: (a) initial stress relaxation rate; 1/k1 and (b) asymptotic residual modulus for 0.4% κ-carrageenan gels with 0.0269M potassium salts, as a function of anionic Hofmeister number. Data for K(sorbate) (♦) has been fitted.

These results indicate that those systems with kosmotropic anions of lower Hofmeister number initially relax faster against the implemented strain, whilst those gel systems in the presence of chaotropic anions of higher Hofmeister number store energy imparted by work done on compression longer. The asymptotic residual modulus E_A was observed to decrease with increasing anion Hofmeister number (Fig. 15b). This indicates that the presence of kosmotropic anions generate a stronger κ-carrageenan aggregate, by comparison to chaotropic anions.

Sorbate monobasic anion effects on the initial stress relaxation constant $\frac{1}{k_1}$ and asymptotic residual modulus E_A of κ-carrageenan gels fitted the trends with an averaged Hofmeister number valuation 11.0.

The trend in asymptotic residual modulus E_A as a measure of solid character with anionic Hofmeister number effects agrees with hypotheses from bulk modulus (Fig. 13) and failure work studies (Fig. 14a), as resilience in storage of potential energy will be defined by the strength of the aggregate polymer network and the degree of intermolecular binding present: more intermolecular bridging spreading an applied load better across a cross section; reducing stress concentration which cumulates in plastic deformation and energy dissipation.

Decreasing initial stress relaxation $\frac{1}{k_1}$ with increasing anion Hofmeister number (Fig. 15a) suggests increasing brittle character and inflexibility of the polymer aggregate in the presence of more kosmotropic anions.

Brittleness will be defined by the concentration of inter molecular cross linkages between aggregate domains. The higher the number of junction zones, the more the aggregate domains will be held in a fixed position, so that greater forces and stresses must be exerted upon them in order to move them out of position in order to achieve and hold the same strain, subsequently

more irreversible displacement of cross linkages will occur, inherently causing more potential energy to be dissipated.

These findings for stress relaxation studies emulate those trending observations throughout this study: that aggregate strength, network development and elastic character increases with decreasing anionic Hofmeister number. For all relaxation studies a constant strain of 20% (of the original sample height) was applied, and all studies throughout contain the same concentration of polymer (0.4%), therefore the origins for distinction in material properties must lie in how the polymer presents itself: either dissolved in the bulk water phase or out of the bulk water phase, and also the extent of the aggregate networking and how it interconnects (i.e. number and strength of junction zones). These findings thus far would appear to support the theory of Hofmeister series ordering of 'salting in/out' effects of anions on κ-carrageenan polymer solutions [55] [93] [94] [108] [85].

As has previously been highlighted, the high charge density on kosmotropic anions is comparable to that of a water molecule, and they subsequently offer preferential (to polysaccharide chain) hydration sites for free water molecules [108] [115] increasing water structuring in the bulk phase (i.e. 'structure making'). Water molecules are less available to the κ-carrageenan to stabilise it, and subsequently, the polymer is not sufficiently solvated and charge on the polysaccharide chain is not stabilised by water molecules in the bulk phase, therefore the polymer stabilises itself by forming the aggregate. Studies of kosmotropic effects on water hydration of proteins by [108] suggested that the kosmotropes themselves did not interfere directly with the protein chain, and that effects on relative protein solution / aggregate stability were a result of indirect anion effects on the availability of free water for hydration of the protein chain. Aggregation and network development is therefore higher in the presence of kosmotropic anions with greater water associative attributes, and less in the presence of chaotropic anions with water structure disrupting character, which is what we have observed

here. It would appear logical therefore that the observed trends in the development of the aggregate network against the comparative charge density of the anions in the series and inherent interactions with water structuring conform to the 'salting in/out' model.

2.4.6. Work Recovery

Compression-decompression cycles are a useful technique in quantifying the recoverability of a polymer gel network. In compressing a gel (or any) system work must be done on it. Upon compression this work is transferred to the gel polymer network. The work is then either stored or dissipated depending on the elastic properties of the specific gel network – the greater the elastic properties, the greater the system's ability to store the work done upon it as potential energy and utilize it upon decompression in returning towards its original state. Inversely, the poorer the elastic character of the system, the more work is dissipated e.g. via bond breaking. In accordance with the fundamental law of energy conservation, all of the work implemented upon the polymer gel sample must be accounted for. By repeating compression / decompression cycles the work recovered from each preceding compression cycle may be determined, and therefore the elastic (and subsequently also plastic) recoverability of the polymer systems quantified and compared.

Gels of 0.4% κ-carrageenan with 0.0269M potassium salt were compressed between parallel plates to 80% of the height of the initial length of the sample (20mm compressed to 16mm) in 4 compression / decompression cycles. The work required for each compression was calculated as the area under the stress / strain curve, and compared as a percentage of the work required on the first compression. Data has been presented as a function of anionic Hofmeister number (Fig. 16). Sorbate anion effects were fitted to the trend with a Hofmeister number valuation of 9.8.

Three trends are distinguishable from the data presented. Firstly, the work recovered by the κ-carrageenan gel systems is less than 100% (Fig. 16). This indicates that the polymer system does not behave as a perfectly elastic material at these strain parameters, and that a portion of the work implemented upon it is lost via irreversible displacement to the network.
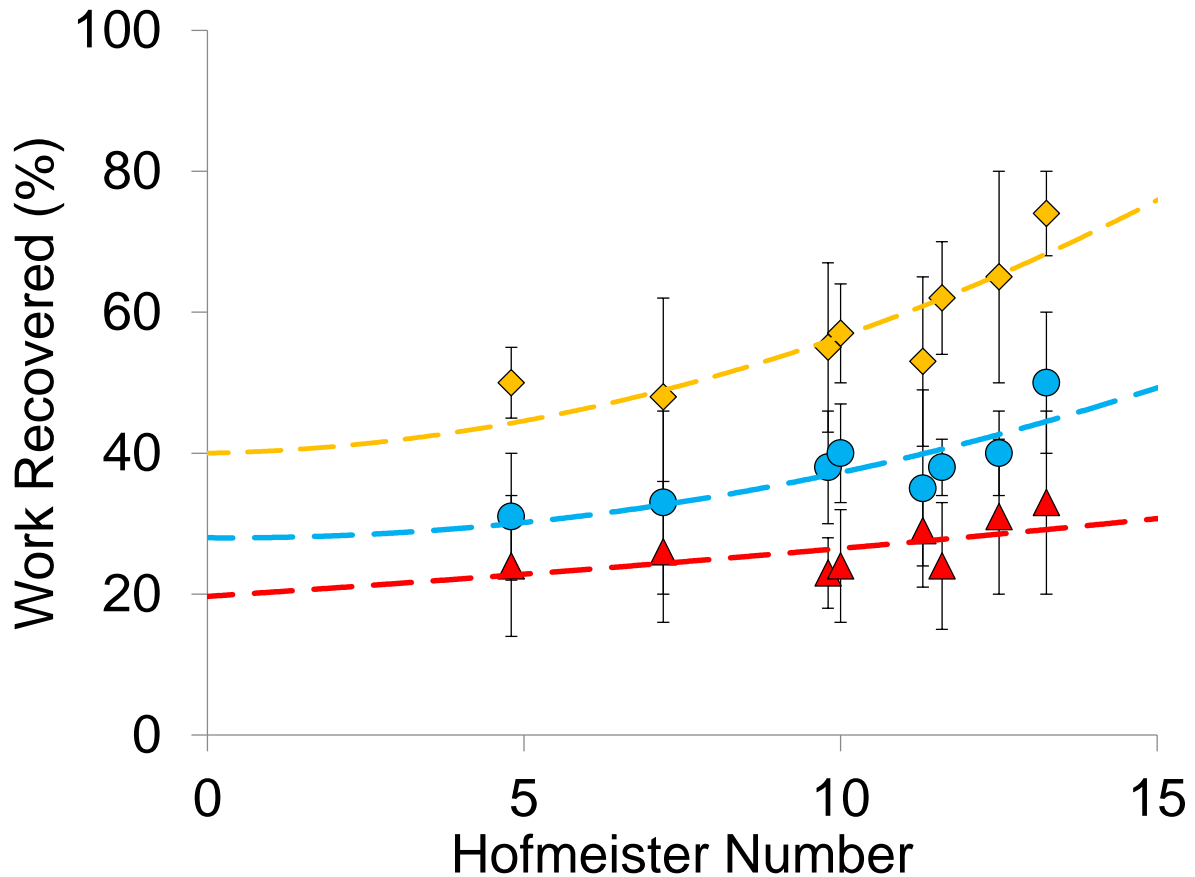
Fig. 16：**Percentage of work done recovered by 0.4% κ-carrageenan gels with 0.0269M potassium salt subject to 20% uniaxial strain after one (◆), two (●) and three (▲) compression cycles, as a function of potassium salt anionic Hofmeister number. Dashed lines are included for the purpose of guiding the readers' eye.**

Secondly, work recovered continues to decrease with the number of compression cycles, with the difference in work recovery between consecutive compression cycles decreasing each time (Fig. 16). Repeated work done on the system will continue to deform the network and displace polymer structuring and intermolecular binding from its initial equilibrium position prior to

deformation. For example a junction zone which may have been deformed irreversibly on the initial compression may be broken completely on the second compression, furthering energy dissipation with continued compression cycles.

The initial compression will cause the most disruption to the aggregate network; bending and deforming any weak points in the microstructure in order to facilitate the 20% compressive strain, the subsequent compression will therefore find less irreversible deformation is required, meaning less work dissipated on bond breaking, and the next compression cycle will find even less irreversible deformation is necessary, etc. Subsequent compression cycles may also start to compact the aggregate structure, which will increase the rigid attributes of the gel and support resistance to further applied force, reducing the relative difference in lost work each time. To this end, a decrease in work recovery between consecutive compression cycles is observed. Compression to 20% strain was selected as uniaxial compression investigations demonstrated that this strain exceeded the linear elastic region of deformation for all samples without initiating complete failure; allowing work recovery to be assessed over multiple cycles.

Finally, the work recovery is observed to exhibit a dependence on the Hofmeister number of the potassium salt anion present in the sample, increasing with Hofmeister number. Over repeated compression cycles however the distinction between different systems recedes (Fig. 16).

This observed behaviour trend in mechanical deformation relative to anion presence is not unlike that observed for initial stress relaxation $\frac{1}{k_1}$ where those κ-carrageenan aggregates in the presence of kosmotropic anions dissipated work stress faster than those in the presence of chaotropic anions. The explanation for that observed behaviour is equally applicable in this instance, in that the work recovery analysis is an indication of the aggregate brittleness, rather than its strength, and work recovery will depend upon the extent of inter-molecular bonding

between the aggregate domains; the more developed aggregates being fixed in position more than those of a less developed aggregate network, and subsequently for a predetermined strain (20% in this instance) the stresses placed upon the junction zones will be far greater in the former than the latter, and potential for work dissipation e.g. through bond breakage is greater.

As has been discussed already, the development of the aggregate will depend on the anion presence, which is believed to impact upon the structuring and availability of water molecules from the bulk phase, and their availability to stabilise the charged polysaccharide double helix. This will in turn affect the thermodynamic driving force towards aggregation, as the κ-carrageenan domain structures not stabilised in solution will look to stabilise themselves via aggregation; leading to more developed aggregate networks and intermolecular bonding in those systems where anions encourage bulk phase water structuring more, i.e. kosmotropic anions of higher charge density.

2.5. Conclusions

Trending behaviour of anion lyotropic effects upon microstructure and physicomechanical properties of κ-carrageenan aggregates has been established over an unprecedented range and number of Hofmeister values. The Hofmeister number valuation of the sorbate monobasic anion – which is presently unassigned – has been proposed at 10.4±0.15, supported by specific physicomechanical attribute trend fitting throughout. This value correlates well with those values of similar organic acid monobasic anions such as citrate$^-$ (7.2), tartrate$^-$ (7.4), and propionate$^-$ (9.8) [82], progressing a suggestive order of decreasing charge density with increasing Hofmeister number which would concur with those trends typically associated with the lyotropic series.

The structure and textural properties of κ-carrageenan aggregates may be predictably manipulated using lyotropy of monovalent anions - even at low (0.0269M) anion concentrations; via control of the bulk water solvent quality and subsequently associated polymer chain intermediate stability, as proposed by Grasdalen et al. [81]. Kosmotropic anions promote destabilisation of the intermediate in the second order aggregation mechanism, reducing the temperature of feasible association onset, and increasing the rate of junction zone formation between intermediates, driving the more stable quaternary structure, whilst chaotropes will indirectly support stabilisation of the intermediate therefore facilitating greater conformational ordering. This has been indicated by optical rotation and ultraviolet light scattering studies, in concurrence with those findings by Norton et al. [55]. Consequently, kosmotropes increase strength of the aggregate, confirmed in these studies by increasing resistance presented towards macroscopic failure and elastic potential energy storage capacity, although gels increase in brittle character as a consequence of increased solid structuring material, as has been demonstrated here using oscillatory rheology, initial stress relaxation rate and work recovery investigations. Correspondingly, chaotropes decrease aggregate physicomechanical strength as a result of reduced thermodynamic drive towards the quaternary aggregate structure, decreasing junction zone formation and subsequently increasing stress concentration and the propagation of failure.

Error - as indicated by error bars of one standard deviation either way throughout, is observed to be consistently low, which would suggest a good level of precision, most significantly in using parallel plate compression texture analysis as this highlights the potential for a more extensive application of this technique towards polymer aggregate physicomechanical studies, where alternative methods such as parallel plate rheology may suffer as a consequence of syneresis and slippage, for example.

Further work could look at verifying the assigned value for sorbate monobasic directly, and pursuing further the material and textural effects of other organic acid (potassium) salts which are FDA approved, for application in the food industry. Alternative composition parameters such as different or additional hydrocolloids should be investigated using the same analysis techniques to study further physicomechanical effects of altering the microstructure.

III

MODELLING PHYSICOMECHANICAL PROPERTIES OF K-CARRAGEENAN AND CROSS-LINKED WAXY MAIZE STARCH COMPOSITE GELS

3 Modelling physicomechanical properties of κ-carrageenan and cross-linked waxy maize starch composite gels

3.1. Abstract

Composites of segregated polymer blends comprising of swollen cross-linked waxy maize (XLWM) starch granules in a quiescent κ-carrageenan gel matrix have been prepared in the presence of different potassium salts of various anionic lyotropic character, and different salt concentrations. Respective partitioning of solvent was calculated using XLWM centrifugation swelling supernatant volumes of XLWM swollen granule solutions, and differential scanning calorimetry was performed in order to confirm neither κ-carrageenan and/or salt impeded the starch granule swelling. G' dependency upon polymer concentration was determined for solutions of XLWM starch and κ-carrageenan gel respectively via oscillatory rheology. Concentration dependencies were then combined with phase partitioning data in order to understand the contribution of either phase towards the composite strength and compare against ideal isostress and isostrain blending law models developed by Takayanagi.

Composite rheology conformed to the isostrain model, suggesting the starch granules behave as a soft filler relative to the continuous κ-carrageenan phase at effective concentration. Addition of XLWM increased aggregate strength within the elastic region of uniaxial compression, beyond which XLWM decreased the mechanical response.

3.2. Introduction

Combining multiple gelling biopolymers in a composite system provides greater variety in microstructure design and tailoring physicomechanical attributes, expanding potential for novel applications within the food industry such as controlling texture, water release, processing response and shelf life [52] [116]. The ability to specify the overall rheological and mechanical behaviour of composites by defining and controlling their individual microstructure systems and combined compatibilities makes these gel mixtures highly lucrative [62] [117].

Polymer blending laws conceptualised by Motowo Takayanagi [118] and later developed specifically for phase separated polymer gel systems [119-121] have previously been used to effectively model the contribution of either polymer phase to the overall rheological and mechanical behaviour of composites, and compare either individual phase to their respective single polymer 'simple' systems to highlight any interactions (direct or indirect) between the two polymers.

Starch composites with gelatin [122] , xanthan [123], and agarose [124] have been studied using Takayanagi's blending model, to explain mechanical response to deformation. Little work appears to exist applying these models to κ-carrageenan / starch composites however, with precursory investigations choosing to focus instead upon the viscoelastic composite properties [125] [126] [127], temperature dependant behaviour [128] [129], compatibility and gelation [127].

In the native form, starch exists as spherical granules, made up of crystalline and amorphous regions of amylopectin (cross linked) and amylose chains [130]; the relative proportions of which define the thermostability of the granule structure. Amylose is a straight chain polymer of D-glucose units, which will dissolve readily in water and leak from the starch granule,

95

undergoing retrogradation on cooling and gelling irreversibly [130] [131]. Amylopectin on the other hand is a branched polymer of D-glucose units which is less soluble in water; the cross linkages presenting a more structured organisation in the native form with increased polymer chain associations, and therefore more energy is required via heating in solution to allow the amylopectin chains to unfold [132], followed by stabilisation of the chains via water molecule polymer association mechanisms.

By chemical modification of starch, chain branching and amylopectin proportion per mass of starch can be increased, in order to improve granule structural durability during heating and gelatinization [133], whereby the crystalline helix regions of the granule unwind allowing the granule to swell in size, absorbing water in the process [95].   Absorption of water into the granule and away from the bulk aqueous phase is referred to as volume exclusion [128]; the other polymer essentially being 'excluded' from that volume of (water) solvent.

K-carrageenan is a sulphated charged polysaccharide able to form high viscosity gels even at low concentrations.   The negative charge of the $(1\rightarrow3)$-β-D-galactose-4SO$_3^-$$(1\rightarrow4)$-3,6,anhydro-$\alpha$-D-galactose alternating chains means it is highly responsive to ionic environment, particularly potassium salts [77]; the potassium cation facilitating junction zone formation between ordered helix domains resulting in aggregation [66] [70].

One particular characteristic associated with κ-carrageenan gels formed in the presence of potassium cations is the tendency for syneresis. Syneresis is the gradual expelling of water from the aggregate over time. Previous studies using light scattering analysis [134] have demonstrated that this behaviour is a consequence of tightening of the κ-carrageenan coils and reorganisation of the aggregate domains over time, as the polymer secondary and tertiary structures seek to achieve the lowest energy arrangement possible.   This characteristic understandably presents some considerable implications for the food industry and longevity of

processed foods, where unbound 'free' water can facilitate microbial growth [39, 40], transport of hydroperoxides and radicals [38], and undesirable interference amongst process reactions [36], as just a few examples.

A potential advantage of chemical modification of starch which has been highlighted [60, 61] is improved water retention over time, and subsequently addition of modified starch to κ-carrageenan aggregate gels to form a mixed polymer composite is suggested as a potential pacifier for the pragmatic water loss behaviour. This can be expected however, to convey implications for the physicomechanical properties of the overall material.

Whilst potassium is well established as the overriding group I cation facilitating quiescent κ-carrageenan gel formation [89, 135, 136], it is the anionic dependency of κ-carrageenan [55] [85] [90] and starch [137] [138] however – depending on the potassium salt added – which provides a fine control by which the final properties of either polysaccharide may be modified, and a central focus in this investigation.

The aim of this study is to apply these isostrain / isostress polymer blending laws to κ-carrageenan / swollen starch granule composites via rheological investigations and conclude how and why the individual phases behave in order to achieve the final composite material properties, and then apply this understanding to the composite behaviour under uniaxial deformation, both at low strains (<10%) and high strains (approaching / at point of failure). Particular interest shall be made towards the effects of potassium salt anion and concentration.

3.3. Materials & Methods

3.3.1. Materials

All samples were prepared by first dissolving K-carrageenan (*Eucheuma Cottonii*, M_W 600-700 kDa, E407A EU specification processed, propan-2-ol washed, cat no.22048, Sigma Aldrich, Gillingham, UK) in deionised water (Aquatron A4000D, Stuart, Staffordshire, UK) at 80˚C under continued mixing using a hot plate stirrer (Stuart, Staffordshire, UK), before adding potassium salts as appropriate. Potassium citrate monobasic, potassium sorbate, potassium chloride and potassium iodide were of analytical grade (Sigma Aldrich, Gillingham, UK). Cross linked waxy maize (XLWM) starch was kindly donated by Ingredion Incorporated (Westchester, IL, USA). Amylopectin fraction of the starch was 99% minimum by mass and acetate stabilized, as declared by manufacturer. Mixed polymer solutions were obtained by preparing separate XLWM starch and κ-Carrageenan solutions of 400ml at twice the required final concentrations (specified in text) before mixing. Mixtures were sealed and then held for 1 h in a water bath at 80°C with occasional gentle stirring using a magnetic stirrer. Materials used were given no further purification or modification of their properties.

Temperature in preparation of all solutions containing XLWM specifically did not exceed denaturing temperature (90°C) of starch granules, and therefore it has been rationalised that they retained a swollen granular structure.

3.3.2. Rheology

Oscillatory tests were performed using a Kinexus rheometer (Malvern, UK) fitted with a Ø60mm roughened parallel plate geometry. XLWM/κ-Carrageenan mixtures were loaded onto the rheometer at 60˚C and a silicon oil water trap applied to the periphery to reduce water loss via evaporation. Samples were then cooled to 5˚C at 1.0 K.min^{-1}, under a constant shear strain

of 0.5% at 1.592 Hz, where they were held for 5 minutes before taking final G' values. Measurements of storage modulus were taken throughout the experiment.

3.3.3. Starch Swelling

Aliquots (~25g) of the XLWM/κ-Carrageenan paste at 80˚C were placed into 50-ml centrifuge tubes then cooled to ambient temperature for 30 minutes. Samples were centrifuged at 4000g for 1hr. Phase volume was estimated by weighing the supernatant and sediment following centrifugation (4000g; 25˚C; 1hr) of gelatinised solution, performed using a Sigma 3K30 refrigerated centrifuge (Sigma, UK). Supernatant and sediment were weighed immediately after centrifugation.

Centrifugal force of 4000g was employed; taken from affiliated literature reports [123] [124]. 4000g was used here as a compromise; it was important to extract maximum free water, whilst water 'squeezed out' of swollen granules should be kept at a minimum for accuracy. Experiments were performed 6 times and results averaged.

3.3.4. Micro Differential Scanning Calorimetry

Thermal analysis of starch/κ-Carrageenan was carried out using μDSC3evo calorimeter (Setaram, France). Approximately 600mg of sample was used each time, using deionised water as a reference. Loading of the DSC cell varied depending on the sample. In the case of starch alone, samples were loaded at room temperature and allowed to equilibrate at 5˚C for 20 minutes. Those solutions containing K-carrageenan alone pipetted into the stainless steel cell at 60˚C, before cooling to ambient temperature, upon which point the DSC analysis cycle was started.

Finally, in the case of bipolymer mixed systems, K-carrageenan / salt solution was prepared as before, then cooled to 50˚C (below starch gelatinisation temperature) before adding XLWM. Samples were loaded at 50˚C and allowed to equilibrate at 5˚C for 20 minutes. In all cases after equilibration, temperature was then raised from 5˚C to 85˚C at heating rate of 0.1∘C/min and held for 20 min before cooling back down to 5˚C at 0.1∘C/min.

Peak enthalpies were normalised to the weight of polymer (i.e. non-water) material in each sample using the following equations 1-3.

$$Mass\ of\ Polymer = Total\ Mass\ of\ Sample\ \times \%\ Concentration\ of\ Polymer \quad (1)$$

$$Enthalpy\ of\ Transition^* = \frac{Peak\ Energy}{Total\ Mass\ of\ Sample} \quad (2)$$

$$Enthalpy\ of\ Transition^{**} = \frac{Energy\ of\ Trans.\,(g^{-1}\ sample)}{Mass\ of\ Polymer} \quad (3)$$

$*\ normalised\ against\ mass\ of\ sample$

$**\ normalised\ against\ mass\ of\ polymer$

As an example, if we are studying a sample of 2% XLWM starch solution weighing 0.589g, and the DSC trace exhibits an endotherm peak attributed to XLWM starch granule swelling of energy 0.67J:

$$Mass\ of\ XLWM = 0.589\ \times \frac{2}{100} = 0.01178g$$

$$Enthalpy\ of\ Transition^* = \frac{0.067}{0.589} = 0.114\ J.\,g^{-1}_{sample}$$

$$Enthalpy\ of\ Transition^{**} = \frac{0.114}{0.01178} = 9.677\ J.\,g^{-1}_{XLWM}$$

3.3.5. *Large Scale Uniaxial Compression Studies*

Mixed polymer hot solutions were poured into Ø20mm x 20mm moulds and stored at 5˚C for 24 hours. Cylindrical gelled samples were then loaded onto a TA.XT.plus® Texture Analyser (Stable Micro Systems, UK) with a 5kg load cell and a cylindrical head geometry (Ø40mm) and compressed 15mm (75% strain) at 0.2 mm.s^{-1}. A force trigger of 0.04903N was used.

Force/distance data taken directly from the texture analyser was converted into true strain ε_H and true stress σ_T using equations 4-7, where ε_E and ε_H are the engineering and true strain, σ_E and σ_T are the engineering and true stress, H_0 and A_0 are the initial height and cross sectional area of the sample, and F and h are the force applied and the height of the sample [99].

$$\varepsilon_E = \frac{(H_0 - h)}{H_0} \tag{4}$$

$$\varepsilon_H = -\ln(1 + \varepsilon_E) \tag{5}$$

$$\sigma_E = \frac{F}{A_0} \tag{6}$$

$$\sigma_T = \sigma_E(1 + \varepsilon_E) \tag{7}$$

Young's modulus, bulk modulus, and work done at total failure values were determined [100] [102] [101]. Stress at total failure was also recorded. No barrelling was observed in κ-carrageenan / XLWM starch mixed systems (Fig. 17), indicating an absence of frictional forces perpendicular to compression between the gel and the plate, and subsequently lubrication was not required. Experiments were performed to 10 repeats and averaged.

Fig. 17: κ-carrageenan / XLWM starch mixed system gelled sample undergoing compression up to and including failure.

3.3.6. *Visual inspection of gels for syneresis*

Two solutions, one of 0.4% K-carrageenan in the presence of 0.0269M potassium sorbate and 2% XLWM starch, and another analogous solution however this time omitting starch, were prepared and poured into Ø20mm x 20mm moulds, sealed as for texture analysis, and stored at 5˚C for 7 days after which they were visually inspected and compared for surface water. Head space of the mould lid was lined with cotton wool so as to minimize distortion of the results as a consequence of condensation, with care taken to ensure the liner did not come into direct contact with the composite. Twelve samples of either solution were prepared for comparison.

3.4. Results & Discussion

3.4.1. Visual Inspection of Gels for Syneresis

Samples containing starch were observed to be light grey and opaque in appearance, whereas samples without starch were colourless and transparent. Both sets of samples formed an odourless, quiescent, firm, free standing gel. Surface texture of both was moist, and shiny in appearance. Shrinkage from the walls of the container was observed in all samples without starch, down to approximately 90% of the original size (i.e. 10% sample diameter lost), comparatively those samples with starch shrank less, with only 3 samples out of the 12 reaching the same degree of size reduction. Expelled water was observed in all those samples without starch, and whilst expelled water was still observed in 10 of the 12 samples containing XLWM starch it was approximately half the volume of that found in samples without starch. These observations indicate that addition of XLWM starch does indeed increase the water retention of composites in comparison to the respective K-carrageenan aggregates, although syneresis is not entirely eliminated, indicating reorganisation of the K-carrageenan aggregate domains is still occurring; helical tightening contributing toward the gel shrinkage observed [134].

3.4.2. Starch Swelling

Native starch exists as semi-crystalline granules that are insoluble in cold water. The granule loses its native crystalline structure upon heating and the granule swells. The transition temperature is specific to the type of starch, in high water concentration conditions this is referred to as the gelatinisation temperature (under lower water concentrations it is referred to as the melting temperature) [139] [140]. The physical consequences of this structural transformation have been studied here in the swelling studies, and the energies accompanying the transformation are studied later in the DSC studies.

The material behaviour and rheology of polymers and their gels formed are polymer concentration dependant and, subsequently, so is the macrostructure of any mixtures formed. Therefore, it is necessary first to establish what proportion of the total water in the system either polymer (starch and κ-carrageenan) occupies and how this varies with starch and salt concentration; the effects of which we are investigating in this study - and thus determine the effective concentration of starch grains and κ-carrageenan. Rheological studies of composite mixed biopolymer systems may then be related to the rheology of either phase at its effective concentration.

$$\phi_{mXLWM} = \frac{m_{total\ sample-(m_{XLWM}+m_{supern.})}}{(m_{sample} - m_{XLWM})} = \frac{m_{water}\ in\ starch\ granules}{total\ m_{water}} \tag{8}$$

$$\phi_{XLWM} = \frac{m_{XLWM}}{\rho_{water}} = \frac{m_{XLWM}}{0.99704} \tag{9}$$

Equations 8 and 9 demonstrate how the starch phase water volume fraction was determined from the weighing values, here Φ_{mXLWM} is the calculated starch phase water mass fraction, Φ_{XLWM} is the calculated starch phase water volume fraction, m_{sample} is the mass of the whole sample, m_{XLWM} is the mass of XLWM starch dissolved in the solution, and $m_{supern.}$ is the mass of supernatant tipped off following centrifugation, and ρ_{water} is the density of water in g.ml^{-1}.

Although starch and K-carrageenan are not expected to interact directly [128] [127], K-carrageenan inclusion will inhibit starch swelling via indirect means. The rate of water molecule migration from the bulk phase into the starch granule is defined by the osmotic gradient. Water is a polar molecule, and subsequently its behaviour will be effected by the presence of charged particles and ions.

The K-carrageenan polysaccharide chains comprise of a series of negative charged regions, and subsequently polar water molecules will move toward and hydrate the chains in order to stabilise them. These water molecules are subsequently not 'free' (here referring to 3 hydration sphere diameters of separation) and therefore less water is freely available for diffusion into the starch granules than if there were no K-carrageenan present, and this factor will oppose osmotic gradient towards water diffusion into the starch granules. The degree to which this will effect starch granule swelling however, is uncertain.

Fig. 18: Starch Phase Volume Fraction dependency on Starch concentration for sample containing 0.0269M of K(sorbate) (◊) and 0.0269M K(citrate) (×) starch and potassium salt solutions, and their corresponding mixed solutions with 0.1% K-carrageenan (Δ and □ respectively). Solutions centrifuged at 4000g for 1 hr, Starch Phase Volume Fraction determined by weighing supernatant and applying Equation 8 & 9. Studies performed at 25°C, n=6.

The starch phase volume with concentration in both pure starch and mixed starch / κ-carrageenan solutions is shown (Fig. 18). In the case of all starch solutions, phase volume fraction absorbed by starch granules was observed to increase linearly with starch concentration in the system. Starch phase volume fraction (Fig. 18) demonstrates no difference upon addition of 0.1% K-carrageenan outside of one standard deviation represented by the error margins shown. It is therefore concluded K-carrageenan effects upon starch swelling are negligible for the range of concentrations studied here [127, 141]. Subsequently, starch phase volume fractions for mixed systems shall be assumed equivalent to those determined from corresponding pure starch-salt solutions, and that therefore XLWM granule swelling behaviour in mixed systems is tantamount to that in corresponding pure starch-salt solutions, as has been similarly employed in previous consubstantial biopolymer studies, e.g. with agarose [124]. Salt type, and concentration, is known to affect both K-carrageenan structure (see Chapter 2.0) and starch swelling in accordance with the Hofmeister Series [85] [55].

In starch systems, increasing Hofmeister number of anions present increases starch swelling, and decreases gelatinization peak temperature [142] [137]. Anions of low Hofmeister number; kosmotropes, or 'salting-out' anions, have a greater charge density and interact more with polar water molecules in the bulk phase than those of higher Hofmeister number; chaotropes, or 'salting-in' anions [115] [108]. Water molecule attraction and binding to the kosmotropes in the bulk phase is therefore strong according to ligand binding theory [79], and this leads to water hydrating the kosmotropic anions preferentially to other, less charge dense, ions or molecules present in solution: the water molecules in the bulk phase are now more structured, as the dipole interactions amongst the bulk phase are now stronger than they would have been without the ions which would be an accumulation of hydrogen bonding and van der waals forces [143] [144]. Water molecules will require more energy to overcome bulk interactive forces and migrate from the bulk phase to stabilise the amylopectin (or amylose) chain, and

this provides reasoning for the trend in increasing starch gelatinization peak temperature with lower anionic Hofmeister number. The inverse is true for chaotropic anions, (being less charge dense) the water-water associations will be stronger than chaotrope-water associations and therefore water molecules in the bulk phase will not be impeded from migrating to hydrate the polysaccharide chains.

Hydrophobic regions on the branched amylopectin chains in the native starch granules will associate with one another in order to stabilize the polysaccharide. Sufficient water molecule availability and applied thermal energy is understood to be able to create ordered water molecule 'shells' about polymer chain hydrophobic patches by tight packing and ordering [108], stabilising them in solution. This will result in a small decrease in enthalpy, and large decrease in entropy of association at these points, causing Gibbs' free energy to increase, thus lowering the polymer-bulk solvent interfacial energy, facilitating dissociation of the amylopectin interconnections, and subsequently the granule structure will increase in flexibility, and allow greater swelling capacity and granule gelatinization. Via this mechanism therefore, those (chaotropic) anions which promote the disruption of bulk phase water structuring can increase the starch phase volume fraction (and vice versa for kosmotropes). The effects of increased starch swelling may be seen in the viscosity and G' of the respective starch gels which we will come to later, as increased swelling in the presence of high Hofmeister numbers leads to less 'free' water in the bulk phase and thus increased viscosity and G' [142].

Fig. 19 shows the relationship of XLWM starch phase volume fraction (and thus starch swelling capacity) with XLWM starch concentration in the presence of Potassium chloride, sorbate, citrate and iodide monovalent salts individually. Starch phase volume fraction exhibited no dependency upon anionic Hofmeister number (Fig. 19a) and K(sorbate) concentration (Fig. 19b) outside of the boundaries of one standard deviation shown.

Fig. 19: Starch Phase Volume Fraction dependency on XLWM Starch concentration for starch-salt solutions in the presence of (a) K(sorbate) (◊), K(citrate) (○), KI (□) and KCl (Δ) at 0.0269M concentration, and (b) 0.0135M (×), 0.0269M (◊), 0.0404M K(sorbate) (+).

Observed starch swelling independency from salt concentration is believed to be a result of the low salt concentrations used, as previous studies where starch swelling dependency on ionic presence has been reported have employed anionic concentrations in the region of a factor of ≈10 higher [142], and as starch swelling is known to be dependant of anionic concentration [137] it is deduced that ionic concentrations used here are simply not high enough to distinguish between different anions via weighing of supernatant alone.

Starch phase volume fraction increases linearly with starch concentration and with good reproducibility. Mean water volume taken up per mass of starch was calculated using equations 10-12, where $m_{water\ in\ granules}$ is the mass of water remaining in the granules after centrifugation, $m_{water\ p.\ mass\ XLWM}$ is the calculated mass of water remaining per gram of XLWM starch, $V_{water\ p.\ mass\ XLWM}$ is the calculated volume of water remaining per gram of XLWM starch.

$$m_{water\ in\ granules} = m_{sample} + \left(m_{XLWM} + m_{supern.} \right) \tag{10}$$

$$m_{water\ p.\ mass\ XLWM} = \frac{m_{water\ in\ granules}}{m_{XLWM}} \tag{11}$$

$$V_{water\ p.\ mass\ XLWM} = \frac{m_{water\ p.\ mass\ XLWM}}{\rho_{water}} = \frac{m_{water\ p.\ mass\ XLWM}}{0.99704} \tag{12}$$

Mean water volume absorbed per gram of XLWM starch granules was calculated at 12.153ml.g_{XLWM}^{-1} ±0.282. This value correlates with those from literature for cross-linked waxy maize starch; 9.0 ml.g^{-1} [122], 10.4 ml.g^{-1} [145], although it is marginally higher even with standard deviation bounds considered; understood to result from bulk (i.e. not in XLWM granules) water remaining in the starch sediment following tipping, which would also

contribute towards a greater standard deviation in data in mixed systems, observed in the increased error bounds for those mixed systems in Fig. 18 compared to their corresponding XLWM starch solutions. Alternatively, this value may be accurate and the deviation simply originates from variation in the XLWM starch. Because standard deviation range is less than 5% of the calculated value $\left(\frac{0.564}{12.153}\right) = 0.0464 = 4.64\%$ this study shall proceed upon the latter assumption.

3.4.3. Thermal Analysis

Differential scanning calorimetry (DSC) is used to detect the transition in single or mixed polymer systems with changes to polysaccharide interactions usually manifesting themselves by distorting the peaks of the individual gels and generating a new thermal event.

Solutions of 0.4% κ-carrageenan, and slurries of 2% XLWM starch in 0.4% K-carrageenan solution were prepared separately in the presence of 0.0269M potassium sorbate, citrate, iodide and chloride salts, as well as lower (0.0135M) and higher (0.0404M) K(sorbate) concentrations. Slurries with the omission of K-carrageenan and salt were also included as a reference, μDSC traces are shown (Fig. 20). No distinction was observed between the endotherm traces for κ-carrageenan solution nor XLWM slurries against the corresponding endotherms in the respective XLWM κ-carrageenan mixed slurries, and subsequently these have been left out. No distinction between μDSC traces for XLWM κ-carrageenan slurries in the presence of 0.0269M K(sorbate), 0.0269M K(citrate) and 0.0269M KCl was observed, therefore represented by 0.0269M K(sorbate) μDSC trace shown (Fig. 20e).

Fig. 20: μDSC heating traces for (a) 2% XLWM starch slurry, and 2% XLWM slurry with 0.4% κ-carrageenan in the presence of (b) no added salt, (c) 0.0269M KI, (d) 0.0135M K(sorbate), (e) 0.0269M K(sorbate), and (f) 0.0404M K(sorbate). Heat flow is relative as indicated on graph, as traces have been separated for visibility.

DSC studies displayed two endotherms; corresponding to either polymer present. The first, observed in all traces (Fig. 20) at higher temperatures around 65°C and correlates to the disordering of the amylopectin crystalline structure [146] [147]. This is caused by amylopectin crystal melting (gelatinisation), allowing water absorption from the free water phase into the swelling starch granules. As a result less free water resides in the bulk phase, the starch solution will exhibit decreased liquid-like flow behaviour, and solid attributes of the system will increase , i.e. shear elastic modulus G'. DSC traces displayed gelatinization endotherm for amylopectin crystal structure gelatinisation, indicating starch granule swelling has occurred to completion [139].

A second endotherm is observed at lower temperatures, between 40-55°C, exhibited only in the presence of salt and κ-carrageenan. This corresponds to κ -carrageenan melting, whereby the cation mediated junction zones holding the aggregate are overcome via thermal energy transfer in order to revert them back to a random coil domain via a reversible transformation [74].

Peak temperatures for aggregate dissociation (T_{K-C}) and starch granule gelatinization (T_{XLWM}) in XLWM / K-carrageenan mixtures exhibited no distinction from those corresponding peaks in K-carrageenan salt-solutions, and XLWM slurries respectively; starch does not directly affect K-carrageenan aggregate dissociation transformation energy, and vice versa for starch gelatinisation, therefore concluding that XLWM starch and κ-carrageenan do not associate via direct interaction.

T_{K-C} showed minimal anion dependency, ranging from 47~50°C (Fig. 20c & Fig. 20e) – 0.0269M K(sorbate) trace representative also of corresponding K(citrate) and KCl systems. Anionic presence exhibits little impact on aggregate dissociation temperature at the concentrations used here.

Peak temperatures for starch granule gelatinization (T_{XLWM}) in XLWM / K-carrageenan salt-solutions are higher ($\approx$64-65°C) than that of (Fig. 20a) without added salt ($\approx$62°C). Comparing XLWM starch solution endotherm (Fig. 20a) to XLWM solution endotherms in the presence of alternative salts and salt concentrations (Fig. 20b-e) indicates this effect is due to the addition of salt.

Metal cations such as K^+ have previously been observed to affect the gelatinization temperature of starch granules; increasing it at lower salt concentrations, as has been observed here [138] [138, 142] [143] [148]. This observed effect is understood to be the cumulative effect of a number of mechanisms, which impact upon T_{XLWM} in opposing ways.

In one instance, electrostatic association with hydroxyl groups on starch will occur, the cation being a positively charged ion and the hydroxyl group being a good electron donor base group [79] [59], this disrupts the structure of the granule, and the electron densities have now shifted towards the cation. The starch polysaccharide branched chains would then carry an overall positive charge, and subsequently water molecules from the free water bulk phase will be more inclined to migrate towards the polysaccharide chain in order to hydrate and stabilise it; the oxygen atom on the water molecule being a good electron donor, this will impact upon the osmotic gradient in favour of polymer solvation, facilitating gelatinization at lower temperatures.

Opposing the above mechanism, in a similar mechanism to the kosmotropic anions, cations will seek stabilisation via direct hydration by water molecules. The potassium monovalent cation carries a high charge density, and therefore water molecules will interact strongly with it, preferentially to the polysaccharide chain of lower charge density [79] and will improve water structuring [143] [115]. Subsequently this will increase the energy boundary which must be overcome by water molecules in order to solvate the starch granules, and the osmotic

gradient is shifted less in favour of polymer solvation. As a result the polymer-solvent interfacial energy is now increased.

It would appear that this later mechanism is the dominant factor in these results here at these relatively low salt concentrations, as we observe T_{XLWM} to increase overall with salt concentration − water requiring more kinetic energy to overcome the potential barrier and migrate towards the starch granules. Whilst kinetic studies have not been included in this investigation here, reasoning for the water structuring mechanism being dominant may stem from the increased mobility, availability, and population of water molecules in comparison to starch hydroxyl groups, which will allow them to move towards, hydrate, and stabilise the cations faster.

The fact T_{XLWM} values are comparable in the presence of all potassium salts suggests that T_{XLWM} bears little dependency on anion lyotropic properties in these results here - although this is known not to be the case at greater concentrations where the impact of anionic charge density difference is observed due to changes in 'free' water structuring [137]. Rather, this marked change in T_{XLWM} is a result of general ionic salt presence and not specific anionic lyotropic properties. However if we consider the energies accompanying these peaks, a fine level of lyotropic distinction may be highlighted.

A change in the starch gelatinization enthalpy was observed with the addition of salt. In all cases - save for in the presence of Iodide, ΔH_{XLWM} increased, where as in the case of Iodide anions a marginal decrease was observed (Table 2). In general, salt effects on starch gelatinization follows the Hofmeister lyotropic series, particularly that of anions [59]. Salt ions are capable of influencing structure making / breaking effects of water in starch gelatinization.

Starch hydroxyl groups exhibit weak acid dissociative behaviour, according to Equation 13, thus rendering the starch chain with a partial negative charge, and the aqueous bulk phase with

a partial positive charge [149]. Those kosmotropic anions with a higher negative charge density are believed to remain in the bulk aqueous phase therefore, and influence starch granule gelatinization indirectly.

$$Starch - OH \leftrightarrow Starch - O^- + H^+ \qquad (13)$$

Salt	[Salt] (M)	[κ-C] (%)	Enthalpy (J.g^{-1})	σ (J.g^{-1})	T$_{PEAK}$ (°C)	T$_{ONSET}$ (°C)	T$_{OFFSET}$ (°C)
-	0	0	9.6	0.85	62.4	54.1	67.9
-	0	0.4	10.1	0.69	62.3	54.0	68.0
K(Sorbate)	0.0269	0.4	11.7	2.00	64.3	59.0	69.8
K(Citrate)	0.0269	0.4	12.6	3.34	64.7	59.7	70.2
KCl	0.0269	0.4	11.4	2.96	64.5	58.4	69.5
KI	0.0269	0.4	9.2	3.13	64.6	59.4	69.6
K(Sorbate)	0.0135	0.4	9.4	1.99	63.8	58.1	69.0
K(Sorbate)	0.0404	0.4	13.6	2.62	64.8	60.8	70.3

Table 2: Data for XLWM starch swelling endotherms with 2% XLWM starch in 4% K-carrageenan solution in the presence of varying potassium salt anions and concentrations. Peak enthalpy has been normalised with regards to the amount polymer.

Chloride, sorbate and citrate anions exhibited similar lyotropic effects. The monobasic sorbate anion does not carry an officially assigned Hofmeister number, however previous work by the author assigned a value of 10.4±0.15. Chloride and citrate monobasic anions carry Hofmeister

numbers of 10.0 and 7.2 respectively). They carry lower Hofmeister valuations than iodide (Hofmeister number 12.5) and subsequently are considered more kosmotropic than iodide, which is considered chaoptropic.

Comparatively therefore, chloride, sorbate and citrate anions interact with and structure the polar water molecules in the bulk phase more; worsening the solvent quality of the bulk phase [59, 137] [150], than iodide anions, which will inversely disrupt water molecule structuring in the bulk phase due to its lower charge density, as per mechanisms previously discussed.

Subsequently, bulk phase water in the presence of more kosmotropic chloride, sorbate and citrate anions will require increased energy to overcome the bulk phase structuring interactions and migrate to the starch granules where water molecules support gelatinisation of the starch cystalline structure, separating chains into amorphous form and instigating granule swelling. The energy required to overcome bulk phase structuring interactions will be less in the presence of iodide anions, as these will decrease the order and quality of water structuring interactions.

The result of this is an increase in the endothermic peak attributed to starch gelatinization [138] (Table 2) in the presence of those kosmotropes stimulation bulk phase water structuring interactions.

Under these conditions and concentrations employed ΔH_{XLWM} was comparable in the presence of chloride, sorbate and citrate, indicating no marked difference in starch gelatinization in the presence of these anions here.

0.4% K-carrageenan solutions and 2% XLWM starch in 0.4% K-carrageenan solution slurries were then prepared in the presence of 0.0135M (Fig. 20d) and 0.0404M (Fig. 20f) potassium sorbate, to assess the impact of salt concentration. As previously reported by [142], those effects on ΔH_{XLWM} observed on addition of salt (in this instance, K(sorbate)) increased under higher salt concentrations; ionic presence was greater and thus water availability to the granule

reduced, and vice versa in the instance of lower salt concentrations, having a less marked change from the control (Fig. 20).

$T_{\text{K-C MELTING}}$ exhibited direct dependency upon salt concentration (Fig. 20d & Fig. 20f), as is to be expected [69] [151]; increased cationic concentration may facilitate a greater number of junction zones in aggregate formation which subsequently must be overcome on dissociation, and will therefore require a greater overall thermal input; the reverse being true for lower salt concentrations. T_{XLWM} dependency upon changing salt concentrations was small, this may have been a result of the concentration range having been too narrow, or speculatively, that the chosen increased concentration had initiated an increase and a subsequent drop in T_{XLWM} that has been observed with higher cation concentrations [143]. Therefore it may be concluded that changing salt concentration bears little control on starch granule swelling behaviour for the concentration range studied here.

3.4.4. Composite Phase Partitioning

3.4.4.1.   Determination $G'_{\text{K-C}}$ dependency on K-carrageenan concentration

Rheology is an effective method of studying the temperature course dependence of polymer solution gelation; typically via low frequency constant shear oscillation under a linear temperature ramp, allowing the gelation temperature and final shear storage behaviour to be studied and compared between polymer systems [152].

A typical temperature course of G' taken from these studies is shown in Fig. 21. G' initially gave no response on cooling from 60˚C for all the polymer systems studied, until T_{gel} (ascertained in the thermal analysis), after which point G' rose very rapidly before reaching a final asymptotic level, due to positive order kinetics of self-assembly (cross-linking) and the requirement for a minimum number of cross-links per 'chain' at the gel point [152]. This final

G' value, taken after 5 minutes of temperature equilibration at 5˚C, was recorded and compared in the following studies.

Fig. 21: An example of original data displaying G' temperature course dependency for 0.4% κ-carrageenan 1% XLWM Starch solution with 0.0269M K(sorbate).

Anion lyotropic attributes will exhibit a control upon K-carrageenan aggregate formation; inhibiting aggregate junction zone formation between domains in the presence of more chaotropic environments with anions of higher Hofmeister number. The physicomechanical properties of the κ-carrageenan gel will reflect this, exhibiting reduced strength and yield stress, as demonstrated earlier (Chapter 2.0). Increasing salt concentration will increase the number of junction zones and aggregation, whilst also increasing syneresis and gel setting speed [85] [55].

G' dependency on K-carrageenan concentration in pure K-carrageenan systems was determined in the presence of a range of K(sorbate) concentrations (Fig. 22a) and in the presence of 0.0269M K(sorbate), K(citrate) monobasic, KCl & KI salts (Fig. 22b).

Data fitted the power law to >98% confidence in all cases, with R^2 values of 0.989, 0.991, 0.994, 0.995, 0.996 and 0.995 for systems with 0.0135M K(sorbate), 0.0269M K(sorbate), 0.0404M K(sorbate), 0.0269M KCl, 0.0269 KI and 0.0269M K(citrate) respectively.

By plotting these values using a power law model (Equation 14 & 15), the relationship between G' and K-carrageenan concentration could then be quantified, where *a* and *b* are constant and have thus been quantified experimentally for each salt environment, $c_{K\text{-Ceff}}$ is the effective concentration of K-carrageenan in its phase, and G' is the shear storage modulus of the K-carrageenan gel.

$$y = ax^b \tag{14}$$

$$G' = a.c_{K-ceff}^{b} \tag{15}$$

Within this relationship, constant *a* represents the gradient of the linear relationship between the effective concentration of K-carrageenan and G' of the aggregate. It represents dependency coefficient of the elastic shear modulus of the system upon concentration of polymer present, and is equal to the true G' at $c_{K\text{-Ceff}} = 1$.

Constant *b* refers to the polymer aggregation exponent, and how (non-)linear the relative dependency of G' upon polymer concentration is. The closer *b* is to 1, the more linear it is, i.e: doubling K-carrageenan concentration will approximately double aggregate shear elastic

modulus. The greater b is than 1, the less linear the relationship will be. For power law relationships, G' will display reduced dependency (relative to the linear relationship) at low polymer concentrations, and higher dependency at higher K-carrageenan concentrations. The greater the power, the more this effect is observed. Experimental values for constants a and b are shown (Table 3).

Salt	[Salt] (M)	a (Pa^{-1})	b
K(Sorbate)	0.0269	1903.1	2.05
K(Citrate)	0.0269	2840.4	2.12
KCl	0.0269	2471.3	2.08
KI	0.0269	1568.3	2.77
K(Sorbate)	0.0135	1383.8	2.58
K(Sorbate)	0.0404	2688.6	1.86

Table 3: Experimental values for a and b constants in the power law relationship between G' and polymer concentration, for K-carrageenan solutions in the presence of potassium salts.

Fig. 22: G' dependency on K-carrageenan concentration with (a) 0.0135M (×), 0.0269M (◊) and 0.0404M (+) K(sorbate), and (b) 0.0269M K(sorbate) (◊), K(citrate) (○), KCl (Δ) and KI (□).

Constant *a* increases with increasing concentration of K(sorbate) present, and decreasing Hofmeister number (kosmotropic character) of anion present. This would indicate elastic shear modulus of the K-carrageenan aggregate is more dependent upon polymer concentration under higher salt concentrations, and in the presence of anions of more kosmotropic character.

Constant *b* decreases (closer to 1) with increasing concentration of K(sorbate) present, and decreasing Hofmeister number (kosmotropic character) of anion present. This would indicate that elastic shear modulus of the K-carrageenan aggregate only starts to show considerable dependence upon polymer concentration at higher (compared to the respective linear model) concentrations of polymer, for systems of lower salt concentration, and in the presence of chaotropic anions.

Shear elastic modulus (G') of K-carrageenan aggregates will be defined by the number and size of cross links between polymer aggregate domains. As K-carrageenan concentration is increased, so more polymer material is present, which may then associate, form double helices, and domains, which may then be stabilised and interconnected at junction zones in the presence of cations. The higher the polymer concentration, the more material there is available for aggregate network growth. Increasing *a* with salt concentration and kosmotropic character simply reflects the increased aggregation stabilisation in these conditions; the thermodynamic drive for stabilisation via aggregation of K-carrageenan double helices is greater as the solvent potential of the bulk phase is decreased (Chapter 2.0), therefore a larger proportion of the polymer available will be forced towards aggregation, and G' exhibits a greater dependency upon polymer concentration.

Constant *b* is arguably even more interesting, as it represents how the influence of K-carrageenan concentration upon G' changes as it (concentration) increases. The aggregation of K-carrageenan double helices is understood to be dependent on both polymer [153] and K^+

[66] concentration. Chaotropes will break up water solvent structuring, facilitating their movement towards the polysaccharide chains to hydrate and stabilise them. Polymer self-stabilisation by aggregation is therefore less thermodynamically favourable.

Concerning reaction kinetics, low concentrations of polymer will decrease the probability of one polymer chain coming into contact with another polymer chain. At low polymer concentrations association and junction zone formation is therefore exponentially less probable as there is neither sufficient thermodynamic drive nor rate of incidence. Hence at low concentrations those chaotropic anions and low salt concentrations carry higher values for constant b as the power factor is greater, as they have little thermodynamic drive towards formation of the aggregate at such low concentrations, therefore G' displays less dependency for early increase in K-carrageenan concentration.

By continuously increasing K-carrageenan concentration, this will in itself decrease the solvent potential. Chaotropes are of a finite concentration in the solution, and therefore the water made available via structure breaking will only be able to successfully stabilise a finite amount of polymer in solution, therefore eventually a critical polymer concentration will be reached where junction zone formation becomes more thermodynamically favourable and aggregation increases with polymer concentration, this explains the late rise in concentration dependency of G' associated with the relationships of higher power order; b.

Inversely, kosmotropes will stabilise water in the bulk phase, reducing its solvent potential for stabilising the K-carrageenan polysaccharide chains. They now are thermodynamically driven towards association with other K-carrageenan chains even at low polymer concentrations in order to stabilise themselves, forming aggregates. As a result the amount of aggregate is dominated by the amount of polymer material present in the system, and therefore the observed G' carries a much more linear relationship upon K-carrageenan concentration.

3.4.4.2.   Takayanagi's isostress & isostrain models applied to biopolymer systems

Having established the power law relationship and constants in each case the elastic shear response of a pure K-carrageenan phase may be predicted so long as the concentration of K-carrageenan is known in that phase volume. $c_{K\text{-}Ceff}$ may be identified, as the mass of K-carrageenan added to each solution is known, whilst starch swelling studies (Fig. 19) were able to identify the starch phase fraction for each system using Equations 8 & 9, and subsequently the K-carrageenan phase fraction may therefore be determined using the Equation 16 for starch / K-carrageenan mixed polymer systems, assuming that all remaining 'free' water not absorbed by starch is occupied by the K-carrageenan phase [62], where $\phi_{K\text{-}C}$ is derived K-carrageenan phase volume fraction and ϕ_{XLWM} is derived XLWM starch phase volume fraction. From this, actual phase volume and effective phase polymer concentrations may be determined.

$$\phi_{K-C} = 1 - \phi_{XLWM} \tag{16}$$

For phase separated composites comprised of a continuous and dispersed phase (as my be hypothesised in this case to a high degree of probability), the moduli of either composite in its respective phase may be studied using isostress and isostrain blending laws [118] adapted to dissociative phase polymer composites [119] [120] [121].

$$G'_{composite} = G'_{K-C}.\phi_{K-C} + G'_{XLWM}.\phi_{XLWM} \tag{17}$$

$$\frac{1}{G'_{composite}} = \frac{\phi_{K-C}}{G'_{K-C}} + \frac{\phi_{XLWM}}{G'_{XLWM}} \tag{18}$$

If the deformation of a weaker dispersed component is inhibited by the rigidity of the stronger component then both phases experience the same deformation [62]. These are known as isostrain conditions and elastic shear modulus of the overall system; $G'_{composite}$ in this ideal case follows the relationship in Equation 17, where $G'_{composite}$ is the elastic shear modulus of the composite, G'_{K-C} is the elastic shear modulus of the K-carrageenan phase, ϕ_{K-C} is the volume phase fraction occupied by K-carrageenan, G'_{XLWM} is the elastic shear modulus of the XLWM starch phase, and ϕ_{XLWM} is the volume phase fraction occupied by XLWM starch.

On the other hand, if the strength of the dispersed phase limits the force (and therefore the stress) transferred to the continuous phase so that both phases are subject to the same stress, deformation of the overall system is weighted on the compliance of either phase [62]. These are known as isostress conditions and the elastic shear modulus of the overall system; $G'_{composite}$ in this ideal case follows the relationship in Equation 18.

Composites comprised of a continuous phase with non-associative dispersed filler particles generally agree reasonably well with either of these models [154]. Thus for either ideal model theoretical G'_{system} values may be determined and plotted and compared to the experimental G'_{system} values, and conclusions drawn accordingly on the phase behaviour, comparative strengths of either phase and the contribution of filler particles to the overall system physicomechanical properties. This analysis assumes Hookean behaviour and, more significantly, that failure only occurs in the matrix; and were the stress high enough to cause failure within the dispersed 'filler' phase it would be unable to cross the continuous-dispersed phase interface. The variables in both of these relationships are the same; ϕ_{K-C} and ϕ_{XLWM} which are both known from starch swelling studies (Fig. 19), G'_{K-C} and G'_{XLWM}. G'_{K-C} values are able to be calculated from the individual K-carrageenan concentration dependency plot relationships (Fig. 22a-b) (Equation 15). G'_{XLWM} values were fitted as all other values were known, using the model relationships.

3.4.4.3.   K-carrageenan / XLWM starch dependency on salt and starch

In the first series of experiments, K-carrageenan concentration and salt type were held constant (0.4% and K(sorbate) respectively) whilst XLWM starch concentration was varied from 0-4 % at increments of 1% for salt concentrations 0.0135M, 0.0269M and 0.0404M (Fig. 23a)

Under all salt concentrations $G'_{composite}$ was observed to increase with XLWM concentration in an approximately linear relationship. Increasing salt concentration subsequently increased $G'_{composite}$. As was previously observed, increasing XLWM starch concentration increased the XLWM starch granule phase volume fraction; ϕ_{XLWM} (Fig. 19) which consequently shall decrease that phase volume fraction occupied by K-carrageenan in the continuous phase. The steady increase in $G'_{composite}$ with increasing XLWM starch concentration irrespective of salt concentration may therefore be accredited to this increasing effective concentration of the K-carrageenan continuous matrix (Fig. 23a), alternatively known as the excluded volume effect [127] [128] [155].

Previous polymer blending studies with agarose and XLWM starch [124] and gelatin and XLWM starch [122] have also shown increasing $G'_{composite}$ with increasing starch concentration. This behaviour is therefore assumed independent of the nature of the continuous polymer structure itself (whilst agarose chemical structure is not dissimilar to that of K-carrageenan; comprising of a D-galactose and 3,6-anhydro-L-galactopyranose linked by α-(1→3) and β-(1→4) glycosidic bonds, gelatin for example is markedly different, its structure comprising of denatured fibrous protein) and rather a result of an indirect excluded volume effect increasing the effective concentration of the continuous phase polymer.

Similarly, increasing salt concentration will increase K^+ cationic presence, which mediate junction zone formation in K-carrageenan aggregation of ordered domains [66], therefore

increasing aggregation in the K-carrageenan continuous phase, increasing G'_{K-C} [91] which is reflected in the overall composite elastic shear response modulus; $G'_{composite}$ (Fig. 23a).

K-carrageenan and salt concentration was then held constant (0.4% and 0.0269M respectively) and potassium salt varied, with K(sorbate), KCl, K(citrate) monobasic and KI tested over a XLWM starch concentration range of 0-4 % at increments of 1% (Fig. 23b). $G'_{composite}$ was observed to increase steadily in an approximately linear relationship with XLWM. Again it is hypothesized to be a result of increased starch phase volume fraction and K-carrageenan effective concentration.

Anion type influenced $G'_{composite}$ considerably, decreasing elastic shear response with increasing Hofmeister number. Chloride (Hofmeister Number 10.0) gave similar $G'_{composite}$ values to citrate (Hofmeister Number 7.2), and sorbate. Earlier (Chapter 2.0) the sorbate anion was assigned with a Hofmeister Number of 10.4±0.15 via trend fitting to a range of anion effects upon structuring and mechanical properties of κ-carrageenan aggregates, and all three of these anions were shown to exhibit similar lyotropic effects (see Chapter 1), whilst the presence of iodide (Hofmeister Number 12.5) decreased $G'_{composite}$.

Anions of higher Hofmeister number are known to entropically stabilise the transitional ordered domain in K-carrageenan aggregate formation [85] [55], decreasing entropic drive toward aggregation of ordered domains and as a result K-carrageenan solutions in the presence of iodide form slower, weaker aggregates, which becomes apparent in the reduced $G'_{composite}$ as the continuous matrix system will be weakened in the presence of I^-.
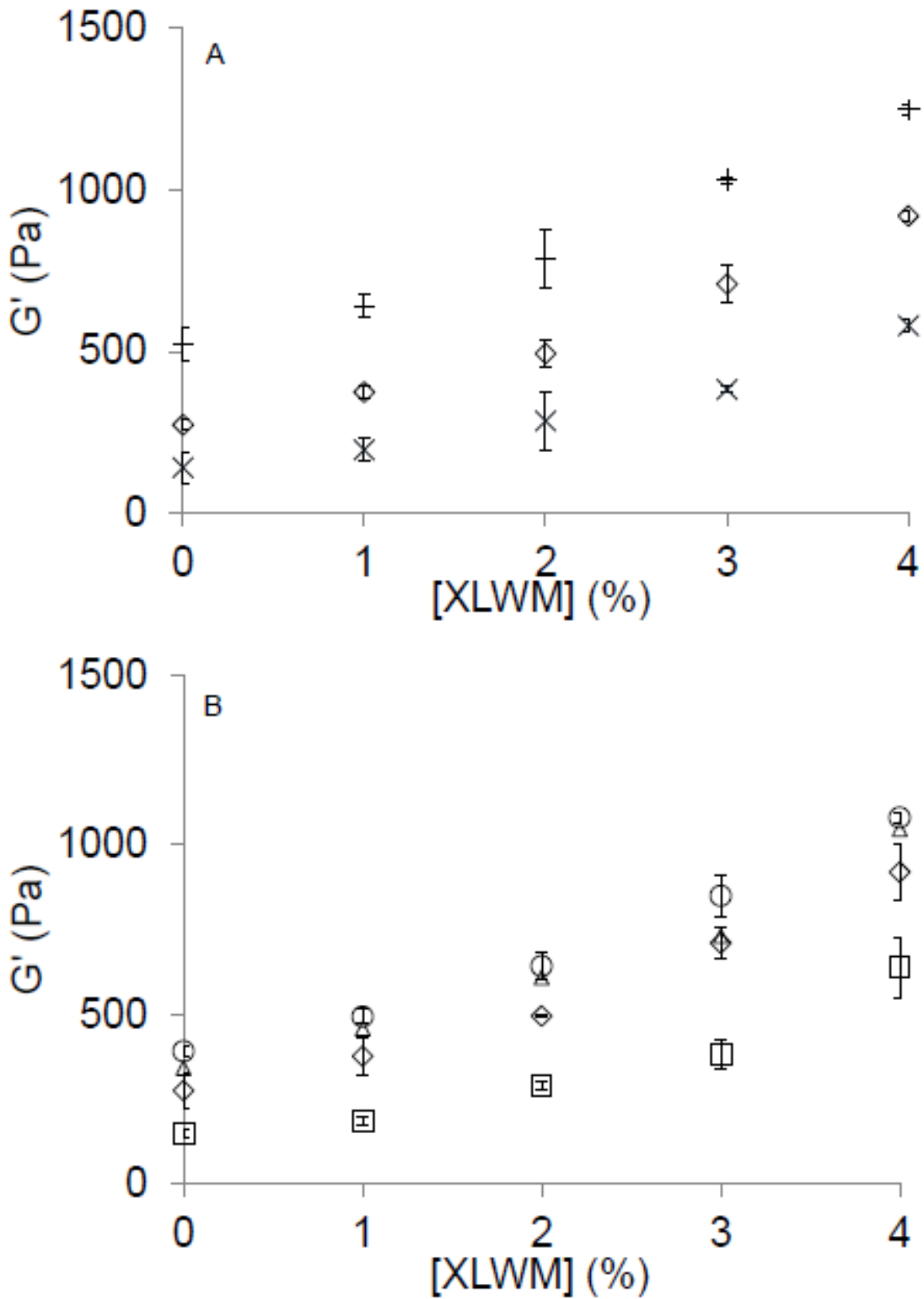
Fig. 23: G'composite dependency on XLWM starch concentration with (a) 0.0135M (×), 0.0269M (◊) and 0.0404M (+) K(sorbate), and (b) 0.0269M K(sorbate) (◊), K(citrate) (○), KCl (Δ) and KI (□).

3.4.4.4.   Applying Takayanagi's models to K-carrageenan/XLWM starch composites

The rheology of the mixtures was rationalised using available constitutive models for polymer blending [123] [124] (Fig. 24a-d).

In compliance with these models, continuous matrix G'_{K-C}; determined from water partitioning data (Fig. 19) and G'_{K-C} dependency on K-carrageenan concentration in pure systems (Fig. 22a-b) was compared to the corresponding value for experimental $G'_{composite}$ at respective XLWM starch concentrations. In the case of all salt types and concentrations sampled composite G' fitted the isostrain modelled G' closely.

The isostrain model in biphasic structures stipulates that either phase experiences the same strain; that is, relative deformation when subject to deformation from its equilibrium resting position [118]. In a system of a dispersed particle phase throughout a continuous phase therefore, this inherently means that the continuous phase supports the dispersed phase, which therefore requires the continuous phase to be the more rigid of the two.

Energy transferred to a system as deforming force is directly related to the stress and strain implemented upon it [156] [101]. Therefore for a given amount of work applied to a model isostrain system, the more rigid continuous phase will experience greater stress than the less rigid dispersed phase, to a degree relative to the distinction between the two respective rigidities.

In correlation with preceding physicomechanical observations within this study no distinction was found between K(sorbate), K(citrate) and KCl composite systems at 0.0269M, subsequently K(citrate) and KCl composite models are displayed in Appendix 1.
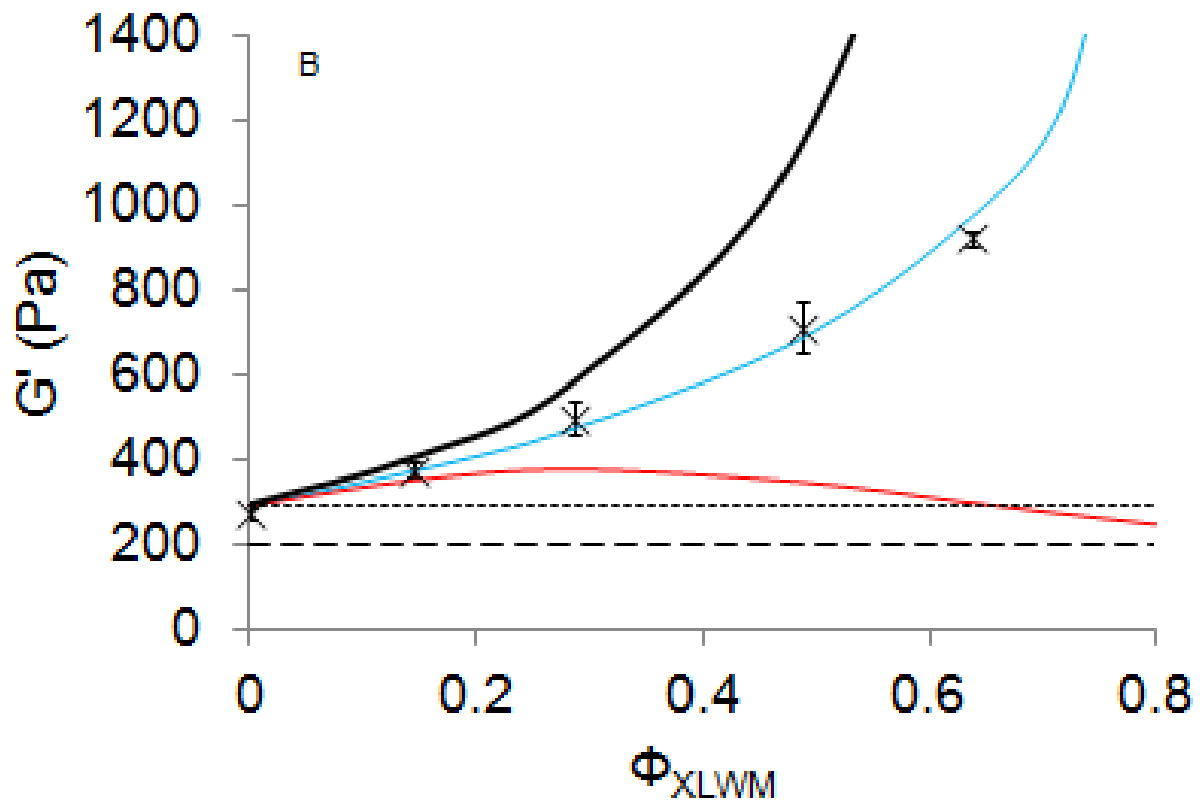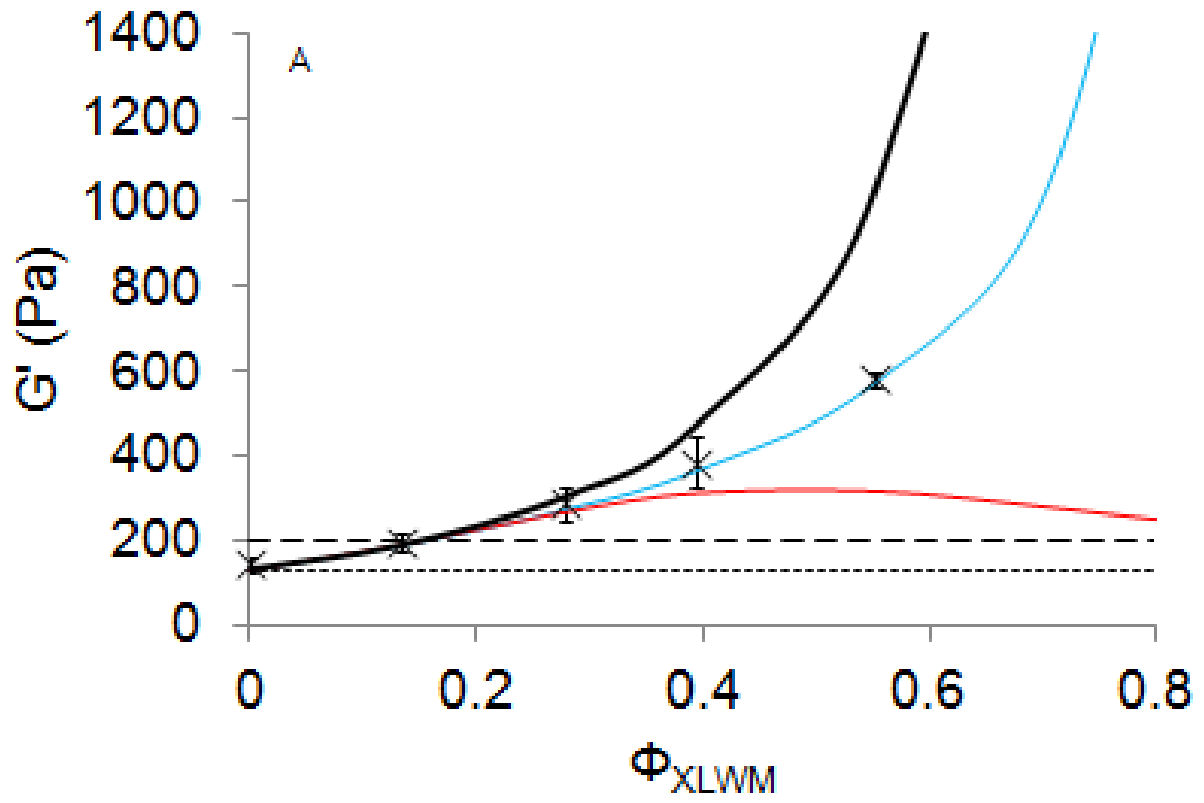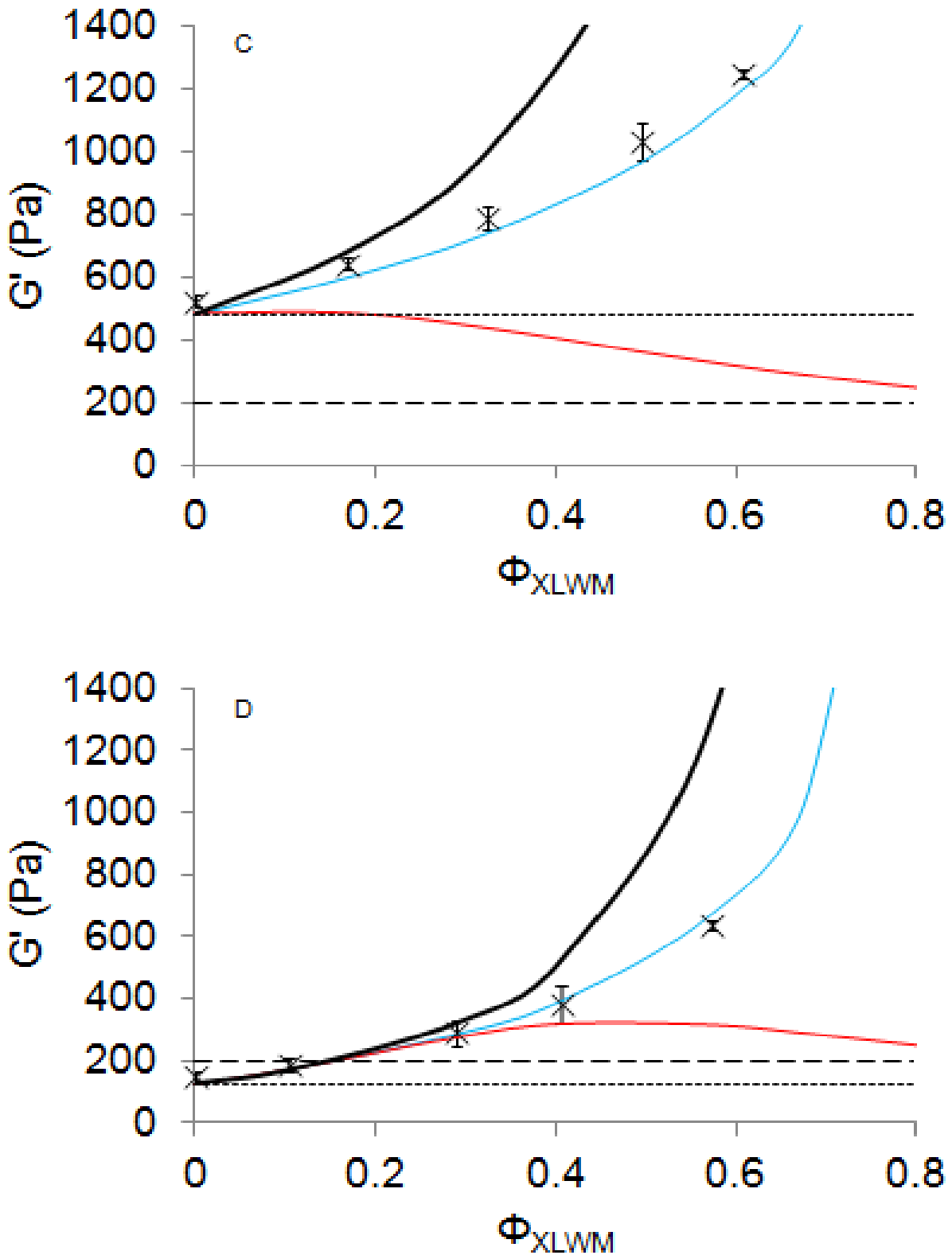
Fig. 24: Experimental dependency of G'composite (×) on XLWM starch concentration in the presence of (a) 0.0135M K(sorbate), (b) 0.0269M K(sorbate), (c) 0.0404M K(sorbate), and (d) 0.0269M KI respectively. Calculated models for isostress (—) and isostrain (—) are shown. Calculated G'K-C is shown (—) as well as fitted G'XLWM (— — —) and G' of corresponding pure K-carrageenan / salt gel (• • •).

In the instance of these composites in this study, the isostrain model indicates that the continuous K-carrageenan phase is more rigid than the XLWM starch dispersed granules (dispersed phase). G'_{K-C} originally correlated with (to within an acceptable margin of error) experimental $G'_{composite}$ at lower XLWM (1<%) starch volume fractions. This implies that sufficiently low concentrations of starch do not inhibit or interfere with the bulk network structure of the K-carrageenan continuous matrix, so that no change in material behaviour is observed from pure K-carrageenan system. Although some solvent exclusion is expected to occur [62] as the granules have swollen (increasing the K-carrageenan effective concentration) this effect is minimal at these lowest concentrations of starch thus a subsequent effect on the material behaviour is negligible. This is in agreement with analogous hydrocolloid – XLWM starch composite studies on gelatin [122] and XLWM starch composite studies on agarose (0.25%) [124] in the presence of low XLWM starch concentrations (≤2.00%).

Separation of model upper and lower bounds, composite, and continuous phase moduli with the progressive addition of starch is dependent on the difference in material strength between the continuous phase and the dispersed starch phase, with separation occurring earlier under lower added starch concentrations where starch is significantly lower in G' than the continuous phase. This effect is observed here in those composites where the modulus of the 0.4% K-carrageenan pure phase is far greater than that of the pure XLWM starch (horizontal dashed line) in the presence of 0.0404M K(sorbate); (Fig. 24c), and less pronounced in those composites where the modulus of the 0.4% K-carrageenan pure phase is lower in the presence of 0.0135M K(sorbate); (Fig. 24a).

Increasing salt concentration – known to increase K-carrageenan gel strengths (below the critical concentration) – decreases the point of starch concentration at which models diverge, as K-carrageenan continuous phase is becoming distinctively stronger than the starch filler. Therefore it may be surmised that higher salt concentrations increase the G' of the K-

carrageenan aggregate and therefore the difference in G' between the K-carrageenan and the starch, which subsequently causes a more radical and earlier divergence in the models; as the individual phases are further apart in physicomechanical response.

Further increasing XLWM starch volume fractions see G'$_{composite}$ fall below the corresponding G'$_{K-C}$ trend, indicating this XLWM / K-carrageenan composite is weaker than its pure K-carrageenan phase at the effective concentration. Now, rather than simply residing in spaces in the K-carrageenan network without impacting the continuous phase matrix as at lower starch concentrations, the starch granules are of sufficient concentration to bear a significant impact upon the overall composite structural strength, existing as softer inhomogeneities in an otherwise continuous network. Upon subject to stress, the distortional forces shall be spread throughout the mixed polymer aggregate structure. The greater the number and size of junction zones in an aggregate system, the greater applied stress may be spread, and subsequently localisation of stress will be less, as discussed previously (refer to Chapter 2.0).

Inclusion of these soft inhomogeneous granules however interrupts this stress dispersion continuity. As the granules are inhomogeneous and comparatively softer, the transfer of stresses from the K-carrageenan aggregate to the granule are believed to be less efficient, and subsequently the stress concentrates in the K-carrageenan aggregate in that region. This subsequently results in increased likelihood for energy dissipation via irreversible bond distortion or breakage, accumulating in crack tip propagation and initial stages of failure.

As a result the overall physicomechanical strength of the composite is decreased and the limitations of pure elastic storage of the system are decreased as failure will occur under less shear. Clearly, as the number of granules is increased, so the interruptions to the continuous K-carrageenan matrix are more regular and subsequently stress concentration is greater, and the mixed polymer system is weakened.

Previous investigations [122] using mixed gelatin and XLWM starch composites reported that upon addition of higher concentrations of XLWM starch (≥3.00%), the modulus of the continuous gelatin phase; G'$_{\text{gelatin eff}}$, instead fell below those respective values for G'$_{\text{composite}}$, the G'$_{\text{composite}}$ itself following the isostress model, as the starch dispersion was stronger than the gelatin continuous phase, and thus increased physicomechanical strength of the overall composite, supporting the (gelatin) continuous phase by sharing the strain.   Upon changing conditions for the continuous phase from 0.88% gelatin at 20°C to 1.50% gelatin at 5°C however, isostrain and isostress models converged and less distinction was observed between experimental values for G'$_{\text{composite}}$, isostress, and isostrain models, as the modulus of the gelatin phase approached that of the starch phase [122].   The same authors reported different hypotheses in xanthan and XLWM starch composite phase partitioning studies [123], where the modulus of the continuous phase at effective concentration; G'$_{\text{xanthan}}$, fell below G'$_{\text{composite}}$, however this time the two trends diverged immediately on the addition of very low concentrations of XLWM starch.   Again, when the continuous phase concentration was increased, the separation of continuous and dispersed phases was reduced.

It was concluded [123] that the increase in elastic shear storage modulus of the composite observed in the case of gelatin / XLWM starch systems was a result of increased gelatin effective concentration in the continuous phase due to the excluded volume effect of starch granule swelling; which exist in that instance as non-interactive dispersed filler particles. Contrastingly, xanthan was understood [123] to actively promote the adhesion of starch granules (in addition to volume exclusion effects of the starch), causing them to flocculate together.

Studies [157] have shown that polymer chains can stimulate flocculation of dispersed particles via two mechanisms: depletion and bridging. Bridging flocculation involving bridging of two starch granules via the polymer chain association to either of them. Depletion flocculation can

occur as two starch granules come within close proximity to one another via random Brownian motion. The polymer chains can't fit in between the two granules comfortably and will diffuse out of the gap between the two granules, along with water molecules hydrating the chains. A region of low concentration now remains between the two granules, and subsequently a temporary loss in entropy. Entropy may be restored by the granules moving together into the gap, and subsequently adhesion can occur. The significance of these mechanisms with regards to the continuous polymer is that the rigidity of the polymer will determine the feasibility of both of these mechanisms. Straight, rigid polymer chains (e.g. xanthan) will have lower entropic barrier to overcome in order to associate to either granule for bridging compared to a random flexible coil (e.g. gelatin). Similarly, rigid polymer chains will be less accommodating to the confines of two particles moving close upon one another, and are more likely to be forced out facilitating depletion flocculation. Abdulmola et al. [123] hypothesized that either or both of these mechanisms were responsible for the increased mechanical strength of the starch phase in the presence of xanthan but not gelatin.

Interestingly, the chemical structure and associations of K-carrageenan would be considered more akin to that of xanthan then that of gelatin, despite studies for K-carrageenan here displaying no such evidence of starch flocculation. It is concluded therefore that there is insufficient evidence here to support a theory of K-carrageenan facilitated XLWM starch granule flocculation.

Studies performed by Mohammed et al. [124] with agarose / XLWM starch composites reported G'$_{composite}$ followed the isostrain model derived from Takayanagi's studies [118] [119], the composite G' modulus falling below that of the continuous phase under higher concentrations of XLWM starch ($\geq 3\%$). As the continuous phase G' was now greater than that of the dispersed starch phase the starch granules were perceived to be acting as less rigid filler particles [124]. The observed mechanical models constructed with K-carrageenan / XLWM

starch composite systems in this study follow those reported by Mohammed et al. [124] closely, and the same hypotheses is therefore proposed in this system.

By comparing and contrasting these results here using K-carrageenan / XLWM starch composites to those using other hydrocolloid continuous phases, the following conclusions may be drawn on the phase partitioning behaviour. Firstly that the composite follows the isostrain model, and falls below the respective modulus for the pure continuous K-carrageenan phase under these conditions and concentrations is indicative that the incorporation of starch granules into the K-carrageenan matrix - as inhomogeneous filler particle defections to its continuous structure - weakens the composite; reducing $G'_{composite}$, as similarly demonstrated in those studies with high concentration agarose [124].

Inversely, starch addition was observed to improve the overall composite modulus at lower agarose concentrations, [124] as in analogous gelatin and xanthan systems [122] [123]. The correlation between these composites strengthened by the addition of starch is that they all have a weaker continuous phase matrices compared to the K-carrageenan gel systems here and those of higher agarose concentration [124].

Therefore, unlike in those systems of weaker matrices where starch is comparatively harder than the continuous phase and thus acts as a hard filler improving the physicomechanical response of the composite, here the starch is weaker than the continuous K-carrageenan matrix, the result of which is observed in the weakened physicomechanical response of the composite compared to the pure continuous phase. Subsequently, the addition of starch is detrimental to the bulk physicomechanical properties of the K-carrageenan system whilst the continuous phase demonstrates greater physicomechanical strength and the starch acts as a soft filler.

Secondly the delayed separation of the upper and lower bounds and composite and continuous phase moduli with the progressive addition of starch as observed in those studies with gelatin

and agarose [124] [122], as oppose to the immediate distinction observed with xanthan [123] would lead to the hypothesis that rheological enhancement of the $G'_{composite}$ is due to the excluded volume effect from water confined within the swollen starch granules as in the case of agarose and gelatin, rather than via promotion of starch granule association, as in the case of xanthan, strengthening those conclusions from thermodynamic studies that K-carrageenan and XLWM starch are not thermodynamically compatible.

Another point noteworthy is the marked difference between either ideal blending model here. Rather than following each other closely to around ~3% XLWM starch [124] [122] here there is a clear distinction as early as 1% XLWM starch. This is not quite so distinguished in the less aggregated KI system however, (Fig. 24f) (clear distinction ~2% XLWM) and even less so in the low salt concentration (0.0135M K(sorbate)) (Fig. 24a) system (clear distinction ~3% XLWM starch) suggesting this originates from lower G'_{K-C} of the K-carrageenan phase in this case, impacted by the ionic effects on K-carrageenan aggregation, as XLWM starch volume fractions were highly comparable for all systems (Fig. 19).

At polymer concentrations and salt conditions employed in this study all systems (Fig. 24a-d) follow the isostrain ideal model closely and therefore the continuous K-carrageenan matrix may be concluded to be far more rigid than the dispersed filler XLWM starch granules. The K-carrageenan matrix dominates the bulk rheological properties of the composite. Generally error bounds are small, insinuating a high degree of precision.

It should be noted that whilst these results are in good agreement with the isostrain model some assumptions were required and as such this hypothesis is entirely dependent on their accuracy.

Firstly, the theory that there are no direct interactions between the two, and that they are indeed incompatible, with no heterogeneous association.

Conflicting theories exist contrary [158] [159] and complimentary [155] [128] to this reasoning. However, one would have to conclude that at these conditions and concentrations at least, K-carrageenan / XLWM starch direct association may be negated, referring in particular towards thermal analysis studies here showing starch granule structure transformation endotherm traces accompanying gelatinization do not show any change from starch solution to starch / K-carrageenan mixed solution, indicative of an absence of mixed heterogeneous association.

Secondly, results have been cumulated and conclusions made using a fitted value of G'_{XLWM} into the models employed here; all other values inserted into the model having been determined experimentally. The agreement between these experimental values and the Takayanagi blending isostrain model; in conjunction with starch granule swelling studies, should be viewed with circumspection. However it is fair - given the close agreement in all cases studied here, to conclude that this model may be used to predict those $G'_{composite}$ values observed experimentally to a reasonably good degree of certainty.

3.4.5. Texture Analysis

Large deformation studies allow an insight into the tertiary and quaternary structure of a polymer system, and how it contributes towards the mechanical properties [97] prior to failure (e.g. Young's modulus, bulk modulus) and during failure (e.g. work done, stress, strain to failure) as demonstrated (Fig. 25). Composite response can correlate with oscillatory rheology measurements, [97, 110] or alternatively it may respond entirely differently [111].

Even upon reflection of those results obtained from rheology phase partitioning studies, it is not immediately clear what is to be expected. Increasing concentrations of starch were established as acting upon the composite material behaviour via multiple conflicting mechanisms: increasing continuous phase strength via volume exclusion effects whilst

simultaneously serving as structural defects and weakening the structure - with indirect volume exclusion effects ultimately prevailing. However, this behaviour was determined over a far lower (shear) strain than those employed in these uniaxial compression studies. Strain rate is known to influence the mechanical response behaviour of a system [160], with a higher dissipation rate of energy through structural defects at higher strain rates, and subsequently trends of decreasing elastic character and strength as represented by G' in rheology studies may be replicated in larger deformation e.g. Young's modulus.
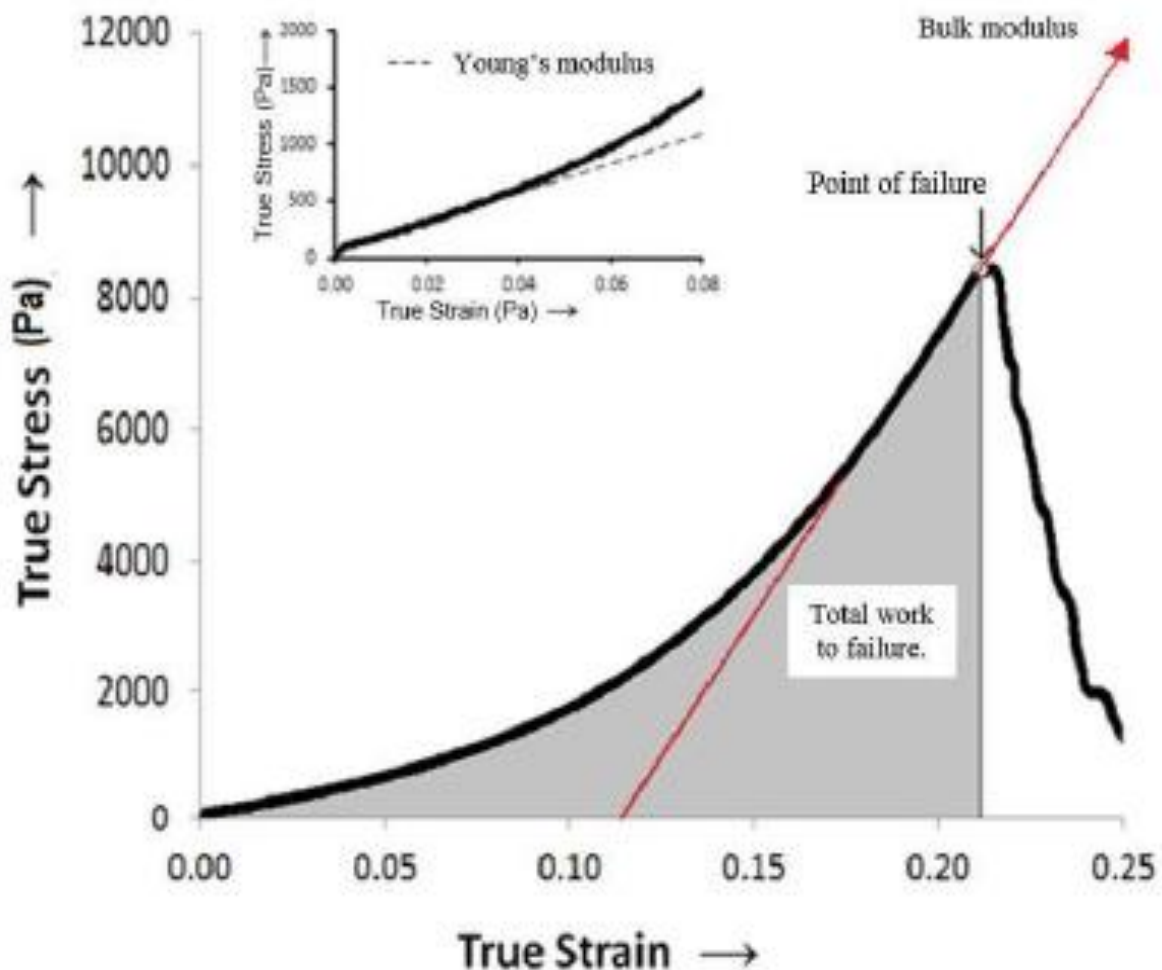
Fig. 25: An example of original data demonstrating typical true stress / strain plot from uniaxial compression of K-carrageenan / XLWM starch composite gels. The interpretations of Young's modulus, bulk modulus and total work to failure are shown.

On the one hand, G' was observed to increase following the addition of XLWM starch, and it was concluded to be a result of the volume exclusion phenomena increasing the continuous phase matrix effective concentration and subsequently its material strength. This phenomenon will similarly be a factor for consideration in the large scale deformation behaviour of the composite; the work to induce complete failure for example – where the number and size of junction zones in the continuous phase will determine the force required to induce permanent deformation, as any load on the composite will be spread across the junction zones in the aggregate network [99] (refer to previous work in Chapter 2.0). Therefore, the more junction zones the further the force is spread and the lower the mean force on any given junction zone, thus greater force shall be required to implement bulk failure.

Inversely, the G' of the composite was observed to fall below that G' of the K-carrageenan continuous phase at the calculated effective concentration, following the isostrain model indicative of a soft filler incorporated into a comparatively hard, strong continuous phase. This soft filler effect may become more prominent under increased stress and strain [160]; with deformable inhomogeneities in an otherwise continuous κ-carrageenan matrix network becoming more significant to stress concentration in the continuous phase, and/or increased strain forcing displacement of the starch granule though the continuous phase. Lyotropic effects upon aggregation in the continuous phase (increasing with lower Hofmeister numbers) are predicted to strengthen the continuous phase and subsequently the overall strength of the composite, as for rheology studies.
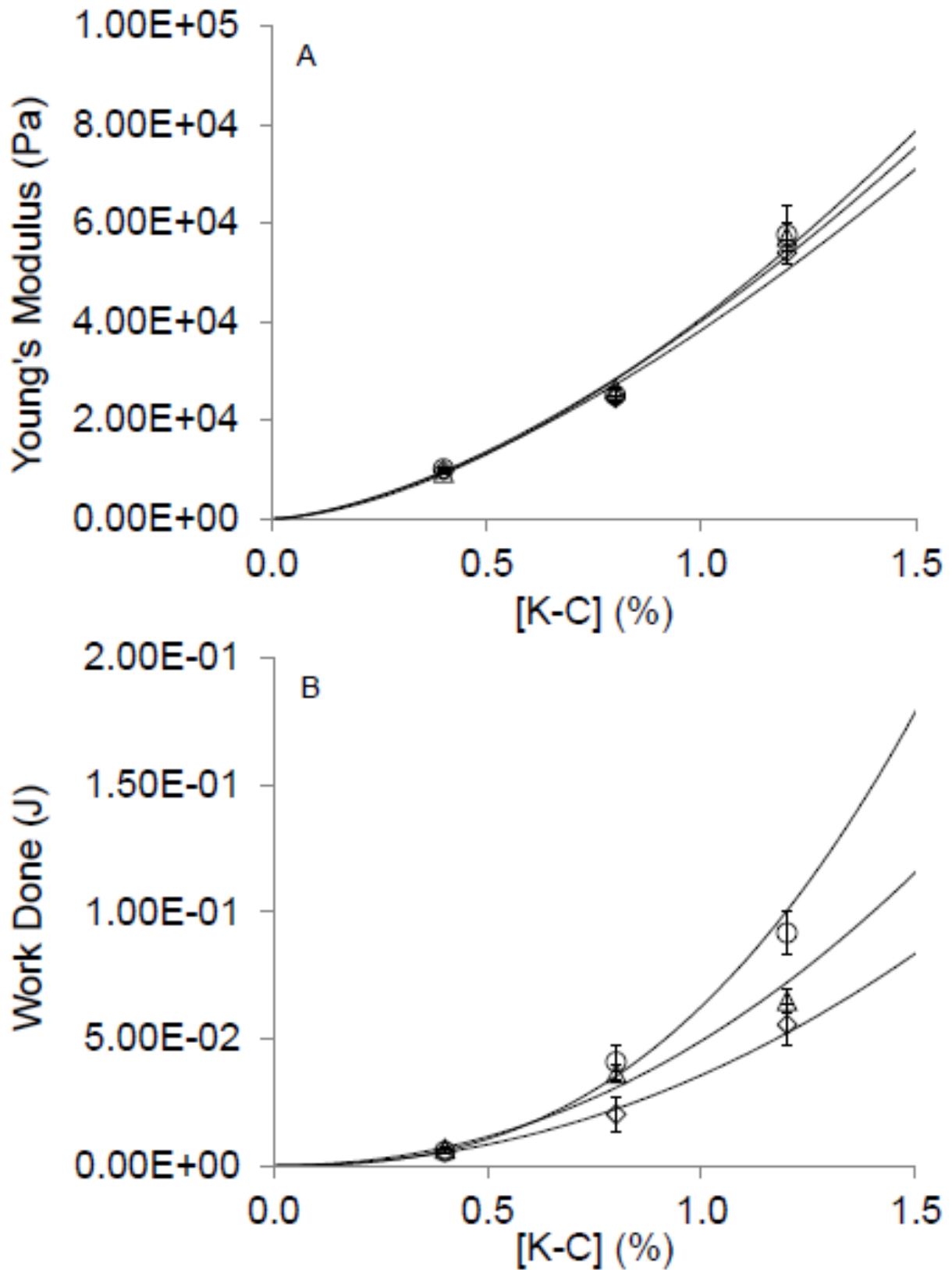
Fig. 26: Dependency of (a) Young's modulus, and (b) work resulting in failure upon polymer concentration in K-carrageenan gels with 0.0269M K(sorbate) (◊), K(citrate) (○) and KCl (Δ).

The stress / strain behaviour of 0.4%, 0.8% and 1.2% K-carrageenan gels in the presence of 0.0269M Potassium salt was studied. Young's modulus and failure work are represented in Fig. 26a-b respectively. Bulk modulus was found to demonstrate analogous dependency trends to work failure, and subsequently was not shown here. Power law relationships between all material properties in turn and K-carrageenan concentration were fitted as for rheology studies.

P (units)	Salt	a (Pa^{-1})	b	R^2
	KCl	40587	1.63	1.00
Youngs (Pa)	K(Citrate)	40089	1.56	0.98
	K(Sorbate)	38240	1.52	0.99
	KCl	708574	1.67	1.00
Bulk (Pa)	K(Citrate)	847987	1.86	0.98
	K(Sorbate)	563368	1.77	1.00
	KCl	0.0491	2.11	0.99
Work (J)	K(Citrate)	0.0627	2.58	0.99
	K(Sorbate)	0.0356	2.10	1.00

Table 4: Experimental values for a and b constants in the power law relationship between mechanical property P and polymer concentration, for K-carrageenan solutions in the presence of 0.0269M K(sorbate). R2 values for this power law fit are also shown.

Physicomechanical strength increased with increasing K-carrageenan concentration. This was to be expected, as the more polymer present, the more material available for junction zone forming and aggregate development. Additionally, the higher the polymer concentration the less the subsequent solvent potential of the bulk water phase molecules to support additional

K-carrageenan polymer in solution via hydration, and the more thermodynamically favourable stabilisation via aggregation will become [69]. The more extensive the aggregate development, the greater the network across which stress may be dispersed and subsequently the less localised stress and the higher the strength of the aggregate.

In this instance here, the power law relationship is represented by Equation 19, where P represents any of the mechanical property values Young's modulus, bulk modulus, or work up to failure. Constant a here represents the dependency coefficient of the respective mechanical property; P, upon concentration of polymer present, and is equal to the true P at $c_{K\text{-Ceff}} = 1$. Constant b refers to the polymer aggregation exponent, and how (non-)linear the relative dependency of P upon polymer concentration is. Data fitted the power law to >97.5% confidence in all cases, values for a, b and R^2 shown (Table 4). Interestingly, polymer aggregation exponent b appears to increase for those mechanical properties referring to inelastic deformation and bulk failure. It is hypothesized that this is accredited to the bulk strength properties dependence upon solid material in the sample; more aggregate increasing resistance to forces driving bulk macroscopic failure.

$$P = a.c_{K-ceff}^{b}$$
(19)

Having established the power law relationships for κ-carrageenan concentration in each case, the models for physicomechanical properties at κ-carrageenan phase effective concentration were determined using the phase volume fraction data established earlier (Fig. 19a), and plotted alongside experimental values for the mixed composites of 0.4% K-carrageenan and 0-4% XLWM starch, in the presence of 0.0269M potassium salts. Young's modulus (Fig. 27), bulk

modulus, and failure work (Fig. 28) models for composites in the presence of K(sorbate) 0.0269M are shown, models for corresponding systems in the presence of 0.0269M K(citrate) and 0.0269M KCl exhibited no distinction from those of K(sorbate) and thus have been included in appendices (Appendix 2, Appendix 3, Appendix 4 respectively).

Young's elastic modulus; as taken from the initial linear region of the stress / strain plot [99] [100] increases (from that of 0.4% K-carrageenan gel) with increasing XLWM starch concentration in the presence of all potassium salts. Anionic lyotropic effects showed no distinction between K(sorbate) (Fig. 27), KCl (Appendix 2a), and K(citrate) (Appendix 2b).
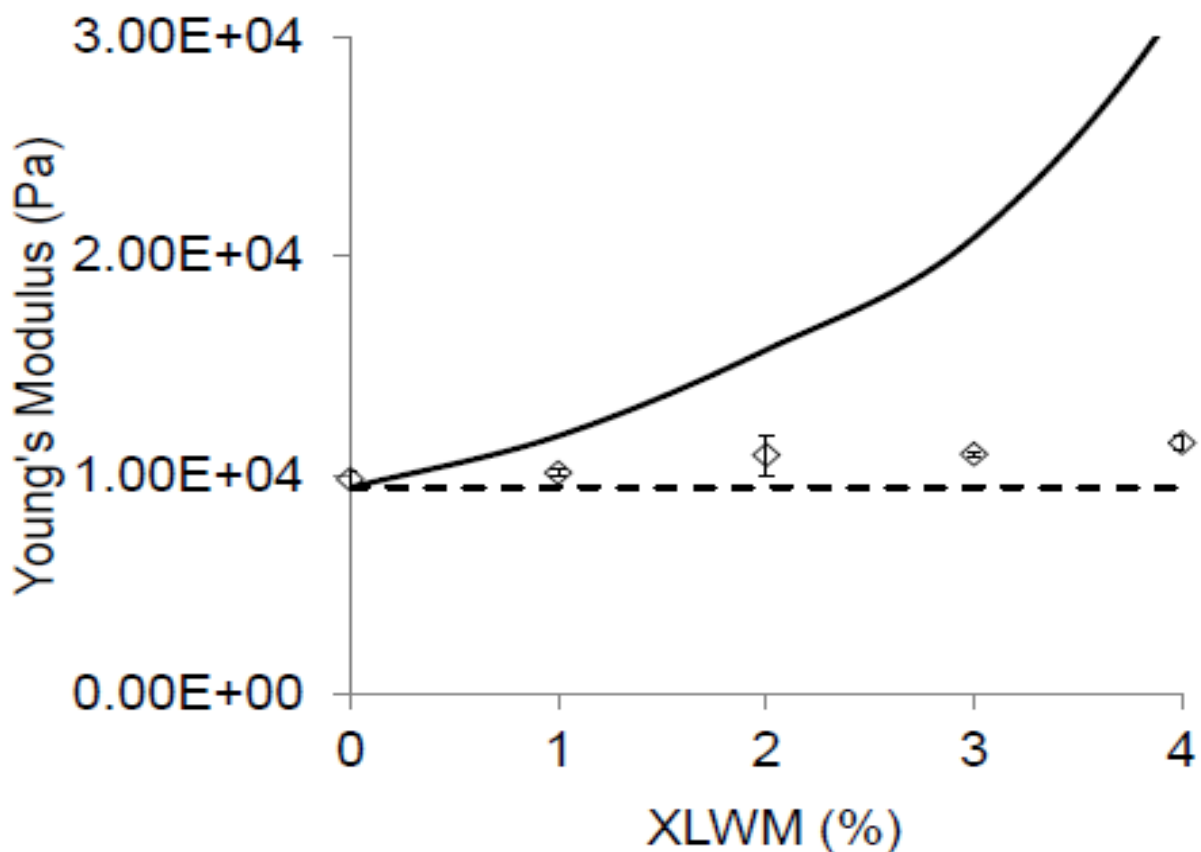
Fig. 27: Experimental dependency of Young's modulus of K-carrageenan and XLWM starch composite gels upon XLWM starch concentration with 0.0269M K(sorbate). Calculated Young's modulus for the effective concentration of the K-carrageenan phase is represented (――――) as well as Young's modulus of corresponding 0.4% K-carrageenan/salt gel (― ― ―).

The experimental Young's modulus of the composite was low relative to that of the calculated effective K-carrageenan concentration; the inhomogeneous swollen starch granules do therefore have some impact in disrupting the continuity of the κ-carrageenan matrix, transferring stress less efficiently than the continuous matrix and allowing it to concentrate. These trends are analogous to those of the rheology G' studies, and so too is the reasoning.

Composite Young's modulus is observed to increase with XLWM addition relative to the respective 0.4% K-carrageenan aggregate, concluding that continuous phase strengthening via indirect solvent volume exclusion effect again prevails above weak filler inhomogeneous disruption to the continuous matrix in the context of composite physicomechanical strength, increasing the effective concentration in the continuous phase, and thus increasing κ-carrageenan network aggregation and the number of junction zones formed which subsequently spreads any applied load better, and reduces the load (on average) on any single aggregate junction. As such, the load which may be applied prior to initiating irreversible plastic deformation [99] of the junction zones is greater, and the elastic Young's modulus is therefore greater. No direct correlation exists between elastic moduli and the physicomechanical properties of polymer systems subject to increased strain approaching macroscopic failure; response can vary greatly, and is strongly influenced by inhomogeneities in the network structure [111] [161] [162]. Consequently, it is not possible to predict accurately the response of the composites beyond the first linear elastic region purely based on the elastic response.

The bulk moduli of composites was taken from the gradient of the final linear region approaching total failure on the stress / strain plot [102] [99] and recorded as a function of their dependency on starch concentration, in the presence of 0.0269M K(sorbate) (Fig. 28a). Uniaxial bulk modulus decreases with increasing XLWM starch concentration from the bulk modulus of the respective 0.4% κ-carrageenan aggregate, in a linear decline.
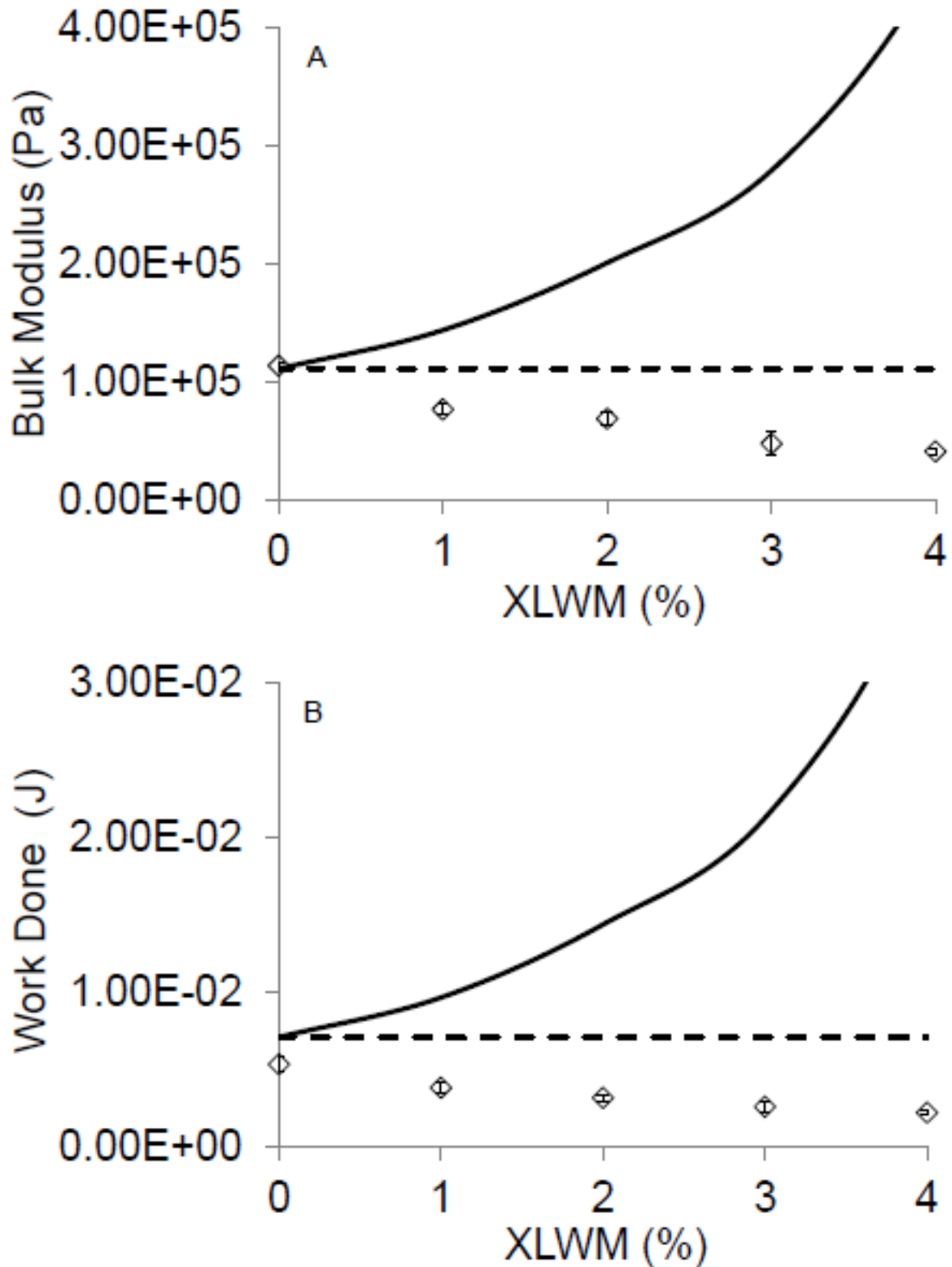
Fig. 28: Experimental dependency of (a) bulk modulus, and (b) work failure of K-carrageenan and XLWM starch composite gels upon XLWM starch concentration with 0.0269M K(sorbate). Calculated values for the effective concentration of the K-carrageenan phase is represented (———) as well as that of corresponding 0.4% K-carrageenan/salt gel (— — —).

Work done to the composite system in order to stimulate complete failure (Fig. 28b) showed analogous results to those of the bulk modulus; as starch concentration increased so work done to failure decreased, despite the respective calculated values for the κ-carrageenan phase at its effective concentration increasing exponentially.

Under deformation at low strains ≥10% (i.e. G' and Young's modulus studies) the addition of starch serves to strengthen the physicomechanical response of the composite; within the elastic region. As strain increases, approaching and at complete failure ≈50% (i.e. bulk modulus and work input to failure) the addition of starch serves to weaken the physicomechanical response of the composite beyond the initial linear elastic region.

In polymer blending rheology models constructed (Fig. 24a-d) it has been concluded that starch retains its granule structure albeit in a swollen state, and these swollen starch granules act as softer filler particles, relative to the K-carrageenan continuous phase following the isostrain model. The addition of less rigid (inactive) filler particles weakens the composite [162] relative to the continuous phase at its effective concentration; however the overall effect at low strains is still to strengthen the overall structure by addition of starch due to the dominant volume exclusion phenomena.

At higher strains beyond the initial linear elastic region this is no longer the case, and other phenomena detrimental to the overall physicomechanical behaviour of the composite must take the principle role, as the addition of starch is not only failing to add to the bulk strength of the structure of the composite relative to that of the equivalent 0.4% κ-carrageenan aggregate, but instead actually weakening it, as demonstrated by bulk modulus (Fig. 28a) and failure work (Fig. 28b). The hypothesis therefore, is that at high strain this direct effect of softer, less rigid filler particle incorporation into the composite structure becomes the dominant phenomena.

Swollen starch granules may be deformed readily with little stress [155], serving a twofold mechanism in weakening the structure. Firstly, they are comparatively less rigid than the κ-carrageenan aggregate forming the continuous matrix, therefore effecting as interstices in the composite structure where (more rigid) κ-Carrageenan aggregate may otherwise fill, offering reduced support towards mechanical deformation of the composite. Secondly, as has been demonstrated, the two polymers are non-associative, and consequently stress transfer efficiency from one polymer type microstructure to another is poor, resulting in stress accumulation in the continuous phase at the points occupied by the starch granules; stress (and potential energy) accumulation ultimately being relieved as kinetic energy via structure/junction zone failure. This is observed on a macro scale as permanent deformation in the system, and clearly the greater the starch concentration, more interstices, the more this will be facilitated, accumulating in a weaker structure.

3.5. Conclusions

The role of XLWM starch in defining the physicomechanical attributes of mixed composite gels with κ-carrageenan is not a straightforward one. Depending upon the conditions (e.g. applied strain, salt concentration, and salt type) granules may function in either of two completely different ways both directly and indirectly, to increase or reduce composite elastic attributes and resistance to macroscopic failure.

κ-carrageenan will not form associative interactions with XLWM starch granules, as has been demonstrated by μDSC studies, however as cross linked waxy maize starch granules swell (16% of the total water volume per gram of starch added) indirect volume exclusion of the bulk solvent will increase κ-carrageenan effective concentration in the continuous phase, strengthening it and creating an isostrain model whereby the more rigid continuous κ-

carrageenan network supports the less rigid starch granule dispersed phase, these effects were demonstrated to increase polymer composite resistance to small deformation using oscillatory rheology studies, by which polymer blending models were able to be constructed. Starch granules simultaneously act directly as inhomogeneous 'defects' in the continuous κ-carrageenan network, weakening the structure by disrupting stress dissolution, allowing it to concentrate and increasing potential for crack tip propagation, as has been demonstrated in large uniaxial deformation studies.

Salt lyotropic effects on solvent quality allow specific alteration of the composite physicomechanical properties via control of both phases as concluded from μDSC studies, controlling starch swelling and κ-carrageenan aggregate development. Salt concentration was found to exhibit a more substantial distinction upon composite material properties than anion type, although a wider range of anion Hofmeister numbers should be investigated, as sorbate and citrate (monobasic) potassium salts studied here affected composite physicomechanical attributes similarly to chloride, and were chosen primarily for their lack of attention in scientific literature prior to this point, despite their popularity in food applications as preservatives.

Further work of particular interest would be to assess the effects of κ-carrageenan concentration; particularly lower concentrations, and to what degree the composites will continue to follow an isostrain model. Additionally it would be interesting to replace cross linked waxy maize starch with a different starch of smaller swollen granule size; quinoa starch for example – and thus smaller 'defect' size at high strains of compression.

IV

EFFECTS OF PROCESSING CONDITIONS IN PALM OIL SHORTENING EMULSION FORMULATION

4 Effects of Processing Conditions in Palm Oil Shortening Emulsion Formulation

4.1. Abstract

The physicomechanical processing conditions upon the physicomechanical properties of 30% water in non-hydrogenated palm shortening emulsions with a monoglyceride emulsifier have been investigated, formulated using a bench scale scraped surface heat exchanger (SSHE) and subsequent pin stirrer (PS) unit. Emulsions' resistance to deformation; defined by work up to failure, bulk modulus of compression, yield stress, and extensional flow yield stress using uniaxial compression studies, increased with increasing SSHE shear rates (up to 1315rpm) and decreasing SSHE jacket temperature (to 16ºC) whilst the inverse was true for the PS processing parameters. It has been demonstrated that SSHE processing parameters promoting rapid cooling of fat crystals; which is known to create more numerous, smaller crystals, and consequently weak linkage association between fat crystals is more profuse, strengthening the overall microstructure, as demonstrated in this study. Inversely, pin stirring softened emulsions disrupting fat matrix extension. This study has concluded processing parameters complimenting emulsion material strength simultaneously increased aqueous phase dispersion, assessed via NMR as surface weighted diameter d3.2 and free water (d3.2 values $\geq 50\mu m$). It is suggested that SSHE shear will directly disperse the aqueous phase, whilst stabilisation of the droplets will be increased by the smaller, more regular, interlocking fat crystal morphology favoured by the same parameter settings. Aqueous phase dispersion was stable from 0.5-504 hours after processing, with solid fat content (SFC) showing no dependency upon processing parameters after 24 hours.

4.2. Introduction

In designing emulsion systems (and indeed any processed food product), the choices of process concept and conditions used are a key factor in deciding the food structure, creating novel food products and structures using new technologies, or improving established technologies and processes, for example from chemical and / or mechanical engineering disciplines [163] [164] [165]. The physical and functional properties of semi solid w/o crystallised fat emulsion food systems will be critically defined by its microstructure organisation: fat crystal shape, organisation and size, melting temperature, emulsifier droplet shell integrity and aqueous phase droplet size (to name but a few) [3]. All of which may be specified, in theory, using processing condition control.

One such crystallising fat with potential basis for emulsion formulation is baking margarine, or shortening. Typically palm oil shortening is used in a refined state, mainly as stearin and olein triacylglyceride (TAG) fractions [166]. Medium melting range (40-44) non-hydrogenated palm oil shortening typically carries a solid fat content of 30% (at 10.0) [167] [168] attributed to the solid TAG concentrations, and the material properties and solid character of the fat under any given conditions are defined by a) the amount of solid fat present, and b) the organisation of that fat [169]. The rest of the shortening structure is comprised of liquid fats. TAGs typically make up for 98% of the composition [166], with the rest comprising of diacylglycerols (DAGs), monoacylglycerols (MAGs) and other minor components.

Ongoing studies at the Centre for Formulation Engineering, University of Birmingham [35] [33] [42] have explored the potential for w/o emulsion formulation with cocoa butter – a fat not dissimilar to palm oil shortening used in baking – substituting a proportion of the cocoa butter fat with water and therefore reducing overall energy density. Studies have reported the successful production of w/o emulsions of up to 60% water [32], formulated using a

conventional bench-scale margarine line incorporating a temperature-controlled scraped surface heat exchanger (SSHE) and subsequent separate pin stirrer (PS).

SSHE's are particularly useful in the production of food emulsion systems where a high degree of fine fat crystallization nucleation is required [170]. The SSHE serves a fourfold purpose in processing the pre-emulsion. It works primarily by sweeping TAG molecules in solution onto a cooling wall where thermal energy is transferred away for the fat, reducing molecular energy until a free energy barrier is overcome and TAG molecules reorganise and associate to form crystal nuclei, this primary crystallisation may then initialise secondary nucleation – whereby the crystal breaks up and seeds multiple crystals [30]. Secondly it disperses the aqueous phase via shear forces, and thirdly serves to sweep emulsifiers and TAG crystals onto the interface, stabilising it. Finally, due to the high shear and heat transfer of the system [171] compared to other conventional heat exchange processing methods [172] [173], it is highly effective at controlling crystal size, polymorphism and number [174] as well as aqueous phase dispersion (and stabilisation) [33], making it a lucrative tool in the formulation of emulsions. The newly formed w/o emulsion was then passed through the PS, the role of which is to break up associations forming between adjacent crystal microstructures preventing an extended fat matrix network structure [175], softening the end product [176] to the organoleptic and textural requirements, and to also prolong heat transfer control, which is specified by controlling water temperature travelling through the jacketing of the vessels.

Upon heat transfer at the cooling wall in the SSHE, TAGs crystallise via first order kinetics [30], firstly adopting either the 'chair' or 'tuning fork' conformation [177]. Such is the shape of these molecules that they are able to align opposite one another and pair up. These pairs may then organise in a number of ways and accumulate to form nanostructures, and these subsequently may aggregate to give the primary crystal structures. Further association and

flocculation can then eventually cumulate into a three dimensional fat matrix structure [30] [178] [179] [177].
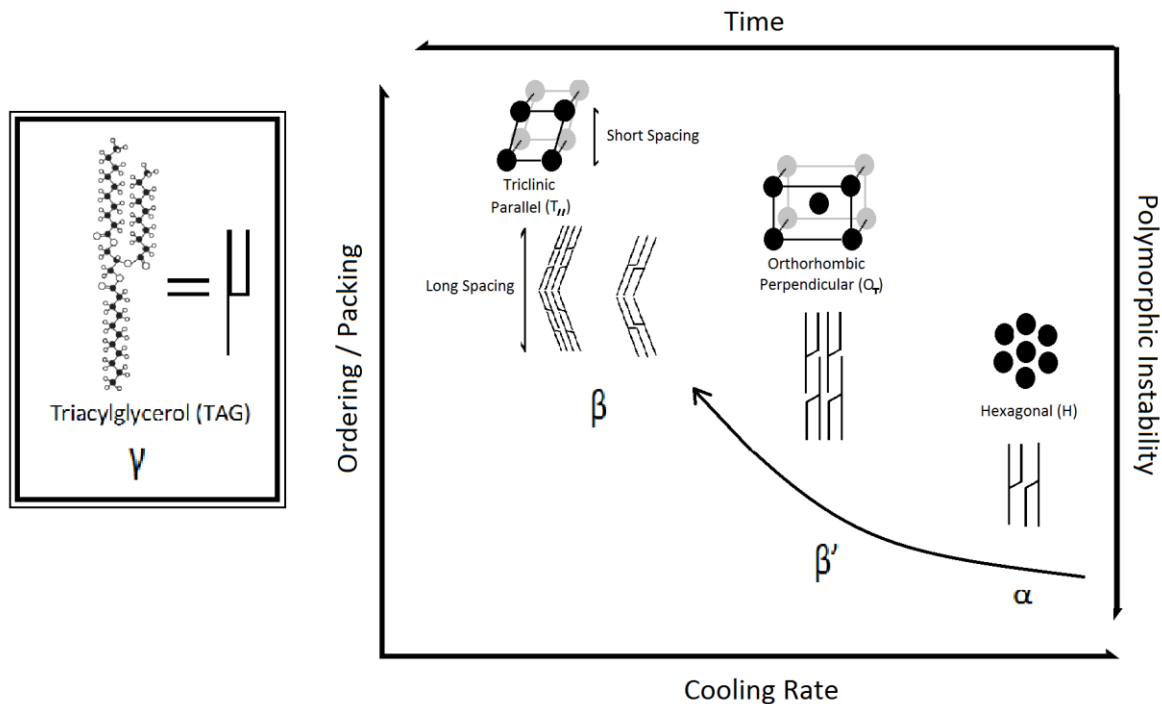
Fig. 29: Schematic visualising the dependency of TAG crystal polymorphic ordering, packing and inherent stability upon cooling rate and resting time [181]. Simplified representations of packing arrangement are included.

TAG molecules are able to adopt different polymorphic crystalline structures as shown in Fig. 29; specifically, hexagonal (H) α, orthorhombic perpendicular (O_T) β', or triclinic parallel (T_{II}) β [180], of increasing structural order, and subsequently increasing energy of packing and polymorphic stability. Polymorphic stabilisation is progressive, and therefore less stable α crystal polymorphs will usually form first, as they are very basic nanostructures compared to the others and require less specific orientation, and therefore less orientation time. These will then organise to form the more stable β' crystal orientation rapidly (typical time scale of microseconds – well within the residence time of the SSHE) and then similarly structure will

then look to further reorganise to achieve maximum stability [169] [178] [179] over time after passing through the SSHE (and continuing after the whole SSHE & PS process) (Fig. 29). The greater the ordering of the polymorphic arrangement, the more specific the organisation of TAGs is. Subsequently, slower cooling rates will provide greater opportunity for sufficient orientation of TAG molecules to adopt more stable, more ordered structures, and will therefore favour these polymorphic forms (Fig. 29). Lower energy structural ordering will inherently require greater energy input to dissociate, and this is reflected by increasing melting point of the crystal polymorphs from α to β' [181] [182] [183].

Three points should be highlighted at this stage, firstly; this is a one way process due to thermodynamic obligation of the molecules to achieve the most stable form, and that the reverse process is thermodynamically unfavourable. Secondly, it is not always necessary for the crystals to adopt each crystal morphology in turn in order to achieve the high energy, and specific temperature, cooling rate and shear conditions may temper the TAG directly to a more stable packing structure [184]. The third and final point is that whilst the β form may be thermodynamically desirable it may not always be viable. Because the β lattice is highly ordered, if the TAG molecules are too dissimilar (TAGs have very different shapes) or are shaped in such a way that packing is difficult (e.g. polyunsaturated) this can make more structurally ordered crystal polymorphs unviable [185]. Marangoni & Narine [167] indicated that typical non-hydrogenated PO shortening favours β' over β polymorph, likely to be a combined result of all of these factors.

Once formed, elements on the crystal microstructures may associate via weak bonding to similar elements on adjacent crystal microstructures (Fig. 30). In this manner an extended fat matrix structure may develop, forming the macrostructure.

156
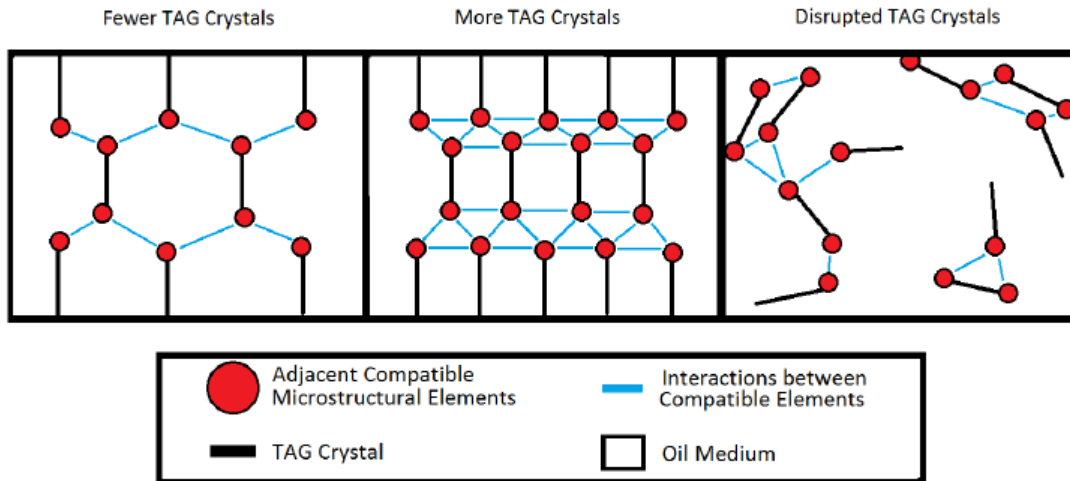
Fig. 30: Idealised schematic of TAG fat crystal organisation in relation to interactions between compatible elements between crystal microstructures. Note the interruption to the extended weak link network in the emulsion system which has been disrupted, for example via pin stirring.

The microstructure of TAG crystals is one of an orthodox amorphous solid, however the macrostructure of multiple microstructures together is fractal in nature. Narine et al. [186] demonstrated a series of models by which the mechanical strength of a TAG macrostructure may be approximately attributed to the microstructure crystal components, and their organisation relative to one another.

The first of these considers a weak-link model; indicating that macroscopic strength and solid character will be defined by the limiting factor; i.e. the strength of the weakest bonding, therefore the strength of association between crystals will define the mechanical properties of the bulk fat network, and not the internal strength of the crystals themselves.

According to the fractal network model however [186]; stress will be more efficiently transferred through microstructures rather than between microstructures, therefore larger crystal sizes will dissolve stress more efficiently, reducing stress concentration.

Finally, the van der waals forces acting within the network are considered (dipole forces are acceptably negated, as for non-polar fat particles in a non-polar oil solvent they are of the order of 10^{10} times smaller). These are the associative forces between compatible elements on adjacent microstructures, which must be overcome in order for microstructures to move past one another, and will define the macrostructures resistance to flow and bulk deformation [187] [28]. According to the model of fractal mechanics of fat crystal structures [186], the (approximate) force in order to overcome the associative forces between two microstructures is given by Equation 1.

$$F = m\left(\frac{A\sigma^2\varepsilon}{4d_0^3}\right)\left(1 - \frac{11\sigma\varepsilon}{2d_0}\right) \tag{1}$$

Here, F is the force required to overcome the association between the two microstructures, m is the number of adjacent identical pairs of microstructural elements, d_0 is the equilibrium distance between the element pair, A is Hamaker's constant, σ is the diameter of the element (assumed spherical), and ε is the deformation strain. This is an approximation, and makes a number of assumptions; most significantly identical elements and perfect spherical shape. However the critical point from this relationship is that as the force F required to overcome the association between the two microstructures is directly related to the number of associations between elements, m.

Braipson-Danthine et al. [188] established a linear relationship between the level of fat phase crystallisation in w/o PO emulsions and perceived hardness of the fat crystal network. By applying this model it is logical that nucleation of a greater number of (smaller) TAG crystals (for a given mass of TAGs) increases the net total TAG crystal surface area in a system,

subsequently increasing potential number of associative elements on crystal surfaces *m* and therefore the number of weak link associations.

These models for defining mechanical strength are considered with regards to the processing focus of this study. Due to the highly efficient thermal transfer and shear exhibited by the SSHE, crystal microstructures are consistently small, and high in number, the exact extent to which will depend upon processing conditions. It is therefore considered highly unlikely that the fractal network model will bear significant bearing upon the mechanical strength of the continuous fat matrix here, and hypotheses here shall be considered based on a weak link model. SSHE is succeeded by a PS, the primary purpose of which is to disrupt crystal weak linkage associations, and therefore consideration should be given not only to number of crystals and associative elements, but also the disruption they will undergo as they attempt to form an extended network.

It is critical to consider the effects of aqueous phase droplet distribution when trying to understand physical material properties of emulsions. Sullo et al. [42] applied particle/matrix studies on silica/polymer composites [189] to water in cocoa butter emulsions, establishing that larger droplet sizes (within the micron range) decreased the strength of the overall emulsion / composite, accredited to increasing surface area to volume ratios. Processing parameter effects and control upon droplet size must therefore be understood, and considered in conjunction with mechanical strength of the emulsion macrostructure.

Droplet size is highly influential in both the way the product is perceived by the customer (organoleptic quality, appearance, functionality) and also the structure and material behaviour [3]. Free water also influences the longevity of the product and potential for microbial growth. In margarine emulsions, typically target water droplet size is approximately 5μm in diameter, with a threshold of around 30μm where they begin to be perceived orally [176].

In the SSHE, emulsifiers and TAG crystals are swept onto the w/o interface, subsequently contributing towards the stability of the newly formed emulsion. Emulsifiers, such as the one used in these studies, are usually amphiphilic organic molecules comprised of an alternate hydrophobic and hydrophilic end [27], which will sit at the interface preferentially, either end demonstrating affinity toward the fat and water phases respectively (Fig. 31).
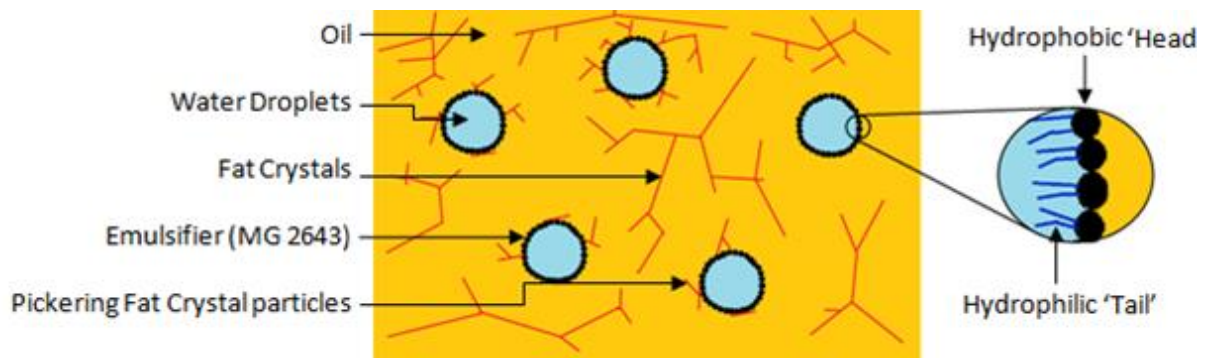
Fig. 31: Schematic representing the structure of Margarine Emulsions.

TAG crystals can associate to those lipophilic emulsifier 'heads' at the interface with sufficient similarity in TAG molecular structure and shape, causing them to sterically inhibit movement and potential coalescence of the droplet (Fig. 31), referred to as the Pickering particle mechanism [190] [191] [192] [30]. The ability of a fat crystal to associate here is referred to as the 'wettability' (albeit confusingly – as the name may incur suggestions of direct water association by TAG crystals, which is not happening), and is partially defined by the steric demands of the crystal morphology: the less stable α polymorph exhibits a higher affinity for the emulsifier monolayer at the o/w interface than β' and β [193], and subsequently they are important in emulsion stabilisation [34] [194] [195]. Higher concentrations of crystal nuclei of wettable character will increase stabilisation effects upon water droplets, simply due to greater numbers available for association (up to the point of saturation – which in itself is

defined by interfacial area), and increased incident probability; reducing the probable time interval from dispersion to TAG crystal association and therefore reducing opportunity for coalescence on the basis of fundamental collision theory [196].

Smaller fat crystals will sit around the interface more comfortably as a result of simple steric inhibition; with greater numbers of TAG crystal association inherently reducing feasibility of droplet migration and coalescence mechanisms. In cases where crystals at the interface are close enough, sintering can actually occur [197] [41] [41] [195] creating a smoothed fat shell around the droplet (Fig. 32). Finally, TAG crystallisation effects upon emulsion stability from the (bulk) continuous phase should be considered, as greater numbers of fat crystal will reduce the spacing in the continuous phase, and increase the degree of adjacent compatible element associations between crystals. Subsequently the continuous phase will be more viscous and droplet movement through the continuous phase will be less energetically viable reducing potential for coalescence and Ostwald ripening [27].
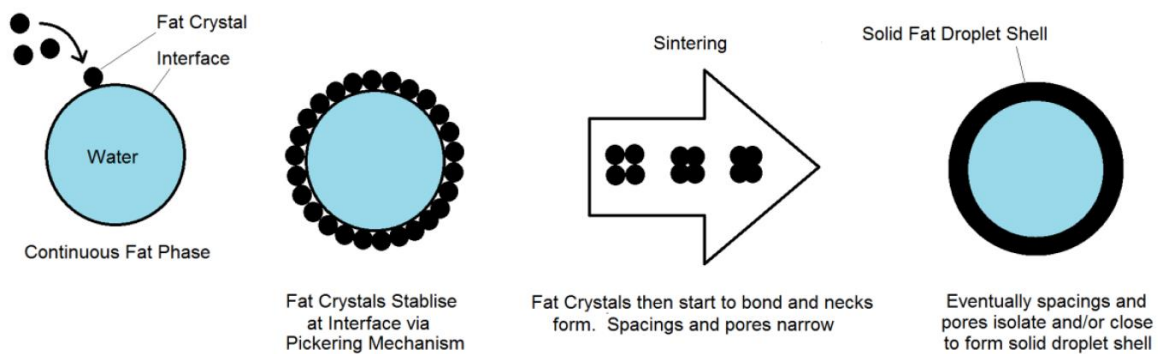
Fig. 32: Mechanism for solid fat droplet shells formation via fat crystal sintering [41] [199] [195].

The implementation of methodical controls on each of the independent process parameters on a conventional margarine line in order to make w/o palm shortening emulsions, and subsequent

systematic interpretation using the physicomechanical studies alongside droplet size studies in particular is a novel approach. Analysis of less conventional material properties such as the bulk modulus have been included within this study alongside more conventional approaches such a yield stress and work done studies, and interpretations cross-compared in order to achieve as broad yet definitive understanding as possible, of how each variable may be used to manipulate the final emulsion.

At this point it is important to highlight that in designing emulsion systems consideration should be given towards emulsion composition: fat type, aqueous/fat phase fraction, emulsifier concentration, emulsifier type, etc. as these will obviously carry a very significant bearing on the emulsion produced. For the purpose of this investigation here however, the emulsion composition was fixed, in order to allow the effects of processing conditions to first be properly defined.

Therefore, by systematically changing processing conditions using a conventional margarine SSHE and PS bench scale processing line this study aims to define the effects of different processing conditions on palm shortening emulsion quality and properties: namely SSHE jacket temperature, SSHE shear rate, PS jacket temperature, PS shear rate, and residence time. Emulsions have been studied using solid fat content (SFC) and Droplet size distribution analysis - which may be considered typical for a study of this nature – and mechanical response aspects towards uniaxial compression – which incorporate a novel physicomechanical approach towards this kind of study.

4.3. Materials & Methods

4.3.1. Materials

TransAdvantage® P-100 NH Palm Shortening was kindly supplied by Cargill™ (Vilvoorde, Belgium). Radiamuls® MG 2643 was purchased from Oleon (Epson, Avril Group, France) and materials were used in varying amounts (defined in text). Radiamuls® MG 2643 emulsifier is a commercially available solid white flake monoglyceride emulsifier blend consisting of 60% glyceryl stearate ($C_{21}H_{42}O_4$). Water used was deionised and distilled from an Aquatron A4000D (Stuart, Staffordshire, UK). Materials used were given no further purification or modification of their properties.

4.3.2. Pre-Emulsion Preparation

Deionised water was held at 80˚C under continued stirring using a hot plate stirrer (Stuart, Staffordshire, UK), prepared in batches of 1 litres. The oil phase was prepared in 1 litre batches by heating the TransAdvantage® P-100 NH Palm Shortening to 90˚C before adding Radiamuls® MG 2643 emulsifier. The oil mixture was then held at 90˚C (well above complete melting point) for 2 hours to ensure complete melting and deletion of any fat crystal memory. Mixture was then cooled to 80˚C prior to mixing with aqueous phase.

The pre-emulsion was prepared in 1.5 litre batches by adding of the required amount of de-ionised water (30% by volume) to the oil phase and mixed using an overhead stirrer (RW20 digital, IKA-Werke GmbH & Co.) at 400 rpm until the mixture appeared homogeneous by visual inspection.

4.3.3. Margarine Line

Water-in-oil emulsions were formed using a bench scale margarine continuous line process (Fig. 33). This comprised of a jacketed scraped surface heat exchanger (SSHE) (volume of 40 ml) followed by a jacketed pin stirrer (PS) (volume of 170 ml), with controllable shear speeds up to 1315rpm and 1345rpm respectively.
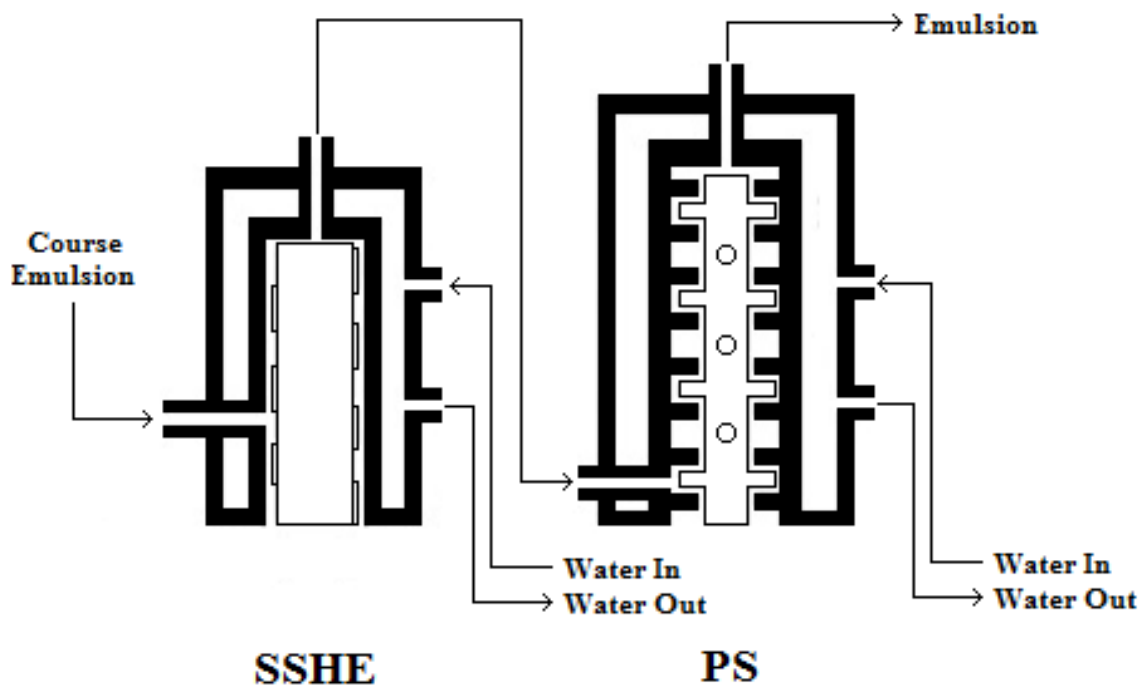
Fig. 33: Cross section schematic of margarine line, dimensions are not necessarily to scale, reproduced from [43].

4.3.4. Emulsification Process

Pre-emulsion was pumped into the SSHE followed by the PS through a silicon flexible pipe (inner diameter 3.2mm; ESCO, SLC, UK) at a constant flow rate controlled by a Masterflex Easy-Load II L/S pump (Cole-Parmer Instrument Company, UK). Jacket temperature (T_{SSHE} & T_{PS} respectively) was controlled by water baths (Julabo, UK) and the emulsion temperature entering and leaving either processing unit was measured ($T_{SSHE\ Enter}$; entering SSHE, $T_{SSHE\ Exit}$; leaving SSHE, $T_{PS\ Enter}$; entering PS, $T_{PS\ Exit}$ leaving PS) using a Data Logger Thermometer (Omega, UK) fitted with a K-Type thermocouple ($\pm0.2\%$ accuracy) via insertion into T-junctions included in the piping. Hot emulsions were poured directly into required moulds depending on analysis (see later) and (unless otherwise stated) allowed to cool to room temperature over approximately 30 minutes before transferring to 5˚C (±1˚C accuracy) storage.

4.3.5. Uniaxial Compression Fracture Studies

Emulsion systems were prepared as above and poured immediately into Ø20mm x 20mm moulds. Cylindrical samples were then loaded onto a TA.XT.plus® Texture Analyser (Stable Micro Systems, UK) with a 5kg load cell and a cylindrical head geometry (Ø40mm). Samples were then compressed at a probe cross head speed of 0.2 mm.s^{-1} to a distance of 5mm from the plate (75% strain). A force trigger of 0.04903N was used. Force/distance data taken directly from the texture analyser was converted into true strain ε_H and true stress σ_T using the Equation 2-5 [98] [99] [136] where ε_E and ε_H are the engineering and true strain, σ_E and σ_T are the engineering and true stress, H_0 and A_0 are the initial height and cross sectional area of the sample, and F and h are the force applied and the height of the sample [99].

$$\varepsilon_E = \frac{(H_0 - h)}{H_0} \tag{2}$$

$$\varepsilon_H = -\ln(1 + \varepsilon_E) \tag{3}$$

$$\sigma_E = \frac{F}{A_0} \tag{4}$$

$$\sigma_T = \sigma_E(1 + \varepsilon_E) \tag{5}$$

From these subsequent true stress / true strain plots, the work done at total failure was determined according to [101], as well as bulk modulus [102]. Stress at total failure was also recorded. Due to the lubricant nature of the fat continuous samples frictional forces perpendicular to direction of compression were negligible and no barrelling occurred. Experiments were performed at 20±1˚C and to 10 repeats and averaged.

4.3.6.   Uniaxial Compression Squeeze Flow Studies

Emulsion systems were prepared as above and poured immediately into Ø30mm x 8mm moulds. Cylindrical samples were then loaded onto a TA.XT.plus® Texture Analyser (Stable Micro Systems, UK) with a 30kg load cell and a cylindrical head geometry (Ø75mm).

Samples were then compressed at a probe cross head constant force of 150 N, and constant sample volume between plates of $5.65 \times 10^{-6}\,\mathrm{m}^3$, until change in sample height was held (to within 5% strain deviation) for 20 seconds. Sample height / time data was taken at a rate of $100\mathrm{s}^{-1}$ and final limiting thickness H_L was recorded. A force trigger of 0.04903N was used and studies were performed at 20±1˚C and in triplicate.

Extensional yield stress (or yield stress parameter), is an analytical assessment for the flow of semi solids and at what sample height or thickness an equilibrium is reached during viscous – plastic fluid flow [198] [199]. Apparent extensional yield stress was determined using the Equation 6 [199], where σ_y is the apparent extensional yield stress, F is the force applied, R_0 is the initial radius of the cylindrical specimen and H_0 is the initial height of the specimen sample. Due to the lubricant nature of the sample, perfect slip has been fairly assumed here in these calculations.

$$\sigma_y = \frac{(FH_L)}{\pi R_0^2 H_0} \tag{6}$$

4.3.7. Droplet Size Measurements

Emulsion systems were prepared as above and poured immediately into 50ml plastic sample pots and stored for 21 days unless otherwise specified. Water droplet size was measured using nuclear magnetic resonance (Minispec Bruker Optics, UK) attached to a LTC4 Refrigerated Circulating Bath with TX150 Circulator (Grant Instruments, Cambridge, UK) for probe chamber temperature control, and analysed using a w/o emulsion specific droplet application software [42]. A detailed explanation of the extended theory behind droplet size calculation and analysis in food emulsions is available [200] but will not be pursued further here.

Samples of approximately 1mL were taken from each emulsion using a metal plunger and transferred into a 10mm glass NMR tube (Bruker Optics, UK). Readings were taken at a chamber / sample temperature of 5˚C. Tests were performed in triplicate.

$$d_{3.2} = d_{3.3} \times e^{-\frac{1}{2}\sigma^2} \tag{7}$$

Direct droplet analysis granted the volume-weighted mean diameter of water droplets; or $d_{3.3}$. This was then converted to the surface-weighted mean diameter; $d_{3.2}$ (whilst $d_{3.3}$ is commonly reported in NMR studies, $d_{3.2}$ is more typically reported across a wider range of techniques [200]) via Equation 7, where $d_{3.3}$ is the volume-weighted mean diameter of water droplets, $d_{3.2}$ is the surface-weighted mean diameter of water droplets, and σ is the standard deviation of the logarithm of the water droplet diameter as recorded by the software. 'Free' water (inclusive of droplet sizes above 50μm in volume weighted diameter) was also recorded.

4.3.8. Solid Fat Content Measurements

Emulsion systems were prepared as above and poured immediately into 50ml plastic sample pots and stored for 21 days unless otherwise specified. Solid fat content (SFC) was measured using nuclear magnetic resonance (Minispec Bruker Optics, UK) and practical set-up was identical to that of water droplet size analysis (above).

The application used this time was liquid fat content specific software specifically designed for the NMR (Bruker Optics, UK). All NMR measurements were then carried out at 20±1˚C, and then afterwards again at 50˚C on the sample samples. A sample of pure sunflower oil was also included for correction using Equation 8 with regards to temperature dependence of liquid proton relaxation time (detector 'dead time' [201] was accounted for in system calibration).

$$C = \frac{Sunflower\ Oil\ FC_{50}}{Sunflower\ Oil\ FC_{20}} \qquad (8)$$

$$SFC\%_{20°C} = \frac{Total\ FC_{50°C} - (C.LFC_{20°C})}{Total\ FC_{50°C}} \times 100 \qquad (9)$$

Using all this data, Solid Fat Content at 20˚C as a percentage of total fat content was then determined for each sample with Equation 9 [201] where $SFC\%_{20°C}$ is the solid fat content as a percentage of all fat in the sample at 20˚C, Total $FC_{50°C}$ is the complete fat content in the sample (measured at 50˚C when all the fat is in the liquid state and is therefore all detectable by the equipment), $LFC_{20°C}$ is the liquid fat content of the sample at 20˚C, and C is the correction factor that is obtained by dividing the sunflower oil liquid fat content reading at 50˚C by that at 20˚C. Results were reported as an average of three replicates.

4.4. Results & Discussion

The organisation of the dispersed phase: defined here using free water and droplet size, is critical to emulsion mechanical and functional behaviour [27]. By defining droplet size distribution it is not only possible to explain the mechanical properties, but also to understand the mechanisms involved in the fat phase development, which accumulate in the final structure.

4.4.1. Droplet Size (d3.2) and Free Water

T_{SSHE} was set at 16˚C, 18˚C, 20˚C and 22˚C and resulting emulsion surface weighted droplet sizes ($d_{3.2}$) and free water values have been compared as a function of emulsion exit temperature from the SSHE (Fig. 34). The NMR regarded any water droplets above ~50μm in diameter as free water. Unless otherwise specified, ω_{SSHE} = 1315rpm, ω_{PS} = 1345rpm, T_{SSHE} = 18˚C, T_{PS} = 20˚C, Q = 0.5ml.s^{-1}.

Increasing T_{SSHE} increased $d_{3.2}$, whilst implementing a higher blade tip speed was observed to decrease $d_{3.2}$. Similarly, free water increased significantly with increasing T_{SSHE} and lower ω_{SSHE}. When studies were performed upon PS parameters, $d_{3.2}$ and free water were observed to be independent of PS temperature (T_{PS} = 18˚C, 20˚C, 22˚C and 24˚C) and pin speed (ω_{PS} = 1345rpm and 672rpm).

These observations closely resemble those reported in studies upon cocoa butter emulsions [33]; T_{SSHE} and ω_{SSHE} displaying significant control over water droplet size, whilst T_{PS} and ω_{PS} exhibit no observed control upon the dispersion of the aqueous phase.

Decreasing T_{SSHE} and ω_{SSHE} favoured smaller free water and droplet size. In order to facilitate this the processing must firstly disperse the aqueous phase sufficiently, and secondly stabilise that dispersion created by reducing interfacial tension and/or preventing coalescence [27].

Fig. 34: (a) Mean surface weighted droplet size (d3.2), and (b) Free water percentage, for PO 68%, HMMGE 2%, water 30% emulsions as a function of exit temperature from the SSHE unit for ωSSHE 1315 rpm (♦) and 657 rpm (◊).

Considering the exclusive dependency [33] upon the SSHE mixing step, the roles of individual processing steps should be considered relative to emulsion (fat and aqueous phase) structuring. As discussed earlier, the SSHE serves to initiate fat crystallisation, control crystal growth (both size and polymorphism), disperse the aqueous phase, and then sweep stabilisers onto the interface, and any or (most likely) a combination of these factors can be used to control the stability of an aqueous dispersion.

Increasing SSHE blade tip speed was observed to decrease water droplet size and free water concentration, improving stability of the emulsion. As blade speed is increased so blades pass through the mixture more often, and therefore increase the shear exhibited upon the water phase. Subsequently the water droplets will be broken up more, and the dispersion will be greater, producing a higher number of smaller droplets which will then require stabilisation to avoid rapid coalescence.

Similarly, as increasing SSHE blade tip speed will increase the pass rate through the aqueous phase, so too will it increase the rate at which emulsifier molecules are swept onto the interface, where they will bind tightly. Subsequently incidence at the interface will be faster, reducing opportunity for coalescence and stabilising smaller droplet sizes.

In addition to this SSHE blade tip speed defines the rate at which TAG molecules are swept onto the jacket cooling wall. At higher blade speeds the rate of transfer to the jacket cooling wall will therefore be greater, and subsequently the heat transfer away from the emulsion will be greater.

TAGs will cool and subsequently start to crystallize by configuring into tuning fork / chair conformations and pairing to form lamella base polymorph (Fig. 29). Because higher SSHE shear rates will increase the rate of the TAG transfer to and from the cooling wall, this will increase the rate of crystal nuclei formation.

As blade speed controls movement of emulsifier onto the interface, so too does it define the rate at which TAG crystal nuclei are swept onto the interface. Therefore increasing the blade tip speed would be expected to also increase the transfer rate of crystal nuclei onto the interface, where Pickering particle stabilisation may potentially occur [195] (Fig. 31), and subsequently speed of droplet stabilisation would be further increased.

Decreasing T_{SSHE} was observed to decrease $d_{3.2}$ and free water. Increased cooling will not impact upon the rigidity nor chemical properties of the water phase to any significant degree for the temperature range used here, and therefore the observed trend of increased emulsion stability - as represented by decreasing droplet size and free water; with decreasing T_{SSHE} is likely to result from control of the fat continuous phase.

Decreasing T_{SSHE} will increase the temperature gradient between the wall and the emulsion mixture, therefore the rate of latent heat conduction away from the TAGs which are moved onto the cooling jacket wall will be higher, and crystal nucleation will occur faster and in favour of higher energy order polymorphic organisation [178] [202] [180] [203].

TAG crystal affinity for emulsifiers (at the interface – which then can lead to stabilisation of droplets via the Pickering particle mechanism) is dependent upon the 'wettable' character of TAG crystals [30] [27] [194]. Less stable crystal polymorphs (e.g. α) as favoured by faster nucleation have been established as exhibiting increased interfacial affinity [193] [190] therefore associating to the interface more effectively, and lowering interfacial tension, stabilising smaller droplet sizes. As less stable crystals are also typically the fastest forming, so they will also be the first to be readily available for movement onto the interface to stabilise via a Pickering particle mechanism [192] [191] [204] [205] [194] decreasing opportunity for coalescence.

Increased nucleation via blade tip speed and/or temperature control will subsequently increase the viscosity of the emulsion, as viscosity is approximately directly related to the amount of solid material present in the system. Subsequently shear viscosity will increase, increasing the shear forces exhibited upon both fat and aqueous phases; further facilitating secondary nucleation [174] [195] [30] and droplet break up [33] respectively, whilst simultaneously increasing the kinetic energy for coalescence of newly formed droplets.

The observation that the aqueous phase dispersion quality is unaffected by the ω_{PS}, as similarly observed by [33] in cocoa butter emulsion studies, suggests that the shear force generated in the PS mixer is not high enough to impact upon the droplets and disperse them further.

Emulsion dispersion was observed to increase with residence time, as defined by $d_{3.2}$ (Fig. 35a) and free water (Fig. 35b). This would agree with above hypotheses regarding dispersion and stabilisation effects of the SSHE, and the null hypothesis with regards to PS effects. Increased residence time will allow for greater exposure to shear in the SSHE, breaking droplets up further, moving more material to the interface and/or the cooling wall, whilst also being subject to fast cooling for longer, promoting rapid crystal nucleation.

Subsequently dispersion of the aqueous phase is greater, and interfacial stabilisation and annealing is more proficient, resulting in stabilisation of smaller stabilised droplet sizes. Resident time in the PS is much greater than that of the SSHE, yet it does not appear to exhibit any emulsion structure breaking effects with regards to droplet size or free water (Fig. 35). This, and the earlier referenced observations that changing PS temperature and pin speed parameters did not impact upon droplet size nor free water concentration lead us to the hypothesis that the PS process step exhibits negligible control over aqueous phase dispersion and stabilisation.
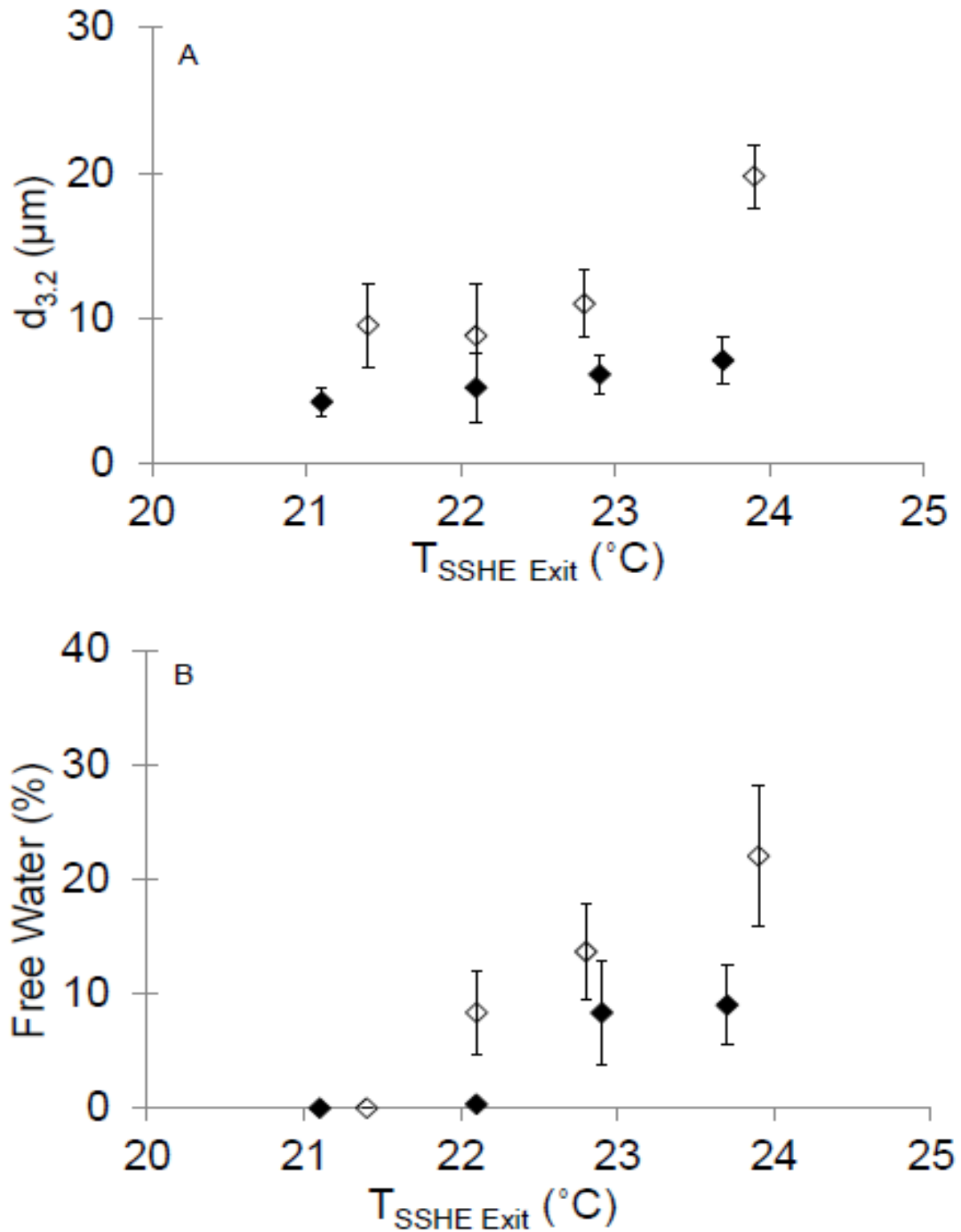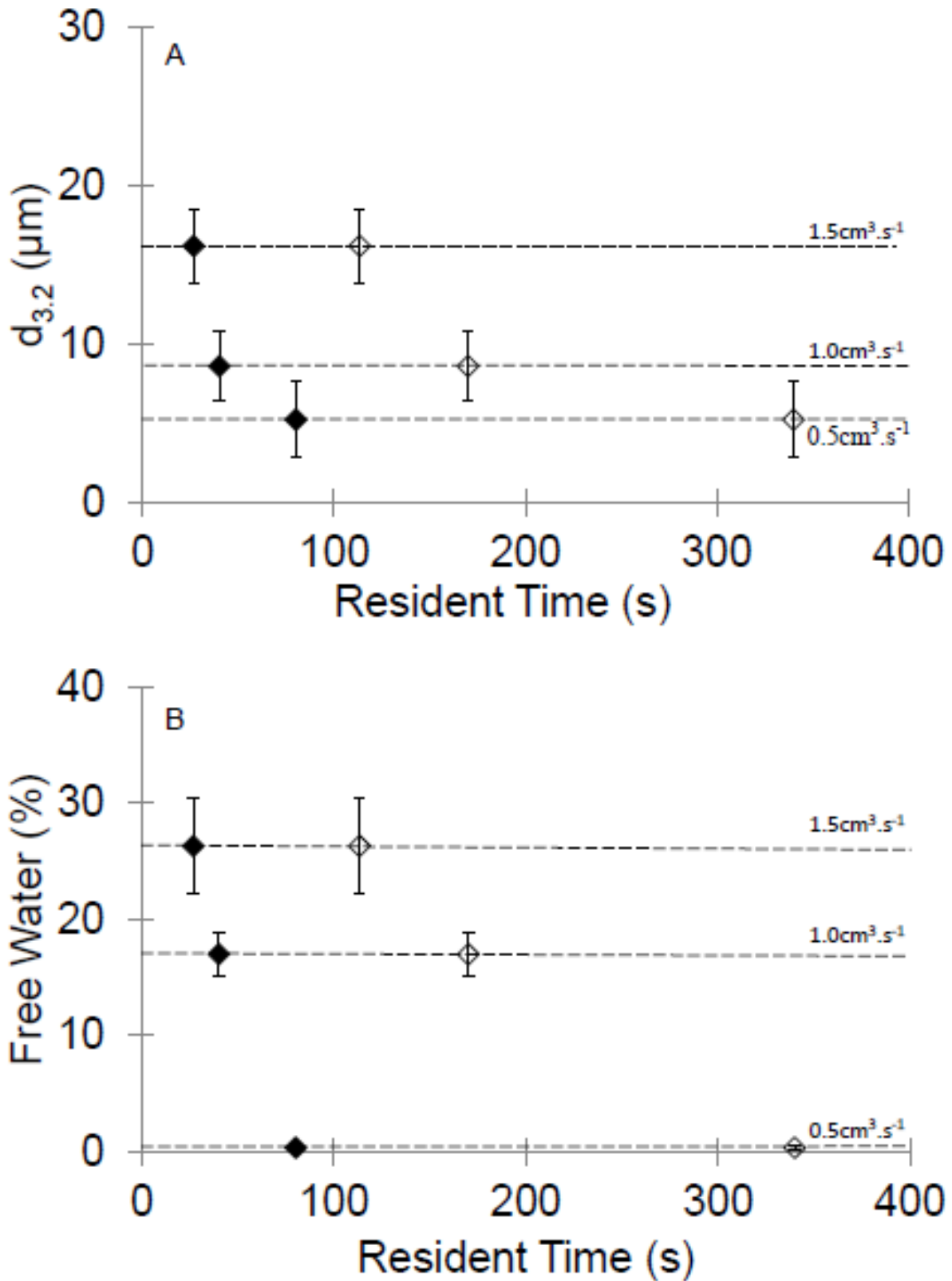
Fig. 35: (a) Mean surface weighted droplet size (d3.2), and (b) free water percentage, for PO 68%, HMMGE 2%, water 30% emulsions as a function of resident time. Respective resident time in SSHE unit (♦) and PS unit (◊) are shown.

Finally, as a broader consideration of industrial application, it should be highlighted that the sensitivity of the physical emulsion properties towards processing temperature is high (to $\pm 1^\circ C$), indicating any scaled up application should give serious consideration to temperature control, precision, and any process variability.

It has been established therefore, that increasing SSHE cooling; which promotes TAG crystal nucleation and typically favours low order energy less stable TAG crystal polymorphism, and increasing SSHE shear rate; which promotes aqueous phase physical break up and movement of particles towards the cooling wall and/or the interface, successfully stabilise smaller aqueous phase droplet sizes (and inherently higher interfacial areas) in water / PO emulsions, understood to result from both increased initial dispersion forces and interfacial stabilisation. Comparatively, PS mixing exhibits no effect upon aqueous phase dispersion and stabilisation. We shall now look to consider the effects of the same processing parameters upon emulsion mechanical properties, and resistance to applied force, bringing forward understandings of the process already discussed, and those hypotheses drawn.

4.4.2. Large Deformation

Uniaxial deformation studies were performed on the PO margarine w/o emulsions. By observing the mechanical property trends over specific controlled processing parameters up to and including the point of macroscopic failure, and making cross comparisons with droplet size analysis, it is possible to construct a strong hypothesis upon how the microstructure has defined each material behaviour trend in turn, attributed to the combined factors [206] [183] [188] [207]. Fat phase structuring has been considered in accordance with weak link theory and van der waals' associations between TAG crystals [186] [183].

A typical true stress vs. true strain plot is shown (Fig. 36). From this stress to failure, 'bulk' modulus and work input to failure were recorded. Area below the plot up to failure is representative of work input to failure.

It can be clearly observed that the initial linear elastic region [100] of typical interest in more elastic systems; polymer gels for example, is extremely short (<0.01) and thus any surface irregularities (which are probable in such crystallised semi solid soft food emulsions) may likely lead to a valuation inaccurate to the true value [208], and as such Young's elastic modulus has not been investigated in these studies here.
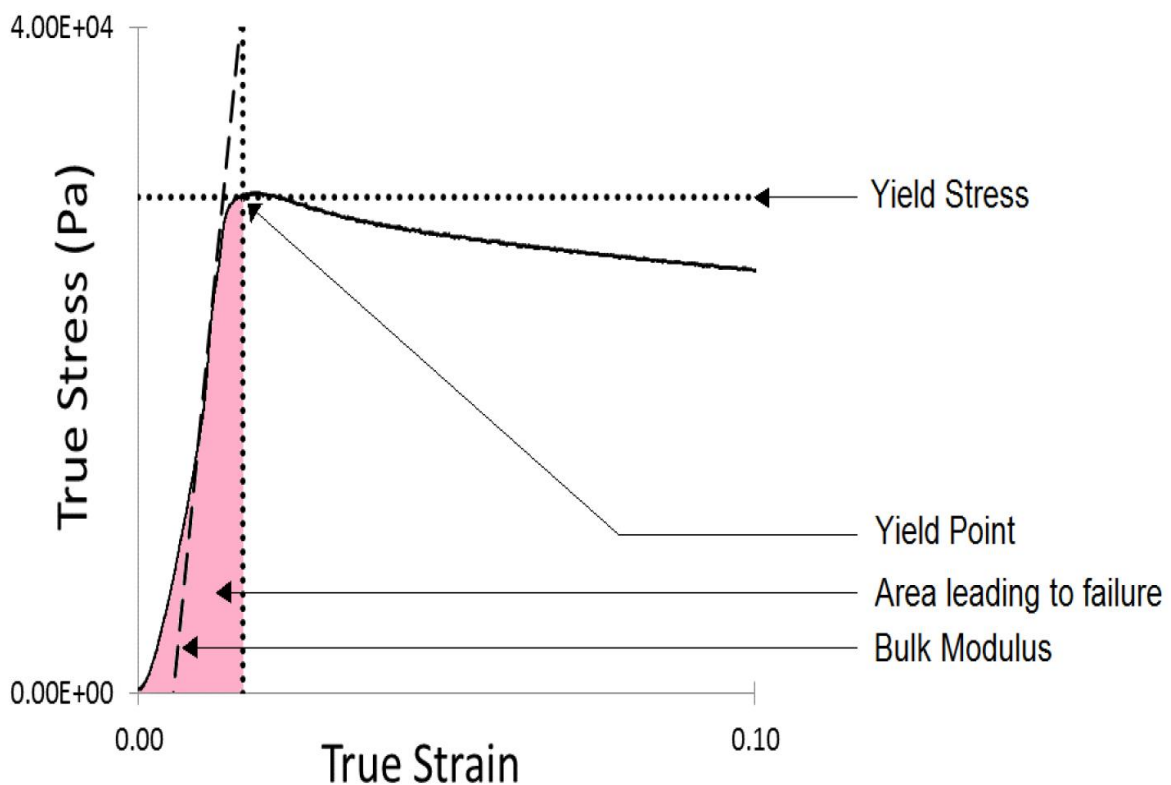
Fig. 36: True stress vs. true strain plot under uniaxial compression to failure, typical of all plots for these systems. Bulk modulus (— — —) for uniaxial compression was assigned by eye as the final extended linear region prior to failure. Vertical and horizontal dotted lines (●●●) indicate strain and stress of fracture, respectively.

All sample plot data fitted the fracture behaviour of a 'brittle' material; whereby limited plastic deformation precedes bulk failure, observed as a failure below 0.2 strain under high stress [116] [42]. Following the point of failure samples are observed (Fig. 36) to adopt less brittle behaviour, rather than falling away sharply they instead continue to withhold high stress to continued increasing strain, decreasing (stress) very gradually.

This is typical of non-Newtonian Bingham plastic behaviour [209]; once the yield stress point is reached the accumulative resistance threshold to macroscopic deformation produced by the bulk extended network of TAG crystals association has been superseded, and they will proceed to move past one another and break apart from one another dependent on the fracture propagation and the unique structure of the individual network, however weak van der waal linkages between associating elements on adjacent microstructures will still be present which must then be overcome for continued progressive strain, thus this brittle-to-spreadable behaviour is observed [208] [210]. This is investigated in more detail later via squeeze flow experiments.

4.4.3. Large Deformation: Macroscopic Failure

Work input to failure for simple emulsions produced as a function of SSHE and PS speeds and temperatures is presented in Fig. 37 a&b respectively. Unless otherwise specified, ω_{SSHE} = 1315rpm, ω_{PS} = 1345rpm, T_{SSHE} = 18˚C, T_{PS} = 20˚C, Q = 0.5ml.s^{-1}.

T_{SSHE} was set at 16˚C, 18˚C, 20˚C and 22˚C and resulting emulsion failure work values have been compared as a function of recorded emulsion exit temperature from the SSHE ($T_{SSHE\,EXIT}$) (Fig. 37a). Increasing T_{SSHE} was observed to decrease failure work of emulsions in a linear relationship. Higher SSHE blade tip speeds (1315rpm) were observed to increase emulsion failure work (Fig. 37a) by comparison to lower blade speed (657rpm).
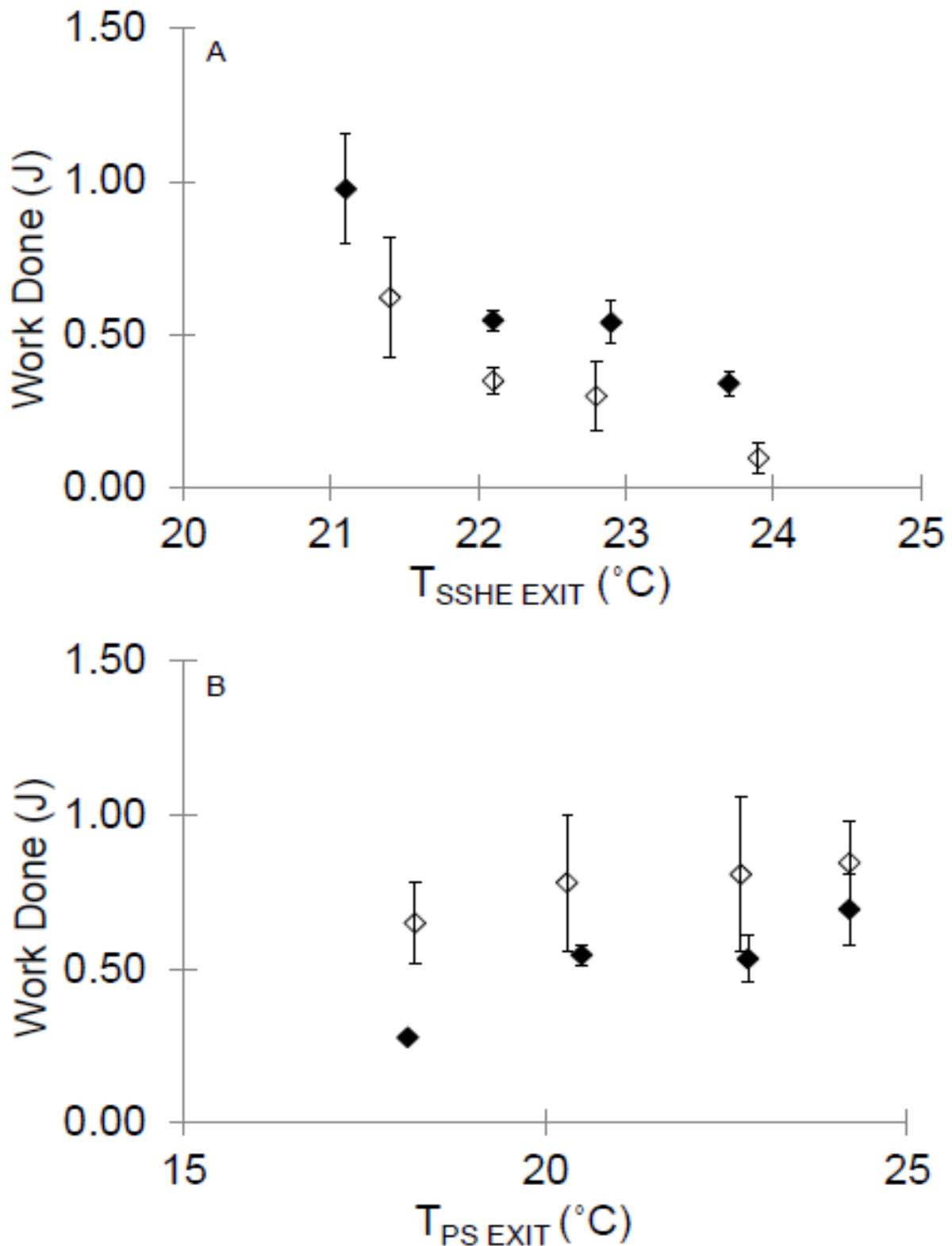
Fig. 37: Work required leading to failure for PO 68%, HMMGE 2%, water 30% emulsions as a function of (a) exit temperature from the SSHE unit for ωSSHE 1315 rpm (♦) and 657 rpm (◊), and (b) exit temperature from the PS unit for ωPS 1345 rpm (♦) and 672 rpm (◊).

Yield stress of emulsions (Fig. 37) was also recorded and similarly analysed in relation to processing parameters. Relationships between processing parameters and emulsion yield stress - of which $T_{SSHE\ EXIT}$ effects are shown in (Fig. 37) as an example; were observed to be analogous to those of failure work studies in all cases. This is considered logical as failure strain is low (Fig. 36) and deviations are small, and the shape of the curve leading to compression is similarly consistent, the emulsions not exhibiting any significant strain hardening / softening behaviour prior to failure.
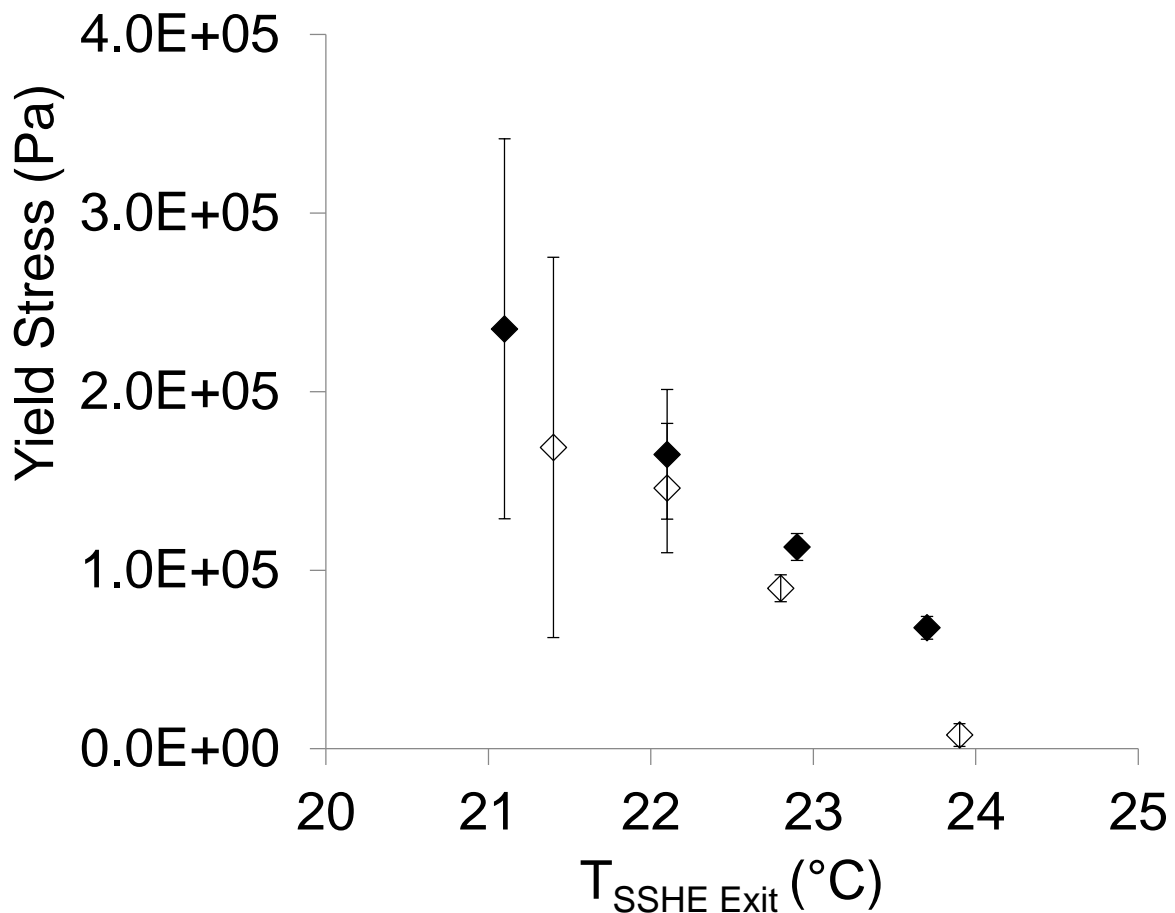
Fig. 38: Yield Stress at point of failure for PO 68%, HMMGE 2%, water 30% emulsions as a function of exit temperature from the SSHE unit for ωSSHE 1315 rpm (♦) and 657 rpm (◊).

A number of trends are observed in resistance to failure (represented by failure work (Fig. 37) and yield stress (Fig. 38) of emulsion macrostructure, relative to process parameters. Increasing T_{SSHE} decreases macrostructure strength - as indicated by decreasing failure work and yield stress; of emulsions in a linear relationship, whilst doubling blade tip speed (ω_{SSHE}) from 657rpm to 1315rpm increases emulsion macrostructure strength.

As discussed earlier, emulsion structure has been considered within a weak link theory model, on the basis that the high shear, rapid cooling nature of the SSHE process heavily restrict the size of TAG crystal growth and fractal nature of the system [186] [206] [183]. Assuming consistently small crystal sizes and constant SFC throughout the investigation therefore, an alternative mechanism attributing to macrostructure strength controlled by the SSHE mixing step must be considered.

Droplet size and free water investigations (Fig. 34 & Fig. 35) demonstrated that the same conditions which promote emulsion macrostructure strength (Fig. 37 & Fig. 38) also decrease average droplet size of aqueous phase distribution. Crack tip propagation, which accumulates in fracture and represents the initial stage of macroscopic failure [208] [160] originates in regions where stress is allowed to concentrate [189].

If a system is able to transfer applied stress efficiently and distribute it evenly throughout the system, the macroscopic strength of the overall system will be higher. If stress is not dissolved efficiently, it will concentrate in regions of inefficient transfer, and cracks will then propagate here to dissipate the concentrated potential energy (as kinetic energy).

Stress transfer across the oil/water interface is known to be inefficient [42] due to the contrasting rigidity of either phase, to a degree which worsens with decreasing surface area to volume ratio of the droplet i.e. increasing droplet size (Fig. 37 & Fig. 38) [160] [42]. Macroscopic strength of emulsions formulated using SSHE processing conditions which

encourage larger droplet size and free water concentration (i.e. low ω_{SSHE} and high T_{SSHE}) (Fig. 34 & Fig. 35) would therefore be reduced by greater number of regions of stress concentration in the emulsion macrostructure facilitating stress concentration, as is observed in the overall mechanical trends (Fig. 37).
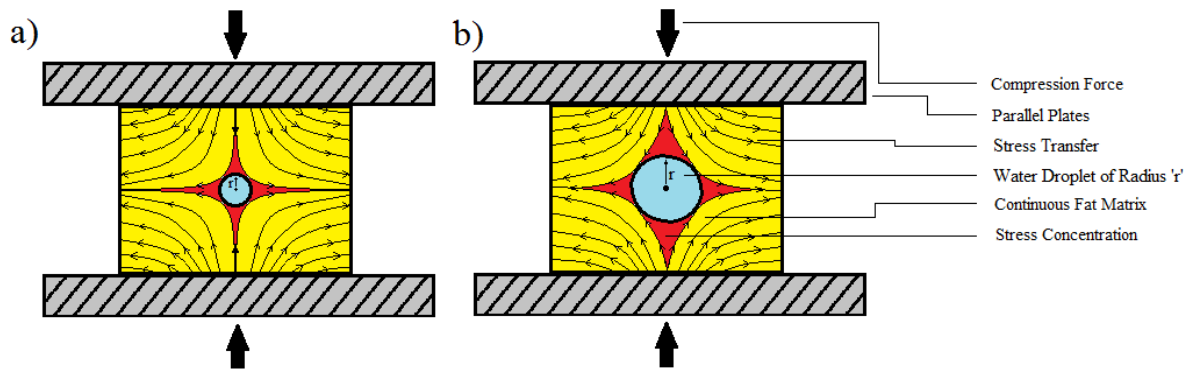
Fig. 39: Diagram demonstrating transfer of stress in emulsion samples with a) smaller water droplet size and b) larger water droplet size, and their respective concentrated stress regions (shown in red).
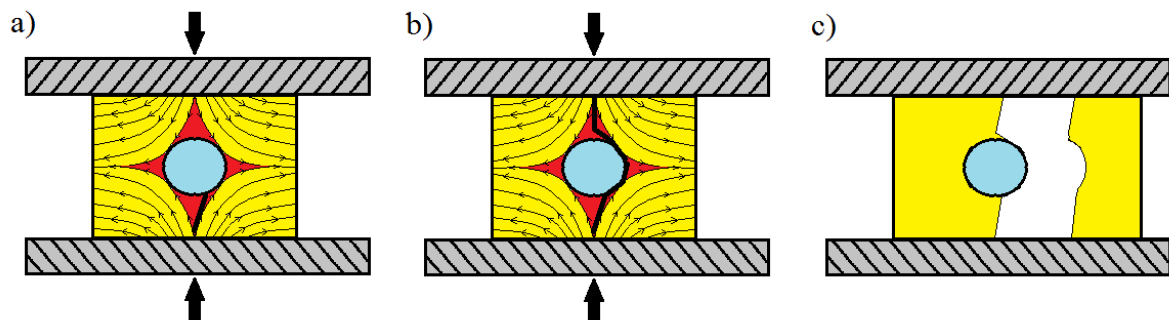
Fig. 40: Stress concentration about droplets (blue) initiating crack propagation (━━━) cumulating in failure of the fat crystal macrostructure (yellow).

T_{PS} was set at 18°C, 20°C, 22°C and 24°C and pin tip speed (ω_{PS}) was set at 1345rpm and 672rpm. Work input up to macroscopic failure has been presented (Fig. 37b) as a function of recorded emulsion exit temperature from the PS ($T_{PS\ EXIT}$). Increasing T_{PS} was observed to increase failure work of emulsions in a linear relationship. Higher SSHE blade tip speeds (1345rpm) were observed to increase emulsion failure work (Fig. 37b) by comparison to lower blade speed (672rpm).

Earlier, emulsion droplet size distribution and free water analysis reported no dependency of aqueous phase distribution upon PS processing within the parameter ranges studied. Consequentially, in order to explain observed macroscopic emulsion strength dependency upon PS processing parameters, the control upon the other, fat continuous phase should be considered.

Upon exiting the SSHE, compatible elements upon adjacent TAG crystal surfaces interact and associate via weak linkage van der waals' forces of attraction (Fig. 30), and subsequently the extended macrostructure of the fat continuous phase develops. The PS, carries a twofold purpose [176]. Firstly, it is employed to work the super cooled crystallising fat, disrupting the development of any extended fat structure. In conventional margarine processing this functions to allow the final hardness and plasticity of the product to be customized to its purpose [211].

Secondly, it is used to increase the overall resident time of the emulsion, so that cooling rate - and therefore fat crystallisation; may be further controlled and fat crystals at the interface of the droplets may be annealed in order to improve shell integrity [212].

TAG crystals will begin to associate once sufficient thermal energy has been removed from the system (via the jacketed cooling system) to overcome a free energy barrier, referred to as the latent heat of fusion. Subsequently, the greater the rate of heat transfer from the emulsion mixture (i.e. lower T_{PS}), the faster this free energy barrier is overcome and the sooner TAG

crystals begin to associate. Correspondingly, lower T_{PS} will facilitate association of TAG crystals faster, and earlier in the PS mixing step, where they will subsequently be subjected to the pin shear forces, disrupting the extended network development and breaking it up. The degree of crystal weak linkage association and extended network development will determine the accumulated associative forces through which a crack must propagate and potential energy required to overcome in order for macroscopic failure to occur, increasing relative to one another, as demonstrated in Fig. 41.
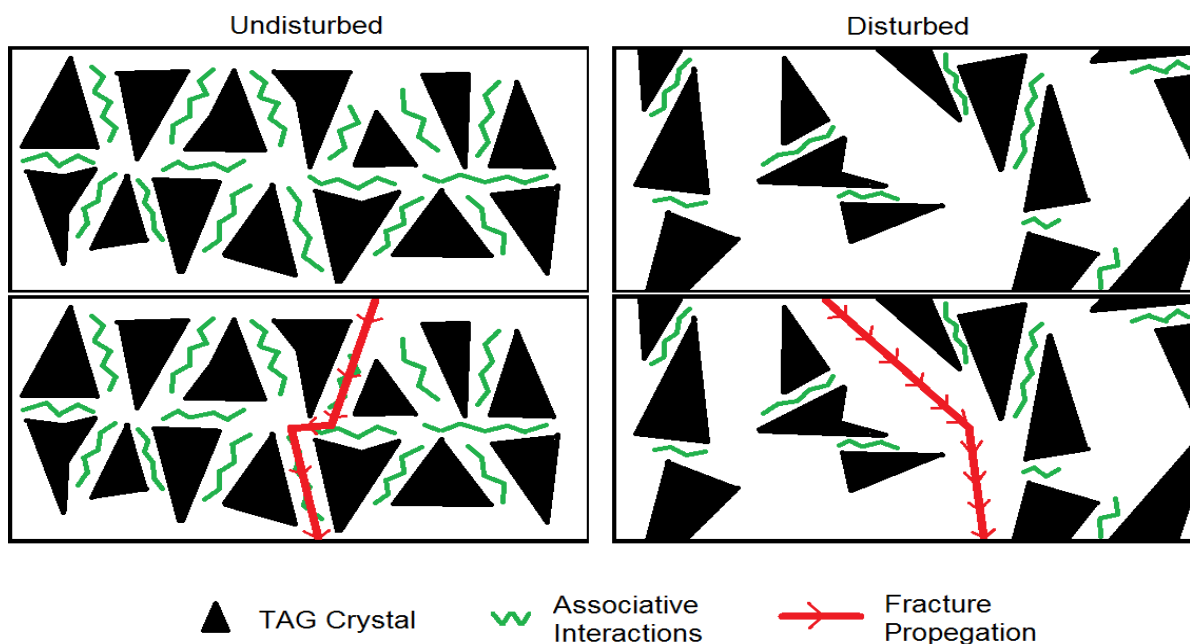
Fig. 41: Simplified schematic indicating how disruption of the TAG crystals in the developing fat matrix affects the associative bonding in the macrostructure.

It is concluded therefore that increasing the cooling rate in the PS, (for a fixed tip speed) would increase the proportion of network development time exposed to PS disruption, and therefore the final fat matrix structure will be less extensive, with less associative linkages to overcome, as demonstrated by increasing emulsion failure work with T_{PS} (Fig. 37b).

Implementing higher jacket temperatures (closer to $T_{PS\ ENTER}$) will encourage higher energy order TAG crystal polymorphism, e.g. β, as it allows time for reorientation of the crystal to achieve more complex arrangements of closer packing (and vice versa with prolonged super cooling and low energy TAG polymorphism). This is unlikely to affect macrostructure strength due to fractal nature of the small crystal sizes, however it could be consequential for reorganisation on the interface for potential fat shell sintering [41] [213] [30] and melting heat resistance of the emulsion.

Building upon this hypothesis, the rationale for ω_{PS} effect on emulsion behaviour is a straightforward one. The greater the pin speed, the more passes through the crystallising fat emulsion structure, and the more the TAG microstructures are broken up and disrupted; resulting in observed (Fig. 37b) decrease in mechanical strength for emulsions processed under high ω_{PS} [175].

Flow rate was set at $0.5ml.s^{-1}$, $1.0ml.s^{-1}$, and $1.5ml.s^{-1}$ and failure work of emulsions presented as a function of time spent in the SSHE and PS units (Fig. 42). Increasing residence time in the SSHE and PS units exhibited an increase in work required to fracture emulsions. Droplet size studies (Fig. 35) showed that increasing residence time decreased droplet sizes and free water percentage, however PS processing conditions were observed to exhibit no effect upon aqueous phase dispersion, relying instead upon SSHE effects. Despite PS process parameters having been established as critically defining emulsion mechanical properties, the structure making effects of the SSHE appear to prevail in resident time dependency, outweighing any accumulative structure breaking effects of increasing time spent in the mixing units proportionally.
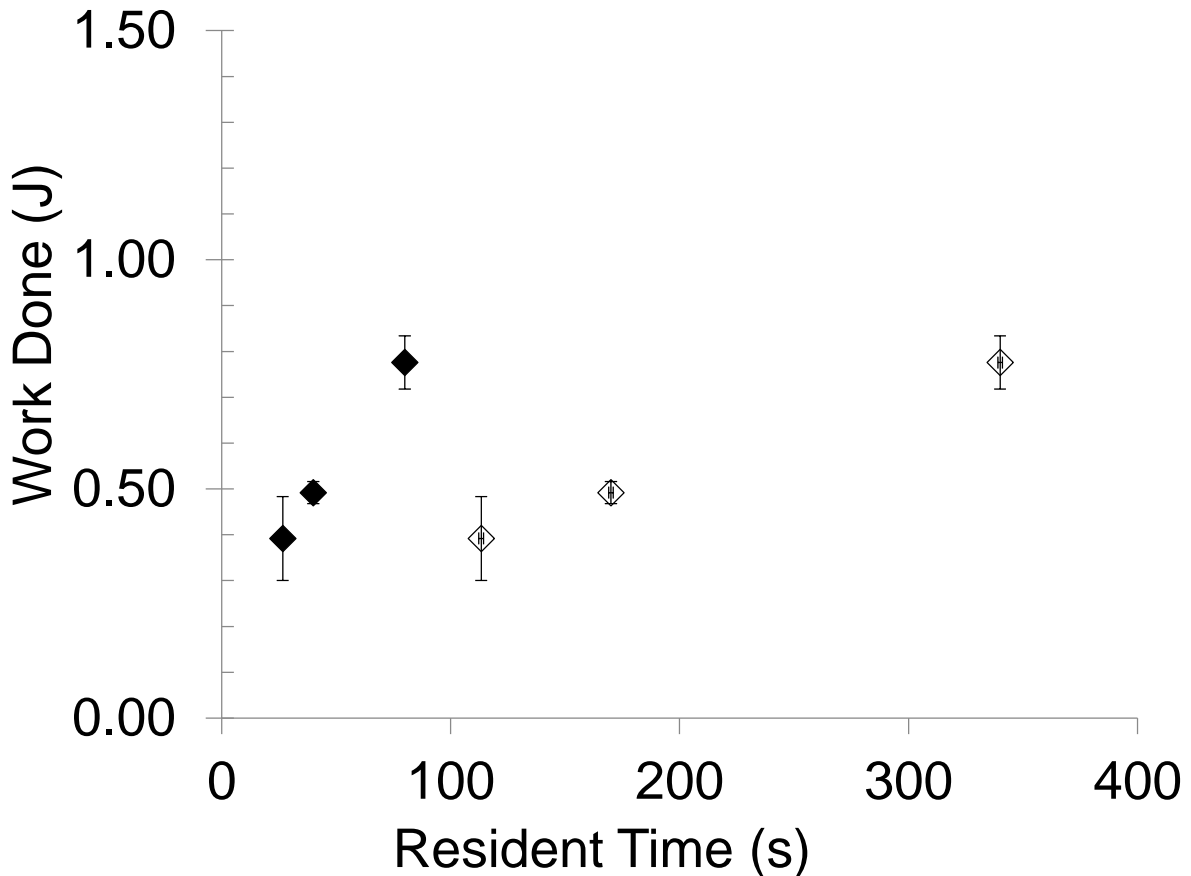
Fig. 42: Work required leading to failure for PO 68%, HMMGE 2%, water 30% emulsions as a function of resident time. Respective resident time in SSHE unit (♦) and PS unit (◊) are shown. Respective flow rates are indicated, horizontal broken lines (▪▪▪) indicate different flow setting investigations.

This reasoning may be developed further when we observe the limited change in material properties of the emulsion when flow rate is then decreased further from 1.0ml.s^{-1} to 0.5ml.s^{-1}. Negligible change indicates that the increased time spent inside the PS unit starts to counter any additional crystal propagation in the SSHE unit as increasing residence time will increase the cooling inside the PS line, and the amount of crystal development and growth occurring inside the processing units which will be subsequently broken up by the PS. Associative network development will progress over an extended period of time, and is not just limited to the time spent within the processing units. As one part of the SSHE purpose is to stimulate

TAG crystal nucleation, it is logical that the effects of this continue to be demonstrated beyond the formulation process, as the crystal nuclei formed in the SSHE continue to grow and develop a network. Contrastingly, the structure breaking action of the PS will seize upon exiting the PS, and therefore SSHE effects would be expected to dominate residence time effects, as demonstrated (Fig. 42).

4.4.4 Large Deformation: Compressibility and Flow

Up until this point studies have considered the mechanical behaviour of emulsions at the point of macrostructure failure. Investigations now turn to consider the mechanical response prior to, and (later) following this point via bulk modulus and squeeze flow analysis respectively, and how these characteristics are defined by the processing parameters.

Uniaxial 'bulk' modulus represents the resistance towards (irreversible) microstructure compaction and distortion prior to macroscopic failure; i.e. the reciprocal of compressibility. It is represented as the gradient of the linear stress vs. strain plot leading up to failure (Fig. 36), as previously used in polymer gel systems [102] [99]. Similarities between the structure development in fat crystal networks and flocculated colloids are well established [186], and subsequently bulk modulus analysis has been applied to the emulsion systems here.

Bulk modulus dependency on SSHE (Fig. 43a) and PS (Fig. 43b) processing parameters is shown. Immediate observations indicate dependency trends of bulk modulus upon processing parameters correlate with those of failure work and yield stress seen earlier (Fig. 37 & Fig. 38 respectively); bulk modulus increasing with ω_{SSHE} (Fig. 43a) and T_{PS} (Fig. 43b), whilst decreasing with T_{SSHE} (Fig. 43a) with ω_{PS} (Fig. 43b), with differences between processing effects appearing to remain proportional to those of work failure (Fig. 37) and yield stress (Fig. 38).

Fig. 43: Bulk modulus for PO 68%, HMMGE 2%, water 30% emulsions as a function of (a) exit temperature from the SSHE unit for ωSSHE 1315 rpm (♦) and 657 rpm (◊), (b) exit temperature from the PS unit for ωPS 1345 rpm (♦) and 672 rpm (◊).

Bulk modulus is a measure of the reciprocal of compressibility for a material prior to the point of bulk failure [214], therefore, as weak link theory dictates the strength of the system is only as great as its weakest bonding, it is the amount of force required to compact the TAG crystals closer together, displacing weak linkages between associating elements irreversibly from their equilibrium position on a micro scale, without causing macroscopic failure through the structure.

The contribution of crystal size and polymorphic packing upon the mechanical strength; and conversely the fractal nature of the systems, has already been assumed negligible; accounting for SSHE regulation of crystal sizes aforementioned. TAG crystal polymorphism will continue to impact affinity towards the interface and subsequently droplet stabilisation and droplet size; which in turn will contribute toward propagation of failure (Fig. 39 & Fig. 40).

SSHE processing parameters will control how droplets are dispersed and stabilised, as previously discussed, and therefore it is concluded that SSHE control mechanisms defining emulsion compression resistance are analogous to those of failure work and stress (Fig. 37 & Fig. 38 respectively); essentially increasing emulsion strength character by increasing droplet stabilisation, decreasing droplet sizes, and subsequently decreasing stress concentration.

Similarly, PS process parameters control bulk modulus via the same principles as for failure work and stress; disrupting weak linkage formation between microstructures and subsequently decreasing the resistance to compaction of the microstructures. Increasing the pin tip speed will logically increase this effect, as will increasing heat transfer (by decreasing T_{PS}), as more weak linkage formation will occur (and subsequently be disrupted) under pin shearing conditions, forming more compressible emulsion systems with less resistance to compaction.

Squeeze flow uses a different experimental technique to the uniaxial compressions used thus far, involving a finite amount of the select sample placed between two surfaces being pushed

out by compressive forces of one or both of the surfaces. Although similar in practice, squeeze

flow studies offer different information to large deformation biaxial compression to fracture

studies, as they define material resistance to flow. A typical sample strain vs. time plot is

shown (Fig. 44).
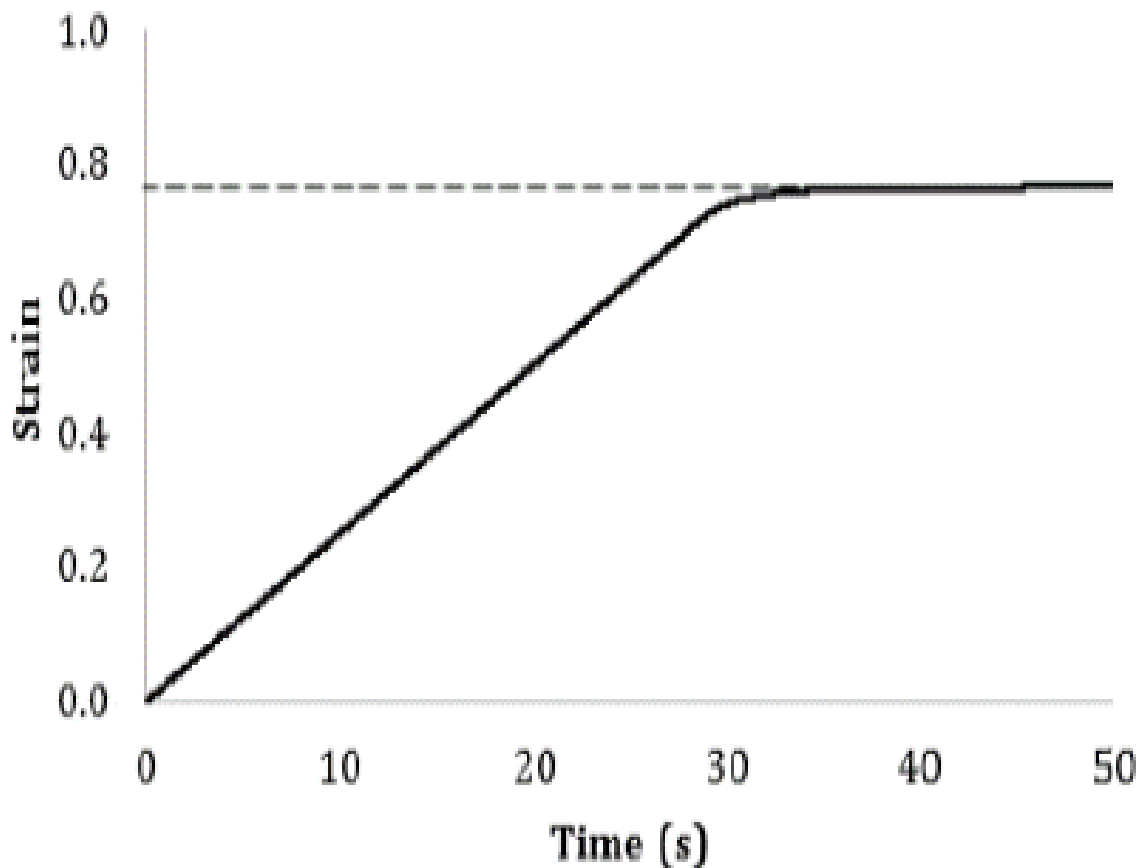
Fig. 44: Typical sample height vs. time plot from squeeze flow studies for emulsion systems. Limiting strain (▬ ▬ ▬) is indicated.

From this data, the limiting strain at which the flow resistance is equal and opposite to the

compressive force may be identified, and subsequently the extensional yield stress

demonstrating the materials ability to resist flow may be determined using Equation 6 [198]

[199].

The flow behaviour of baking shortening is governed by the microstructure, and the organisation of these microstructures to form the macrostructure [215] [176] [27]. In order for squeeze flow to occur the microstructures must move past one another; requiring those weak linkages holding the position of one TAG crystal relative to another to be overcome. As the flow character will be defined by extent of weak link association between adjacent compatible elements, so flow behaviour is predicted to exhibit similar processing parameter dependencies to failure and compression behaviour, which was dominated by weak linkage association.

The effects of the ω_{SSHE} and T_{SSHE} (Fig. 45a), and ω_{PS} and T_{PS} (Fig. 45b), on the extensional yield stress is shown. As for bulk modulus, results display analogous trends to the mechanical property process parameter dependencies observed thus far under large deformation; extensional yield stress increasing with ω_{SSHE} (Fig. 45a) and T_{PS} (Fig. 45b), whilst decreasing with T_{SSHE} (Fig. 45a) with ω_{PS} (Fig. 45b).

As resistance to flow of TAG crystals will be defined by the strength of the interactions holding them in place relative to one another, it is logical that the continuing theme through these studies is equally applicable here; SSHE processing parameters will define the droplet size and inherent stress accumulation, increasing the resistance to flow (represented by extensional yield stress in Fig. 45a) as conditions promote smaller droplet sizes (high ω_{SSHE} and low T_{SSHE}), whilst PS processing parameters control resistance to flow (Fig. 45b) by disrupting network extension of the fat continuous matrix (increasing with high ω_{PS} and low T_{PS}).

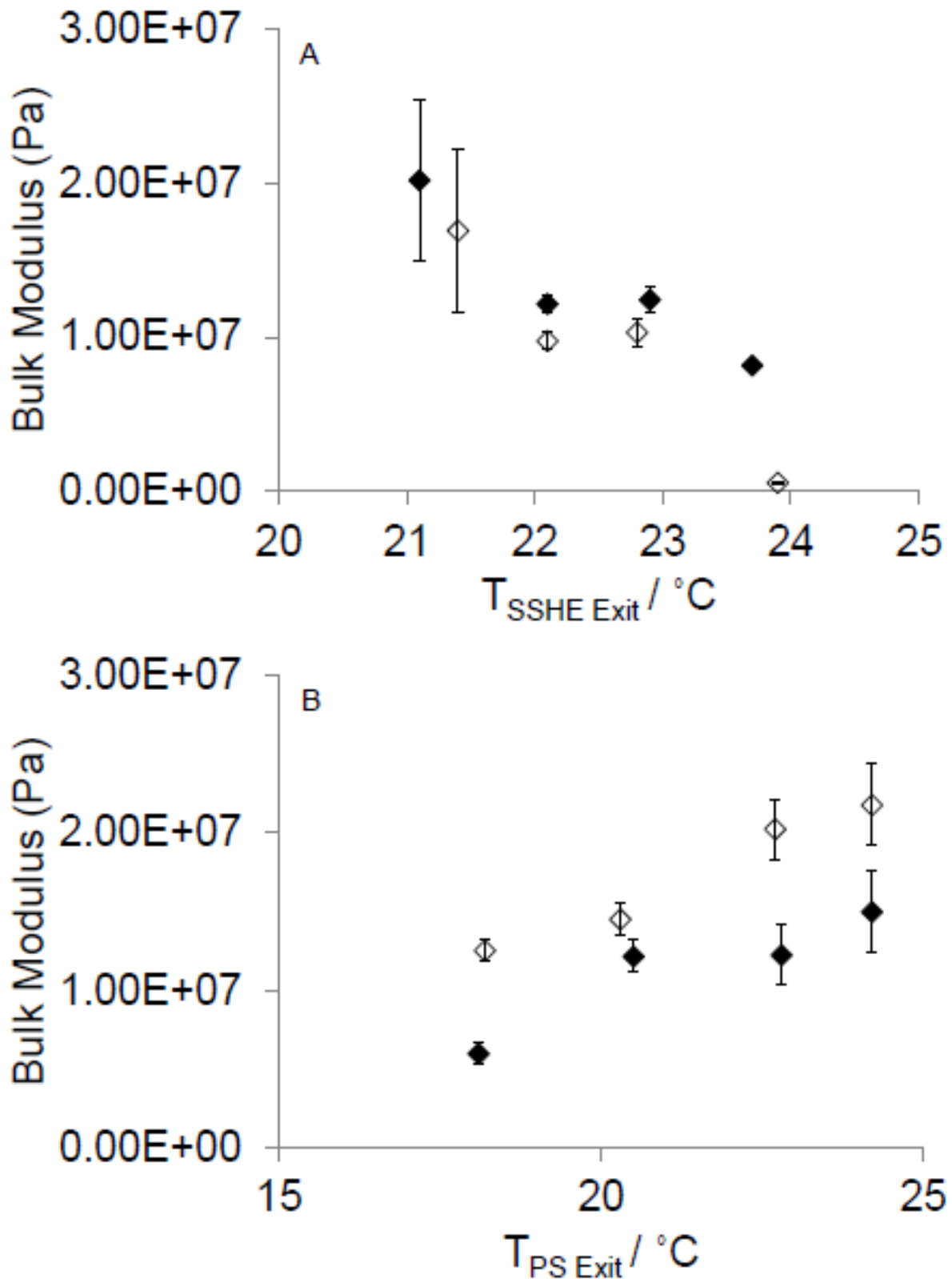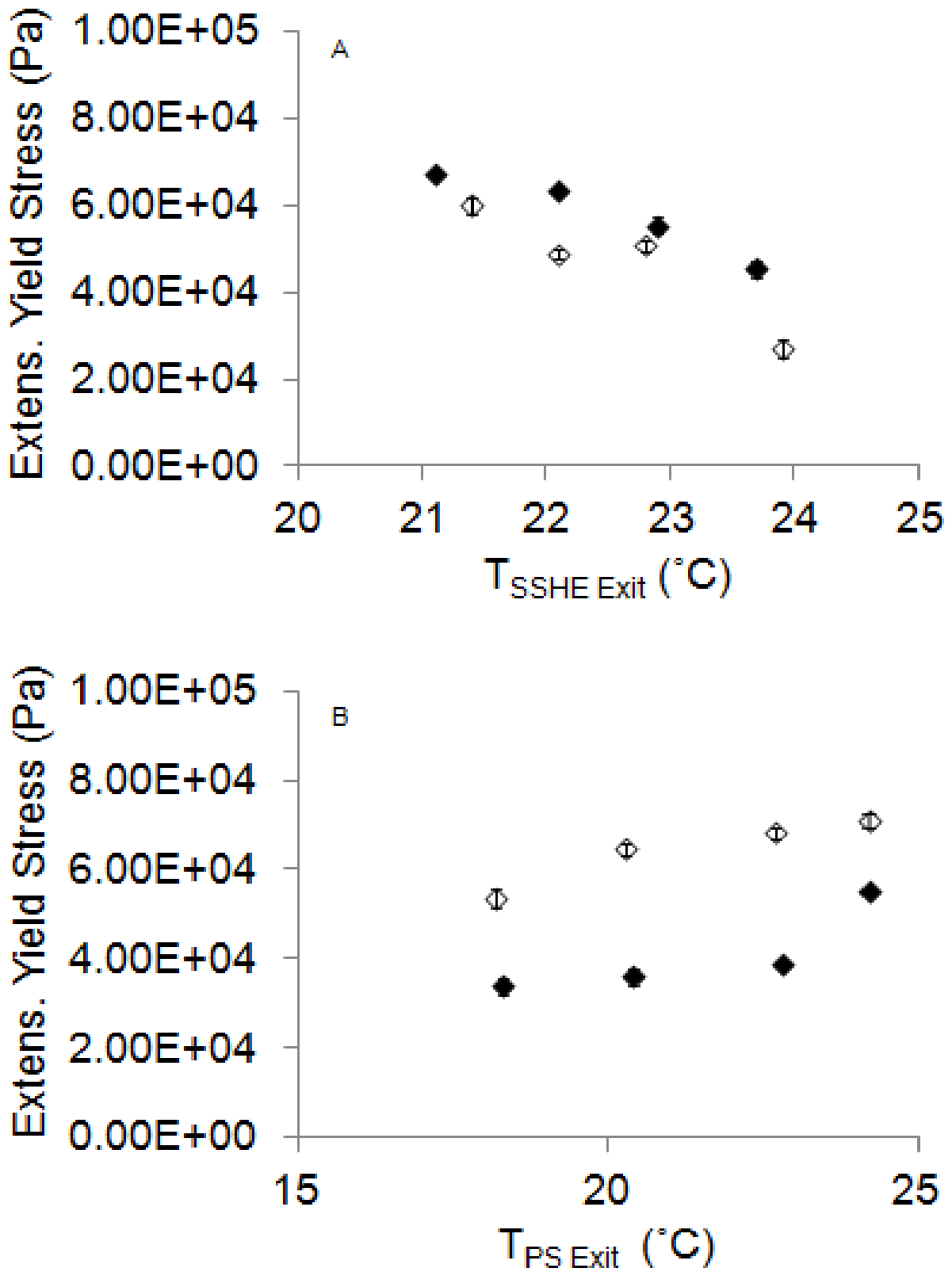**Fig. 45: Extensional Yield Stress for PO 68%, HMMGE 2%, water 30% emulsions as a function of (a) exit temperature from the SSHE unit for ωSSHE 1315 rpm (♦) and 657 rpm (◊), and (b) exit temperature from the PS unit for ωPS 1345 rpm (♦) and 672 rpm (◊).**

4.4.4. Time Dependency Studies

Thus far in this investigation, all studies have been performed on samples which have been stored for 21 days (504 hours) in order to ensure valid comparisons within this investigation. It is important however, to understand the development of the solid fat proportion of the continuous matrix directly after formulation, and the effects of processing upon this, as this will arbitrate the final structural arrangement (assumed here at 21 days). The rate of fat crystallisation in the continuous phase is directly related to the Pickering stabilisation of the aqueous phase dispersion, as higher concentrations of solid fat will present a greater physical barrier towards coalescence and migration mechanisms. Processing conditions would be expected to exhibit some control over this, not only via (latent) heat transfer within the mixing steps themselves stimulating physical state change, but also by controlling TAG crystal seeding and subsequently fat crystal nuclei growth and matrix development after processing [30].

Solid fat content was measured as a function of time after formulation for emulsions formulated using select processing conditions. Emulsion samples were prepared as before. Control conditions were set at $\omega_{SSHE} = 1315$rpm, $\omega_{PS} = 1345$rpm, $T_{SSHE} = 18°C$, $T_{PS} = 20°C$, $Q = 0.5$ml.s^{-1}. Subsequent samples were then prepared to explore the effects of processing conditions systematically. Samples of each processing batch were then allowed to cool to room temperature before storing at 5°C, as for the preceding studies. Solid fat content as a function of SSHE conditions (Fig. 46a) and PS conditions (Fig. 46b) was measured using NMR at time $t = 0.5, 1, 6, 24, 48, 168$, and 504 hours (21 days). Time $t=0$ was set as the time upon which emulsion entered the sample pot (approximately 20 seconds after leaving the PS).

In all cases SFC (Fig. 46a) was observed to increase with time up to a plateau, as ultimate SFC under a given environment will be defined by the composition [33] [188]. Rate of solid fat development decreased with time, as the concentration of TAG crystals capable of crystallising (under these conditions) decreased.
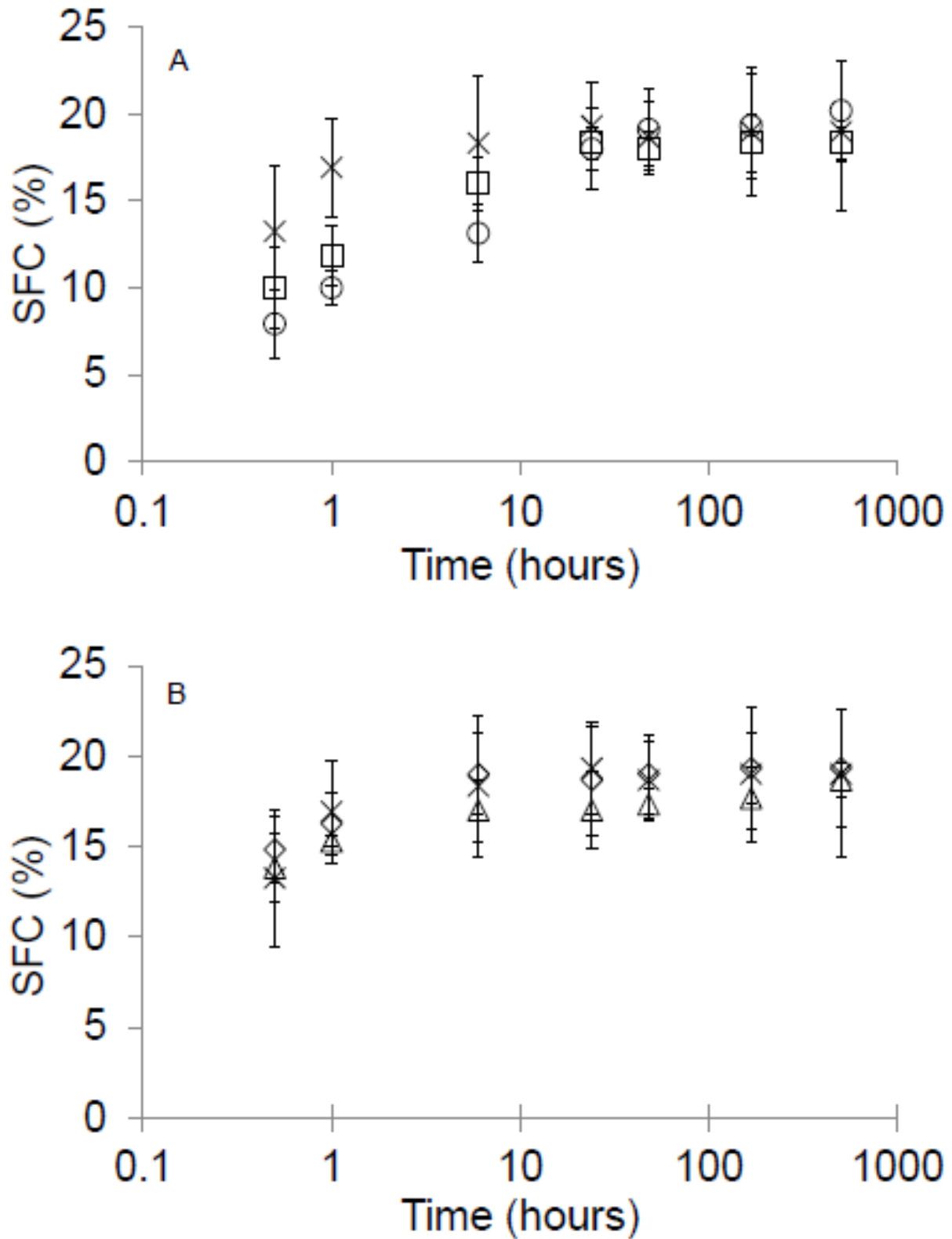
Fig. 46: Solid fat content development with time from formulation for PO 68%, HMMGE 2%, water 30% emulsions created under varying (a) SSHE, and (b) PS processing conditions: (×) control; (□) increased (22°C) TSSHE; (○) decreased (657.5rpm) ωSSHE; (Δ) increased (24°C) TPS; and (◊) decreased (672.5rpm) ωPS.

As a general observation, solid fat content was equilibrated approximately 6 hours after processing emulsion systems, except for those emulsions formulated under increased T_{SSHE} (22˚C) and decreased ω_{SSHE} (657.5rpm), where SFC plateaued 12 hours after processing. No significant change in SFC was observed between 12 hours and 504 hours for all emulsions outside of the bounds of one standard deviation as indicated by the error bars.

The data presented here (Fig. 46a&b) supports earlier conclusions regarding the respective roles either mixing stage plays with regards to emulsion structuring. By lowering ω_{SSHE}, fat crystal seeding in the SSHE is reduced, and subsequently the development of TAG crystals is slower, as it has less seed points from which to extend [216], the effects of this are seen in Fig. 46a, as low ω_{SSHE} conditions reduce the rate of SFC development relative to the (high ω_{SSHE}) control. Similarly, increasing T_{SSHE} from 18˚C (control) to 22˚C increases the time taken to reach SFC equilibrium (Fig. 46a), as the heat transfer gradient is decreased, and subsequently less (latent) heat is removed from the fat and less crystal seeding occurs in the SSHE, similarly reducing the number of crystal seed points from which secondary nucleation may proceed.

Contrastingly, low ω_{PS} and high T_{PS} processing conditions exhibit no distinction upon the rate of SFC relative to the control (Fig. 46b), indicating – as earlier concluded – that the PS mixing step exhibits no significant control upon solid TAG crystal formation for the conditions used in these studies, instead defining the extended macrostructure, and polymorphic rearrangement of the crystals formed.

Aqueous phase distribution (Fig. 34) indicated that lower ω_{SSHE} and higher T_{SSHE} conditions resulted in increased droplets sizes and free water concentration. Less crystal nucleus seeding in the emulsion will result in slower fat crystal matrix growth, and subsequently slower dissolution of the solid fat (Fig. 46a) and therefore greater window for coalescence occurring. Once the solid fat crystal network has formed about the droplet dispersion it is very hard for

aqueous droplets to move and coalesce, and Ostwald ripening becomes the most likely source of (if any) regression in aqueous phase dispersion quality [27] [33]. Using increased ω_{SSHE} and reducing T_{SSHE} the degree of coalescence and aqueous phase dispersion breakdown immediately post-processing can therefore be reduced.

This data would therefore be a good basis for the hypothesis that material behaviour of emulsions 12 hours after formulation would be similar to analogous emulsions 504 hours after formulation. This analysis however does not account for reorganisation of the fat crystal structure after dissolution, and subsequently it would be advisable to pursue further investigations into the progression of emulsion material properties over time.

4.5. Conclusions

Water-in-palm oil shortening emulsions of 30% aqueous fraction stable to 21 days have been successfully formulated, achieving mean droplet diameters as low as 4.26µm and 0% free water, using a conventional bench scale SSHE and PS margarine line.

It is concluded that by specifying SSHE shear, resident time and temperature parameters dispersion of the emulsion aqueous phase may be controlled via multiple mechanisms; initially controlling the dispersion forces exerted upon the aqueous phase in the crude emulsion, controlling the rate of TAG crystal nucleation, and then subsequently controlling the rate at which emulsifiers and TAG crystals serving as Pickering particles are transferred onto the interface, and therefore the barriers resisting coalescence; conclusions supported by NMR $d_{3.2}$ and free water studies presented. The rate at which the solid fat phase will grow and develop similarly depends upon SSHE conditions, and will define the physical barriers opposing emulsion breakdown mechanisms; namely coalescence and Ostwald ripening, established with SFC NMR time studies. The aqueous phase droplet dispersion and emulsification is concluded

to have finished upon exiting the SSHE, confirmed by aqueous phase droplet size or free water exhibiting independence to PS shear and temperature parameters.

Emulsions macrostructures produced using this method have been safely assumed highly fractal due to the high shear rapid cooling nature of the SSHE processing step. Resistance to failure, microstructure compaction and flow all displayed similar behaviour trends, further suggesting a structure dominated by weak linkage associations on compatible adjacent elements. It has been concluded therefore that SSHE processing parameter control upon emulsion microstructure strength characteristics are due to droplet size effects on stress transfer efficiency and stress concentration, accumulating in crack propagation, as indicated in these studies by increasing bulk modulus, failure work, yield stress and extensional yields stress with increased shear and heat transfer processing parameters which correspondingly decreased mean droplet and free water concentration. Contrastingly, the PS processing step is understood to regulate the emulsion macrostructure by disrupting the weak link associations forming between TAG crystal microstructures. These studies have therefore successfully established the roles of the SSHE and PS as a structure creator and subsequent structure regulator, respectively.

Advancing forward, the effects of composition upon emulsion quality and mechanical properties should be investigated under fixed processing parameters, having now benchmarked their effects here.

V

FORMULATION OF BAKING MARGARINE EMULSIONS WITH MIXED HYDROCOLLOID GELS

5 Formulation of Baking Margarine Emulsions with Mixed Hydrocolloid Gels

5.1. Abstract

Palm oil baking margarine emulsions of up to 30% aqueous phase were formulated successfully using a conventional bench scale margarine line of combined scraped surface heat exchanger and pin stirrer. Studies structured the aqueous phase by addition of κ-carrageenan, cross linked waxy maize starch and K(sorbate), prior to emulsion formulation in order to predictably control the texture of the resulting emulsion. Emulsion droplet size distribution assessed by surface weighted mean diameter and free water percentage was measured via NMR. Physicomechanical properties of emulsions were studied using uniaxial compression in order to quantify microstructure resistance to deformation. The resistance of emulsion structure to deformation is increased by multiple factors: (i) improved droplet shell hardness due to emulsifier hardness, (ii) sintering of fat droplet shells, hardening them, (iii) improved interactions with surrounding PO matrix, (iv) smaller droplets exhibiting improved stress transfer efficiency in comparison to larger droplets, however cryogenic scanning electron microscopy images showed smooth shell fat sintering was not completely successful. Cryo-SEM images concluded XLWM granules do not get broken up in the emulsification process, but weaken the fat matrix as the number of inhomogeneous defects is increased, facilitating stress concentration. Higher water phase fraction and lower emulsifier concentration similarly increased droplet sizes and weakened the structure.

5.2. Introduction

Emulsions exist in a huge number of foods eaten by the modern day consumer, with the potential for an enormous variety of different organoleptic and physical properties, defined by the structuring of the phases of which it is composed [27]. Despite the extensive range of potential forms and textures the central problems associated with emulsions remain prevalently in emulsion structure stabilisation and understanding of mechanisms at the boundary between either phase(s), known as the interface.

The mechanism by which fat and emulsifiers act at the w/o interface and the subsequent action they bear in stabilising a dispersion is highly complex, and still not entirely understood [30]. Previous studies on cocoa butter emulsions [32, 42] have reported that solid fat cocoa butter particles could undertake a Pickering particle mechanism by absorbing onto the w/o interface, immobilizing the dispersed particles and inhibiting coalescence [192] [191]. More recent studies demonstrated Pickering particles could fuse and form a smooth sintered shell around the droplet, entirely enclosing it [41]. Such fat integration about the dispersed water droplets is of a core interest here, as it poses high potential for control in water release and retention of shortening's textural properties.

One way in which textural and emulsion stability challenges may be tackled is by addition of further agents to the phases in order to modify their physical and chemical behaviour in favour of the attributes which are desired. Inclusion of hydrocolloids into the aqueous phase of an emulsion is of particular interest as it may allow the texture properties of the fat to be mimicked in the dispersed water phase [217] [218] as well as controlling water release and simulating the material behaviour of the continuous phase. If we consider shortening emulsions, structuring of the aqueous phase using hydrocolloids may provide some control over water release during baking, and help define the physicomechanical response in such a way as to emulate the response of regular shortening during mixing.

Whilst existing works have investigated hydrocolloid dispersion in w/o emulsion systems, examples using the κ-carrageenan polymer specifically remain exiguous. Studies performed by Sullo et al. [42] incorporated 2% κ-carrageenan solutions in cocoa butter (CB) emulsions, however the unanimous thermal distinction of polymorphic crystal forms in cocoa butter is not replicated in PO shortening, and the addition of monovalent salts to the κ-carrageenan solutions was not explored in that instance, the presence of which are known to influence κ-carrageenan conformer behaviour and aggregate stability [55, 69, 74].

Further studies have focussed upon κ-carrageenan solutions dispersed in low fat spreads [48], with particular interest highlighted towards the potential for improved dispersion stability as a consequence of increased aqueous phase viscosity [218], and enhanced textural and mouth feel [219].

Here, we present a novel systematic investigation of κ-carrageenan aggregate dispersion in PO shortening emulsions, and the implications for emulsion physicomechanical behaviour properties. Preceding this work, the Author has implemented an extensive holistic strategy to carefully define the numerous control parameters affecting the structuring of κ-carrageenan aggregates in the presence of salts (see Chapter 2.0), and their mixed composite systems with modified starch in an effort to inhibit the archetypal syneresis behaviour (see Chapter 3.0). Using this understanding, this work now looks to instigate gelation and aggregate structuring of the dispersed aqueous phase after complete emulsification within droplets, the clear advantages to this being reduced viscosity and therefore resistance to shear induced dispersion of the aqueous phase during the processing, but then increased viscosity and aqueous phase structuring after the mixing step, where it will oppose instability mechanisms. Processing effects have been systematically defined on water in palm oil emulsions (refer to Chapter 4.0), and this understanding is now applied to understanding drawn from the preceding chapters on

κ-carrageenan aggregate thermostability in order to precisely manage the onset of aqueous phase gelation relative to the emulsification and mixing process.

This work focusses upon emulsion composition; ingredient components involved in emulsification and stabilisation mechanisms of palm oil emulsions, and how effective they are in doing so. Direct stabilisation mechanisms are both physical (e.g. continuous phase viscosity) and energetically (e.g. interfacial energy reduction) driven in nature [30], and subsequently both are explored here.

5.3. Materials & Methods

5.3.1. Materials & Emulsion Preparation

The aqueous phase was prepared separately before combining with the oil phase. Solutions 0.4% K-carrageenan (*Eucheuma Cottonii*, M_W 600-700 kDa, E407A EU specification processed, propan-2-ol washed, cat no.22048, Sigma Aldrich, Gillingham, UK) with 0.0135M K(sorbate) (Sigma Aldrich, Gillingham, UK) were prepared in batches of 1 litre by dissolving in deionised and deionized water from a Aquatron A4000D (Stuart, Staffordshire, UK) at 80°C under continued mixing using a hot plate stirrer (Stuart, Staffordshire, UK). Potassium sorbate was of analytical grade and also purchased from Sigma Aldrich (Gillingham, UK). Materials used were given no further purification or modification of their properties.

Mixed polymer solutions were prepared by mixing separate Cross Linked Waxy Maize (XLWM) Starch and κ-Carrageenan solutions each of 500ml at twice the required final concentrations (4% and 0.8% respectively). XLWM was kindly donated by Ingredion Incorporated (Westchester, IL, USA). Amylopectin fraction of the starch was 99% minimum by mass and acetate stabilized, as declared by manufacturer. Mixtures were then held for 1 hour at 80°C with occasional gentle stirring using a magnetic stirrer.

The oil phase was prepared in 1 litre batches by heating the TransAdvantage® P-100 NH Palm Shortening to 90˚C before adding Radiamuls® MG 2643 , 1-Oleon-rac-glycerol, and / or TransAdvantage® P-130 NH Flake double fraction palm oil (DFPO) as applicable (specific concentrations in text). Radiamuls® MG 2643 emulsifier is a commercially available solid white flake monoglyceride emulsifier blend consisting of 60% glyceryl stearate ($C_{21}H_{42}O_4$). Both Radiamuls® MG 2643 and 1-Oleon-rac-glycerol were kindly supplied by Oleon (Avril Group, France). TransAdvantage® P-100 NH Palm Shortening and TransAdvantage® P-130 NH Flake double fraction palm oil was kindly supplied by Cargill™ (Vilvoorde, Belgium). Radiamuls® MG 2643 was purchased from Oleon (Epson, UK), 1-Oleon-rac-glycerol was purchased from Sigma Aldrich (Gillingham, UK) and materials were used in varying amounts as specified.

The oil mixture was then held at 90˚C (well above complete melting point) for 2 hours to ensure complete melting and deletion of any fat crystal memory. Mixture was then cooled to 80˚C prior to mixing with aqueous phase, to ensure no thermal degradation of starch granules. Finally a 1.5 litre pre-emulsion was prepared by adding the required amount of aqueous phase (10-60% w.v.) to the oil phase and mixed using an overhead stirrer (RW20 digital, IKA-Werke GmbH & Co.) at 400 rpm until the mixture appeared homogeneous by visual inspection.

Water-in-oil emulsions (batch size 1.5 litres) were formed using the same bench scale margarine continuous line unit [32, 33, 35, 42] comprised of a jacketed Scraped Surface Heat Exchanger (SSHE) followed by a jacketed Pin Stirrer (PS); volumetric capacities of 40 ml and 170ml respectively. Shear speeds were controllable up to 1315rpm and 1345rpm respectively.

5.3.2. Emulsification Process

Pre-emulsion was pumped into the SSHE followed by the PS through a silicon flexible pipe (inner diameter 3.2mm; ESCO, SLC, UK) at a constant flow rate controlled by a Masterflex Easy-Load II L/S pump (Cole-Parmer Instrument Company, UK). Jacket temperature (T_{SSHE} & T_{PS} respectively) was controlled by water baths (Julabo, UK) and the emulsion temperature entering and leaving either processing unit was measured using a Data Logger Thermometer (Omega, UK) fitted with a K-Type thermocouple ($\pm0.2\%$ accuracy) via insertion into T-junctions included in the piping.

Hot emulsions were poured directly into required moulds depending on analysis (see later) and (unless otherwise stated) allowed to cool to room temperature over approximately 30 minutes before transferring to 5˚C (±1˚C accuracy) storage. The emulsification process used here emulated those methods employed by the Author in preceding work using water in palm oil emulsions (refer to Chapter 4.0). Unless otherwise stated, conditions were fixed at ω_{SSHE} = 1315rpm, ω_{PS} = 1345rpm, T_{SSHE} = 26˚C, T_{PS} = 20˚C, Q = 0.5ml.s^{-1}.

5.3.3. Thermal Analysis

Thermal analysis of emulsions was carried out using DSC 8000 calorimeter (Perkin Elmer, UK) and digitally processed using the equipment software (Pyris, Perkin Elmer DSC 8000, UK). Approximately 5mg (±1mg) of sample was used each time, using an empty cell as a reference. Samples were loaded at room temperature into aluminium pans of 40μL, which were then hermetically sealed and loaded into the calorimeter. Furnace temperature was equilibrated at 20˚C for 1 minute before initiating temperature sweep from 20˚C, to 80˚C, and back to 20˚C at a constant rate of 10˚C.min^{-1}. The area under endotherm(s) was calculated automatically by the Pyris software, representing the fat crystal / aqueous phase polymer melting enthalpy, and

this was normalised by the weight of component: i.e. fat or polymer material respectively, in each sample using the following equations 1-3. Studies were performed in triplicate.

$$Energy\ of\ Transition = \frac{peak\ enthalpy}{total\ mass\ of\ sample} \tag{1}$$

$$Mass\ of\ component = total\ mass\ of\ sample \times \%\ concentration\ componant \tag{2}$$

$$Enthalpy\ normalised\ per\ component = \frac{Energy\ of\ Transition}{Mass\ of\ Componant} \tag{3}$$

5.3.4. Cryogenic Scanning Electron Microscopy

Emulsions were prepared as above and poured immediately into 50ml plastic sample pots. Cryogenic scanning electron microscopy was carried out using a XL30 ESEM FEG (Philips, Netherlands) with a Polaron PolarPrep 2000 cryo preparation chamber, where the sample was held at -90°C for 4 minutes whilst being etched with 5-10nm platinum in order to allow electrical conductivity on the surface, before being cooled to -180°C and scanned with an electron beam in order to produce the image.

5.3.5. Uniaxial Compression Fracture Studies

Emulsion systems were prepared as above and poured immediately into Ø20mm x 20mm moulds. Cylindrical samples were then loaded onto a TA.XT.plus® Texture Analyser (Stable Micro Systems, UK) with a 5kg load cell and a cylindrical head geometry (Ø40mm). Samples were then compressed at a probe cross head speed of 0.2 mm.s^{-1} to a distance of 5mm from the plate (75% strain). A force trigger of 0.04903N was used.

Force/distance data was converted into true strain ε_H and true stress σ_T using equations 4-7 where ε_E and ε_H are the engineering and true strain, σ_E and σ_T are the engineering and true stress, H_0 and A_0 are the initial height and cross sectional area of the sample, and F and h are the force applied and the height of the sample [99]. Work done at total failure was determined according to the method employed by Kaletunc [101]. Due to the lubricant nature of the fat continuous samples frictional forces perpendicular to direction of compression were negligible and no barrelling occurred. Experiments were performed at 20±1°C, to 10 repeats and averaged.

$$\varepsilon_E = \frac{(H_0 - h)}{H_0} \tag{4}$$

$$\varepsilon_H = -\ln(1 + \varepsilon_E) \tag{5}$$

$$\sigma_E = \frac{F}{A_0} \tag{6}$$

$$\sigma_T = \sigma_E(1 + \varepsilon_E) \tag{7}$$

5.3.6. Uniaxial Compression Squeeze Flow Studies

Emulsion systems were prepared as above and poured immediately into Ø30mm x 8mm moulds. Texture Analyser was now fitted with a 30kg load cell and a cylindrical head geometry (Ø75mm). Samples were then compressed at a probe cross head constant force of 150 N, and constant sample volume between plates of $5.65 \times 10^{-6}\,m^3$, until change in sample height was held (to within 5% strain deviation) for 20 seconds. Sample height / time data was taken at a rate of $100s^{-1}$ and final limiting thickness H_L was recorded. A force trigger of 0.04903N was used and studies were performed at 20±1˚C and in triplicate.

Apparent extensional yield stress was determined using the following equation, where σ_y is the apparent extensional yield stress, F is the force applied, R_0 is the initial radius of the cylindrical specimen and H_0 is the initial height of the specimen sample [199]. Due to the lubricant nature of the sample, perfect slip has been judged a reasonable assumption here in these calculations.

$$\sigma_y = \frac{(FH_L)}{\pi R_0^2 H_0} \tag{8}$$

5.3.7. Droplet Size Measurements

Water droplet size was measured using nuclear magnetic resonance (Minispec Bruker Optics, UK). Probe chamber temperature was controlled using a LTC4 Refrigerated Circulating Bath with TX150 Circulator (Grant Instruments, Cambridge, UK). Specific droplet application software [42] was used to analyse the data. Samples (1 mL) were taken from each emulsion using a metal plunger and transferred into a 10mm glass NMR tube (Bruker Optics, UK). Readings were taken at a chamber / sample temperature of 5˚C. Tests were performed in triplicate.

Direct droplet analysis presented droplet size distributions based upon the volume-weighted mean diameter of dispersed aqueous phase droplets; or $d_{3.3}$. This was then converted to the surface-weighted mean diameter; $d_{3.2}$ using the following equation where $d_{3.3}$ is the volume-weighted mean diameter of aqueous phase droplets, $d_{3.2}$ is the surface-weighted mean diameter of the droplets, and σ is the standard deviation of the logarithm of the droplet diameter as recorded by the software. Free water (droplet diameter > 50µm) was also recorded.

$$d_{3.2} = d_{3.3} \times e^{-\frac{1}{2}\sigma^2} \tag{9}$$

5.3.8. Solid Fat Content Measurements

Emulsions were prepared as above and poured immediately into 50ml plastic sample pots and stored for 21 days. Solid fat content (SFC) was measured using nuclear magnetic resonance (Minispec Bruker Optics, UK) and practical set-up was identical to that of water droplet size analysis. The application used this time was liquid fat content specific software specifically designed for the NMR (Bruker Optics, UK).

All NMR measurements were then carried out at 20±1˚C, and then afterwards again at 50˚C on the sample samples. A sample of pure sunflower oil was also included for correction (Equation (10)) with regards to temperature dependence of liquid proton relaxation time [201]. Using all this data, Solid Fat Content at 20˚C as a percentage of total fat content was then determined for each sample using the following equations [201] where $SFC\%_{20°C}$ is the solid fat content as a percentage of all fat in the sample at 20˚C, Total $FC_{50°C}$ is the complete fat content in the sample (measured at 50˚C when all the fat is in the liquid state and is therefore all detectable by the equipment), $LFC_{20°C}$ is the liquid fat content of the sample at 20˚C, and C is the correction factor that is obtained by dividing the sunflower oil liquid fat content reading at 50˚C by that at 20˚C. Results were reported as an average of three replicates.

$$C = \frac{Sunflower\ Oil\ FC_{50}}{Sunflower\ Oil\ FC_{20}} \tag{10}$$

$$SFC\%_{20°C} = \frac{Total\ FC_{50°C} - (C.LFC_{20°C})}{Total\ FC_{50°C}} \times 100 \tag{11}$$

5.4. Results & Discussion

5.4.1. Structuring the Aqueous Phase

The effect of heat transfer away from the emulsion in the SSHE (interpreted by $T_{SSHE\ Exit}$) upon the aqueous phase distribution in palm oil emulsions with a structured hydrocolloid aqueous dispersed phase was assessed by NMR and physicomechanical properties cross compared.

The aqueous phase was prepared as a 0.4% κ-carrageenan solution with 0.0135M K(sorbate). This was chosen as a compromise, high enough to ensure formation of a quiescent gel at ambient temperature (refer to previous Chapter 2.0) but low enough to facilitate fat crystal seeding. K(sorbate) was chosen based upon a continuum of preceding research performed by the Author. Aqueous phase of 0.4% κ-carrageenan solution with no added salt (non-quiescent gel at ambient temperature) and water aqueous phases were also included for relative comparison. T_{SSHE} was set at 18˚C, 21˚C, 24˚C and 26˚C. All other conditions were fixed at $\omega_{SSHE} = 1315$rpm, $\omega_{PS} = 1345$rpm, $T_{PS} = 20$˚C, $Q = 0.5$ml.s^{-1}. Emulsion formulation consisted of 68% PO, 2% HMMGE and 30% aqueous phase.

Droplet size and free water of emulsions was studied using NMR (Fig. 47a-b respectively). Those emulsions with aqueous phases incorporating water, or 0.4% κ-carrageenan solution with no added K(sorbate), increased in mean droplet size diameter with increasing $T_{SSHE\ Exit}$, with no distinction between the two aqueous phases once standard deviation was accounted for (error bars indicate ± one standard deviation Fig. 47a).
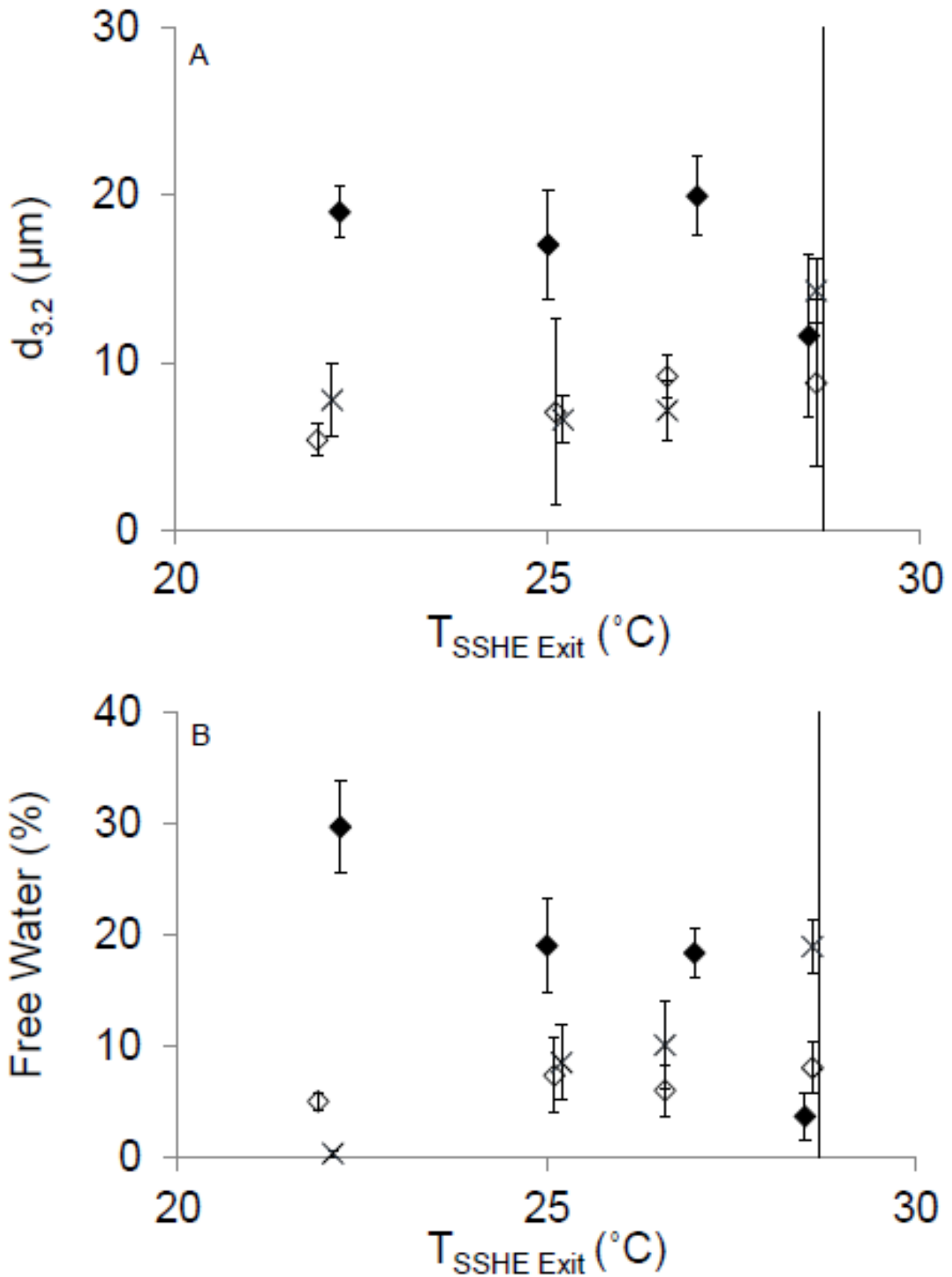
Fig. 47: (a) droplet size, and (b) free water for emulsions with aqueous phase of (×) water, (◊) 0.4% κ-carrageenan solution, and (♦) 0.4% κ-carrageenan 0.0135M K(sorbate), as a function of TSSHE Exit. κ-carrageenan / K(sorbate) gel setting temperature indicated (▬).

Free water (Fig. 47b) demonstrated greater distinction between water and 0.4% κ-carrageenan solution aqueous phases, as a function of $T_{SSHE\ Exit}$. At lowest $T_{SSHE\ Exit}$ (22.1ºC) 0.4% κ-carrageenan solution rose above the water aqueous phase (0.33%) to 5%, and inversely at highest $T_{SSHE\ Exit}$ (28.6ºC) water aqueous phase free water was recorded at 18.9%, whilst 0.4% κ-carrageenan solution recorded only (8.0%). Percentage of free water was observed to increase with $T_{SSHE\ Exit}$ in 0.4% κ-carrageenan solution and (more so) in water dispersions.

Addition of 0.0135M K(sorbate) to 0.4% κ-carrageenan solution aqueous phase increased both mean droplet diameter and free water values (Fig. 47a-b respectively) up until emulsion temperature leaving the SSHE; $T_{SSHE\ Exit}$, approached setting temperature for the (now) ambient thermo-reversible gelling aqueous phase; $T_{gelation}$. At this point both mean droplet diameter and free water values decreased (11.6μm diameter and 3.6% free water), below that of water and 0.4% κ-carrageenan solution aqueous phases.

The aqueous phase structuring (and subsequently viscosity) increases in the order water < 0.4% κ-carrageenan < 0.4% κ-carrageenan with 0.0135M K(sorbate). Previous studies [220] have established droplet dispersion is dependent on the ratio of the viscosities of the aqueous phase to that of the continuous phase: the shear energy required in order to disperse the aqueous phase equally will increase as the difference between the two viscosities decreases. This is evident in general data trends observed here: as aqueous phase structuring increases (water < 0.4% κ-carrageenan < 0.4% κ-carrageenan with 0.0135M K(sorbate)) so the viscosity of the aqueous phase increases, and subsequently achieved dispersion decreases and mean droplet diameter and free water increase.

As T_{SSHE} is increased, so the heat transfer gradient driving heat removal from the emulsion system is decreased, and subsequently $T_{SSHE\ Exit}$ increases. As a result of this latent heat removal from TAGs in order to initiate crystal seeding will be less prolific, and less

crystallisation will occur within the SSHE. Consequently upon leaving the SSHE the crystal structure will be less developed at increasing $T_{SSHE\ Exit}$, and the opportunity for dispersed water droplets to coalesce and reform larger droplets / 'free water' increases. Droplet coalescence will decrease with the (continuous and) aqueous phase structuring/viscosity, as mobility is restricted.

This mechanism contrasts with that of the above relating an increase in aqueous phase structuring and viscosity to a decrease in successful initial dispersion, and therefore the observed results (Fig. 47) are a compromise of the two attributed to whichever becomes prominent depending upon the individual test parameters. For example, whilst the 0.4% κ-carrageenan solution aqueous phase is more structured than the corresponding water aqueous phase and subsequently less effectively dispersed under synonymous processing parameter settings, 0.4% κ-carrageenan aqueous phase emulsion mean droplet diameter and free water values were considerably lower than that of the corresponding water aqueous phase emulsions at the highest $T_{SSHE\ Exit}$ of 28.6ºC, as SSHE temperature was high and subsequently TAG crystal seeding was reduced, allowing greater opportunity for coalescence. In this instance the increased structuring of the 0.4% κ-carrageenan solution aqueous phase (relative to water) was beneficial to opposing coalescence mobility and dispersion reversal.

Emulsions containing the quiescent gelling aqueous phase of 0.4% κ-carrageenan with 0.0135M K(sorbate) exhibited increased droplet size and free water until $T_{SSHE\ Exit}$ was increased to $T_{gelation}$; gelation temperature of the dispersed phase. Studies [42] performed over a range of κ-carrageenan concentrations cocoa butter emulsions observed that in the presence of high enough κ-carrageenan concentrations (2%, no salt) droplet size abruptly increased, suggested this was due to gelation within the SSHE processing step, and subsequently aggregate pieces were cut up in the shear unit and dispersed ineffectively.

It is therefore concluded that a similar process is occurring in this instance at lower $T_{SSHE\ Exit}$ below $T_{gelation}$, and as a result the dispersion is ineffective , and mean droplet diameter (Fig. 47a) and free water (Fig. 47b) are observed to increase. The subsequent drop at $T_{SSHE\ Exit}$ 28.6ºC is accredited to the aqueous phase now gelling immediately after the SSHE, thus viscosity in the shear processing step is lower; allowing for more effective aqueous phase dispersion, viscosity then increasing after processing; reducing droplet mobility and counteracting coalescence migration.

In order to study emulsions for practical application, it is important to consider the response toward mechanical deformation, and the resistance they provide towards applied forces. Furthermore, the information from such studies may provide valuable insight as to how the aqueous phase interacts both directly and indirectly with the fat continuous phase. For the purpose of these studies we have chosen to compare cumulative work required up to the point of bulk failure in uniaxial deformation, and extensional yield stress under squeeze flow.

Squeeze flow compresses a sample of defined volume between two parallel surfaces being pushed out by measurement of the compressive forces and the strain, knowing the sample volume, allows the samples resistance to flow to be quantified, and the extensional yield stress demonstrating the materials ability to resist flow may be determined (Equation 8) [198] [199]. Apparent extensional yield stress (or yield stress parameter), is an analytical assessment for the flow of Herschel-Bulkley semisolids, and at what sample height or thickness an equilibrium is reached during viscous–plastic fluid flow [198] [199]. The flow behaviour will be defined by the microstructure, and the extent of weak link associations between adjacent compatible elements on TAG crystals as they must be displaced in order to move relative to one another, initiating flow.
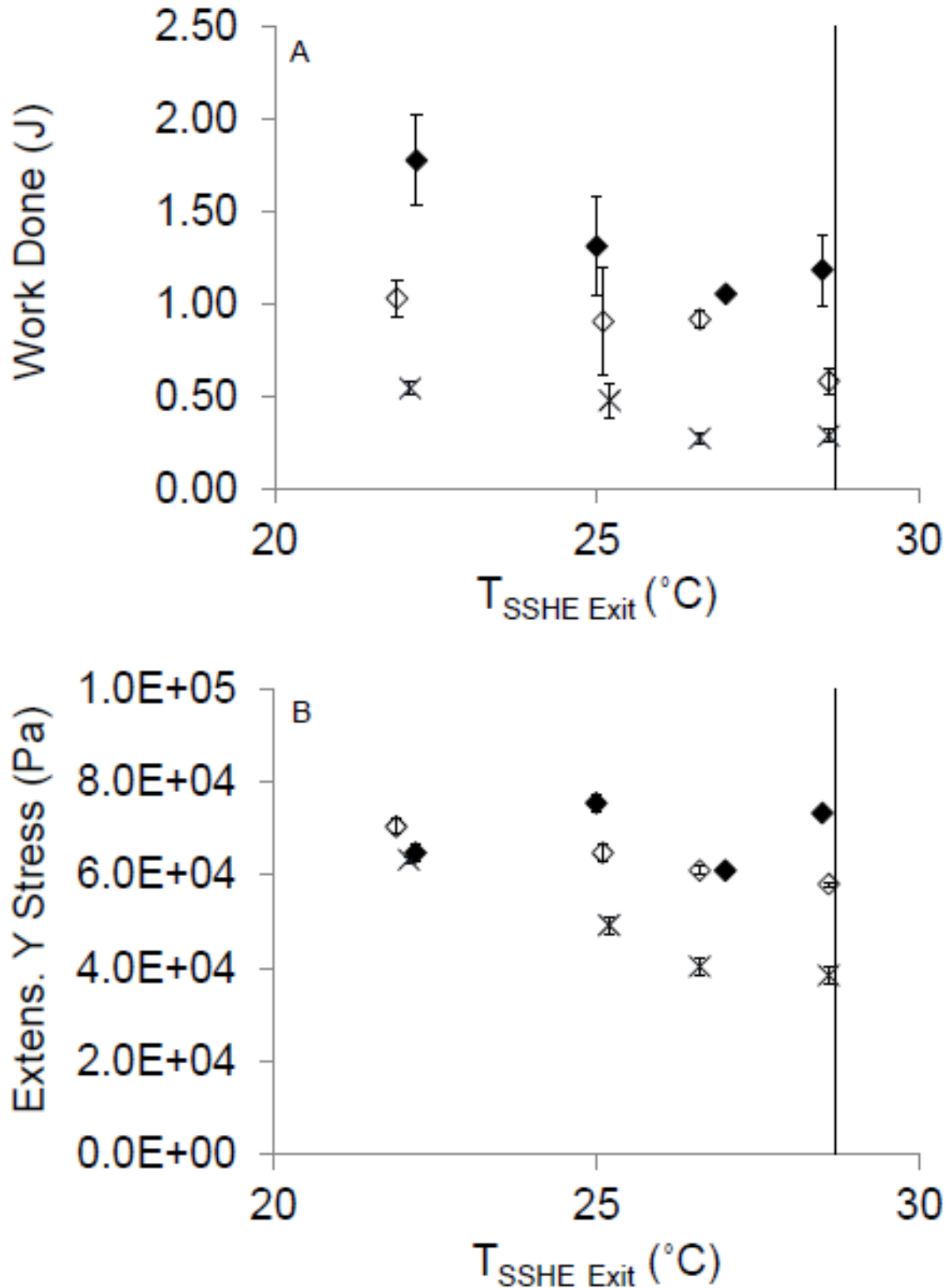
Fig. 48: (a) failure work, and (b) extensional yield stress for emulsions with aqueous phase of (×) water, (◊) 0.4% κ-carrageenan solution, and (♦) 0.4% κ-carrageenan 0.0135M K(sorbate), as a function of TSSHE Exit. κ-carrageenan / K(sorbate) gel setting temperature indicated (━ ━ ━). Error bars within symbols.

Failure work (Fig. 48a) and extensional yield stress (Fig. 48b) values were observed to decrease linearly with increasing $T_{SSHE\ Exit}$ for those emulsions with water or 0.4% κ-carrageenan solution aqueous phase. Emulsions were observed to follow a trend of increasing strength properties with increasing aqueous phase structuring – aggregating 0.4% κ-carrageenan solution with 0.0135M K(sorbate) giving the highest failure work (Fig. 48a) and extensional yield stress (Fig. 48b) followed by 0.4% κ-carrageenan solution and water respectively.

Emulsions containing the quiescent gelling aqueous phase with K(sorbate) displayed a linear decrease in material strength up until $T_{SSHE\ Exit}$ reached 28.5˚C, at which point both failure work (Fig. 48a) and extensional yield stress (Fig. 48b) increased sharply; indicating that at this point emulsion strength has significantly increased.

The sudden rise in emulsion strength distinguished this emulsion formulation significantly from the other emulsions containing water or polymer solution dispersions. Critically, this sudden increase in emulsion strength occurred at approximately $T_{gelation}$ for 0.4% κ-carrageenan with K(sorbate), as established by the Author (see Chapter 2.0).

If droplet analysis data is considered (Fig. 47) it is observed that emulsion strength and resistance to deformation generally increases with increasing aqueous phase structuring in the order of: water < 0.4% κ-carrageenan < 0.4% κ-carrageenan with 0.0135M K(sorbate). The aqueous phase droplets are considerably weaker relative to the continuous TAG semi-crystalline matrix, and subsequently they act as defects about which stress transfer is highly inefficient; increasingly so as the distinction between the two relative strengths is increased. Subsequently, structuring in the aqueous phase will increase solid character of the droplets, improving stress transfer efficiency and reducing stress concentrated about the disperse particles, reducing the likelihood of crack tip propagation and macroscopic failure, increasing

the strength of the emulsion as perceived by failure work (Fig. 48a) and extensional yield stress (Fig. 48b).

As $T_{SSHE\ Exit}$ is further increased to 28.6°C, gelation of the droplet particles is delayed until after dispersion in the SSHE, and subsequently droplet size (Fig. 47a) and free water (Fig. 47b) were observed to decrease. Failure work (Fig. 48a) and extensional yield stress (Fig. 48b) consequently exhibit a sudden increase at this point. As droplet size is decreased so surface area to volume ratio increases. This in turn means increased stress transfer efficiency onto the dispersed particles away from the continuous matrix, and as a result a stronger overall emulsion [189].

Previous studies [221] modelled on polymer composites and applied to w/o emulsions [42] related the yield stress of emulsions to those of the individual components accounting for droplet size using equation 12, where σ_e, σ_w, and σ_{PO} are the stress to fracture of the emulsion, aqueous phase, and PO continuous phase respectively.

$$\sigma_e = A\phi_w\sigma_w + (1 - \phi_w^S).\sigma_{PO} \qquad (12)$$

Φ_w is the aqueous phase volume fraction, S is the strength reduction parameter [0,1] accounting for weakening of the fat matrix due to filler droplets, and A is the adhesion number [0,1] accounting for the stress transfer between the droplets and the fat matrix.

If A remains approximately constant due to the two phases maintaining the same compositions, ϕ_w is kept constant at 0.3, and σ_w increases as the aqueous phase is structured and becomes more rigid, so $A\phi_w\sigma_w$ (accounting for the filler particle / droplet effect on the yields stress of the emulsion) will increase and stress to fracture the emulsion will increase. Similarly as the

droplet size becomes smaller for a given aqueous phase composition (water/hydrocolloid solution/quiescent gel), so the adhesion parameter A will change depending on surface area to volume ratio and subsequent stress transfer efficiency, and therefore stress to fracture the overall emulsion will change.

As the T_{SSHE} increases so the crystal nucleation in the SSHE is decreased, as latent heat transfer away from the mixture is less effective, and control on crystal sizes (being kept small and high in number) is reduced, subsequently weak linkage association between adjacent elements will decrease and movement of the final structure past itself – i.e. flow, will encounter less resistance. Larger droplet sizes, originating for aqueous phase gelation prior to or within the SSHE mixing as a consequence of excessively low SSHE jacket temperature, will reduce stress transfer efficiency at the interface, and consequently the adhesion between the phases will be reduced and therefore, in accordance with equation 12, stress at which the material will yield will be reduced.

Raising SSHE temperature to ensure gelation of the aqueous phase occurs after the SSHE mixing step facilitates improved dispersion (reduced free water and droplet size) and subsequently stress transfer efficiency and phase adhesion will improve, increasing the apparent overall extensional yield stress to initiate flow.

By changing the composition of the aqueous dispersed phase in PO emulsions it is possible to structure it accordingly in order to define the microstructure and material properties of the overall emulsion system. Gelation of the aqueous phase (0.4% κ-carrageenan with 0.0135M K(sorbate)) before and after exiting the SSHE effected dispersion and mechanical behaviour significantly, and subsequently studies forthwith shall be performed at $T_{SSHE} = 26°C$; ensuring aqueous phase gelation occurs after SSHE mixing.

Typically (as has been observed above) a lower temperature would be chosen to create a quality emulsion and water droplets would coalesce prior to fat network establishment, however the viscosity of the gelling 0.4% κ-carrageenan 0.0135M K(sorbate) aqueous phase inhibits mobility and coalescence, whilst reduced energy input for cooling is beneficial from an industrial perspective.

Furthermore, gelation of the hydrocolloid dispersed phase at lower temperatures in the SSHE will assumedly result in gelled fragments being sheared and dispersed throughout the emulsion, which will result in irregular droplet shapes and sizes (as oppose to approximately spherical), which further complicates measurements; droplet diameter being based on a surface-weighted mean, and as such apparent mean diameters for droplet size and free water may be inaccurate. Finally (and most significantly), the emulsion quality; on the evidence gathered thus far, is far superior when the gelling aqueous phase aggregates after the SSHE.

5.4.2. *Emulsifiers*

Thus far studies have focussed on emulsions stabilised by the presence of the high melting (60˚C) monoglyceride 'MG2643' at a concentration of 2%. In order for an emulsifier to be effective it must fulfil the following criteria [222]: (i) it must absorb strongly to the interface between the two immiscible phases, (ii) it must cover the interface completely, (iii) it must be energetically favourable in either phase – generally indicative of amphiphilic character. Monoglycerides (MG) suit this role well due to their structure (Fig. 49), whereby one end (the head) comprises of two alcohol groups and an ester, and the other (the tail) consists of a long carbon chain with none or a varying number of alkene groups. The 'head' therefore is polar due to the number of electrophilic oxygen atoms, whilst the 'tail' end is non-polar. As a result of this, the polar head of the molecule will liken to other polar molecules: such as water, whilst

the non-polar tail of the molecule will liken to non-polar molecules: such as fats. Either end

of the molecule will correspondingly be repelled by the antipodal phase; referred to as the

hydrophobic (repelled form water) or lipophobic (repelled from fat) effect. MGs are therefore

drawn towards the interface between oil and water in preparing emulsions, behaving as small

molecule surfactants [222].
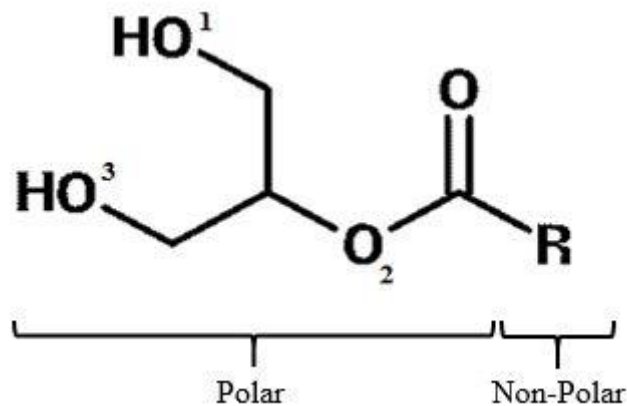
Fig. 49: Structure of monoglycerides. Esterification may also occur at Oxygen 1 or 3 however oxygen 2 is the most stable. R group may be alkane or alkene chain and may vary in length. Polar and non-polar regions are indicated.

By changing the length and structure of the MG carbon R chain (Fig. 49), the physical and

chemical properties - and therefore the emulsifying attributes, may be modified. For example,

increasing chain length will increase the melting point of the MG, and therefore the thermal

behaviour. Inserting alkene bonds into the chain will also cause steric problems and generate

a 'kink' in the tail – making close packing unfavourable at the tail end. In solid fat crystal

matrices, the compatibility of the tail with the triglycerides in the fat phase is also highly

important, if the two are to interact effectively to allow the fat crystals in the continuous matrix

to interact and stabilise at the interface, initializing interfacial heterogeneous nucleation [30]

[31]. It is not necessary however, for the emulsifier tail and triglycerides to be completely

identical in length [185] and structure [31]. It is therefore obligatory to investigate the effects of different MG emulsifiers here in these studies.

A high melting MG (MG2643) and a low melting MG (1-Oleon-rac-glycerol) were compared; referred to forthwith as HMMG and LMMG. The LMMG selected is liquid at room temperature, and in concept may move towards the interface much faster and more freely than longer, higher melting MG emulsifiers, and as a relatively short MG (17 carbon R chain alkene) is adaptable [223]. However inversely this may have a detrimental impact on the droplet shell quality compared to high melting fats which will form a harder shell, such as MG2643. Emulsifiers may also interact differently with κ-carrageenan and metal ions in the aqueous dispersed phase, as both will affect water structuring away from the hydrophilic heads affecting their stability [222].

5.4.3. Processing Effects on High vs. Low Melting Emulsifiers

The effect of SSHE temperature on 2% LMMG emulsion properties was studied and compared against corresponding 2% HMMG emulsions, investigated using uniaxial compression to failure, squeeze flow, and droplet analysis as before. The aqueous phase contained 0.4% κ-carrageenan solution with 0.0135M K(sorbate). NMR demonstrated no distinction in the mean droplet diameter (Fig. 50a) or free water (Fig. 50b) between LMMG and HMMG corresponding emulsions outside of one standard deviation, as indicated by error boundaries. Standard deviation is reasonably high in this instance, and it could be construed that free water is marginally lower in LMMG emulsions.

1-Oleon-rac-glycerol is liquid at room temperature, the structure of the emulsifier chain making it difficult to close pack in order to form a solid structure (at room temperature). Consequently the LMMG emulsifier is more mobile and could move to the interface faster.

It would therefore be rational to hypothesise that the free water is reduced from that of the HMMG, which sets at 60˚C. As $T_{SSHE\ Exit}$ reaches $T_{gelation}$ mean droplet diameter and free water decrease significantly (Fig. 50a & b respectively) due to the aqueous phase aggregation onset now occurring after the SSHE. Subsequently aqueous phase structuring in the mixing step is lower and dispersed more effectively [220].

Failure work (Fig. 51a) and extensional yield stress (Fig. 51b) dependency on $T_{SSHE\ Exit}$ for LMMG emulsions was analogous to that of corresponding HMMG emulsions: decreasing with increasing $T_{SSHE\ Exit}$ up until $T_{gelation}$. At this point a similar increase in resistance to deformation was observed. LMMG emulsions were significantly lower in material strength (approximately 30% lower for work failure and 40% for extensional yield stress). Visual inspection of emulsions observed them to be identical in appearance after 24 hours, and again after 21 days.

Decreasing emulsion physicomechanical strength as indicated by failure work (Fig. 51a) and extensional yield stress (Fig. 51b) with increasing $T_{SSHE\ Exit}$, prior to a sudden increase as $T_{SSHE\ Exit}$ approaches $T_{gelation}$ is explained similarly as for HMMG emulsions: increasing T_{SSHE} will decrease heat transfer away from the emulsion, reducing latent heat removal for TAG molecule crystal seed formation, subsequently TAG crystal nucleation will be slower [206] [203].

Reduced TAG crystal seeding would be expected to affect emulsion macrostructure strength by increasing the time taken for the fat crystal matrix in the continuous phase to develop fully, both as a result of reduced primary and secondary nucleation [178, 179, 202]. Prior to this, mobility of the dispersed phase droplets remains relatively unrestricted, and consequently maintains opportunity for coalescence of the aqueous dispersed phase, leading to increased droplet size and subsequently increased stress localisation, reducing the work required before cracks will begin to propagate and accumulate as macroscopic failure.
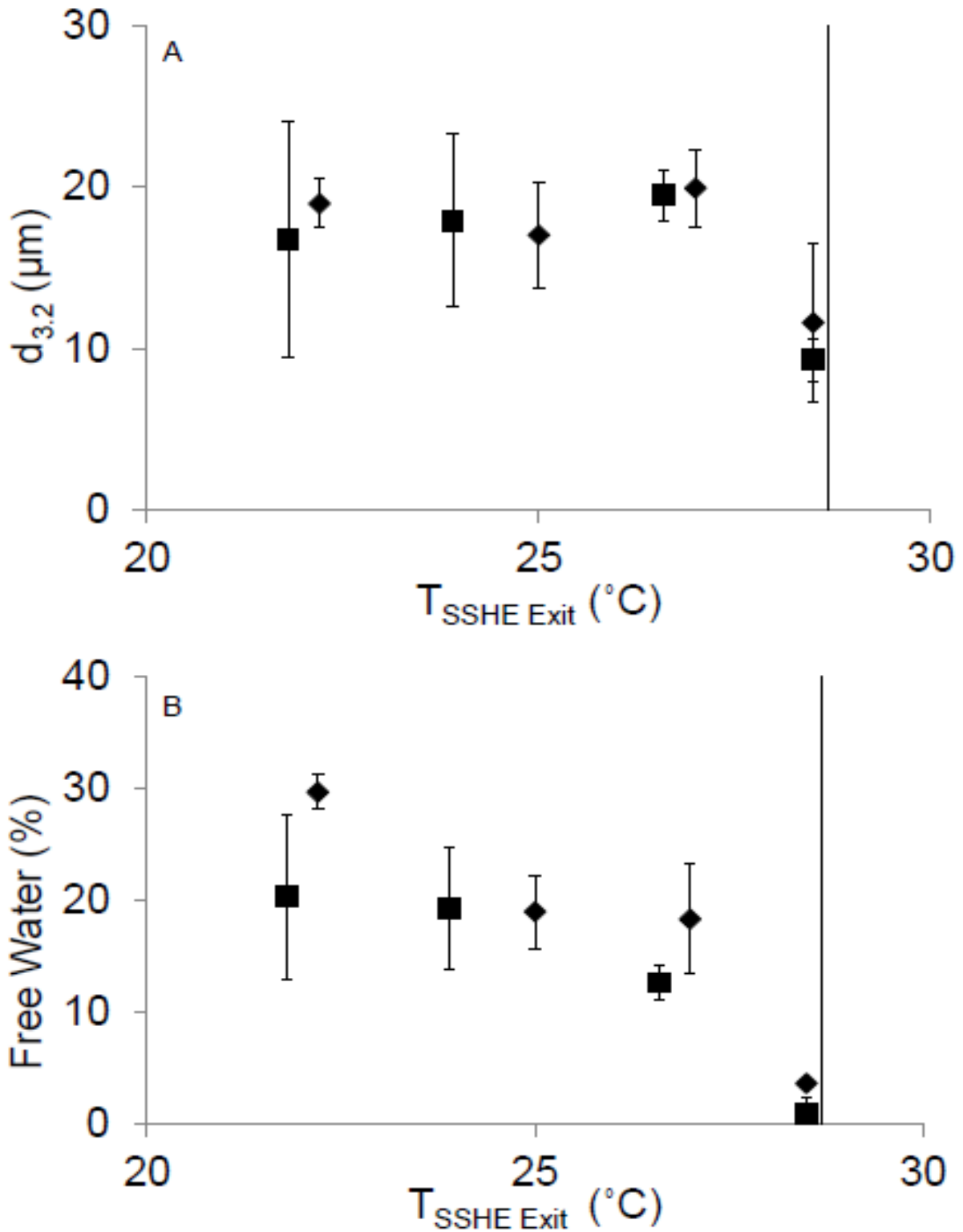
Fig. 50: (a) droplet size and (b) free water for emulsions with 2% HMMG (♦), and 2% LMMG .(■), as a function of TSSHE Exit. Aqueous phase contained 0.4% κ-carrageenan 0.0135M K(sorbate). Setting temperature for κ-carrageenan / K(sorbate) indicated (—).
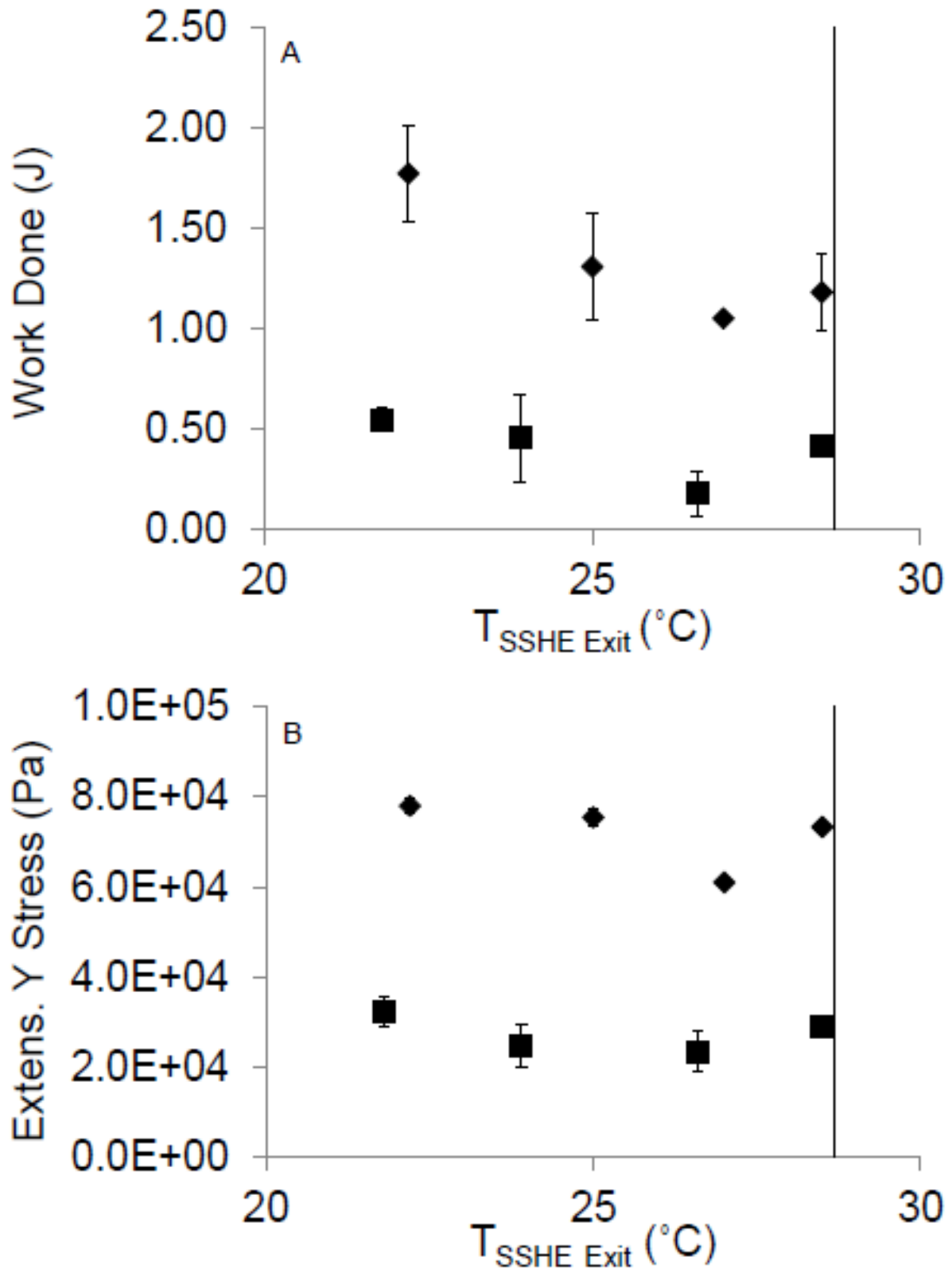
Fig. 51: (a) failure work and (b) extensional yield stress for emulsions with 2% HMMG (♦), and 2% LMMG (■), as a function of TSSHE Exit. Aqueous phase contained 0.4% κ-carrageenan 0.0135M K(sorbate). Setting temperature for κ-carrageenan / K(sorbate) indicated (—).

Similarly, as the TAG network has developed from fewer seeding points the network of crystals and associative weak linkages between adjacent compatible elements would be expected to be less intensive, and subsequently the force required in order for one microstructure to displace relative to the next would be less, and extensional yield stress lower. As in the case of failure work, the larger droplet sizes representing more substantial defects interrupting the fat continuous phase would also further disrupt weak link associations between microstructures, reducing the resistance to flow.

Failure work (Fig. 51a) and extensional yield stress (Fig. 51b) studies indicate LMMG emulsions were consistently weaker than those of HMMG, however there is no distinction in mean droplet diameters between the two sets of emulsions, and free water is actually recorded as lower in those emulsions with LMMG, which would improve stress transfer efficiency from the fat continuous crystal matrix, increasing the strength of the macrostructure. Therefore an alternative mechanism must be responsible for the observed decrease in emulsion physicomechanical strength attributes.

One possible consideration is that the emulsion strength is increased by hardening of the droplet shells in using the higher melting emulsifier. HMMG sets at temperatures far higher than PO, and is hard and solid upon visual inspection under ambient conditions. Subsequently this may increase the perceived rigidity of the dispersed droplets allowing them to act as a much harder filler, supporting the fat continuous matrix more effectively [208] [189].

Alternatively it may be that the LMMG does not interact as well with the continuous fat matrix, subsequently this may lead to a region or space about the droplet with little solid material. On a simplified like-for-like theory the hard fat triglycerides in the PO may be expected to interact better with the harder MG emulsifier accounting for chain lengths etc. If not successfully interacting with triglycerides in the continuous phase [30] adhesion and stress transfer will be

less efficient, the dispersed droplet will represent a more substantial interstice or defect 'hole' in the matrix which will present minimal support upon subjection to compressive forces, weakening the macrostructure.

In a similar argument to the above point, better interaction with the triglycerides in the fat continuous phase would instigate fat crystal stabilisation and sintering on the surface of the droplet [41], again leading to harder droplet shells and improving the adhesion to the surrounding matrix [189].

5.4.4. *Aqueous Phase Fraction*

Perhaps the inevitable sequential question after whether or not fat can be reduced or replaced in food is 'by how much?' Previous studies on cocoa butter emulsions with PGPR [32] [35] [42] have demonstrated that incorporation of hydrocolloids within the aqueous phase can facilitate the successful dispersion of an aqueous phase of up to 50%-60%, while contrastingly a simple water aqueous phase could achieve only 20% (successful being deemed as approximately 5μm mean droplet diameter and 0% free water).

Aqueous phase volume (0-60%) effects on the physical properties of emulsions were investigated, whilst systematically varying emulsifier (LMMG and HMMG) and aqueous phase composition. Work failure, squeeze flow, and NMR droplet size analysis studies were performed. Mean surface weighted droplet diameter ($d_{3.2}$) (Fig. 52a) and free water (Fig. 52b) were observed to increase with aqueous phase volume irrespective of aqueous phase composition in 2% HMMG emulsions, concurring with those observations reported in CB emulsion studies [42]. This is a consequence of increasing volume requiring greater force input in order to disperse it to the same degree, and increased event probability of droplets coming into contact with one another and coalescing.
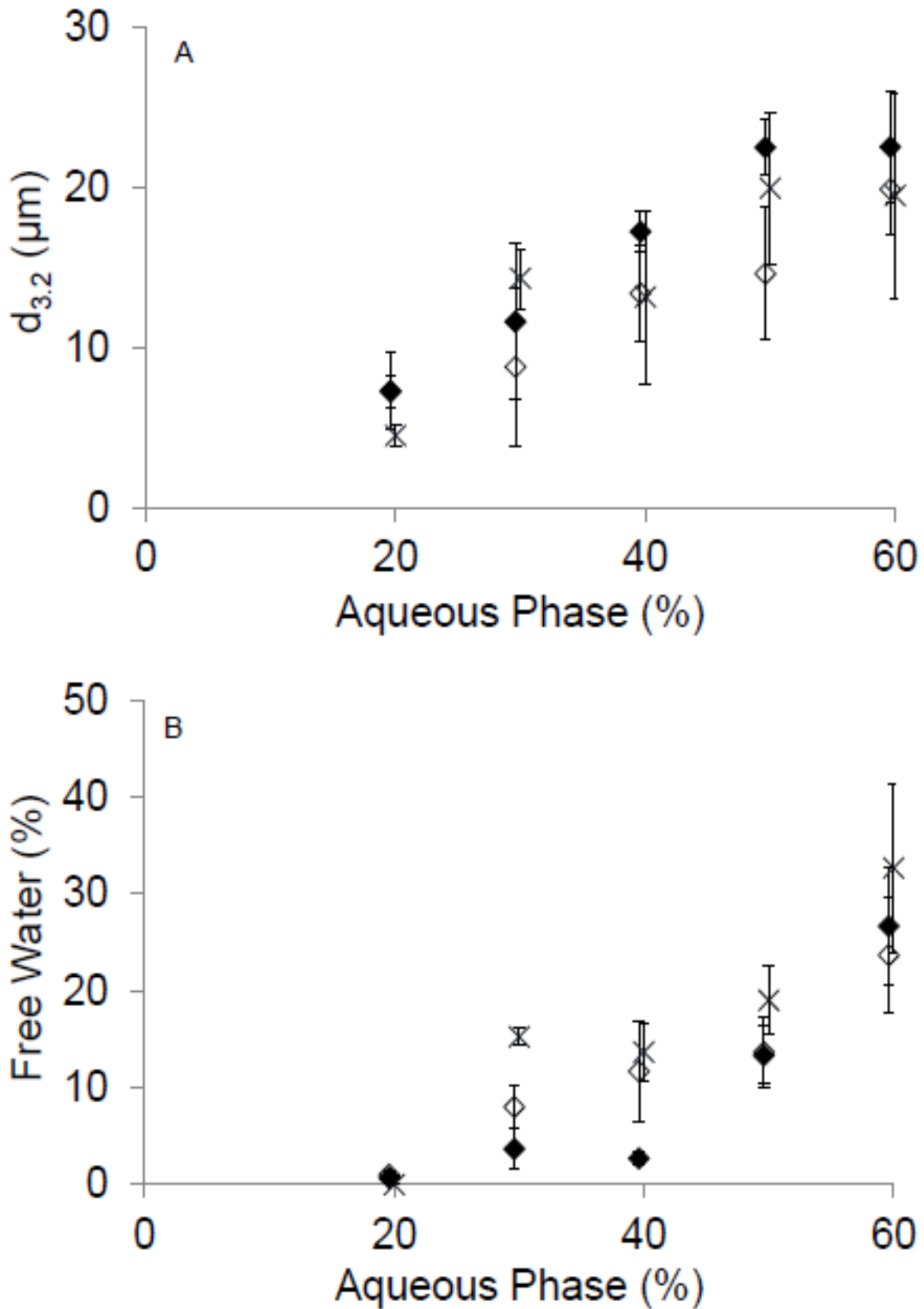
Fig. 52: (a) mean droplet diameter and (b) free water in PO emulsions with 2% HMMG, as a function of percentage aqueous phase. Aqueous phase contains (×) water, (◊) 0.4% κ-carrageenan solution, and (♦) 0.4% κ-carrageenan 0.0135M K(sorbate).
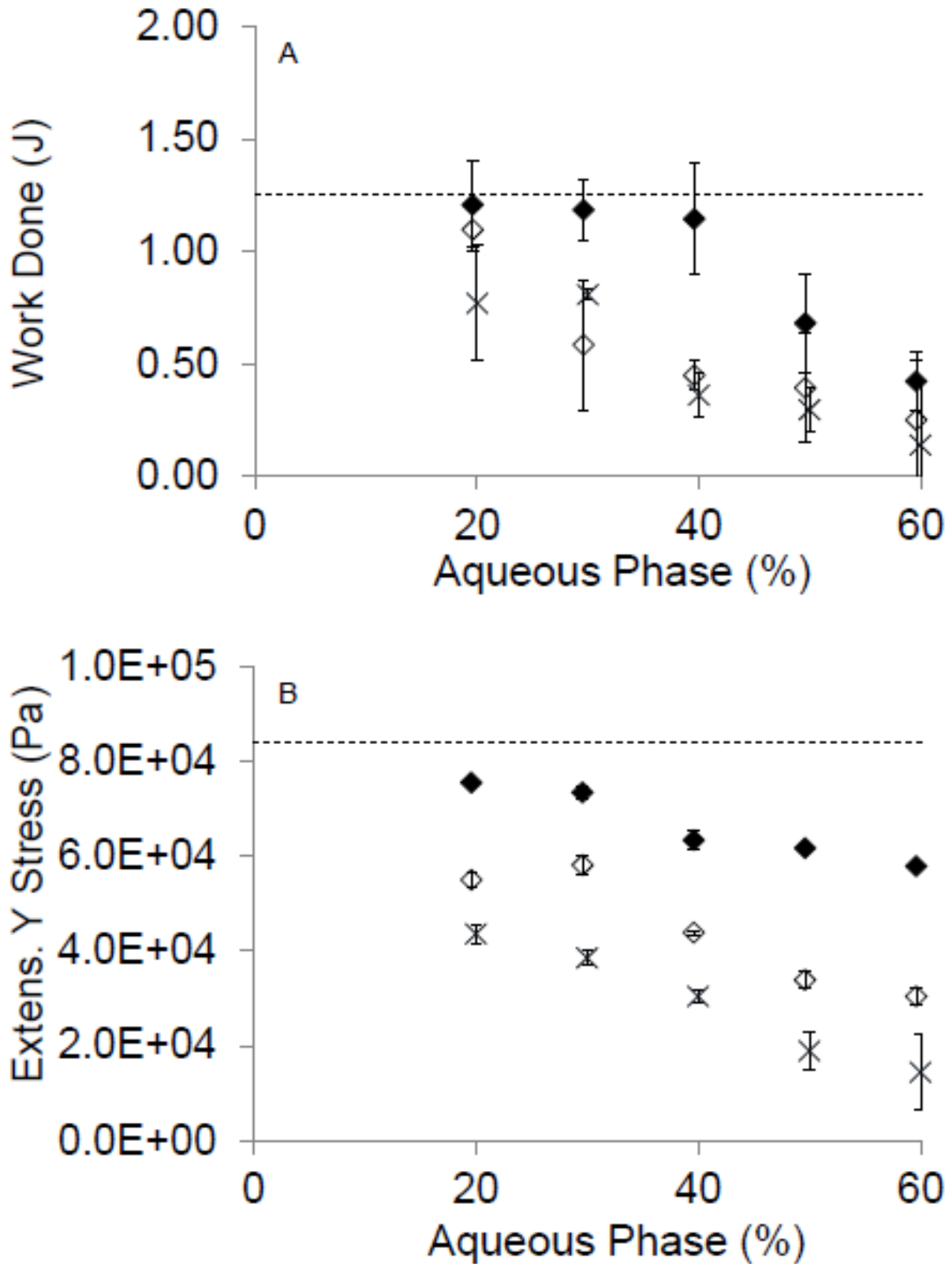
Fig. 53: (a) failure work and (b) extensional yield stress in PO emulsions with 2% HMMG, as a function of percentage aqueous phase. Aqueous phase contains (×) water, (◊) 0.4% κ-carrageenan solution, and (♦) 0.4% κ-carrageenan 0.0135M K(sorbate). Respective values for PO shortening indicated (▬ ▬ ▬).

No distinction was observed in mean droplet diameter (Fig. 52a) between water and 0.4% κ-carrageenan solution aqueous phase compositions outside of indicated error boundaries representing one standard deviation, whilst 0.4% κ-carrageenan 0.0135M K(sorbate) emulsions (arguably) were only marginally higher.

Free water (Fig. 52b) increased significantly in those HMMG emulsions with water, and 0.4% κ-carrageenan solution aqueous phases at 30% volume and above. This also occurred in emulsions with 0.4% κ-carrageenan 0.0135M K(sorbate) aqueous phase, but only at 50% aqueous phase volume.

This evidence presented would further indicate towards multiple conflicting mechanisms driving droplet size distribution. Whilst water would disperse most readily in SSHE mixing as the least structured of the three aqueous phase compositions, increased mobility of the water aqueous phase compared to 0.4% κ-carrageenan solution and 0.4% κ-carrageenan 0.0135M K(sorbate) aqueous phases conversely increases susceptibility to coalescence.

As a result, water droplet distribution will partially reverse as droplets seek to re-merge; driven by the thermodynamic drive to reduce surface area to volume ratio and the proportion of polar water molecules in proximity immiscible non-polar fat. This mechanism will become less prevalent with additional structuring to the aqueous phase; for example in 0.4% κ-carrageenan solution and (more so) 0.4% κ-carrageenan 0.0135M K(sorbate) aqueous phases.

Increased mean droplet diameter of 0.4% κ-carrageenan 0.0135M K(sorbate) aqueous phase emulsions reflects the implications increasing aqueous phase structuring presents towards aqueous phase dispersion; break up will be less effective, and subsequently droplet size will be larger.

Free water at 60% aqueous phase is very high, increasing above 30% for water aqueous phases. This is concluded to represent early stages of phase inversion, as the aqueous phase is becoming larger and so fat can start to become dispersed in the aqueous phase (i.e. o/w emulsion) [224].

This is understood to be due to the higher temperature of the SSHE slowing fat crystal network development allowing droplets to coalesce following dispersion. Previous work on CB emulsions [42] successfully dispersed a 0.6 phase volume fraction of 2% κ-carrageenan (no salt) solution in CB emulsions using an analogous process, using a highly effective PGPR emulsifier. By altering emulsifiers or concentration of emulsifiers droplet size, and free water may therefore be decreased.

Increasing aqueous phase volume decreased physicomechanical strength of the emulsions, as represented by failure work (Fig. 53a) and extensional yield stress (Fig. 53b). Both attributes demonstrated clear distinction on aqueous phase composition, increasing with increasing structure in the order 0.4% κ-carrageenan 0.0135M K(sorbate) >> 0.4% κ-carrageenan solution > water (water giving the weakest emulsions).

All emulsions fell below the measured work failure for pure PO shortening, apart from 0.4% κ-carrageenan 0.0135M K(sorbate) emulsions containing 20, 30 and 40% gelling aqueous phases. Non gelling aqueous phases (0.4% κ-carrageenan solution / water) exhibited a sharp fall in material strength at approximately 30% aqueous phase. All emulsions fell below measured extensional yield stress for PO shortening.

As in HMMG emulsions of varying aqueous phase structure, mean droplet diameter (Fig. 54a) and free water (Fig. 54b) increase in LMMG emulsions with increasing aqueous phase percentage. Both droplet diameter and free water values fell consistently below those of HMMG for corresponding emulsions, as was previously construed (Fig. 50).
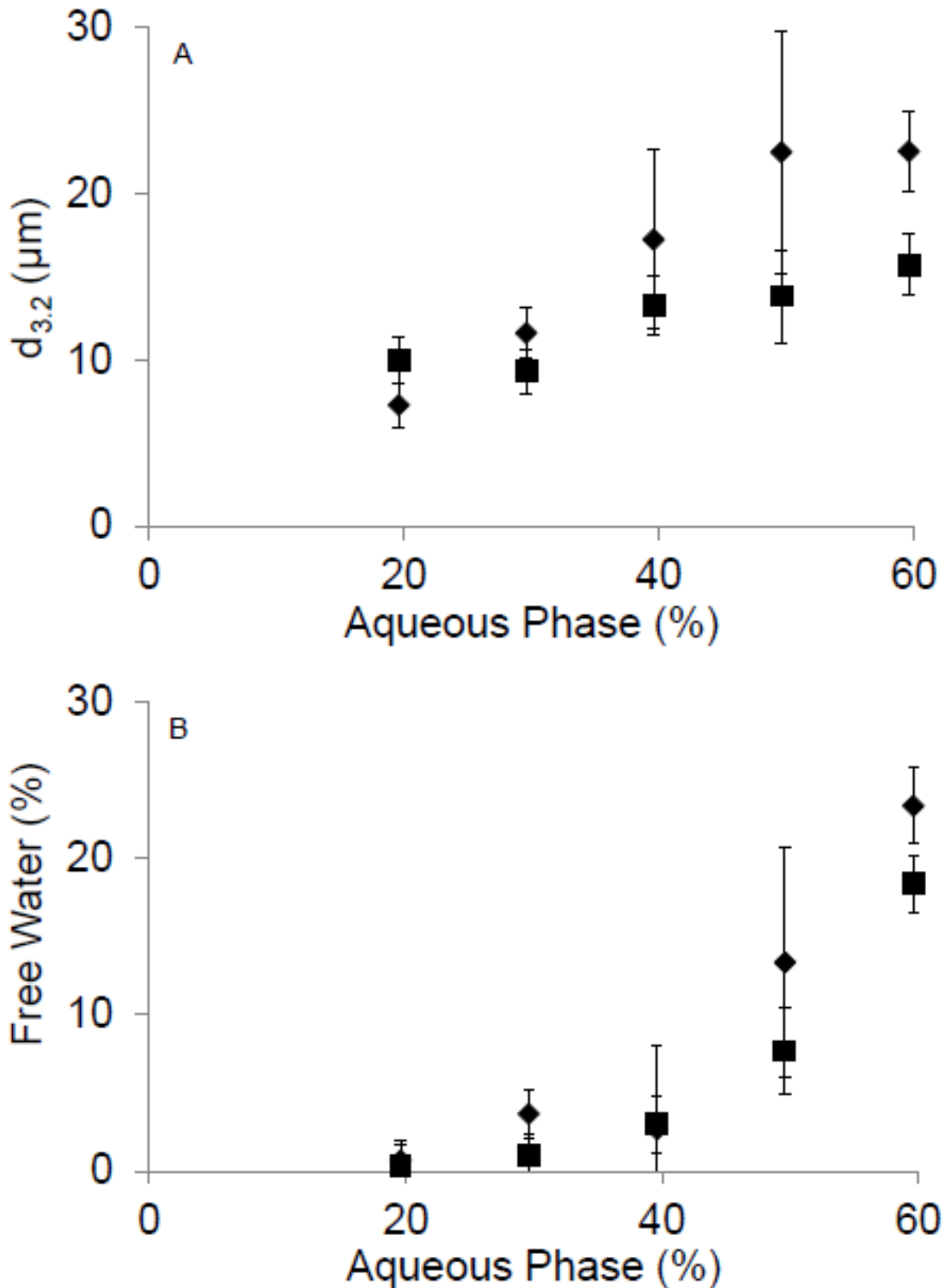
Fig. 54: (a) mean droplet diameter (d3.2), and (b) free water for PO emulsions with 2% HMMG (♦), and 2% LMMG (■) as a function of percentage aqueous phase. Aqueous phase contained 0.4% κ-carrageenan 0.0135M K(sorbate).
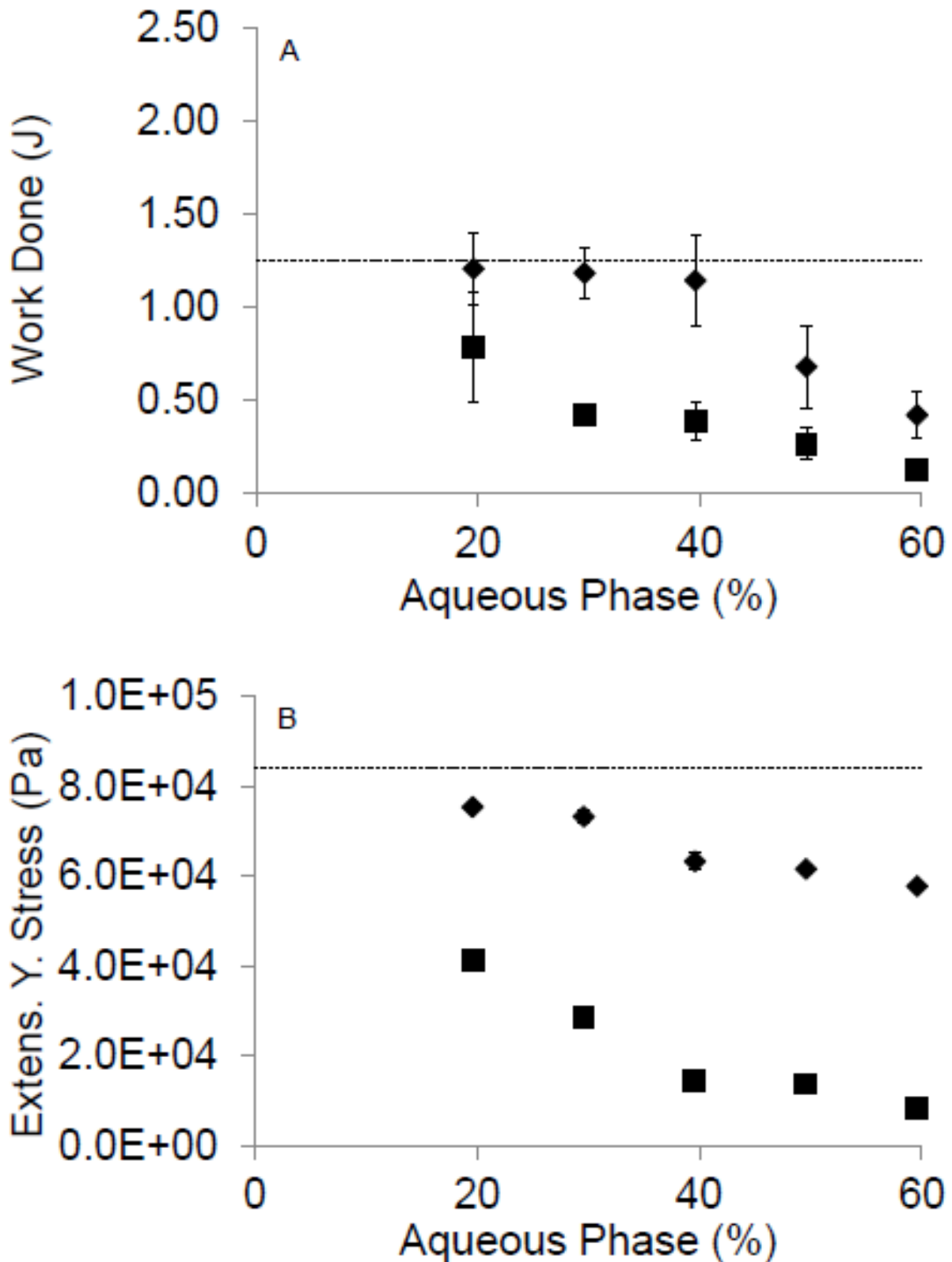
Fig. 55: (a) failure work and (b) extensional yield stress for PO emulsions with 2% HMMG (♦), and 2% LMMG (■) as a function of percentage aqueous phase. Aqueous phase contained 0.4% κ-carrageenan 0.0135M K(sorbate). Respective values for PO shortening indicated (— — —). Error bars within symbols.

Increased aqueous phase volume would correspond to more, and larger, defects in the fat crystal matrix, as confirmed in NMR droplet analysis (Fig. 52), subsequently stress transfer efficiency is expected to decrease, increasing potential for crack propagation in regions where stress concentrates [189].

LMMG emulsifier decreased the failure work and extensional yield stress of emulsions in contrast to HMMG (Fig. 55) in excess of 50%, as previously observed in T_{SSHE} investigations (Fig. 51).

Physicomechanical strength of a material is dependent on a number of factors; predominantly the strength of either phase, the stress transfer defined by interfacial adhesion, and the proportion of the overall composite taken up by the filler particles (Equation 12). It has been established that increasing fat crystalline material in an emulsion increases the material strength and hardness of the resulting macrostructure [188], therefore by increasing the aqueous phase percentage, and thereupon decreasing the fat fraction, the amount of fat crystalline matter is decreased so the fat matrix strength is decreased, resulting in the general trend of decreasing emulsion strength with increased aqueous phase fraction observed here (Fig. 53 & Fig. 55).

The aqueous phase, irrespective of additional structuring imposed here is comparatively much weaker than the TAG crystalline matrix. Correspondingly, increasing volume of weaker non-continuous material further interrupts the fat continuous matrix and van der waal associations between adjacent compatible elements on TAG crystal microstructures [186] [187] [28].

Cross sectional area of the fat crystal continuous network supporting applied loads during deformation will consequentially be decreased, and the net strength of continuous TAG matrix crystal bonding which must be overcome in order to initiate crack propagation and failure is decreased, as has been demonstrated (Fig. 53a & Fig. 55a). Interruption to van der waals associations between adjacent TAG crystal faces similarly decreases the resistance to those

crystal faces moving relative to one another, facilitating flow of the emulsion; represented by decreasing extensional yield stress (Fig. 53b & Fig. 55b).

To the same reasoning, emulsions are observed to be weaker than regular PO shortening, as crystal fat is higher, and network is not at all interrupted by dispersed aqueous phase droplets. Emulsions using HMMG emulsifier with a quiescent gelling structured aqueous phase were able to replicate work failure of PO shortening, indicating that selected compositional parameters in this instance were capable of counteracting the detrimental effects of aqueous phase inclusion (up to 40%) on some physicomechanical properties. This decreased below PO shortening values as rigidity of the aqueous phase was decreased, and HMMG was replaced with softer LMMG emulsifier.

It is therefore concluded that physicomechanical strength of emulsions is related to the mechanism at the interface originating from any or a number of; LMMG emulsified droplets transfer stress inefficiently due to poorer adhesion to the surrounding fat network, or sintering is favoured in one and not the other, or simply HMMG is more rigid than LMMG.

If HMMG emulsifier shells were considerably harder than the PO crystal network itself then it would be expected that the microstructure would exhibit crack propagation through the PO matrix, and not through the droplets, as this is the weakest course [208]. Strengthening of the aqueous phase (assuming complete emulsification) would exhibit no effect upon emulsion strength, which is obviously not the case. Therefore, it is unlikely that the HMMG emulsifier droplet shell structuring is comparatively stronger than the continuous PO crystal network, possibly due to sintering incompletion.

LMMG is liquid at room temperature indicating increased mobility relative to HMMG. It would therefore be expected to associate and interact with the interface within the SSHE faster, stabilising droplets. Subsequently smaller droplet sizes are stabilized, the fat crystal matrix

later developing to fix them in place. Interestingly, smaller droplet sizes and improved dispersion quality would impart strength towards the macrostructure of the emulsion, however the LMMG emulsion is still observed as weaker than the HMMG in mechanical studies (Fig. 55). Emulsion strength therefore must also rely upon droplet shell strength and interactions with the continuous structure. Studies will now turn to focus on the components at the interface between the two phases.

5.4.5. Emulsifier Concentration

Emulsions tend towards separation due to the thermodynamic drive to reduce incompatible phase contact. Reducing the number and increasing the size of droplets will decrease the interfacial surface area between the two phases for a given phase volume. This will reduce the number of adjacent molecules of opposing polarity in the system, and net repulsive force potential energy. Emulsifier molecules orientate themselves at the interface, in order to decrease this potential energy favouring separation, and reduce (or ideally eliminate) it [27] [31]. Subsequently, the greater the aqueous phase volume, or the smaller droplet sizes the aqueous phase is dispersed into, the greater the interfacial surface area, and subsequently the greater the surface area the emulsifier must stabilise [220]. Analogous studies [42] successfully incorporated 60% aqueous phase of 1.5% κ-carrageenan in cocoa butter emulsions, whilst separate investigations [35] have reported the successful incorporation of 50% aqueous phase of 2.5% gelatin, also in cocoa butter emulsions, both using the highly effective but food standards restrictive PGPR emulsifier. It was therefore critical to consider the effects of emulsifier concentration within this investigation.

The effect of emulsifier concentration (0.5-3.0%), for both HMMG and LMMG emulsifiers was investigated in w/o PO emulsions incorporating a 30% aqueous phase of 0.4% κ-

carrageenan with 0.0135M K(sorbate), quantifying the physicomechanical and microstructure properties via work leading to failure studies, squeeze flow, and NMR droplet analysis. Surface weighted mean droplet diameter ($d_{3.2}$) and free water (water droplets exceeding 50μm in diameter) decreased with increasing emulsifier concentration for both emulsifiers studied (Fig. 56a&b). For all emulsions, 3% emulsifier concentration was sufficient to successfully obtain complete emulsification (considered 0% free water: i.e. all water dispersed in droplets below 50μm in diameter) with mean droplet diameters of approximately 10μm diameter in both LMMG and HMMG emulsions with gelled aqueous phase (Fig. 56a) (10μm diameter or less is desirable).

This is concluded to be the result of two factors acting upon the emulsion stability. Firstly, greater dispersion of the aqueous phase into smaller droplets will create a greater surface area:volume ratio, and subsequently a greater total surface area for the emulsifier to cover in order to achieve the same stabilisation potential, requiring higher concentrations of emulsifier will facilitate this. The second factor is increased incident probability: the more emulsifier in the sample, the less the average time delay before a droplet broken up in the SSHE is intercepted by emulsion particles and stabilised, therefore there is less opportunity for coalescence to occur, and smaller droplets in the resulting emulsion.

Emulsifier concentration has a greater relative effect upon droplet sizes in LMMG emulsions. The LMMG emulsifier is liquid in the SSHE, and therefore availability for migration and reorganisation at the interface is increased, subsequently increasing emulsification effectiveness, the results of which are displayed in (Fig. 56b) where only 1% LMMG emulsifier was required in order to obtain 0% free water. Decreased droplet size will reduce the defect action of droplets and localisation of stress in emulsions as discussed explaining observed increase in work to fracture (Fig. 57a), and extensional yield stress (Fig. 57b) in both HMMG and LMMG emulsions..

Fig. 56: (a) mean droplet diameter (d3.2), and (b) free water for PO emulsions with HMMG (♦), and LMMG (■) as a function of emulsifier concentration. Aqueous phase contained 0.4% κ-carrageenan 0.0135M K(sorbate).
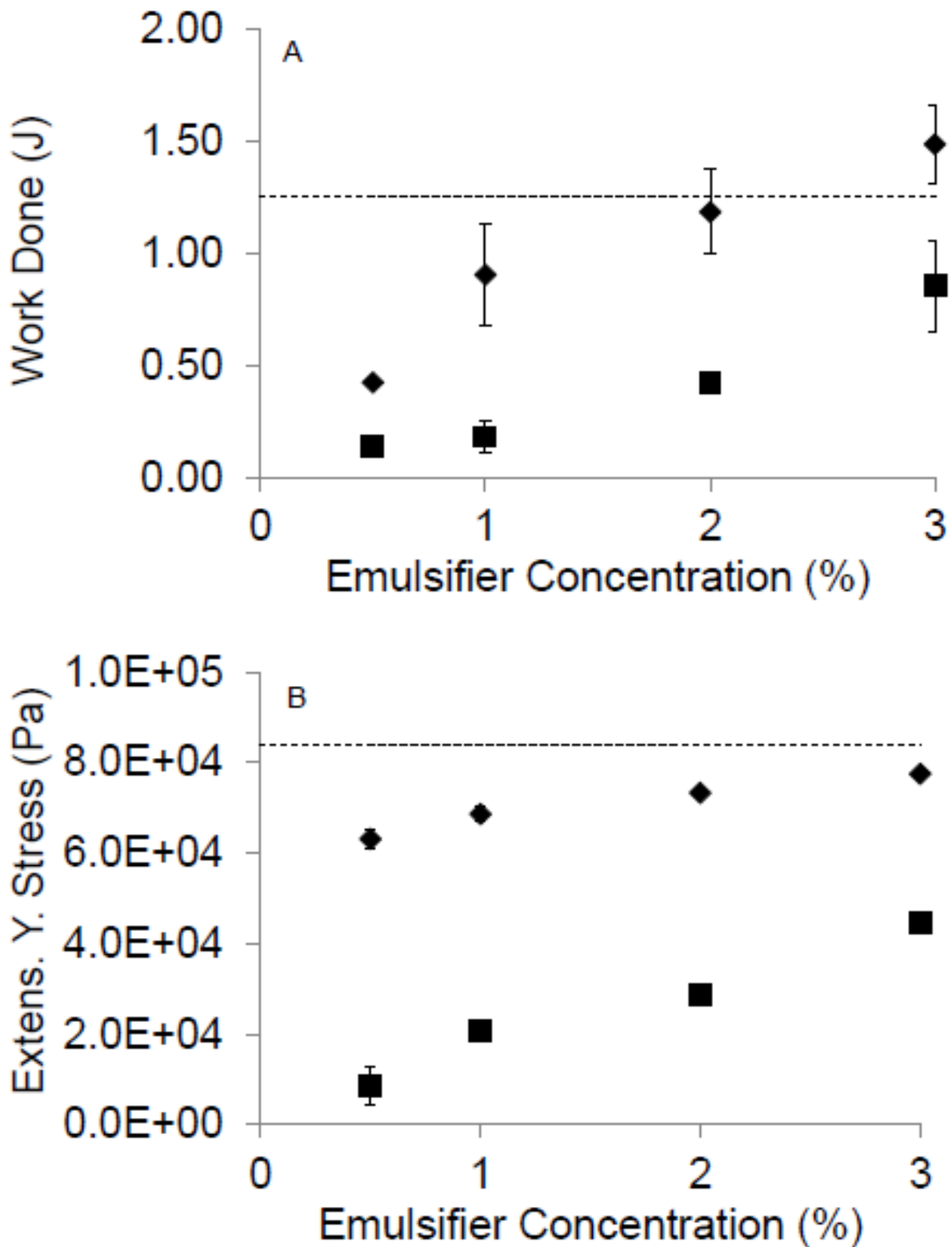
Fig. 57: (a) failure work and (b) extensional yield stress for PO emulsions with HMMG (♦), and LMMG (■) as a function of emulsifier concentration. Aqueous phase contained 0.4% κ-carrageenan 0.0135M K(sorbate). Respective values for PO shortening indicated (— — —).

Work input to fracture studies (Fig. 57a) exhibited decreased compression resistance in LMMG emulsions therefore indicating lower material strength properties to those corresponding HMMG emulsions. As in the case of HMMG emulsions, resistance to compression increased with increasing emulsifier concentration. Increasing emulsifier concentration was also found to induce higher extensional yield stress values (Fig. 57b), with LMMG emulsions exhibiting lower extensional yield stress values than HMMG emulsions.

Emulsions containing 3% HMMG emulsifier matched those material properties of pure PO shortening (Fig. 57). It is concluded that droplet shell strength matches or exceeds the strong bonding in the PO fat crystal matrix at this point, as according to straightforward fracture mechanics [189] [208] [206] the weakest point in a composite will define the macroscopic strength, in this case the PO matrix, as this is where cracks are most likely to propagate from.

5.4.6. Double Fraction Palm Oil

Thus far, HMMG emulsions have persistently given stronger emulsions than those of LMMG (Fig. 51, Fig. 54, Fig. 57). It is insufficient to suggest that the small increase in solid fat content via emulsifier concentration of the magnitude here (0.5%-3%) is likely to stimulate such a gross margin in bulk emulsion strength on its own simply by means of adding solid structuring material [167, 180].

It is hypothesised that addition of HMMG (by comparison to LMMG) to the emulsion increases the hardness of the interface surrounding the droplet shell, and subsequently the composite strength increases on the basis of increased filler particle rigidity [225] [188] [183]. HMMG moves to the interface and cools, so the droplet shells solidify and harden, which cannot occur in the case of the ambient free-flowing LMMG. Depending on emulsifier – fat crystal interactions [30], TAG crystals may associate at the surfactant-stabilised interface immobilise

the droplet via a Pickering mechanism [191, 192]. TAG crystal seeds may accumulate about the droplet, potentially accumulating in a smooth fat sintered shell [41]. Accordingly, addition of high melting fat fractions would be expected to increase the mechanical response of emulsions by strengthening the fat crystal matrix, and/or moving towards the interface and improving droplet shell structure [30].

PO emulsions with a 30% aqueous phase of 0.4% κ-carrageenan solution with 0.0135M K(sorbate) were prepared, with specific concentrations (0-3%) of DFPO incorporated into the fat phase. Emulsions made using 2% HMMG and 2% LMMG emulsifier were compared. DFPO was chosen as it is similar in structure to the triglycerides in the PO continuous fat matrix, and therefore is deemed as having greater potential for interaction with the fat crystal network [30]. It is generated by extracting the two highest melting fractions from standard palm oil by fraction distillation, thus removing the oil from the solid fat.

Increasing DFPO concentration decreased mean droplet diameter and free water percentage in both HMMG and LMMG emulsions only marginally (Fig. 58), with no distinction being drawn between the two sets of emulsifiers.

Solid fat content as a percentage of all fat in the sample was measured using NMR. SFC increased from 16.5-18% by approximately 2.5% with addition of (up to) 3% DFPO (Fig. 59); approximating to the concentration of DFPO added. HMMG emulsions exhibited higher SFC than LMMG emulsions by approximately 1-2%, assumed a result of the solid state of the HMMG emulsifier (2%).

Addition of DFPO appears to improve droplet dispersion stability (Fig. 58). Increased SFC in the fat crystal matrix (Fig. 59) will increase TAG crystal particles available for Pickering stabilisation [204], restricting the mobility of aqueous phase droplets, impeding coalescence mechanisms.
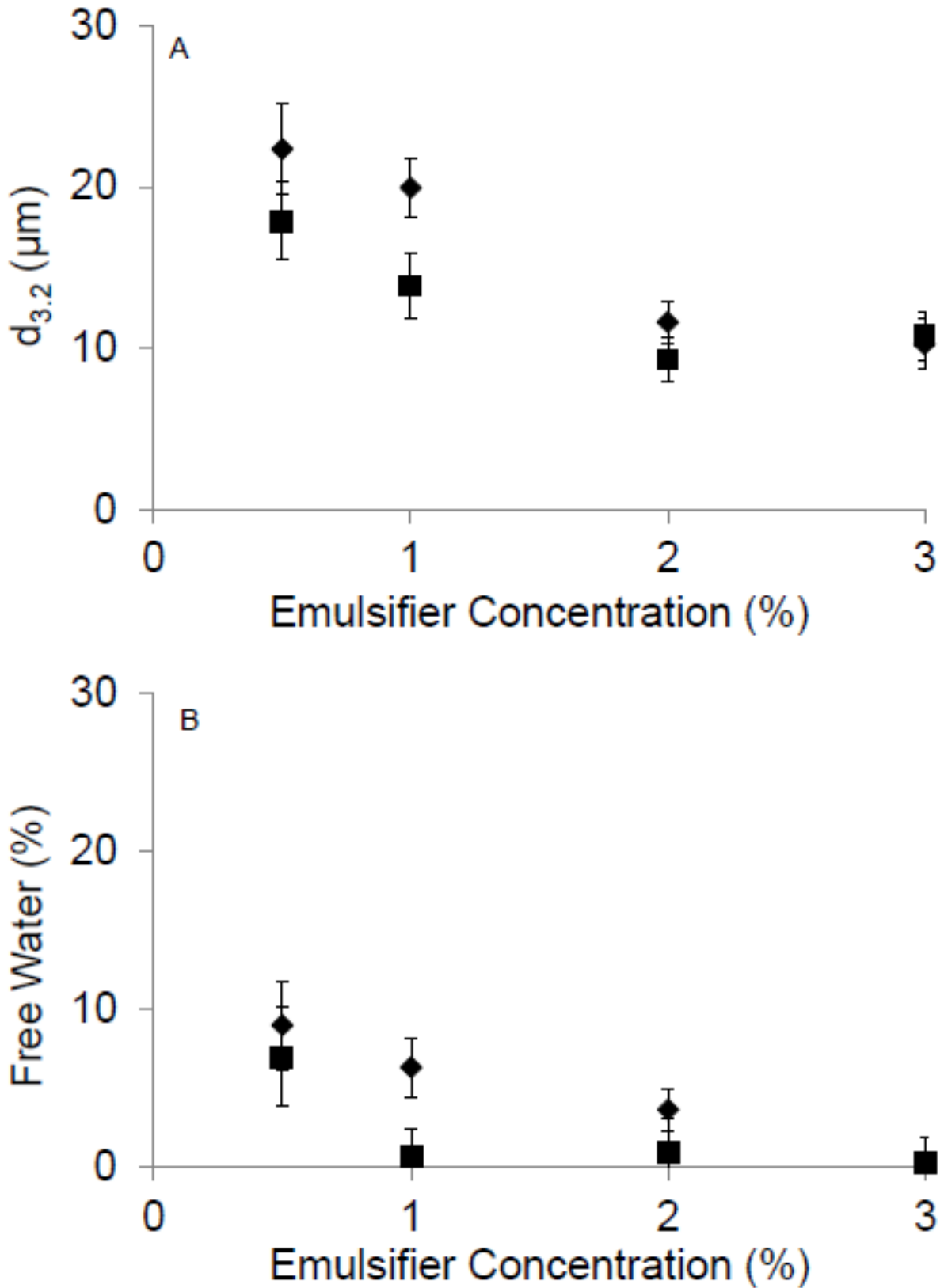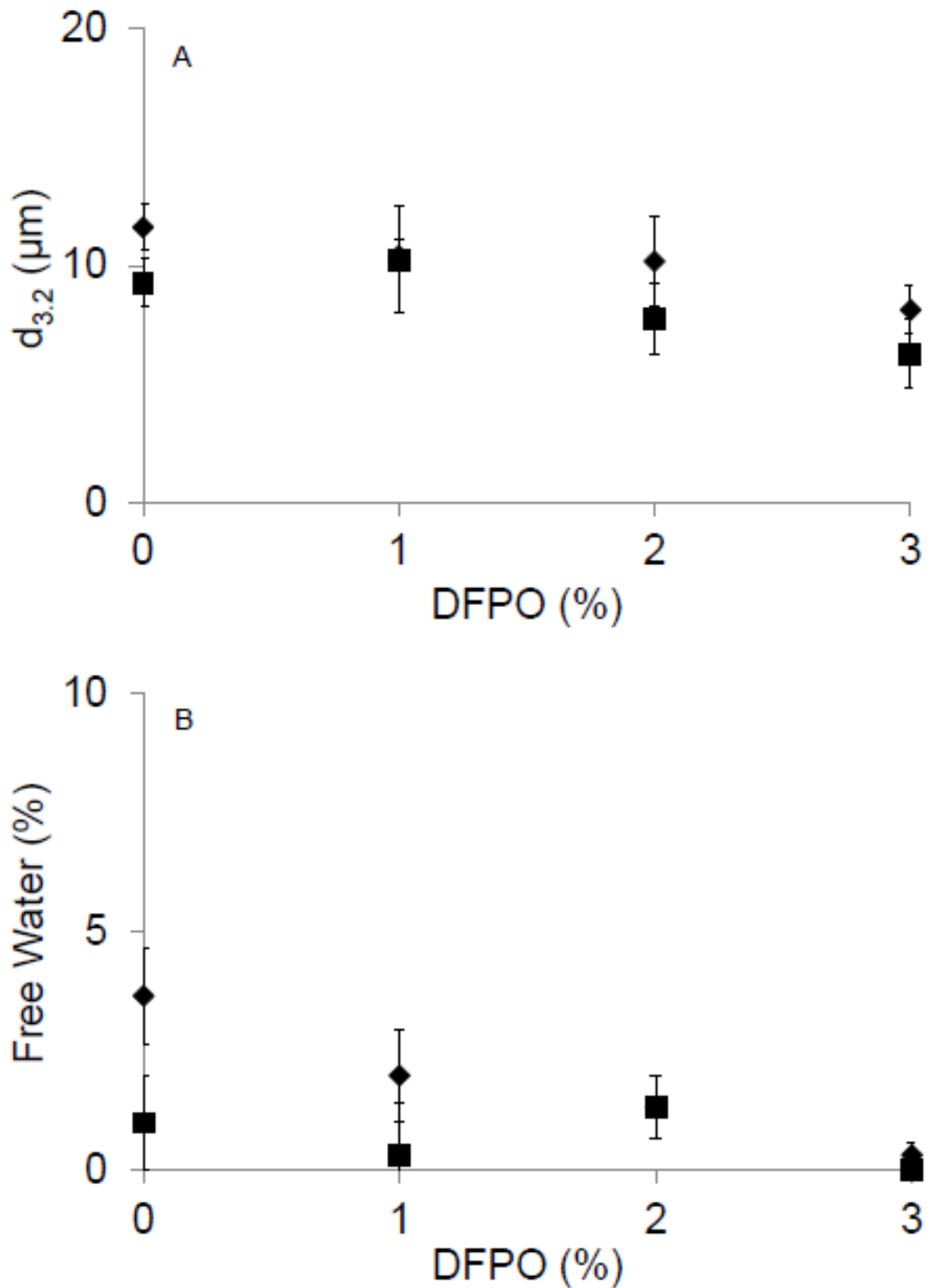
Fig. 58: (a) mean droplet diameter (d3.2), and (b) free water for PO emulsions with 2% HMMG (♦), and LMMG (■) as a function of DFPO added. Aqueous phase contained 0.4% κ-carrageenan 0.0135M K(sorbate).

Higher concentrations of solid fat TAG crystals will increase the incidence probability upon the interface in the SSHE processing unit, decreasing the mean time before crystal seeds stabilise at the interface – increasing the speed of droplet stabilisation. Increased solid TAG concentration will also increase proximity of solid fat crystals associating at the interface, increasing opportunity to congeal and sinter.
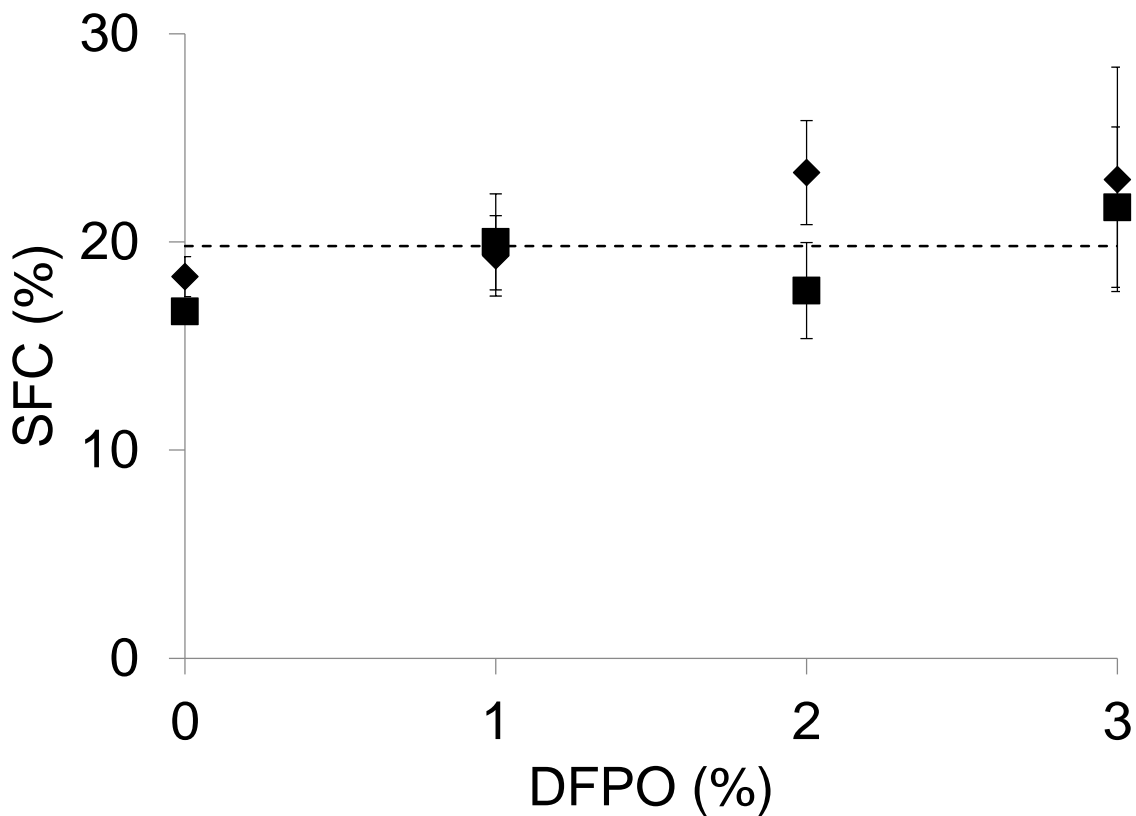
Fig. 59: Solids percentage of the total fat phase for PO emulsions with 2% HMMG (♦), and LMMG (■) as a function of DFPO added. Aqueous phase contained 0.4% κ-carrageenan 0.0135M K(sorbate). The horizontal dashed line indicates the solid fat content of Pure Shortening.

Work input to fracture and extensional yield stress increased with increasing DFPO concentration from 0-3% (Fig. 60) for LMMG emulsions. HMMG emulsions exhibited no distinguished dependency upon addition of DFPO up to 3%. Failure work (Fig. 60a) for

HMMG emulsions reciprocated that of pure PO shortening, whilst only those HHMG emulsions incorporating 2% (and above) DFPO reciprocated PO shortening extensional yield stress values. Addition of DFPO has been shown to implicate the resistance to deformation of LMMG PO emulsions greater than those respective HMMG emulsions (Fig. 60), despite exhibiting no distinction between the two in droplet size (Fig. 58) or solid fat studies (Fig. 59). It is therefore concluded that addition of DFPO implicates microstructure strength and mechanical properties beyond simple increasing solid material mechanisms [180, 202, 203].

The difference in margins of emulsion strength and resistance to compressive force between respective HMMG and LMMG emulsions upon the addition DFPO compared to the equivalent emulsions without, would indicate toward DFPO strengthening a particular aspect of the microstructure, more prominently in LMMG emulsions. The greatest distinction between the two emulsion series is most definitely the comparative physical structuring of either emulsifier at the interface surrounding the dispersed aqueous phase droplets; HMMG existing as a very hard solid under ambient conditions, whilst LMMG is (semi) liquid.

Consequentially, the HMMG emulsified droplets will increase the hardness of the dispersed droplets as it encapsulates them, whilst the softer LMMG will not. Upon addition of DFPO however, the high melting fraction hard fat may associate to the emulsifier at the interface, strengthening the fat layer about the interface and increasing the perceived hardness of the droplets in the emulsion macrostructure. As the hardness of the droplets increases, so the stress transfer efficiency between the TAG continuous matrix and the droplet 'defects' increases, and stress localisation and concentration is decreased, raising the overall emulsion physicomechanical resistance to deformation.
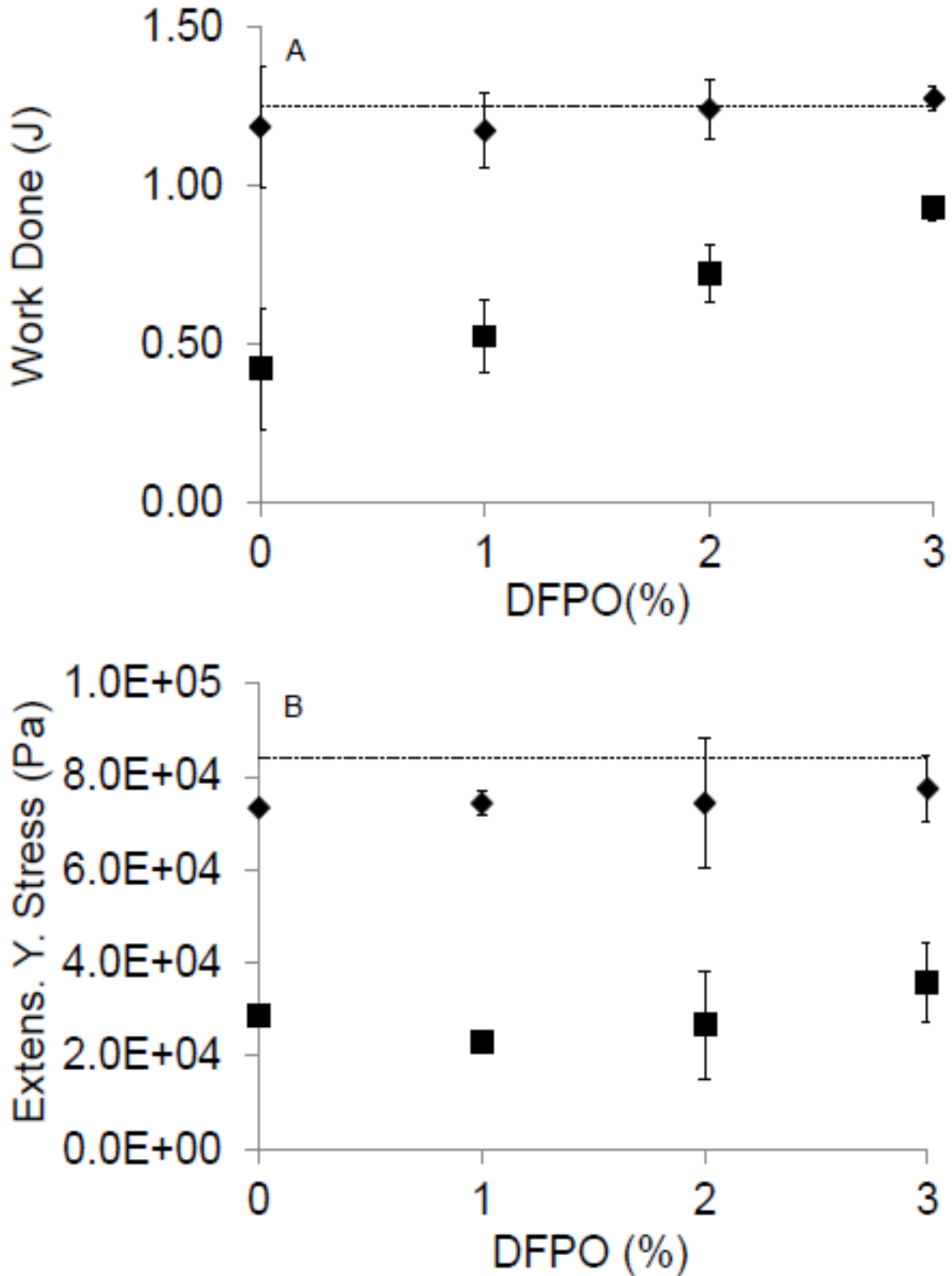
Fig. 60: (a) failure work and (b) extensional yield stress for PO emulsions with 2% HMMG (♦), and LMMG (■) as a function of DFPO added. Aqueous phase contained 0.4% κ-carrageenan 0.0135M K(sorbate). Respective values for PO shortening indicated (━ ━ ━). Error bars within symbols.

Understanding of the specific mechanisms for enhanced DFPO effects on LMMG emulsion mechanical properties at this point remain ambiguous, however it is suggested that the LMMG interacts better with the particular DFPO TAGs added, whether by correlations in chain length [226] or structure [31], improving the DFPO templating about the interface [30]. Alternatively, DFPO action in the two emulsion sets; HMMG and LMMG, may be equivalent, and as distinction is based on the difference in droplet rigidity prior to DFPO addition: any increase will be more apparent in the less rigid LMMG stabilised droplets than in HMMG droplets, which are considerably more rigid to begin with. Furthermore, HMMG emulsions exhibit physicomechanical properties comparable to PO, at which point the fat continuous phase will be the limiting weakness in the macrostructure strength.

5.4.7. K-Carrageenan & XLWM Starch Aqueous Dispersions

Use of κ-carrageenan in structuring the aqueous phase has enabled a varying degree of control both on aqueous phase droplet size and emulsion mechanical behaviour. The effects of increasing complexity in aqueous phase structuring via addition of a cross linked waxy maize starch, for extended control of the dispersed phase was therefore investigated, and effects upon the overall emulsion physical properties with a view to mimicking Palm shortening behaviour and material properties, whilst maintaining a reduced fat content.

Addition of XLWM starch to 0.4% κ-carrageenan gels with 0.0135M K(sorbate) is understood to increase the physicomechanical strength of the composite by increasing the effective concentration of the κ-carrageenan gel continuous phase via a volume exclusion effect (refer to previous Chapter 3.0).

XLWM starch was used in particular as it has a good water holding potential and amylopectin cross-linkages improve resistance to thermal degradation, allowing swollen granules to keep

their structure, whilst amylose concentration is low (<5%) to avoid leakage. Additionally, chemically treated starches such as this have been modified specifically so as to improve resistance to water leakage over time by syneresis. Addition of XLWM starch will improve the rigidity of the composite aqueous phase from that of 0.4% κ-carrageenan 0.0135M K(sorbate) alone; increasing mechanical strength of the overall emulsion macrostructure allowing for a closer replication of those material properties of the pure PO shortening. Furthermore, it enables increased control in water release on practical application (i.e. baking).

Surface weighted mean droplet diameter $d_{3.2}$ and free water for HMMG and LMMG emulsions of varying aqueous phase composition is presented (Fig. 61 & Fig. 62 respectively). Those emulsions incorporating XLWM starch into aqueous phase exhibit a significant increase in both droplet diameter (Fig. 61a & Fig. 62a) and free water (Fig. 61b & Fig. 62b). No marked distinction was observed between emulsifier types, nor between aqueous dispersions with XLWM with κ-carrageenan and DFPO, XLWM with κ-carrageenan, and just XLWM.

Failure work of 2% HMMG emulsions incorporating 2% XLWM starch decreased below that of emulsions with 0.4% κ-carrageenan 0.0135M K(sorbate) aqueous phase (Fig. 63a). Interestingly, mixed polymer emulsions exhibited a marginally higher failure work than 2% XLWM alone, but still considerably below 0.4% κ-carrageenan 0.0135M K(sorbate). Addition of 2% DFPO increased failure work of the mixed polymer emulsion, however no distinction was observed with corresponding emulsion without 2% XLWM. Failure work of 2% LMMG emulsions was consistently lower than respective HMMG emulsions (Fig. 63b). No distinction was possible between those emulsions with XLWM starch, and with water.
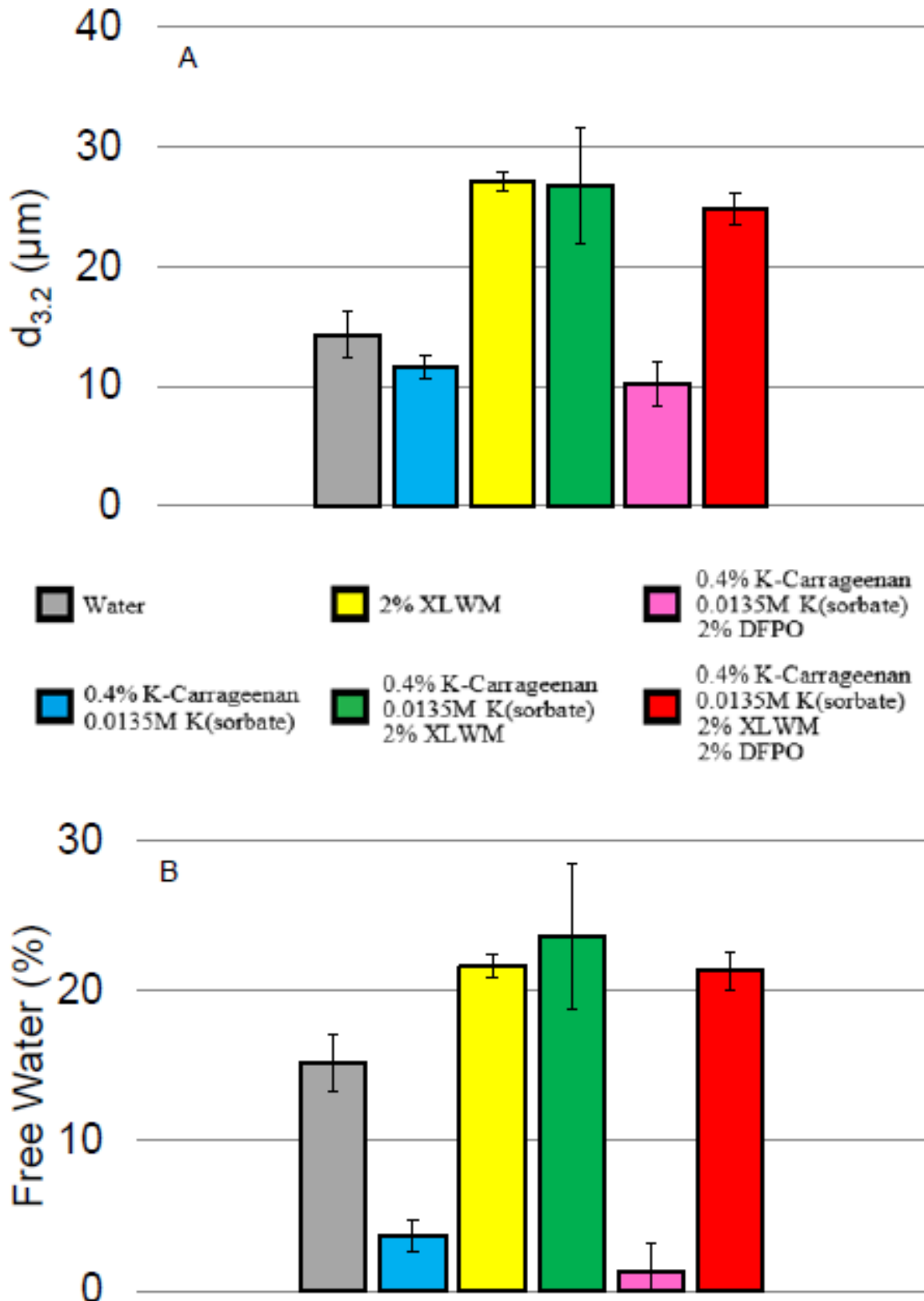
Fig. 61: (a) mean droplet diameter (d3.2), and (b) free water for 2% HMMG PO emulsions. All emulsions included 30% aqueous phase.
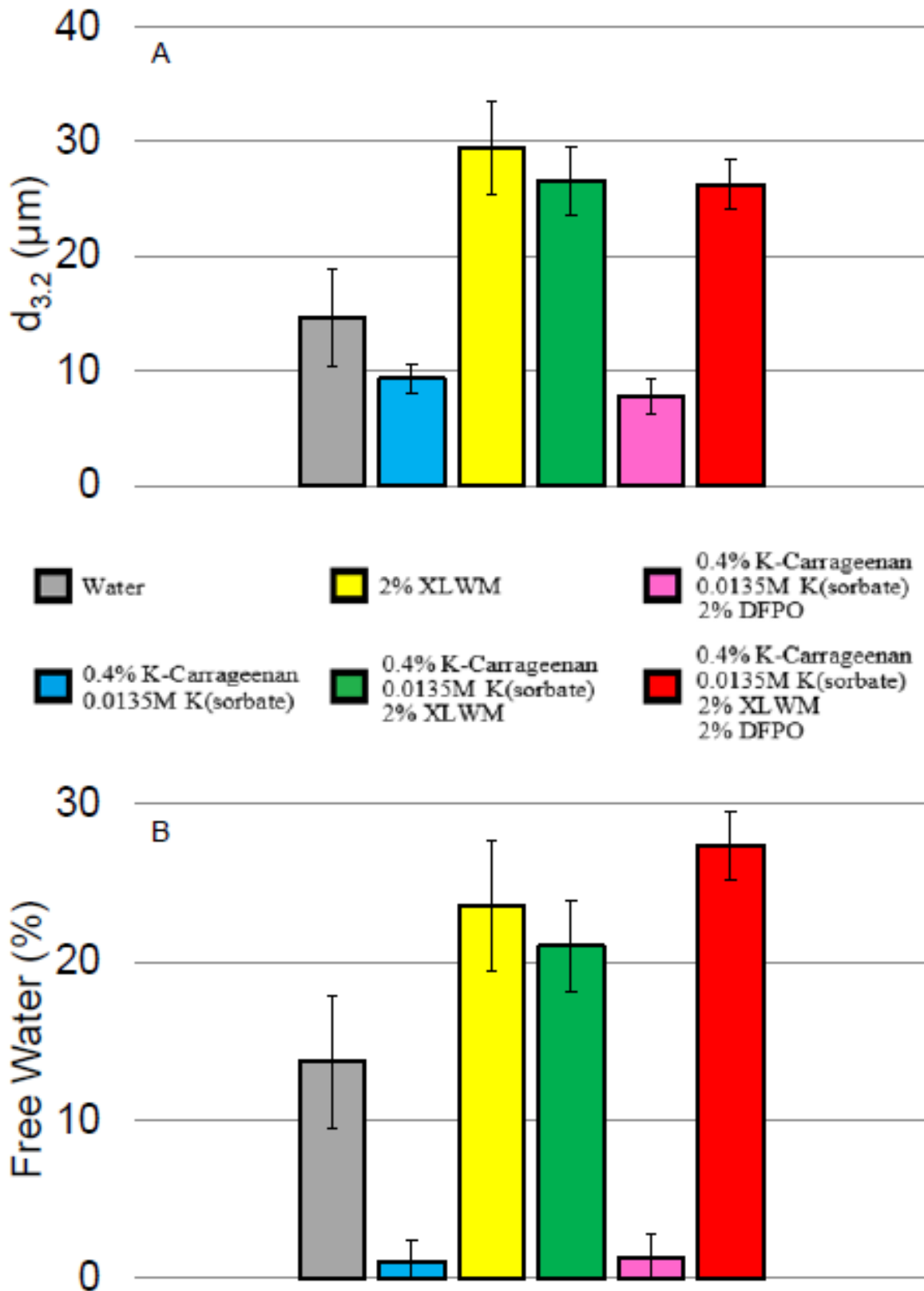
Fig. 62: (a) mean droplet diameter (d3.2), and (b) free water for 2% LMMG PO emulsions. All emulsions included 30% aqueous phase.
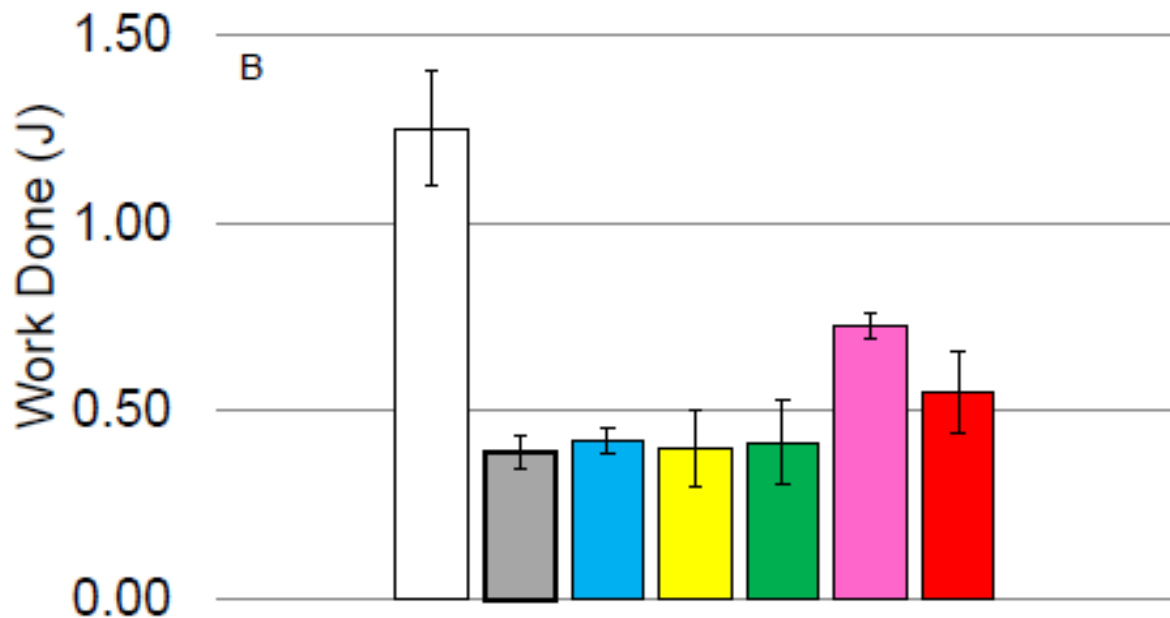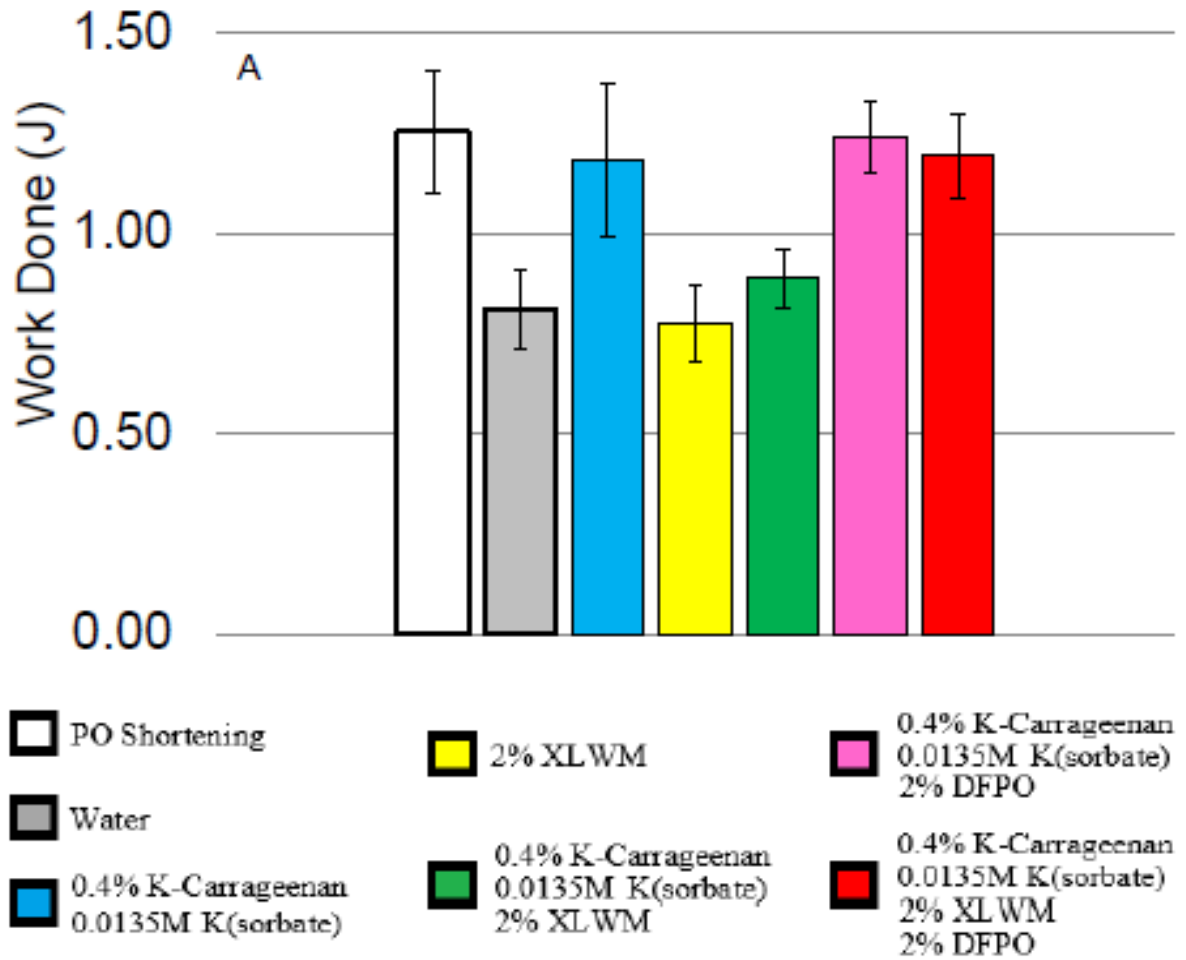
Fig. 63: Failure work for PO emulsions with (a) 2% HMMG, and (b) 2% LMMG. All emulsions included 30% aqueous phase.

Addition of DFPO increased failure work in both 0.4% κ-carrageenan 0.0135M K(sorbate) and mixed polymer emulsions, however the latter fell below the former. Both sets of emulsions using either emulsifier would therefore indicate that XLWM starch addition weakens the emulsion structure.

Cross linked waxy maize starch was quoted as having a granule swelling size of approximately 30-50μm in diameter; corresponding to the mean droplet diameter in both HMMG (Fig. 61a) and LMMG (Fig. 62a) emulsions of 25-30μm (droplet size average will still be decreased by small dispersed droplets containing no XLWM). Granules do vary in size, and any granules greater than 50μm in diameter will likely register as free water; which would explain the high free water values in XLWM emulsions (Fig. 61b & Fig. 62b).

A number of conclusions may be made. Firstly, it would appear that the NMR technique used to analyse droplet size does register swollen starch granules as 'droplets'.

Secondly, it would appear that at least a majority proportion of swollen XLWM granules do not get broken up mechanically in the SSHE given the high droplet sizes and free water values.

Thirdly, the comparatively larger starch granules (compared to mean droplet sizes in non-XLWM dispersions) decrease emulsion mechanical strength. Granules will represent themselves as larger defects in the fat continuous matrix with a low surface area to volume ratio, and concentrate applied stress to propagate crack formation. This is still the case in mixed polymer dispersions with κ-carrageenan gel systems despite increasing the aqueous phase effective κ-carrageenan concentration, and therefore droplet rigid character (see Chapter 3.0). This indicates that the increased defect size is more influential than any impact of increased κ-carrageenan gel strength in impacting emulsion mechanical properties.

An additional hypothesis is that increasing κ-carrageenan effective concentration may increase the gel setting temperature enough to cause it to aggregate prior to or inside the T_{SSHE}, which

would increase droplet size and lead to a poor dispersion as shown earlier in this report, however there seems no significant difference in dispersion quality between those emulsions with XLWM dispersed phases and those with mixed polymer dispersed phases, whereupon if gelation was occurring during the SSHE mixing step the sheared gel fragments might be expected to further reduce the physicomechanical resistance to deformation of the emulsions.

5.4.8. Thermal Analysis

Differential Scanning Calorimetry can be a useful technique when analysing TAG crystal networks, allowing measurement of the temperature and thermal energy transfer associated with latent heat transformations which may be interpreted to provide information on fat crystal polymorphism and thermal stability. More stable close packed crystal polymorphic arrangements will melt at higher temperatures, requiring a greater latent heat as order of the structure increases, and specific TAG crystal melting endotherms may be related to specific crystal polymorphs once energy transfers are normalised by TAG crystal weight. Differential Scanning Calorimetry has been used extensively to assess tempering effects in cocoa butter emulsions formulated using a SSHE margarine line [42] [33] [32] [35] [206] [183], and also in PO margarine fats [207] - although the crystal morphology is not as definitive here.

DSC was used to investigate κ-carrageenan, XLWM starch and DFPO effects upon TAG crystal polymorphism in PO emulsions. PO shortening was also studied in order to provide a reference. For all emulsions aqueous phase was accountable for 30% of the volume of the emulsion, again processing parameters were fixed at ω_{SSHE} = 1315rpm, ω_{PS} = 1345rpm, T_{SSHE} = 26°C, T_{PS} = 20°C, Q = 0.5ml.s^{-1}. Emulsions contained 2% HMMG emulsifier. DSC traces are presented (Fig. 64) alongside peak temperature and enthalpy values (Table 5).

All traces display a single large endotherm from approximately 22 to 40˚C (Fig. 64). This broad peak is attributed to triglycerides making up the solid fat content of the PO shortening, namely dipalmitoyl-oleoyl-glycerol, tripalmatin, dipalmitoyl-stearoyl-glycerol, and dipalmitoyl-linoleoyl-glycerol [207]. The breadth of the peak is attributed to the range of crystallising fats present in the PO shortening; the multiple slight variations in polymorphic form and orientation specific to particular TAG structure lending themselves to a lack of definition in the peak observed [227].

Melting of thermo reversible 0.4% κ-carrageenan / 0.0135M K(sorbate) aqueous phase aggregate occurs at 39.6˚C (see previous, Chapter 3.0), and subsequently any attributable melting endotherm is indistinguishable to that of the collective PO TAG broad endotherm (Table 5).

Aqueous Phase	[DFPO]	T_{onset}	T_{offset}	T_{peak}	Peak Enthalpy
	%	˚C	˚C	˚C	$J.g_{-1}$
-	-	24.2	40.7	35.9	24.3
Water	-	25.0	41.3	36.2	23.8
0.4% K-carrageenan / 0.0135M K(sorbate)	-	24.3	40.2	35.5	19.2
2% XLWM starch	-	24.1	40.0	31.6	17.5
0.4% K-carrageenan / 0.0135M K(sorbate)	3	24.5	39.6	35.6	20.4

Table 5: DSC heating endotherm values for PO emulsions with 2% HMMG.
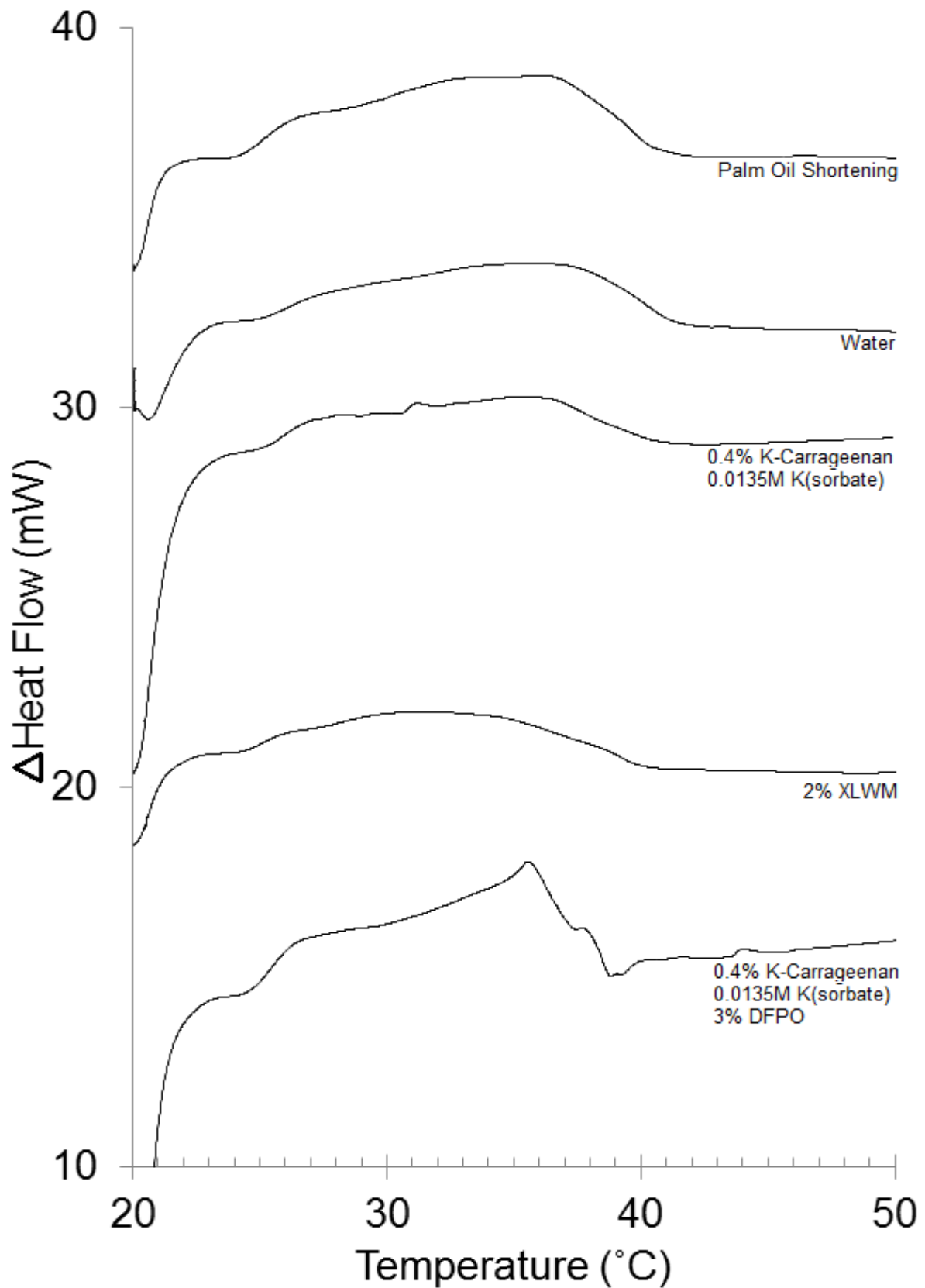
Fig. 64: DSC heating endotherm traces for PO emulsions with 2% HMMG. All emulsions included 30% aqueous phase.

Addition of a 0.4% κ-carrageenan 0.0135M K(sorbate) to the aqueous phase exhibited negligible impact upon peak positioning (relative to water aqueous phase; Table 5). Peak enthalpy decreased by approximately 20%, indicating that the κ-carrageenan did implicate PO fat phase crystallisation.

Structuring of the aqueous phase will increase the viscosity of the aqueous phase in the SSHE processing step, and consequently the localised shear on the PO fat phase will be altered. The SSHE creates TAG crystal nuclei by moving the fat molecules in their molten form in the hot solution onto the jacketed cooling wall on the mixing unit, where heat is transferred away. Sufficient transfer cumulating in latent heat initiates TAG crystal seed nucleation, the blades then sweep the crystal nuclei back in to the bulk mixture and this cycle will repeat, gradually building up the number of TAG crystal nuclei in the bulk mixture.

Increasing aqueous phase viscosity would therefore be expected to oppose this transfer, decreasing the rate of TAG crystal nucleation. Subsequently the fat nuclei seeding will be less effective, and there will be decreased cumulative formation of weak linkages between adjacent elements on TAG crystals and therefore the energy input required to overcome the solid structure bonding upon melting; decreasing the normalised endotherm enthalpy, as observed here (Fig. 64, Table 5). Similar findings were made by Sullo et al. [42] with 1.5% κ-carrageenan solutions (no salt) dispersed in cocoa butter emulsions. The effect observed here is still quite small, and this is likely because the 0.4% κ-carrageenan 0.0135M K(sorbate) solution has not begun aggregation until leaving the SSHE.

Incorporation of 2% XLWM starch in the aqueous phase of PO emulsions decreased T_{peak} and peak enthalpy from those of water, and 0.4% κ-carrageenan 0.0135M K(sorbate) emulsions (Table 5). The reasoning for this is concluded as analogous to that of 0.4% κ-carrageenan /0.0135M K(sorbate) aqueous phase, the effect is amplified in this instance as the swollen

XLWM starch granules are more rigid than the pre-gelled κ-carrageenan aqueous phase, therefore aqueous phase viscosity and thereupon its inhibitory effect upon TAG crystal nucleation rate is more pronounced.

Finally, when 3% DFPO was added a sharp peak rose from the broad peak at 34-40˚C (Fig. 64, Table 5), attributed to particular Palm Stearin addition [207]. The broad peak attributed to various PO TAGs is a merging of many multiple, slightly offset peaks, each representing a particular crystal and polymorphic arrangement or shape which will require a specific enthalpy of latent heat in order to transform from solid crystalline state to liquid. As the DFPO represents two particular fraction(s) of PO, the corresponding peak will be far more distinct. The added DFPO allows the corresponding endotherm for these fractions to rise above the others, distinguishing itself.

5.4.9. *Cryogenic Scanning Electron Microscopy*

Images of PO emulsions were captured using cryogenic scanning electron microscopy in order to try and better understand the mechanisms at the interface, and develop those conclusions from mechanical and droplet distribution studies regarding the action of different emulsifiers, structuring hydrocolloids and specific PO fractions in stabilising the emulsion. Images are displayed in appendices.

Images of emulsions formulated with 2% HMMG, and 2% LMMG (Appendix 5) displayed spherical droplets dispersed evenly in a continuous network of sintered PO fat crystals. Droplet diameters correlated with those recorded in NMR analysis. Droplets stabilised with HMMG (Appendix 5a) were observed to be entirely encapsulated in emulsifier therefore confirming successful emulsification of droplets as concluded previously from droplet analysis (Fig. 47).

The surface is rough and uneven in appearance, and therefore it is concluded sintering was not successful [30] [41] in this instance. Droplets do appear well embodied in the fat continuous

phase however, and droplets appear largely complete, with shells unbroken even in the fracture plane. The mosaic appearance on the surface of the droplet is understood to be HMMG crystals (approximately $0.1\mu m$ in diameter) tessellating on the interface [205] [30]. As a visible distinction is possible between HMMG crystals on the droplet surface it is concluded that complete triglyceride bridging and congealing to create a complete shell about the droplet has not been successful, possibly due to crystal size or shape [30] [195].

Corresponding emulsions stabilised with 2% LMMG showed much smoother droplet shells, however in this case a large proportion were observed to be broken on the sample fracture plane (Appendix 5b). It is concluded therefore that LMMG emulsifier covers the interface better than HMMG, due to increased mobility of the low melting monoglyceride allowing it to firstly associate to the interface more effectively (compared to HMMG), and thereupon reorganise to accommodate the droplet surface, resulting in the smoothed droplet surface (Appendix 5b), these observations would further support conclusions from droplet size analysis where LMMG emulsifier improved stabilisation of droplets compared to HMMG, accredited to increased emulsifier mobility (Fig. 54).

In contrast to HMMG emulsion, a significant number of LMMG droplet shells were unable to withstand sample fracture, the droplet shells rupturing (Appendix 5b). The LMMG emulsified shells are therefore concluded to be weaker than those of HMMG, hypothesised earlier from mechanical studies (Fig. 55). Stress transfer at droplets would therefore be less efficient, facilitating localised stress concentration and inherently crack propagation through droplets in LMMG emulsions.

Fracture around droplets in HMMG emulsions (Appendix 5a) is indicative of increased droplet shell strength relative to the continuous fat matrix [189]. LMMG droplets appear detached from the fat continuous phase (Appendix 5b) suggesting poor adhesion, indicating that the

LMMG shell does not interact well with PO fat crystals, which would contribute towards decreased stress transfer efficiency, allowing stress to concentrate at droplets and cracks to propagate through them, as observed here [208].

Breakages in the LMMG shells reveal κ-carrageenan K(sorbate) aggregate within (Appendix 5b), confirming the hydrocolloid aggregate was successfully formed within emulsified droplets. The κ-carrageenan aggregate appears shrunken away from the inside walls of the droplet, however this is believed to be a result of the freeze treatment during cryo SEM sample preparation.

Emulsions were prepared and analysed as before this time with 3% DFPO added (Appendix 6). HMMG emulsion droplets again appeared uneven on the surface (Appendix 6a), however droplet shells appeared complete and mosaic pattern was not observed, indicating that addition of DFPO has instigated successful bridging at the droplet shells with HMMG emulsifier.

Droplet shells in LMMG emulsions with 3% DFPO are observed to be complete (Appendix 6b), indicating droplet shells have been strengthened with the addition of the small proportion of the high melting fat fraction. Droplets this time appear less smooth: indicating DFPO crystals sintering at the surface are large (close to micron scale in diameter) and do not fit at the droplet surface as well as LMMG emulsifier.

Previous studies [41] have reported similar findings in water/sunflower oil emulsions with monoglyceride emulsifiers, where sintering at the droplet surface was observed to improve considerably when a blend of MG and Tripalmatin was used. The uneven surface observed in this study is concluded to result from MG emulsifier and DFPO structuring limitations. The appearance of the fat continuous matrix in emulsions with DFPO (Appendix 6) appears less even than those corresponding emulsions without DFPO (Appendix 5). This is understood to be a result of greater solid fat crystal structuring in the continuous matrix with added DFPO.

Emulsions incorporating 2% XLWM starch were studied (Appendix 7). Both emulsions formulated with 2% HMMG (Appendix 7a) and 2% LMMG (Appendix 7b) showed well dispersed granules of approximately 30-50μm in diameter, corresponding to estimated swollen starch granule size, confirming that swollen starch granules are not broken up in the SSHE mixing process. This agrees with earlier hypotheses suggesting whole XLWM starch granules would contribute towards increasing droplet size and free water, exhibited in NMR studies (Fig. 61, Fig. 62). Smaller droplets of 5-15μm are visible and this would correspond with droplet sizes for κ-carrageenan.

Sample fracture plane appears to have broken through all larger XLWM granules for both emulsions (Appendix 7). Due to the large size of the starch granules, the surface area to volume ratio will be low and correspondingly the stress transfer will be inefficient [208]. This will weaken the emulsion structure and propagate crack formation; verifying those conclusions drawn from mechanical deformation studies (Fig. 63).

Finally, emulsions with both 2% XLWM starch and 3% DFPO were studied. Starch granules droplet shells were again broken on sample fracture in both 2% HMMG and 2% LMMG emulsions (Appendix 8a & Appendix 8b respectively). Additional structuring effect of DFPO is therefore insufficient to successfully encapsulate XLWM starch granules, as they are too large to avoid breakage of the shells. Smaller droplets believed to contain κ-carrageenan aggregates were found in HMMG emulsions, all with complete shells (again uneven in surface). As observed in earlier DFPO emulsions appearance of the fat continuous matrix appeared uneven, further indicating that this effect is due to inclusion of DFPO.

5.5. Conclusions

In a novel study, palm oil baking shortening emulsions incorporating a quiescent gelled aqueous phase using κ-carrageenan and K(sorbate), a common FDA approved preservative, have been successfully formulated using a conventional bench scale margarine line. Emulsions successfully incorporated up to 30% aqueous phase, based upon mean droplet diameters of approximately 10μm, which were entirely encased within HMMG emulsified fat shells, as confirmed by NMR and cryo-SEM imaging. The use of a firm quiescent gel forming hydrocolloid in a single-step emulsion formulation process in application to PO shortening emulsions in particular represents a novel area of research, and the use of mechanical studies in parallel with more traditional NMR droplet size emulsion analysis has been exhibited to give a reliable in depth understanding of emulsion microstructure(s) and the control this bears on the mechanical response.

Addition of gelling polysaccharide to the aqueous phase implicated processing parameter selection, as lower SSHE temperatures which typically favour TAG crystal nucleation conversely will cause κ-carrageenan aggregation within the shearing step, as demonstrated in droplet analysis. Contrastingly, high SSHE temperatures will reduce TAG crystal nucleation and post-processing coalescence will increase as a consequence. A compromise temperature is therefore required, taken as 28.5°C exiting the SSHE in this study.

It is concluded that by controlling the structuring of the aqueous phase using hydrocolloids, it is possible to define the distribution and droplet size of the aqueous phase in the fat matrix and the subsequent effects this may have upon the physicomechanical properties and functionality of emulsions by modifying both the hardness of dispersed droplets and their shells, and by controlling the size of the droplets, which implicates the efficiency of stress transfer through the emulsion macrostructure, as confirmed here using uniaxial deformation studies, droplet size analysis and cryo SEM. Effects of structuring of the aqueous phase upon TAG crystallisation

should be considered however, as increased aqueous phase viscosity will reduce fat crystal nucleation rate in the SSHE, as indicated in NMR studies.

Droplet shell structuring may be modified depending upon selection of emulsifier type and/or additional structuring material, such as DFPO. Low melting monoglyceride emulsifiers may exhibit increased mobility at the interface, to associate and reorganise to stabilise the droplet, however the weak droplet shell strength facilitates stress concentration, accumulating in reduction of the emulsion resistance to deformation. Harder, high melting emulsifiers will create a harder shell, and subsequently this effect will be less, however it is necessary to consider the restrictions this may create in association at the interface, cryo-SEM studies exhibiting uneven, rough droplet surfaces in those emulsions using HMMG. Addition of DFPO may contribute toward shell sintering, and increase emulsion macrostructure strength attributed to increased droplet shell hardness. Interestingly, swollen starch granules were not broken up upon emulsion formation using this process, however for this particular application the large (~30μm) diameter size of the granules meant that the stress transfer at these filler particles was simply too poor and stress therefore concentrated about the granules, weakening the emulsion structure and resulting in cracks propagating through the granules, almost all droplet shells viewable by cryo-SEM having been ruptured.

A suggested solution to incomplete sintering of shells is modification of the process to include a heat cycle step, in order to facilitate rearrangement of the droplet shell crystals, facilitating improved tessellation in order to form a smoother shell, strengthening shells, and improving control of water release [30]. Further studies should consider alternative emulsifiers and effects on shell structuring and fat crystallisation and interaction.

VI

CONCLUSIONS
&
FURTHER WORK

6   Conclusions

The principle objective of this work was to investigate the capability for emulsion formulation design as a strategy for baking margarine fat reduction via holistic approach by systematically studying the effect of controlled parameters upon microstructure, conjunctive macrostructure, and physicomechanical properties and responses. More specifically, these studies included:

Investigations into monobasic anion lyotropic effects upon K-carrageenan; (de)stabilisation affects upon the ordered domain structure, the subsequent aggregate microstructure, and the impact this has upon the mechanical response of gels formed.

Modelling of the physicomechanical properties of K-carrageenan and cross linked waxy maize starch mixed polymer systems, based upon solvent partitioning and polymer chemical and physical interactions.

Processing parameter optimisation for formulation of w/o Palm Oil baking margarine emulsions using a temperature controlled scraped surface heat exchanger and pin stirrer process.

Composition and processing parameter optimisation formulation of palm oil baking margarine emulsions with a gelling aqueous phase matching those mechanical characteristics of the original full fat shortening.

6.1. Anionic lyotropy studies

The relationship between physicomechanical properties of 0.4% κ-carrageenan aggregates and the anionic lyotropic number (or Hofmeister number) has been clearly defined within these studies; decreasing lyotropic number increased the thermodynamic driving force toward polymer coil aggregation as a consequence of bulk water solvent structuring, decreasing water

molecule migration to partially stabilise the ordered K-carrageenan conformer intermediate. As a consequence of this microstructure control, anionic lyotropy similarly defines the response of the aggregate towards mechanical deformation; those systems driven towards aggregate formation in the presence of kosmotropic anions forming stronger, more rigid gels, than those in the presence of chaotropic anions. The number and range of monovalent anions included within the study itself demonstrates a novel approach, in particular the comprehensive implementation of uniaxial compression to the point of failure as a means of assessing mechanical properties of quiescent gels; offering significant advantages over those perhaps more conventional rotational and oscillatory rheology approaches.

The common food additives potassium sorbate and potassium citrate were included in their monobasic forms, and the Hofmeister number valuation of sorbate anion – which is presently unassigned – has been proposed at 10.4±0.15, supported by specific physicomechanical attribute trend fitting throughout, and conforming to the general trending of organic acid lyotropy.

Studies of potassium sorbate and potassium citrate as those presented in this work are the first of their kind - whilst the monobasic citrate anion does carry an assigned Hofmeister valuation of 7.2; lyotropic behavioural trend fitting and physicomechanical characterisation of the impact upon hydrocolloid aggregate formation is scarce. These studies demonstrated that the potassium salts of monobasic citrate and sorbate exhibit analogous lyotropic control to those of potassium chloride, widely accepted as the most commonly used potassium salt form additive for achieving K-carrageenan aggregate formation of a quiescent gel, and subsequently are proposed as an attractive alternative, given their additional capabilities as acidity regulator and preservative, respectively, and the current consumer demands for clean labelling and fewer ingredients.

6.2. K-Carrageenan & XLWM starch mixed systems

Having performed a comprehensive characterisation of anionic lyotropic effects upon 0.4% K-carrageenan aggregate formation and physicomechanical properties, four specific K-carrageenan / potassium salt combinations; chloride, citrate monobasic, sorbate, and iodide - were chosen for a novel investigation modelling the physicomechanical attributes of mixed composite gels produced by addition of cross linked waxy maize starch, having highlighted the chemically modified polymer as potential solution to counteract the inclination of K-carrageenan aggregates toward syneresis.

These studies have shown K-carrageenan and amylopectin-based starch do not form associative bonding interactions with one another. Interactions between the two are both direct and indirect, and either may present itself as the dominant factor depending upon applied deformation and salt presence. Indirectly, starch granules increased κ-carrageenan effective concentration in the continuous phase via volume exclusion, subsequently strengthening the continuous matrix and the overall composite in accordance with Takayangi's isostrain model. Starch granules were shown to weaken composite resistance towards further deformation and macroscopic failure as a consequence of crack propagation facilitated by their relatively less rigid structure. Both starch swelling and κ-carrageenan aggregate development was able to be controlled via potassium salt concentration and type.

Addition of modified cross linked waxy maize starch decreased syneresis observed over 21 days by comparison to those 0.4% K-carrageenan samples without, and therefore presents a useful solution towards stabilisation of water retention in K-carrageenan aggregates, with additional scope towards other quiescent hydrocolloid systems, all of which exhibit syneresis to some degree. The different mechanisms attributed to starch inclusion upon the resistance towards mechanical deformation of K-carrageenan composites depending on the level of deformation also presents an opportunity for tailoring the flow behaviour of the composite to

suit the particular requirements of the application based upon these holistic studies, specifying flow yield stress, or shear thinning character, for example.

6.3. Process capability & optimisation for W/O emulsions

A conventional bench scale scrape surface heat exchanger and subsequent pin stirrer was used to successfully incorporate30% water by mass within palm oil baking margarine to form an emulsion with 2% high melting monoglyceride emulsifier, achieving target free water of 0% and mean droplet diameter below 5µm (4.26µm achieved).

The two mixing stages of the process – which is an unprecedented format in specific application to baking margarine emulsion formulation – control the organisation of the system in very different ways in order to achieve the final microstructure; the SSHE controlling aqueous phase dispersion, the triacylglyceride crystal nucleation rate and size, and the movement of crystals and emulsifier molecules to the interface to stabilise the emulsion, whilst the PS manipulates the fat continuous phase, disrupting TAG network associations and consequently defining the texture of the final macrostructure, and resistance to mechanical deformation.

6.4. Palm oil baking margarine emulsions with gelling aqueous phase

By incorporating the understanding drawn from the holistic investigation strategy upheld over the previous three chapters, the bench scale scrape surface heat exchanger and subsequent pin stirrer sequence was used to successfully formulate a palm oil baking margarine emulsion, incorporating a 30% gelling hydrocolloid solution aqueous phase of 0.4% K-carrageenan with 0.0125M potassium sorbate, achieving target free water of 0% and mean droplet diameter of 10µm. The holistic strategy exercised throughout allowed for aqueous phase gelation to occur

after emulsion formulation by optimization of process cooling parameters and salt / K-carrageenan concentrations to control fat crystal nucleation and hydrocolloid aggregate formation; facilitating effective aqueous phase distribution and emulsification.

Studies found that in no instance was droplet shell sintering entirely successful, with high melting monoglyceride emulsifiers producing the best shell structures in the presence of additional small concentrations of high melting fat factions, as demonstrated by SEM imaging. These investigations have demonstrated that whilst lower melting monoglyceride emulsifiers formed a smoother, more complete shell structure than their high melting counterparts, they were also weaker.

Using 2% high melting monoglyceride emulsifier in the presence of additional small concentrations of high melting fat factions, palm oil baking margarine emulsions incorporating a fully emulsified 30% aqueous phase were formulated which emulated those physicomechanical properties of the conventional full-fat shortening, therefore proving capability for this novel processing sequence to formulate a 30% reduced fat baking margarine which fulfils all the (pre-baking) functional demands of conventional baking margarine.

The strategy outlined from the preliminary stages of this study has been to develop a comprehensive understanding for microstructure design of reduced fat baking margarine emulsions via systematic control of individual parameters. This holistic approach will enable the learnings from this work to be applied correspondingly to various baking processes, depending upon the requirements and/or limitations of the role which fat must fulfil in the recipe.

For example, in short doughs the role of the fat is to smother the gluten particles of the flour completely preventing hydrolysis and formation of a gluten network – creating the signature crumbly texture, and therefore the 30% reduced fat emulsion described above would be suitable

in this instance, as these studies have demonstrated that none of the water incorporated within the emulsion is available, and it is hypothesised that mildly less hydro-sensitive doughs such as cookie doughs would facilitate even 40% reduced fat emulsions formulated here, as even these has been shown to exhibit only 3% free water. Cake; whose springy, elastic character is attributable to the formation of a more developed gluten network, would be expected to support further increased baking margarine emulsion fat reductions of up to 50%.

Finally, the incorporation of an aqueous phase within the making margarine microstructure may, in some particular applications, be beneficial. Puff pastry is formed by layering sheets of pastry upon one another, separating each layer by a layer of baking margarine. The fat serves to prevent gluten network extending between the layers, keeping it unilateral. Upon baking the steam produced from the pastry dough aerates the region between the layers, producing the signature 'puff'.

Reduced fat baking margarine emulsions as designed within this study would therefore comply particularly well in this application therefore, as vaporisation of the emulsion aqueous phase on baking would enhance the puff effect, whilst the softening in texture as recorded at high aqueous phase volumes would ease the application process, and therefore it is hypothesised a fat reduction of as great as 60% can be supported in such applications.

6.5. Further Work

The following are particular areas the Author feels warrant further investigation as a result of the findings presented from this work:

6.5.1. *Practical application*

Arguably the most pertinent opportunity for further study is to investigate the performance of reduced fat baking emulsions designed within these studies as replacements for the conventional full fat ingredient in a practical baking application. It was suggested within the preliminary stages of this work that a fat mimetic may serve as a fat extender; improving the efficiency in delivery of the fat within the recipe mixture and subsequently reducing the actual fat required by the recipe.

The inherent implications for organoleptic characteristics upon removal of fat from a baking process are well established [18, 19, 29], and reduced fat baking margarine effects upon colouring, rise, odour, hardness, brittleness and crunchiness should be investigated systematically, and benchmarked against those of the conventional full fat shortening. As indicated above, a variety of baking techniques and applications should be assessed.

6.5.2. *Extending the κ-carrageenan / XLWM starch composite model*

Throughout these studies the concentration of κ-carrageenan has been held at 0.4% (by mass) concentration; a concentration chosen initially based upon concentrations used in prior investigations using uniaxial compression studies as a method for κ-carrageenan quiescent gel characterisation [97], and whilst systematic studies were performed measuring physicomechanical response as a function of κ-carrageenan concentration as part of the mixed polymer studies, this was principally targeted at understanding the implications of the starch

granule volume exclusion phenomenon within mixed composites, as κ-carrageenan concentration in the overall system remained the same whilst starch concentration was presented as the main focus.

An interesting opportunity for further investigation is therefore to investigate the change (if any) to the isostrain composite model which has been established from these studies with varying κ-carrageenan concentration. κ-carrageenan aggregates exhibit increasing stress resistance with increasing polymer concentration [153], as has again been quantified here in these studies via oscillatory rheology. This relationship is not necessarily linear however, and also depends upon salt availability, as demonstrated within these studies.

By reducing κ-carrageenan polymer concentration within the continuous phase of the non-associative composite therefore this aqueous fraction would become less rigid, in which case the starch granules may now support the weaker κ-carrageenan phase and the composite structure may now conform to an isostress model, accompanied by different physicomechanical responses.

Alternatively, the κ-carrageenan concentration may be increased further. This may lead to a closed packing effect of the system, which could be expected to increase the yield strength of the composite attributable to further junction zone formation, whilst brittle nature of the aggregate may be amplified, based upon hypotheses drawn within this study.

Additionally, it has been suggested [158, 159] that in some circumstances κ-carrageenan chains may perforate the swollen starch granule and become caught; subsequently linking the K-carrageenan aggregate domains and starch granules as an associated mixture. Such behaviour may be supported by increased κ-carrageenan concentration, forcing the two closer together, and further studies in this area could look towards any indication of an associative composite mechanical behaviour, in order to further extend the physicomechanical modelling of κ-

carrageenan / XLWM composites and the inherent hypotheses on the direct and indirect interactions involved, and understand the parameters for the model behaviour concluded within this work.

6.5.3. *Optimisation of the process*

Emulsions designed within this study were produced using a bench scale scraped surface heat exchanger and subsequent, separate, pin stirring unit in series, to a high degree of success. Images taken using cryo-SEM later revealed however that whilst emulsification was successful in some circumstances, the sintering of fat crystals around the droplet to form a smooth shell was not achieved, observing instead a tessellated mosaic appearance on the surface of the droplet, notably in those emulsions produced using monoglyceride emulsifiers with higher melting points around 60ºC.

One suggestion to potentially improve the sintering of the droplet shells is to introduce an additional SSHE step following the first, prior to the PS mixer. This second SSHE is purposed to oscillate the temperature of the emulsion mixture just above and below the peak temperature of TAG crystallisation. This will encourage TAG crystals to reorganise and reset, in theory supporting a final arrangement in the most compact form; i.e. a smother shell, any inherent effects this might have on the fat in the continuous matrix being manipulated later in the PS mixing step.

Droplets should be supported during temperature oscillation due to the higher melting temperature of the HMMG emulsifier, however further studies would be required to assess the optimum temperature oscillation range and rate.

Throughout the studies the opposing structure forming and structure breaking processes of the SSHE and PS mixing steps respectively have been discussed. One limitation of the equipment

used in this study was the series throughput and single flow speed. It would be recommended therefore, that the flow rate of either stage was separated to create additional parameters for greater control.

Finally, the shear speeds of both SSHE and PS units were restricted to the limitations of the operating equipment, and further studies should look at processing with higher shear speeds, which could be expected to achieve increased aqueous phase distribution and therefore smaller droplet sizes. This work has demonstrated that droplet size exhibits a control upon the physicomechanical properties of the emulsion, and further investigations should look at the possibility of achieving smaller droplet sizes with increased shear forces, and (if achieved) whether they continue to exhibit similar control upon the physicomechanical properties of the emulsion.

6.5.4. *Emulsifier optimisation*

Throughout these studies emulsions have been stabilised using single monoglyceride emulsifiers, in order to focus upon characterising the effects of emulsifier concentration and melting point.

Previous studies have demonstrated [41] combinations of different emulsifiers can be more effective than one emulsifier alone in stabilising small droplet sizes. Additionally emulsifiers are understood to interact differently with TAG molecules, depending upon chemical structure and inherent affinity for one another [30]. Consequentially this can effect facilitation of fat sintering about the droplet.

VII

BIBLIOGRAPHY

7   Bibliography

1.   AlChE. *Chemical Engineering Innovation in Food Production*. Chemical Engineers in Action: Innovation 2009 [cited 2015 11th April].
2.   Berryman, P., *Advances in Food and Beverage Labelling: Information and Regulations*. 2014: Elsevier Science.
3.   Norton, I., P. Fryer, and S. Moore, *Product/Process integration in food manufacture: Engineering sustained health.* AIChE Journal, 2006. **52**(5): p. 1632-1640.
4.   HSCIC, *Statistics on Obesity, Physical Activity, and Diet: England 2015*. 2015: http://www.hscic.gov.uk/catalogue/PUB16988/obes-phys-acti-diet-eng-2015.pdf.
5.   WHO. *WHO Fact Sheet 311*. 2015 [cited 2015 27/07].
6.   Butland, B., et al., *Tackling Obesities: Future Choices: Project Report*. 2007: Citeseer.
7.   WHO, *Global strategy on diet, physical activity and health.* 2004, World Health Organisation. p. 18.
8.   Norton, I., S. Moore, and P. Fryer, *Understanding food structuring and breakdown: engineering approaches to obesity.* Obesity Reviews, 2007. **8**: p. 83-88.
9.   iChemE *Food engineering solution to obesity*. 2013.
10.   AIoM, *Dietary Reference Intakes for Energy, Carbohydrate, Fiber, Fat, Fatty Acids, Cholesterol, Protein, and Amino Acids (Macronutrients)*. 2005, Washington, DC: The National Academies Press. 1357.
11.   McGuire, M. and K. Beerman, *Nutritional Sciences: From Fundamentals to Food*. 2012: Cengage Learning.
12.   Blundell, J.E. and J.I. Macdiarmid, *Fat as a Risk Factor for Overconsumption: Satiation, Satiety, and Patterns of Eating.* Journal of the American Dietetic Association, 1997. **97**(7, Supplement): p. S63-S69.
13.   Blundell, J.E., et al., *Dietary fat and the control of energy intake: evaluating the effects of fat on meal size and postmeal satiety.* Am J Clin Nutr, 1993. **57**(5 Suppl): p. 772S-777S; discussion 777S-778S.
14.   Egger, G. and B. Swinburn, *An "ecological" approach to the obesity pandemic*. Vol. 315. 1997. 477-480.
15.   Mostofsky, D.I. and S. Yehuda, *Handbook of Essential Fatty Acid Biology: Biochemistry, Physiology, and Behavioral Neurobiology*. 2013: Humana Press.
16.   Gropper, S. and J. Smith, *Advanced Nutrition and Human Metabolism*. 2008: Cengage Learning.
17.   BNF. *Foods and drinks high in fat and/or sugar*. [Electronic] 2014 February 2014 [cited 2015 11 April].
18.   Freeman, I.P., *Margarines and Shortenings*, in *Ullmann's Encyclopedia of Industrial Chemistry*. 2000, Wiley-VCH Verlag GmbH & Co. KGaA.
19.   Roller, S. and S.A. Jones, *Handbook of Fat Replacers*. 1996: CRC Press.
20.   Hahn, N.I., *Replacing Fat With Food Technology: A brief review of new fat replacement ingredients.* Journal of the American Dietetic Association, 1997. **97**(1): p. 15-16.
21.   Downs, S.M., A.M. Thow, and S.R. Leeder, *The effectiveness of policies for reducing dietary trans fat: a systematic review of the evidence.* Bulletin of the World Health Organization, 2013. **91**(4): p. 262-269h.
22.   ADA, *Position of the American Dietetic Association: Fat Replacers.* Journal of the American Dietetic Association, 2005. **105**(2): p. 266-275.

23. Barlam, T.F. and E. McCloud, *Severe Gastrointestinal Illness Associated With Olestra Ingestion.* Journal of Pediatric Gastroenterology and Nutrition, 2003. **37**(1): p. 95-96.

24. TIME. *The 50 Worst Inventions*. 2010 [cited 2015 02/08].

25. CSPI. *The Problems with Olestra*. [cited 2015 02/08].

26. Khan, R., *Low-Calorie Foods and Food Ingredients*. 2012: Springer US.

27. McClements, D.J., *Food Emulsions: Principles, Practices, and Techniques, Second Edition*. 2004: Taylor & Francis.

28. McClements, D.J., *Understanding and Controlling the Microstructure of Complex Foods*. 2007: Elsevier Science.

29. Hui, Y.H., et al., *Bakery Products: Science and Technology*. 2008: Wiley.

30. Douaire, M., et al., *Fat crystallisation at oil-water interfaces.* Adv Colloid Interface Sci, 2014. **203**: p. 1-10.

31. McClements, D.J., et al., *Droplet Size and Emulsifier Type Affect Crystallization and Melting of Hydrocarbon-in-Water Emulsions.* Journal of food science, 1993. **58**(5): p. 1148-1151.

32. Norton, J.E., et al., *Development and characterisation of tempered cocoa butter emulsions containing up to 60% water.* Journal of Food Engineering, 2009. **95**(1): p. 172-178.

33. di Bari, V., J.E. Norton, and I.T. Norton, *Effect of processing on the microstructural properties of water-in-cocoa butter emulsions.* Journal of Food Engineering, 2014. **122**(0): p. 8-14.

34. Ghosh, S. and D. Rousseau, *Fat crystals and water-in-oil emulsion stability.* Current Opinion in Colloid and Interface Science, 2011. **16**(5): p. 421-431.

35. Norton, J.E. and P.J. Fryer, *Investigation of changes in formulation and processing parameters on the physical properties of cocoa butter emulsions.* Journal of Food Engineering, 2012. **113**(2): p. 329-336.

36. Schroeder, L.J., M. Iacobellis, and A.H. Smith, *THE INFLUENCE OF WATER AND pH ON THE REACTION BETWEEN AMINO COMPOUNDS AND CARBOHYDRATES.* Journal of Biological Chemistry, 1955. **212**(2): p. 973-984.

37. Duckworth, R., *Water Relations of Foods: Proceedings of an International Symposium held in Glasgow, September 1974*. 2012: Elsevier Science.

38. Heidelbaugh, N.D. and M. Karel, *Effect of water-binding agents on the catalyzed oxidation of methyl linoleate.* Journal of the American Oil Chemists Society, 1970. **47**(12): p. 539-544.

39. Rahman, S., *Handbook of Food Preservation, Second Edition*. 2007: CRC Press.

40. Brown, A.D., *Microbial water stress.* Bacteriological Reviews, 1976. **40**(4): p. 803-846.

41. Frasch-Melnik, S., I.T. Norton, and F. Spyropoulos, *Fat-crystal stabilised w/o emulsions for controlled salt release.* Journal of Food Engineering, 2010. **98**(4): p. 437-442.

42. Sullo, A., M. Arellano, and I.T. Norton, *Formulation engineering of water in cocoa – Butter emulsion.* Journal of Food Engineering, 2014. **142**(0): p. 100-110.

43. Beri, A., J.E. Norton, and I.T. Norton, *Effect of emulsifier type and concentration, aqueous phase volume and wax ratio on physical, material and mechanical properties of water in oil lipsticks.* International Journal of Cosmetic Science, 2013. **35**(6): p. 613-621.

44. Beri, A., R. Pichot, and I.T. Norton, *Physical and material properties of an emulsion-based lipstick produced via a continuous process.* International Journal of Cosmetic Science, 2014. **36**(2): p. 148-158.

45. McClements, D.J. and K. Demetriades, *An Integrated Approach to the Development of Reduced-Fat Food Emulsions.* Critical Reviews in Food Science and Nutrition, 1998. **38**(6): p. 511-536.

46. Jones, M. and I. Norton, *Low-fat spread.* European Patent Application, 1990(EP 0 372 625 A2).

47. Nielsen, B.U. and C. Food Ingredients Europe, *Low fat spreads - SLENDID(TM) gives splendid results.* Food Ingredients Europe Conference Proceedings 1992. 1993. 202-205.

48. Clegg, S.M., A.K. Moore, and S.A. Jones, *Low-fat Margarine Spreads as Affected by Aqueous Phase Hydrocolloids.* Journal of food science, 1996. **61**(5): p. 1073-1079.

49. Hofmeister, F., *Zur Lehre von der Wirkung der Salze.* Archiv für experimentelle Pathologie und Pharmakologie, 1888. **24**(4-5): p. 247-260.

50. Kunz, W., J. Henle, and B.W. Ninham, *'Zur Lehre von der Wirkung der Salze' (about the science of the effect of salts): Franz Hofmeister's historical papers.* Current Opinion in Colloid & Interface Science, 2004. **9**(1–2): p. 19-37.

51. Phillips, G.O. and P.A. Williams, *Handbook of Hydrocolloids.* 2009: Elsevier Science.

52. Banerjee, S. and S. Bhattacharya, *Food gels: gelling process and new applications.* Crit Rev Food Sci Nutr, 2012. **52**(4): p. 334-46.

53. Commission, E. *Opinion of the Scientific Committee on Food on Carrageenan.* 2003 [cited 2015 09/08].

54. WHO. *JOINT FAO/WHO EXPERT COMMITTEE ON FOOD ADDITIVES.* 2014 [cited 2015 09/08].

55. Norton, I.T., E.R. Morris, and D.A. Rees, *Lyotropic effects of simple anions on the conformation and interactions of kappa-carrageenan.* Carbohydrate Research, 1984. **134**(1): p. 89-101.

56. Saltmarsh, M., M. Saltmarsh, and S. Barlow, *Essential Guide to Food Additives.* 2013: Royal Society of Chemistry.

57. Theron, M.M. and J.F.R. Lues, *Organic Acids and Food Preservation.* 2010: Taylor & Francis.

58. Nagle, B.J., et al., *Waxy maize starch derived from grain of a plant which is heterozygous for the sugary-2 allele.* 1999, Google Patents.

59. BeMiller, J.N. and R.L. Whistler, *Starch: Chemistry and Technology.* 2009: Elsevier Science.

60. Han, J.-A., et al., *Utilization of Hydroxypropylated Waxy Rice and Corn Starches in Korean Waxy Rice Cake to Retard Retrogradation.* Cereal Chemistry Journal, 2005. **82**(1): p. 88-92.

61. Waliszewski, K.N., et al., *Changes of banana starch by chemical and physical modification.* Carbohydrate Polymers, 2003. **52**(3): p. 237-242.

62. Morris, E.R., *CHAPTER 5 - Functional Interactions in Gelling Biopolymer Mixtures*, in *Modern Biopolymer Science*, S. Kasapis, I.T. Norton, and J.B. Ubbink, Editors. 2009, Academic Press: San Diego. p. 167-198.

63. Anderson, N.S., et al., *Carrageenans. Part IV. Variations in the structure and gel properties of [small kappa]-carrageenan, and the characterisation of sulphate esters by infrared spectroscopy.* Journal of the Chemical Society C: Organic, 1968(0): p. 602-606.

64. Anderson, N.S., et al., *X-ray diffraction studies of polysaccharide sulphates: Double helix models for κ- and ι-carrageenans.* Journal of Molecular Biology, 1969. **45**(1): p. 85-88,IN5,89-97.

65. Anderson, N.S., T.C.S. Dolan, and D.A. Rees, *Carrageenans. Part VII. Polysaccharides from Eucheuma spinosum and Eucheuma cottonii. The covalent*

structure of [iota]-carrageenan. Journal of the Chemical Society, Perkin Transactions 1, 1973(0): p. 2173-2176.

66. Morris, E.R., D.A. Rees, and G. Robinson, *Cation-specific aggregation of carrageenan helices: Domain model of polymer gel structure.* Journal of Molecular Biology, 1980. **138**(2): p. 349-362.

67. Smidsrød, O., et al., *Evidence for a salt-promoted "freeze-out" of linkage conformations in carrageenans as a prerequisite for gel-formation.* Carbohydrate Research, 1980. **80**(1): p. C11-C16.

68. Smidsrød, O. and H. Grasdalen, *Some physical properties of carrageenan in solution and gel state.* Carbohydrate Polymers, 1982. **2**(4): p. 270-272.

69. Morris, E.R., et al., *Calorimetric and chiroptical evidence of aggregate-driven helix formation in carrageenan systems.* Carbohydrate Research, 1980. **80**(2): p. 317-323.

70. Rochas, C. and M. Rinaudo, *Mechanism of gel formation in κ‐carrageenan.* Biopolymers, 1984. **23**(4): p. 735-745.

71. Borgström, J., et al., *On the structure of aggregated kappa-carrageenan helices. A study by cryo-TEM, optical rotation and viscometry.* International Journal of Biological Macromolecules, 1996. **18**(3): p. 223-229.

72. Nickerson, M.T., A.T. Paulson, and F.R. Hallett, *Dilute solution properties of κ-carrageenan polysaccharides: effect of potassium and calcium ions on chain conformation.* Carbohydrate Polymers, 2004. **58**(1): p. 25-33.

73. Rochas, C. and M. Rinaudo, *Activity coefficients of counterions and conformation in kappa-carrageenan systems.* Biopolymers, 1980. **19**(9): p. 1675-1687.

74. Norton, I.T., et al., *Role of cations in the conformation of iota and kappa carrageenan.* Journal of the Chemical Society, Faraday Transactions 1: Physical Chemistry in Condensed Phases, 1983. **79**(10): p. 2475-2488.

75. Grasdalen, H. and O. Smidsroed, *Cesium-133 NMR in the sol-gel states of aqueous carrageenan. Selective site binding of cesium and potassium ions in .kappa.-carrageenan gels.* Macromolecules, 1981. **14**(1): p. 229-231.

76. Zhang, W., et al., *Cation specificity and cation binding to low sulfated carrageenans.* Carbohydrate Polymers, 1994. **23**(2): p. 105-110.

77. Núñez-Santiago, M.C., et al., *Rheology and microstructure of κ-carrageenan under different conformations induced by several concentrations of potassium ion.* Food Hydrocolloids, 2011. **25**(1): p. 32-41.

78. Nilsson, S. and L. Piculell, *Helix-coil transitions of ionic polysaccharides analyzed within the Poisson-Boltzmann cell model. 2. Effects of salt concentration on the thermal transition.* Macromolecules, 1989. **22**(7): p. 3011-3017.

79. Pearson, R.G., *Hard and Soft Acids and Bases.* Journal of the American Chemical Society, 1963. **85**(22): p. 3533-3539.

80. Hancock, R.D. and A.E. Martell, *Ligand design for selective complexation of metal ions in aqueous solution.* Chemical Reviews, 1989. **89**(8): p. 1875-1914.

81. Grasdalen, H. and O. Smidsroed, *Iodide-specific formation of .kappa.-carrageenan single helixes. Iodine-127 NMR spectroscopic evidence for selective site binding of iodide anions in the ordered conformation.* Macromolecules, 1981. **14**(6): p. 1842-1845.

82. Ohki, S., *The Origin of Electrical Potential in Biological Systems*, in *Comprehensive Treatise of Electrochemistry*, S. Srinivasan, et al., Editors. 1985, Springer US. p. 1-130.

83. Voet, A., *Quantative Lyotropy.* Chemical Reviews, 1937. **20**(2): p. 169-179.

84. Schott, H., *Lyotropic numbers of anions from cloud point changes of nonionic surfactants.* Colloids and Surfaces, 1984. **11**(1–2): p. 51-54.

85. Austen, K.R.J., D.M. Goodall, and I.T. Norton, *Anion effects on equilibria and kinetics of the disorder–order transition of κ-carrageenan.* Biopolymers, 1988. **27**(1): p. 139-155.

86. Slootmaekers, D., et al., *Static light scattering from κ-carrageenan solutions.* International Journal of Biological Macromolecules, 1988. **10**(3): p. 160-168.

87. Slootmaekers, D., M. Mandel, and H. Reynaers, *Dynamic light scattering by κ- and λ-carrageenan solutions.* International Journal of Biological Macromolecules, 1991. **13**(1): p. 17-25.

88. Hermansson, A.-M., *Rheological and microstructural evidence for transient states during gelation of kappa-carrageenan in the presence of potassium.* Carbohydrate Polymers, 1989. **10**(3): p. 163-181.

89. Hermansson, A.M., E. Eriksson, and E. Jordansson, *Effects of potassium, sodium and calcium on the microstructure and rheological behaviour of kappa-carrageenan gels.* Carbohydrate Polymers, 1991. **16**(3): p. 297-320.

90. Ciancia, M., M. Milas, and M. Rinaudo, *On the specific role of coions and counterions on κ-carrageenan conformation.* International Journal of Biological Macromolecules, 1997. **20**(1): p. 35-41.

91. Chen, Y., M.-L. Liao, and D.E. Dunstan, *The rheology of K+-κ-carrageenan as a weak gel.* Carbohydrate Polymers, 2002. **50**(2): p. 109-116.

92. Núñez-Santiago, M.d.C. and A. Tecante, *Rheological and calorimetric study of the sol–gel transition of κ-carrageenan.* Carbohydrate Polymers, 2007. **69**(4): p. 763-773.

93. Watase, M. and K. Nishinari, *THE EFFECT OF MONOVALENT CATIONS AND ANIONS ON THE RHEOLOGICAL PROPERTIES OF KAPPA-CARRAGEENAN GELS1.* Journal of Texture Studies, 1988. **19**(3): p. 259-273.

94. Watase, M. and K. Nishinari, *Thermal and rheological properties of kappa-carrageenan gels containing alkali metal salts – Effect of anions.* Journal of Japanese Society of Biorheology, 1988. **2**: p. 9.

95. Stephen, A.M. and G.O. Phillips, *Food Polysaccharides and Their Applications.* 2006: Taylor & Francis.

96. Richardson, R.K. and F.M. Goycoolea, *Rheological measurement of κ-carrageenan during gelation.* Carbohydrate Polymers, 1994. **24**(3): p. 223-225.

97. Thrimawithana, T.R., et al., *Texture and rheological characterization of kappa and iota carrageenan in the presence of counter ions.* Carbohydrate Polymers, 2010. **82**(1): p. 69-77.

98. Moresi, M. and M. Bruno, *Characterisation of alginate gels using quasi-static and dynamic methods.* Journal of Food Engineering, 2007. **82**(3): p. 298-309.

99. Norton, A.B., P.W. Cox, and F. Spyropoulos, *Acid gelation of low acyl gellan gum relevant to self-structuring in the human stomach.* Food Hydrocolloids, 2011. **25**(5): p. 1105-1111.

100. Smidsrød, O., A. Haug, and B. Lian, *Properties of poly(1,4-hexuronates) in the gel state. I. Evaluation of a method for the determination of stiffness.* Acta Chemica Scandinavica,, 1972. **26**: p. 7.

101. Kaletunc, G., et al., *Determination of elasticity of gels by successive compression–decompression cycles.* Food Hydrocolloids, 1991. **5**(3): p. 237-247.

102. Nussinovitch, A., *From simple to complex hydrocolloid cellular solids.* Gums and stabilizers for the food industry, 2004. **12**: p. 32-42.

103. Koliandris, A., *Relationship between texture of gels and flavour release.* 2009, University of Nottingham.

104. Peleg, M., *CHARACTERIZATION OF THE STRESS RELAXATION CURVES OF SOLID FOODS.* Journal of food science, 1979. **44**(1): p. 277-281.

105. Peleg, M., *Linearization of Relaxation and Creep Curves of Solid Biological Materials.* Journal of Rheology (1978-present), 1980. **24**(4): p. 451-463.

106. Peleg, M. and N. Pollak, *THE PROBLEM OF EQUILIBRIUM CONDITIONS IN STRESS RELAXATION ANALYSES OF SOLID FOODS1.* Journal of Texture Studies, 1982. **13**(1): p. 1-11.

107. Nussinovitch, A., et al., *RECOVERABLE WORK VERSUS ASYMPTOTIC RELAXATION MODULUS IN AGAR, CARRAGEENAN AND GELLAN GELS1.* Journal of Texture Studies, 1990. **21**(4): p. 427-438.

108. Russo, D., *The impact of kosmotropes and chaotropes on bulk and hydration shell water dynamics in a model peptide solution.* Chemical Physics, 2008. **345**(2–3): p. 200-211.

109. Blanshard, J.M.V. and J.R. Mitchell, *Polysaccharides in Food.* 2013: Elsevier Science.

110. Menard, K.P., *Dynamic Mechanical Analysis: A Practical Introduction.* 1999: Taylor & Francis.

111. van Vliet, T., H. Luyten, and P. Walstra, *Fracture and Yielding of Gels*, in *Food Polymers, Gels and Colloids*, E. Dickinson, Editor. 1991, Woodhead Publishing. p. 392-403.

112. Lindstrom, S.B., et al., *Structures, stresses, and fluctuations in the delayed failure of colloidal gels.* Soft Matter, 2012. **8**(13): p. 3657-3664.

113. Moreyra, R. and M. Yeleg, *COMPRESSIVE DEFORMATION PATTERNS OF SELECTED FOOD POWDERS.* Journal of food science, 1980. **45**(4): p. 866-868.

114. Nussinovitch, A., et al., *CHARACTERIZATION OF GELLAN GELS BY UNIAXIAL COMPRESSION, STRESS RELAXATION AND CREEP 1.* Journal of Texture Studies, 1990. **21**(1): p. 37-50.

115. Marcus, Y., *Effect of ions on the structure of water: structure making and breaking.* Chem Rev, 2009. **109**(3): p. 1346-70.

116. Aguilera, J.M. and D.W. Stanley, *Microstructural Principles of Food Processing and Engineering.* 1999: Springer.

117. Norton, I.T., F. Spyropoulos, and P. Cox, *Practical Food Rheology: An Interpretive Approach.* 2010: Wiley.

118. Takayanagi, M., H. Harima, and Y. Iwata, *Viscoelastic behaviour of polymer blends and its comparison with model experiments.* Mem. Fac. Eng. Kyusha Univ., 1963. **23**: p. 1–13.

119. A.M. Clark, R.K.R., G. Robinson, S.B. Ross-Murphy, A.C. Weaver, *Structural and mechanical properties of agar/BSA co-gels.* Prog. Food Nutr. Sci., 1982. **6**: p. 149–160.

120. McEvoy, H., S.B. Ross-Murphy, and A.H. Clark, *Large deformation and ultimate properties of biopolymer gels: 2. Mixed gel systems.* Polymer, 1985. **26**(10): p. 1493-1500.

121. Kasapis, S., et al., *Phase equilibria and gelation in gelatin/maltodextrin systems — Part IV: composition-dependence of mixed-gel moduli.* Carbohydrate Polymers, 1993. **21**(4): p. 269-276.

122. Abdulmola, N.A., et al., *Application of polymer blending laws to starch-gelatin composites.* Carbohydrate Polymers, 1996. **31**(1–2): p. 53-63.

123. Abdulmola, N.A., et al., *Effect of xanthan on the small-deformation rheology of crosslinked and uncrosslinked waxy maize starch.* Carbohydrate Polymers, 1996. **31**(1–2): p. 65-78.

124. Mohammed, Z.H., et al., *Application of polymer blending laws to composite gels of agarose and crosslinked waxy maize starch.* Carbohydrate Polymers, 1998. **36**(1): p. 27-36.

125. Verbeken, D., O. Thas, and K. Dewettinck, *Textural properties of gelled dairy desserts containing κ-carrageenan and starch.* Food Hydrocolloids, 2004. **18**(5): p. 817-823.

126. Tye, R.J., *The rheology of starch/carrageenan systems.* Food Hydrocolloids, 1988. **2**(4): p. 259-266.

127. Chaudemanche, C. and T. Budtova, *Mixtures of pregelatinised maize starch and κ-carrageenan: Compatibility, rheology and gelation.* Carbohydrate Polymers, 2008. **72**(4): p. 579-589.

128. Tecante, A. and J.L. Doublier, *Steady flow and viscoelastic behavior of crosslinked waxy corn starch-κ-carrageenan pastes and gels.* Carbohydrate Polymers, 1999. **40**(3): p. 221-231.

129. Loisel, C., et al., *EFFECT OF TEMPERATURE ON THE RHEOLOGICAL PROPERTIES OF STARCH/CARRAGEENAN MIXTURES*, in *Gums and Stabilisers for the Food Industry 10*, P.A. Williams and G.O. Phillips, Editors. 2000, Woodhead Publishing. p. 181-187.

130. Eliasson, A.C., *Starch in Food: Structure, Function and Applications.* 2004: Taylor & Francis.

131. Pometto, A., et al., *Food Biotechnology, Second Edition.* 2005: Taylor & Francis.

132. Hirsch, J.B. and J.L. Kokini, *Understanding the Mechanism of Cross-Linking Agents (POCl3, STMP, and EPI) Through Swelling Behavior and Pasting Properties of Cross-Linked Waxy Maize Starches.* Cereal Chemistry Journal, 2002. **79**(1): p. 102-107.

133. Szymanski, C.D. and O.B. Wurzburg, *Modified starches for the food industry.* Journal of Agricultural and Food Chemistry, 1970. **18**(6): p. 997-1001.

134. Dunstan, D.E., et al., *Syneresis of k-carrageenan gels at different KCl and LBG concentrations.* Gums and Stabilisers for the Food Industry, 2000. **10**(251): p. 137.

135. Michel, A.S., M.M. Mestdagh, and M.A.V. Axelos, *Physico-chemical properties of carrageenan gels in presence of various cations.* International Journal of Biological Macromolecules, 1997. **21**(1–2): p. 195-200.

136. Tang, J., M.A. Tung, and Y. Zeng, *Compression strength and deformation of gellan gels formed with mono- and divalent cations.* Carbohydrate Polymers, 1996. **29**(1): p. 11-16.

137. Jane, J.-L., *Mechanism of Starch Gelatinization in Neutral Salt Solutions.* Starch - Stärke, 1993. **45**(5): p. 161-166.

138. Jane, J.-L., *13C-NMR Study of Interactions between Amylodextrin and Neutral Salts.* Starch - Stärke, 1993. **45**(5): p. 172-175.

139. Steeneken, P.A.M. and A.J.J. Woortman, *Identification of the thermal transitions in potato starch at a low water content as studied by preparative DSC.* Carbohydrate Polymers, 2009. **77**(2): p. 288-292.

140. Parker, R. and S.G. Ring, *Aspects of the Physical Chemistry of Starch.* Journal of Cereal Science, 2001. **34**(1): p. 1-17.

141. Autio, K., E. Vesterinen, and M. Stolt, *Rheological properties of mixed starch-κ-carrageenan gels in relation to enzymatic digestibility.* Food Hydrocolloids, 2002. **16**(2): p. 169-174.

142. Ahmad, F.B. and P.A. Williams, *Effect of Salts on the Gelatinization and Rheological Properties of Sago Starch.* Journal of Agricultural and Food Chemistry, 1999. **47**(8): p. 3359-3366.

143. Gough, B.M. and J.N. Pybus, *Effect of Metal Cations on the Swelling and Gelatinization Behaviour of Large Wheat Starch Granules.* Starch - Stärke, 1973. **25**(4): p. 123-130.

144. Tro, N.J., *Chemistry A Molecular Approach.* 2010.

145. Steeneken, P.A.M., *Rheological properties of aqueous suspensions of swollen starch granules.* Carbohydrate Polymers, 1989. **11**(1): p. 23-42.

146. Donovan, J.W., *Phase transitions of the starch–water system.* Biopolymers, 1979. **18**(2): p. 263-275.

147. Cooke, D. and M.J. Gidley, *Loss of crystalline and molecular order during starch gelatinisation: origin of the enthalpic transition.* Carbohydrate Research, 1992. **227**(0): p. 103-112.

148. Rendleman, J.A., *Complexes of alkali metals and alkaline earth metals with carbohydrates.* Adv. Carbohydr. Chem., 1966. **21**: p. 62.

149. Oosten, B.J., *Substantial Rise of Gelatinization Temperature of Starch by Adding Hydroxide.* Starch - Stärke, 1979. **31**(7): p. 228-230.

150. Paquette, J. and C. Jolicoeur, *A near-infrared study of the hydration of various ions and nonelectrolytes.* Journal of Solution Chemistry, 1977. **6**(6): p. 403-428.

151. Snoeren, T.H.M. and T.A.J. Payens, *On the sol-gel transition in solutions of Kappa-carrageenan.* Biochimica et Biophysica Acta (BBA) - General Subjects, 1976. **437**(1): p. 264-272.

152. Clark, A.H. and S.B. Ross-Murphy, *CHAPTER 1 - Biopolymer Network Assembly: Measurement and Theory*, in *Modern Biopolymer Science*, S. Kasapis, I.T. Norton, and J.B. Ubbink, Editors. 2009, Academic Press: San Diego. p. 1-27.

153. Rochas, C., M. Rinaudo, and S. Landry, *Role of the molecular weight on the mechanical properties of kappa carrageenan gels.* Carbohydrate Polymers, 1990. **12**(3): p. 255-266.

154. Manson, J.A. and L.H. Sperling, *Polymer Blends and Composites.* 1977.

155. Alloncle, M., et al., *A Rheological Characterization of Cereal Starch-Glactomannan Mixtures.* Cereal Chemistry, 1989. **66**: p. 90-93.

156. International, A., *Atlas of Stress-strain Curves.* 2002: ASM International.

157. Walstra, P. *Introduction to aggregation phenomena in food colloids.* in *Proc. Conf. Food, colloids and polymers: stability and mechanical properties, E. Dickinson, P. Walstra (eds.). Lunteren, The Netherlands 1992. Royal Soc. Chem. (1993) 3-15.* 1993.

158. Matignon, A., et al., *Starch/carrageenan mixed systems: Penetration in, adsorption on or exclusion of carrageenan chains by granules?* Food Hydrocolloids, 2014. **35**(0): p. 597-605.

159. Huc, D., et al., *Interactions between modified starch and carrageenan during pasting.* Food Hydrocolloids, 2014. **36**(0): p. 355-361.

160. Sala, G., et al., *Deformation and fracture of emulsion-filled gels: Effect of gelling agent concentration and oil droplet size.* Food Hydrocolloids, 2009. **23**(7): p. 1853-1863.

161. Vliet, T.v., *Mechanical Properties of Concentrated Food Gels*, in *Food Macromolecules and Colloids*. 1995, The Royal Society of Chemistry. p. 447-455.

162. Dickinson, E., *Emulsion gels: The structuring of soft solids with protein-stabilized oil droplets.* Food Hydrocolloids, 2012. **28**(1): p. 224-241.

163. Van Der Goot, A.J. and J.M. Manski, *14 - Creation of novel microstructures through processing: structure formation in (semi-)solid food materials*, in *Understanding and Controlling the Microstructure of Complex Foods*, D.J. McClements, Editor. 2007, Woodhead Publishing. p. 389-410.

164. EUFIC. *EUFIC REVIEW 06/2010: The greatest thing since sliced bread? A review of the benefits of processed foods*. 2010 15/07/2014 [cited 2014 20/07].

165. Aguilera, J.M., *Why food microstructure?* Journal of Food Engineering, 2005. **67**(1–2): p. 3-11.

166. Metin, S. and R.W. Hartel, *Crystallization of Fats and Oils*, in *Bailey's Industrial Oil and Fat Products*. 2005, John Wiley & Sons, Inc.

167. Marangoni, A.G. and S.S. Narine, *Physical Properties of Lipids*. 2002: CRC Press.

168. Erickson, D.R., *Edible Fats and Oils Processing: Basic Principles and Modern Practices : World Conference Proceedings*. 1990: American Oil Chemists' Society.

169. O'Brien, R.D., *Fats and Oils: Formulating and Processing for Applications, Third Edition*. 2008: CRC Press.

170. Rao, C.S. and R.W. Hartel, *Scraped surface heat exchangers*. Critical Reviews in Food Science and Nutrition, 2006. **46**(3): p. 207-219.

171. Dumont, E., F. Fayolle, and J. Legrand, *Flow regimes and wall shear rates determination within a scraped surface heat exchanger*. Journal of Food Engineering, 2000. **45**(4): p. 195-207.

172. Wang, L., *Energy Efficiency and Management in Food Processing Facilities*. 2008: Taylor & Francis.

173. Mabit, J., F. Fayolle, and J. Legrand, *Shear rates investigation in a scraped surface heat exchanger*. Chemical Engineering Science, 2003. **58**(20): p. 4667-4679.

174. Miskandar, M.S. and I.N. Aini, *Properties of palm oil margarine during storage: effects of processing conditions*. Palm Oil Developments, 2006. **45**: p. 7.

175. Lefébure, É., et al., *Investigation of the influence of processing parameters on physicochemical properties of puff pastry margarines using surface response methodology*. LWT - Food Science and Technology, 2013. **51**(1): p. 225-232.

176. A. Bot, E.F., J.G. Lammers, E.G. Pelan, *The texture and microstructure of spreads*, in *Understanding and Controlling the Microstructure of Complex Foods*, D.J. McClements, Editor. 2007, Woodhead Publishing: Cambridge.

177. Acevedo, N.C., F. Peyronel, and A.G. Marangoni, *Nanoscale structure intercrystalline interactions in fat crystal networks*. Current Opinion in Colloid & Interface Science, 2011. **16**(5): p. 374-383.

178. Acevedo, N.C. and A.G. Marangoni, *Characterization of the nanoscale in triacylglycerol crystal networks*. Crystal Growth and Design, 2010. **10**(8): p. 3327-3333.

179. Acevedo, N.C. and A.G. Marangoni, *Toward nanoscale engineering of triacylglycerol crystal networks*. Crystal Growth and Design, 2010. **10**(8): p. 3334-3339.

180. Sato, K. and S. Ueno, *Physical properties of fats in food*, in *Fats in Food Technology 2e*. 2014, John Wiley & Sons, Ltd. p. 1-38.

181. Clarkson, C.E. and T. Malkin, *139. Alternation in long-chain compounds. Part II. An X-ray and thermal investigation of the triglycerides*. Journal of the Chemical Society (Resumed), 1934(0): p. 666-671.

182. Chapman, D., *The Polymorphism of Glycerides*. Chemical Reviews, 1962. **62**(5): p. 433-456.

183. Marangoni, A.G. and S.S. Narine, *Identifying key structural indicators of mechanical strength in networks of fat crystals*. Food Research International, 2002. **35**(10): p. 957-969.

184. Higaki, K., et al., *In situ optical observation of microstructure of β-fat gel made of binary mixtures of high-melting and low-melting fats*. Food Research International, 2004. **37**(1): p. 2-10.

185. Shinohara, Y., et al., *Microbeam X-ray Diffraction Analysis of Interfacial Heterogeneous Nucleation of n-Hexadecane inside Oil-in-Water Emulsion Droplets*. Crystal Growth & Design, 2008. **8**(9): p. 3123-3126.

186. Narine, S.S. and A.G. Marangoni, *Mechanical and structural model of fractal networks of fat crystals at low deformations*. Physical Review E - Statistical Physics, Plasmas, Fluids, and Related Interdisciplinary Topics, 1999. **60**(6 B): p. 6991-7000.

187. Nederveen, C.J., *Dynamic mechanical behavior of suspensions of fat particles in oil*. Journal of Colloid Science, 1963. **18**(3): p. 276-291.

188. Braipson-Danthine, S. and C. Deroanne, *Influence of SFC, microstructure and polymorphism on texture (hardness) of binary blends of fats involved in the preparation of industrial shortenings.* Food Research International, 2004. **37**(10): p. 941-948.

189. Fu, S.-Y., et al., *Effects of particle size, particle/matrix interface adhesion and particle loading on mechanical properties of particulate–polymer composites.* Composites Part B: Engineering, 2008. **39**(6): p. 933-961.

190. Garti, N., H. Binyamin, and A. Aserin, *Stabilization of water-in-oil emulsions by submicrocrystalline α-form fat particles.* JAOCS, Journal of the American Oil Chemists' Society, 1998. **75**(12): p. 1825-1831.

191. Pickering, S.U., *CXCVI.-Emulsions.* Journal of the Chemical Society, Transactions, 1907. **91**(0): p. 2001-2021.

192. Ramsden, W., *Separation of Solids in the Surface-Layers of Solutions and 'Suspensions' (Observations on Surface-Membranes, Bubbles, Emulsions, and Mechanical Coagulation). -- Preliminary Account.* Proceedings of the Royal Society of London, 1903. **72**(477-486): p. 156-164.

193. Johansson, D., B. Bergenståhl, and E. Lundgren, *Wetting of fat crystals by triglyceride oil and water. 1. The effect of additives.* Journal of the American Oil Chemists' Society, 1995. **72**(8): p. 921-931.

194. Ghosh, S., T. Tran, and D. Rousseau, *Comparison of Pickering and network stabilization in water-in-oil emulsions.* Langmuir, 2011. **27**(11): p. 6589-97.

195. Ghosh, S. and D. Rousseau, *Triacylglycerol interfacial crystallization and shear structuring in water-in-oil emulsions.* Crystal Growth and Design, 2012. **12**(10): p. 4944-4954.

196. Trautz, M., *Das Gesetz der Reaktionsgeschwindigkeit und der Gleichgewichte in Gasen. Bestätigung der Additivität von Cv-3/2R. Neue Bestimmung der Integrationskonstanten und der Moleküldurchmesser.* Zeitschrift für anorganische und allgemeine Chemie, 1916. **96**(1): p. 1-28.

197. Johansson, D., B. Bergenstahl, and E. Lundgren, *Sintering of Fat Crystal Networks in Oils*, in *Food Macromolecules and Colloids*. 1995, The Royal Society of Chemistry. p. 418-425.

198. Ak, M.M. and S. Gunasekaran, *Simulation of lubricated squeezing flow of a Herschel-Bulkley fluid.* Applied Rheology, 2000. **6**(10): p. 5.

199. Sun, A. and S. Gunasekaran, *MEASURING RHEOLOGICAL CHARACTERISTICS AND SPREADABILITY OF SOFT FOODS USING A MODIFIED SQUEEZE-FLOW APPARATUS.* Journal of Texture Studies, 2009. **40**(3): p. 275-287.

200. van Duynhoven, J.P.M., et al., *Scope of droplet size measurements in food emulsions by pulsed field gradient NMR at low field.* Magnetic Resonance in Chemistry, 2002. **40**(13): p. S51-S59.

201. AOCS, *AOCS Official Method Cd 16b-93. Solid fat content (SFC) by low-resolution nuclear magnetic resonance - the direct method. Official methods and Recommended Practices of the AOCS, 6th Ed. 2009. 2011-2012 Methods and Additions and Revisions.* 2009.

202. Marangoni, A.G. and L.H. Wesdorp, *Structure and Properties of Fat Crystal Networks, Second Edition*. 2012: Taylor & Francis.

203. Litwinenko, J.W., et al., *Relationship between crystallization behavior, microstructure, and mechanical properties in a palm oil-based shortening.* Journal of the American Oil Chemists' Society, 2002. **79**(7): p. 647-654.

204. Rousseau, D., *Fat crystals and emulsion stability — a review.* Food Research International, 2000. **33**(1): p. 3-14.

205. Binks, B.P., *Particles as surfactants—similarities and differences.* Current Opinion in Colloid & Interface Science, 2002. **7**(1–2): p. 21-41.

206. Narine, S.S. and A.G. Marangoni, *Relating structure of fat crystal networks to mechanical properties: a review.* Food Research International, 1999. **32**(4): p. 227-248.

207. Saadi, S., et al., *Effect of Blending and Emulsification on Thermal Behavior, Solid Fat Content, and Microstructure Properties of Palm Oil‐Based Margarine Fats.* Journal of food science, 2011. **76**(1): p. C21-C30.

208. Kloek, W., T.O.N. Van Vliet, and P. Walstra, *LARGE DEFORMATION BEHAVIOR OF FAT CRYSTAL NETWORKS.* Journal of Texture Studies, 2005. **36**(5-6): p. 516-543.

209. Steffe, J.F., *Rheological Methods in Food Process Engineering.* 1996: Freeman Press.

210. Haighton, A.J., *Worksoftening of margarine and shortening.* Journal of the American Oil Chemists' Society, 1965. **42**(1): p. 27-30.

211. Miskandar, M.S., et al., *Effect of scraped-surface tube cooler temperatures on the physical properties of palm oil margarine.* Journal of the American Oil Chemists' Society, 2002. **79**(9): p. 931-936.

212. Norton, I.T. and J.E. Norton, *Low Fat Bakery Product.* 2013, Google Patents.

213. Frasch-Melnik, S., *Fat crystal-stabilised double emulsions*, in *Chemical Engineering.* 2011, University of Birmingham: Birmingham.

214. BEOnline, *bulk modulus.* 2014.

215. Borwankar, R.P., et al., *Rheological characterization of melting of margarines and tablespreads.* Journal of Food Engineering, 1992. **16**(1–2): p. 55-74.

216. Garside, J., et al., *Measurement of Crystal Growth and Nucleation Rates.* 2002: Institution of Chemical Engineers.

217. Chronakis, I.S. and S. Kasapis, *Preparation and Analysis of Water Continuous Very Low Fat Spreads.* LWT - Food Science and Technology, 1995. **28**(5): p. 488-494.

218. Alexa, R.I., et al., *Effect of κ-carrageenan on rheological properties, microstructure, texture and oxidative stability of water-in-oil spreads.* LWT - Food Science and Technology, 2010. **43**(6): p. 843-848.

219. Mounsey, J.S., et al., *Effect of zinc fortifications on rheological properties and micro-structure of water-in-oil spreads containing κ-carrageenan.* European Food Research and Technology, 2008. **227**(3): p. 675-681.

220. Walstra, P., *Principles of emulsion formation.* Chemical Engineering Science, 1993. **48**(2): p. 333-349.

221. Li, G., et al., *Analytical modeling of tensile strength of particulate-filled composites.* Polymer Composites, 2001. **22**(5): p. 593-603.

222. Dickinson, E., *Hydrocolloids at interfaces and the influence on the properties of dispersed systems.* Food Hydrocolloids, 2003. **17**(1): p. 25-39.

223. Kulkarni, C.V., et al., *Monoolein: a magic lipid?* Physical Chemistry Chemical Physics, 2011. **13**(8): p. 3004-3021.

224. Campbell, Norton, and Morley, *Factors controlling the phase inversion of oil-in-water emulsions.* Netherlands Milk and Dairy Journal, 1996. **50**: p. 16.

225. Rattanasom, N., S. Prasertsri, and T. Ruangritnumchai, *Comparison of the mechanical properties at similar hardness level of natural rubber filled with various reinforcing-fillers.* Polymer Testing, 2009. **28**(1): p. 8-12.

226. Wassell, P., et al., *Synchrotron Radiation Macrobeam and Microbeam X-ray Diffraction Studies of Interfacial Crystallization of Fats in Water-in-Oil Emulsions.* Langmuir, 2012. **28**(13): p. 5539-5547.

227. Chiavaro, E., *Differential Scanning Calorimetry: Applications in Fat and Oil Technology.* 2014: Taylor & Francis.
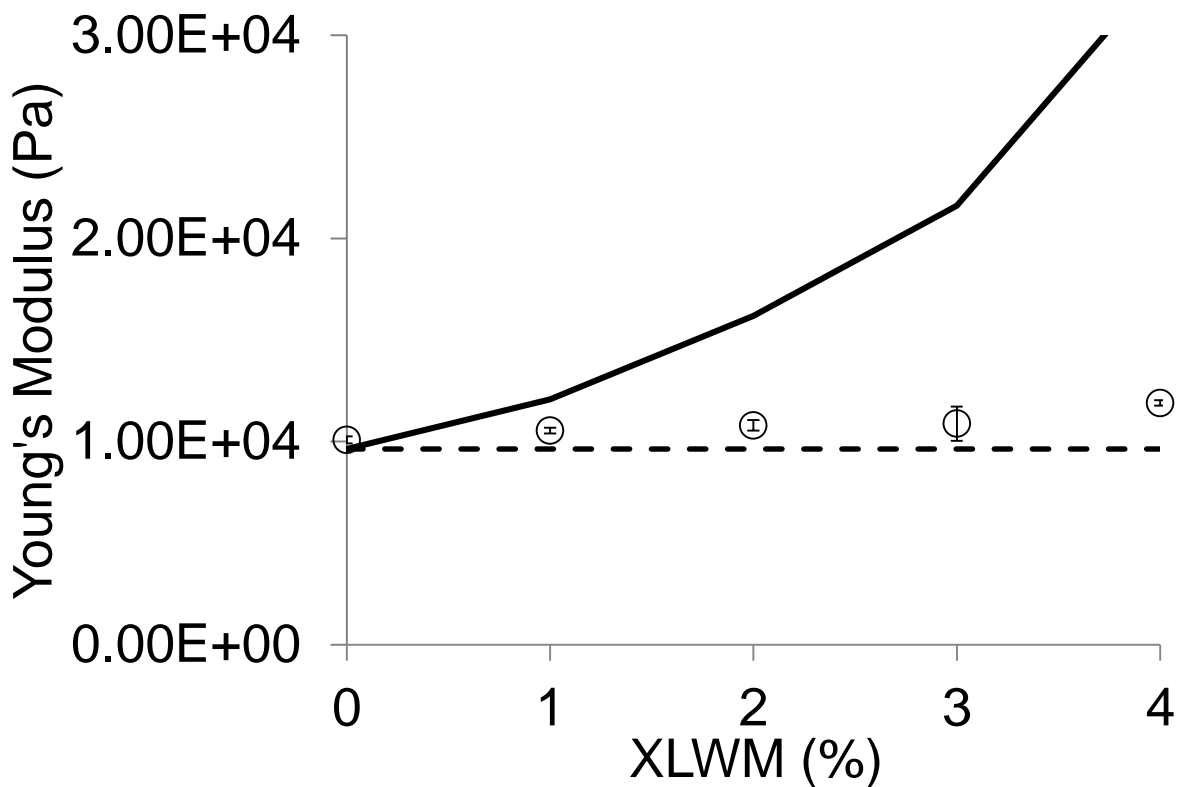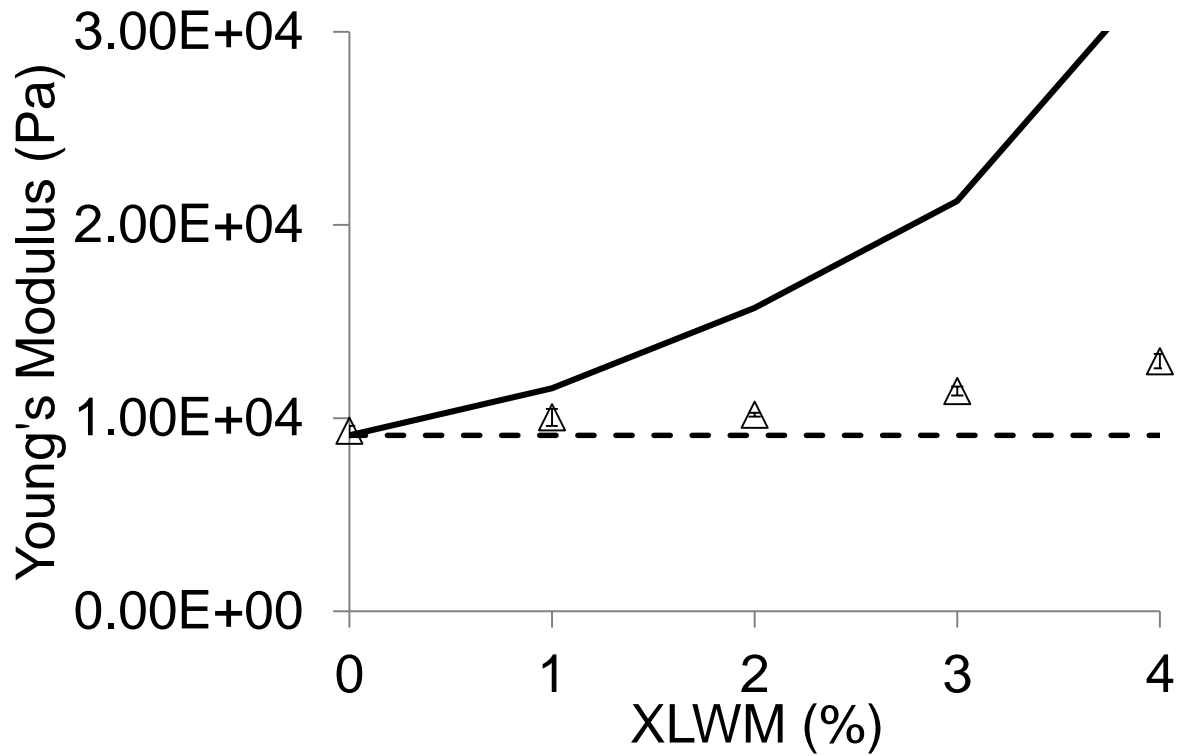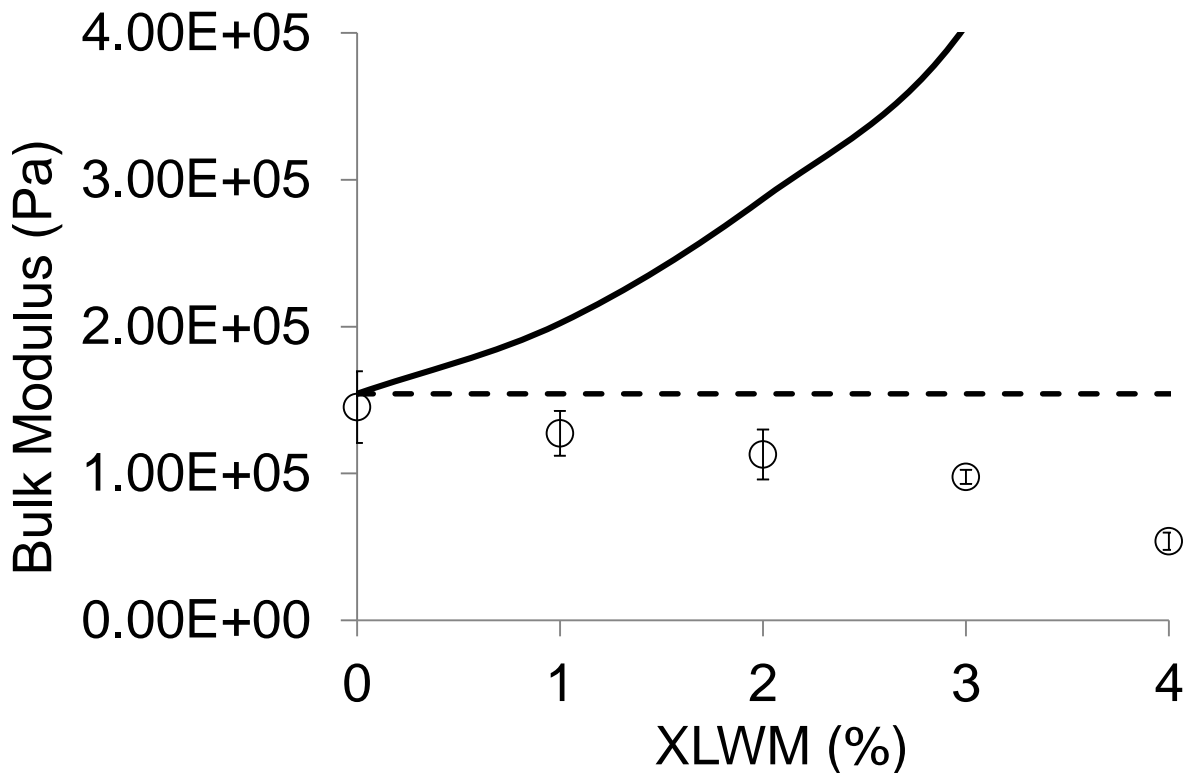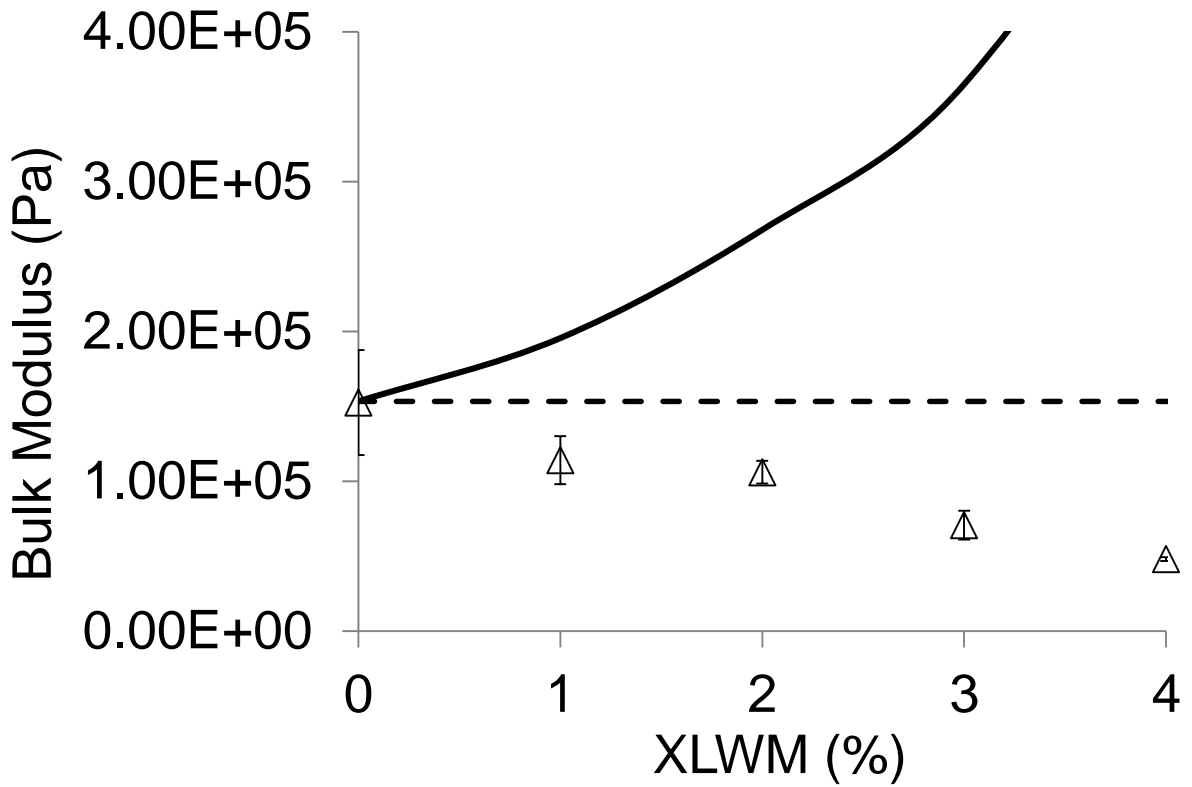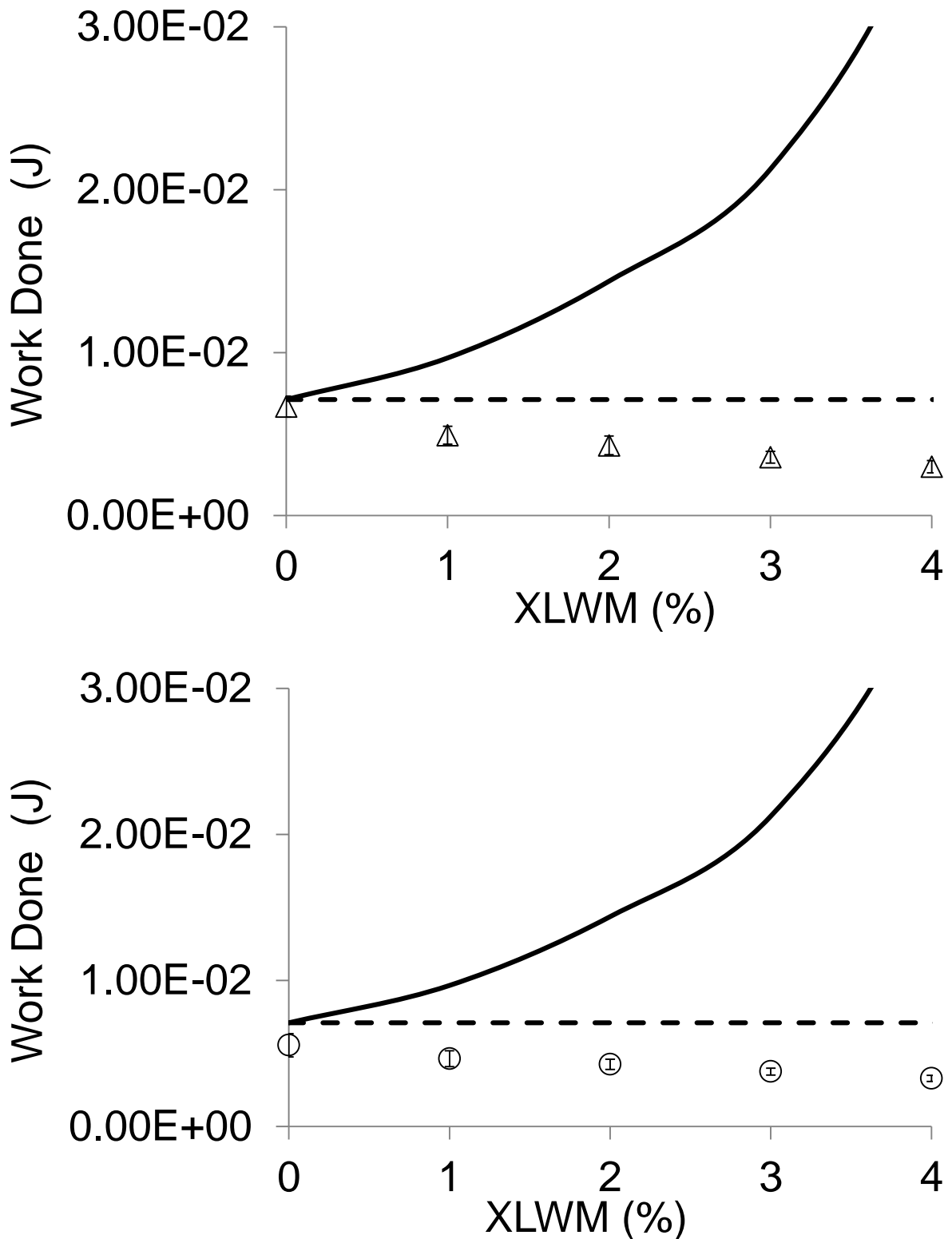
VIII

APPENDIX

8 Appendix
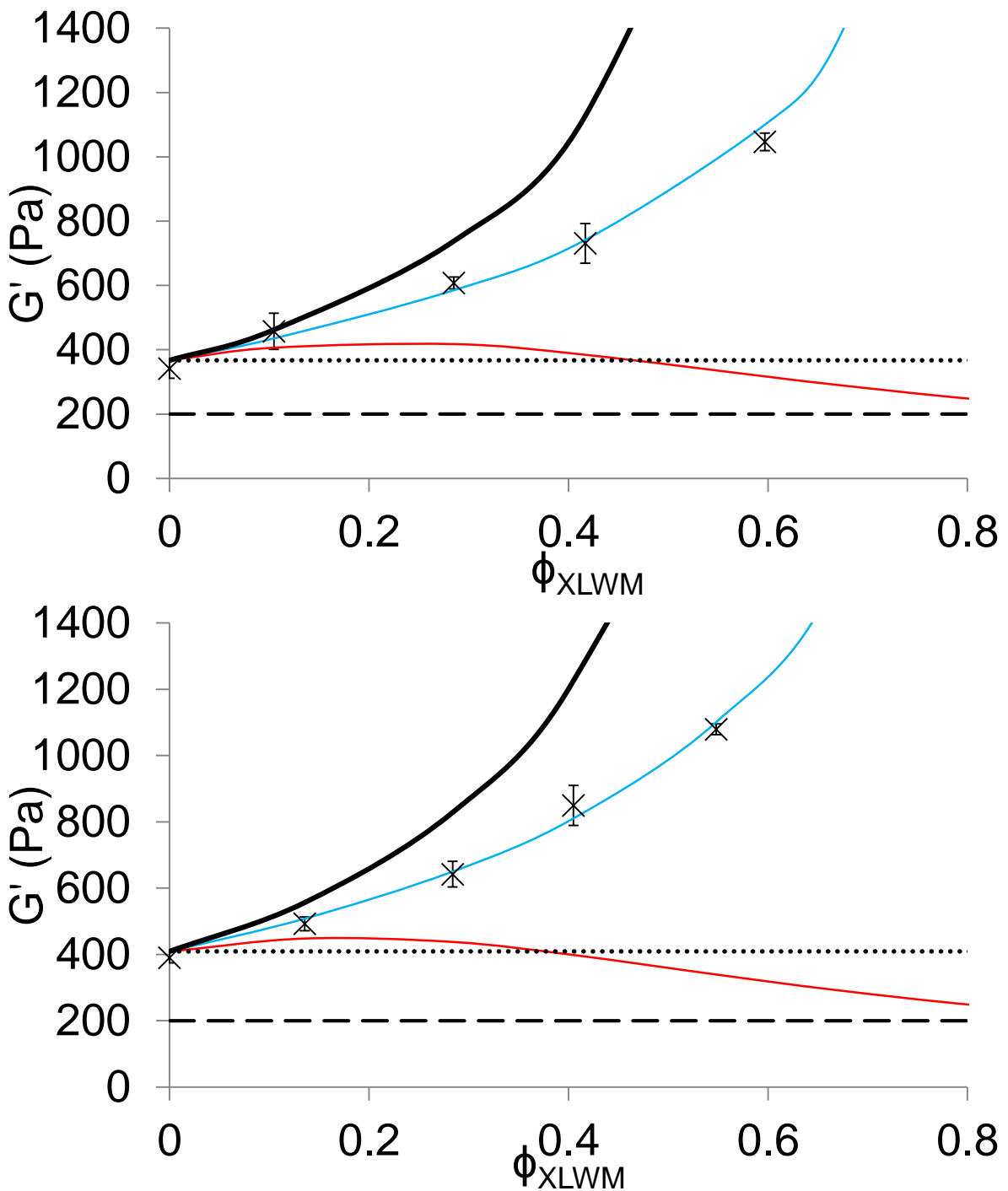
Appendix 1: Experimental dependency of G'$_{composite}$ (×) on XLWM starch concentration in the presence of (a) 0.0269M KCl and (b) 0.0269M K(citrate). Calculated models for isostress (——) and isostrain (——) are shown. Calculated G'$_{K-C}$ is shown (——) as well as fitted G'$_{XLWM}$ (— — —) and G' of corresponding pure K-carrageenan / salt gel (• • •).

Appendix 2: Experimental dependency of Young's modulus of K-carrageenan and XLWM starch composite gels upon XLWM starch concentration in the presence of (a) 0.0269M KCl (Δ), and (b) 0.0269M K(citrate) (○). Calculated Young's modulus for the effective concentration of the K-carrageenan phase is shown (————) as well as Young's modulus of corresponding 0.4% K-carrageenan/salt gel (— — —).

Appendix 3: Experimental dependency of bulk modulus of K-carrageenan and XLWM starch composite gels upon XLWM starch concentration in the presence of (a) 0.0269M KCl (△), and (b) 0.0269M K(citrate) (○) respectively. Calculated bulk modulus for the effective concentration of the K-carrageenan phase is shown (━━━━) as well as bulk modulus of corresponding 0.4% K-carrageenan/salt gel (━ ━ ━).

Appendix 4: Experimental dependency of work to failure of K-carrageenan and XLWM starch composite gels upon XLWM starch concentration in the presence of (a) 0.0269M KCl (Δ), and (b) 0.0269M K(citrate) (○). Calculated work to failure for the effective concentration of the K-carrageenan phase is shown (━━━) as well as work to failure of corresponding 0.4% K-carrageenan/salt gel (━ ━ ━).
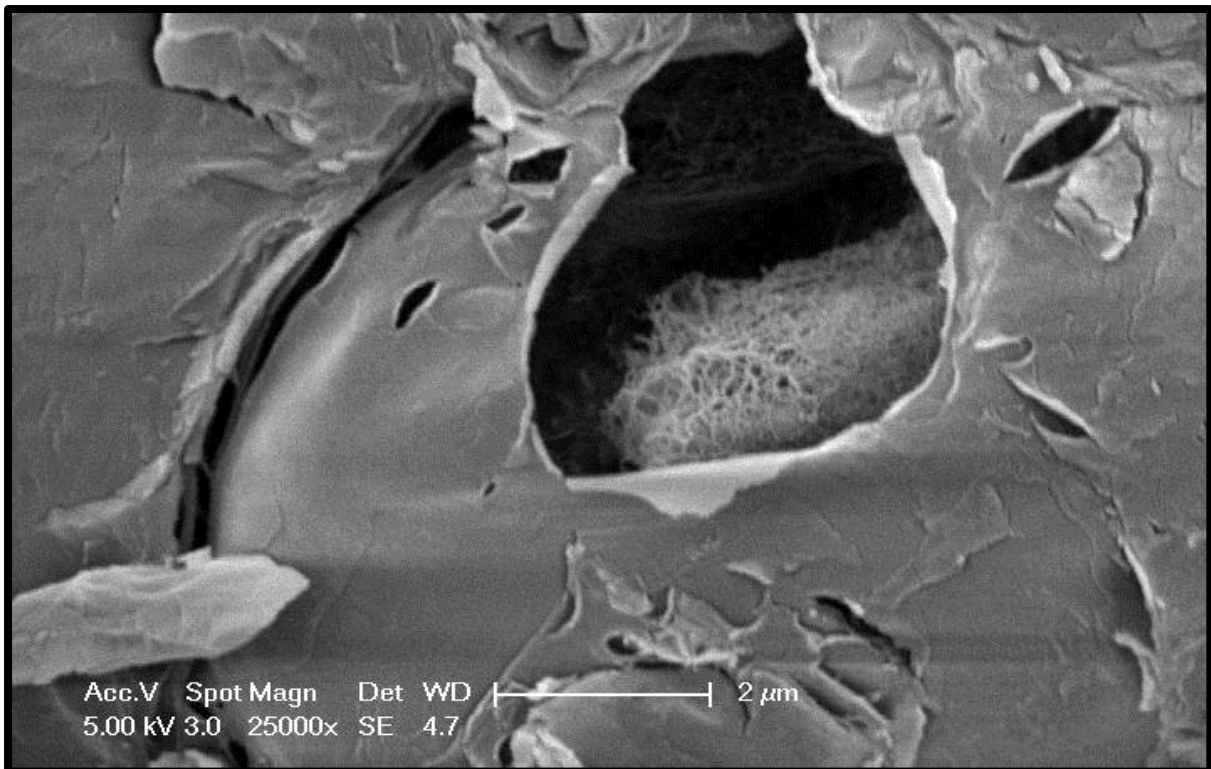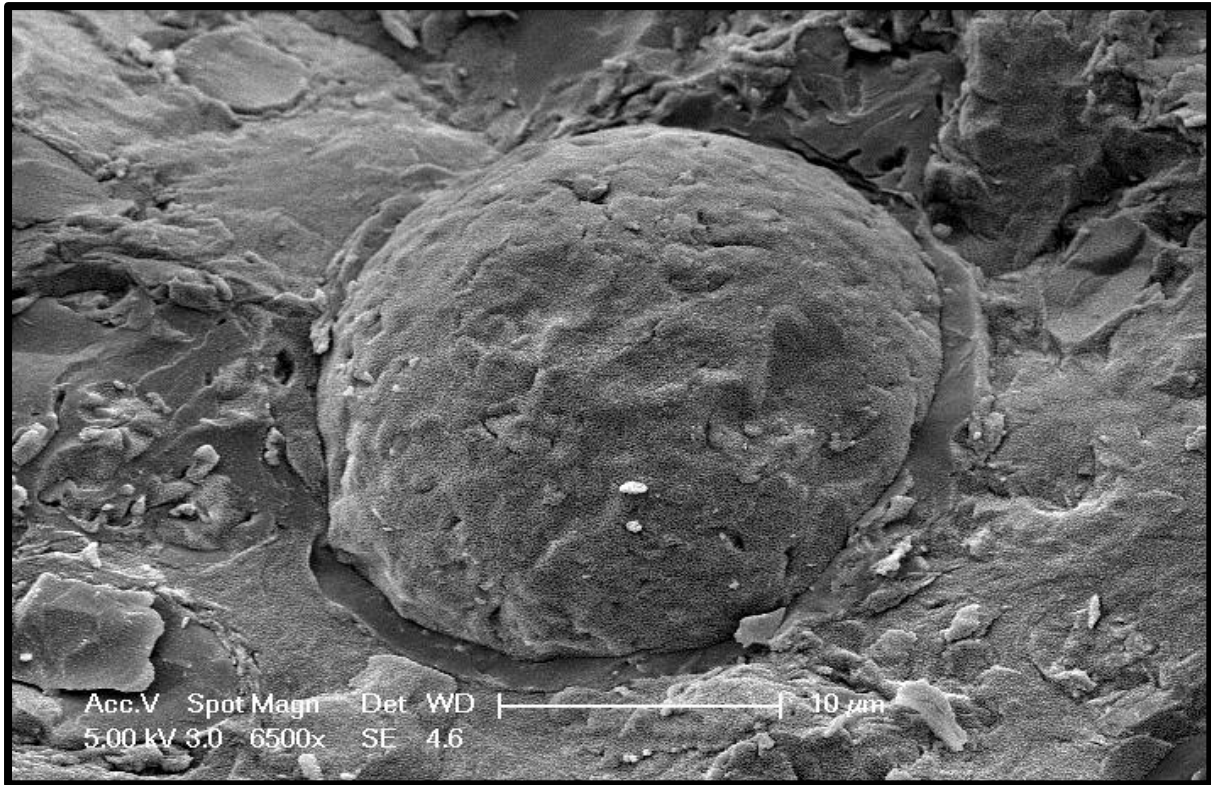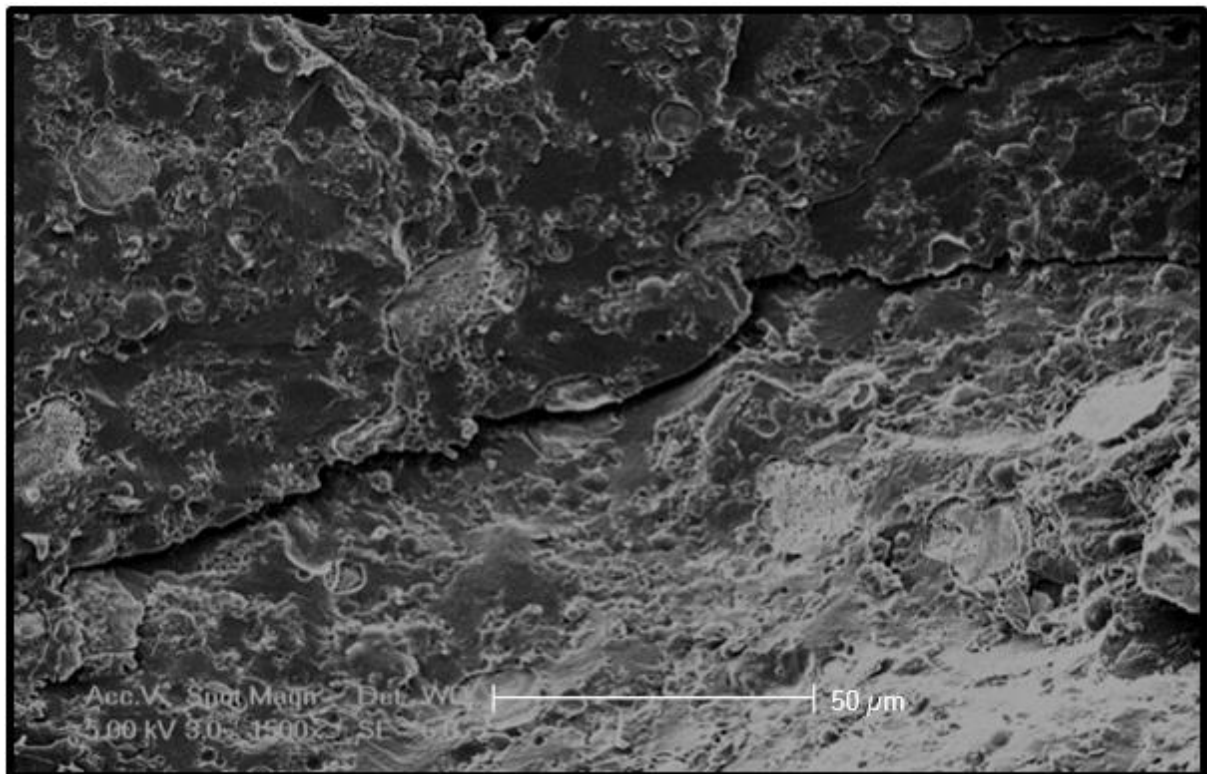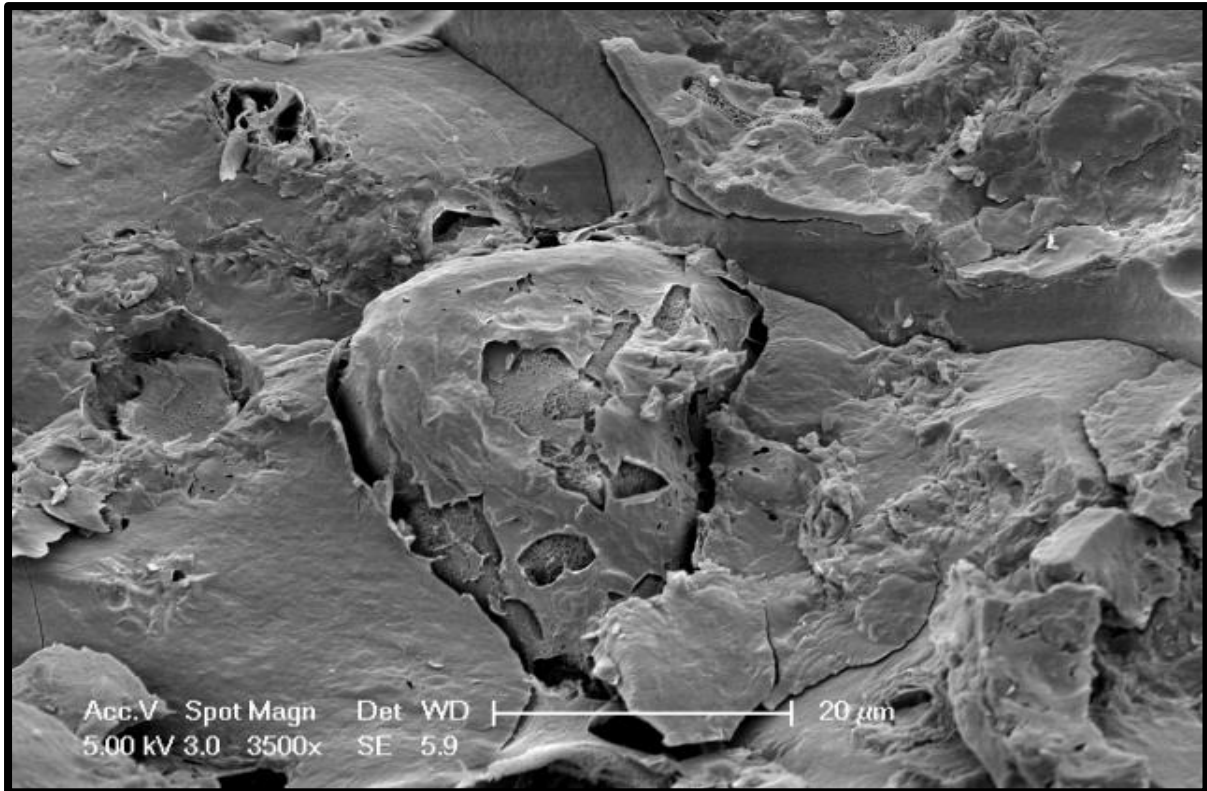
Appendix 5: Cryo SEM images of (a) 2% HMMG, and (b) 2% LMMG PO emulsions with 30% aqueous phase containing 0.4% κ-carrageenan with 0.0135M K(sorbate). Scaling indicated individually.
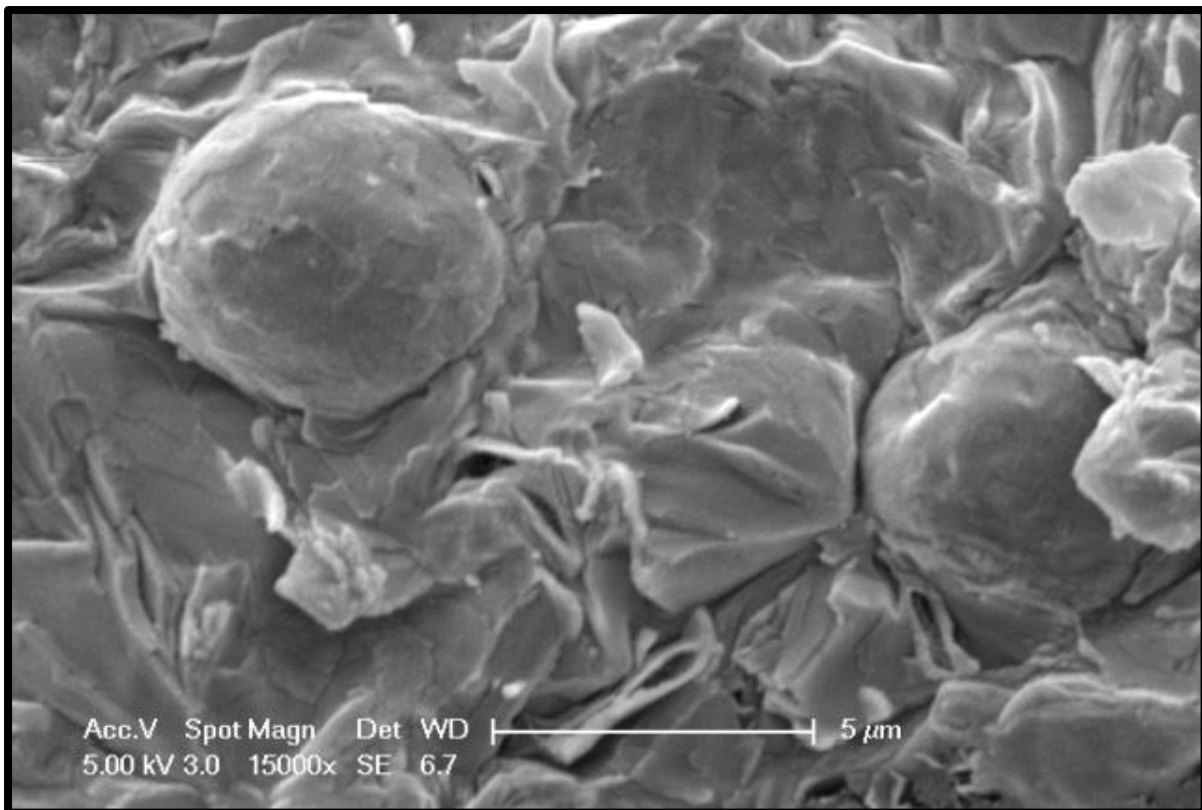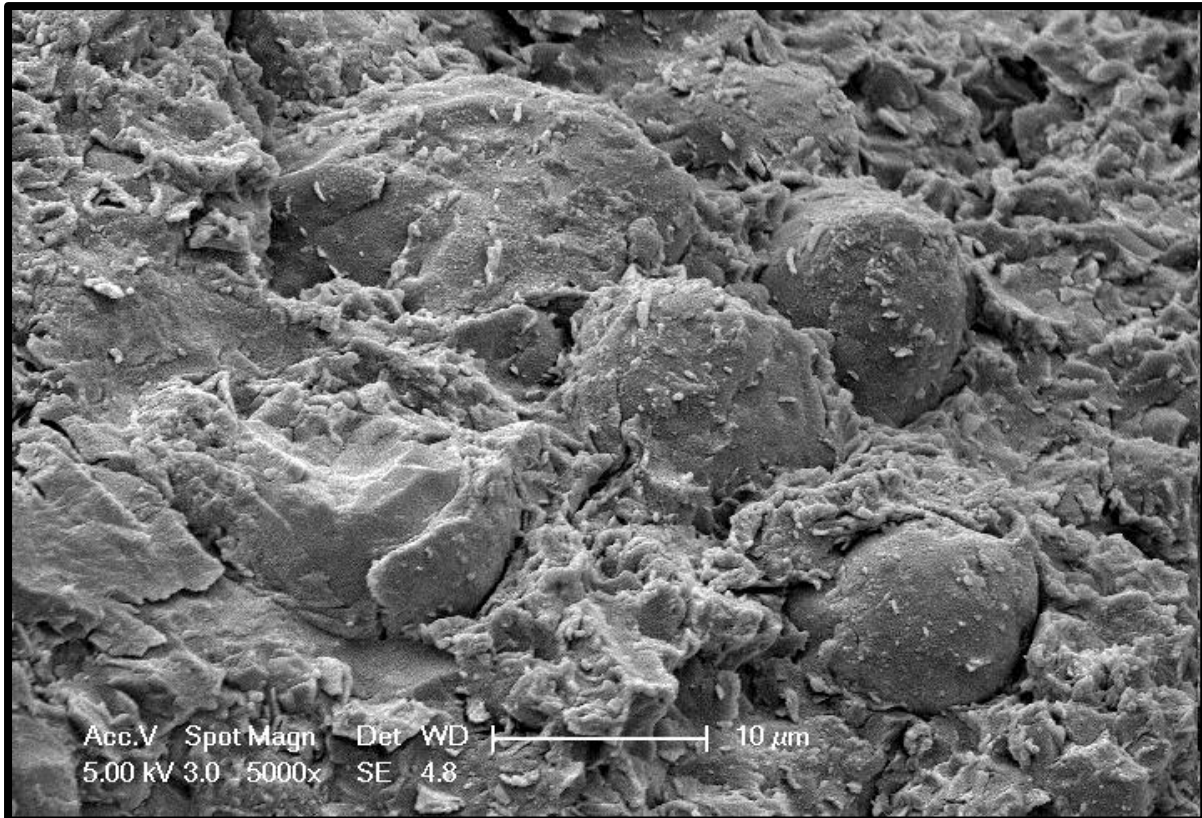
Appendix 6: Cryo SEM images of (a) 2% HMMG, and (b) 2% LMMG PO emulsions with 30% aqueous phase containing 0.4% κ-carrageenan with 0.0135M K(sorbate), with 3% DFPO added. Scaling indicated individually.
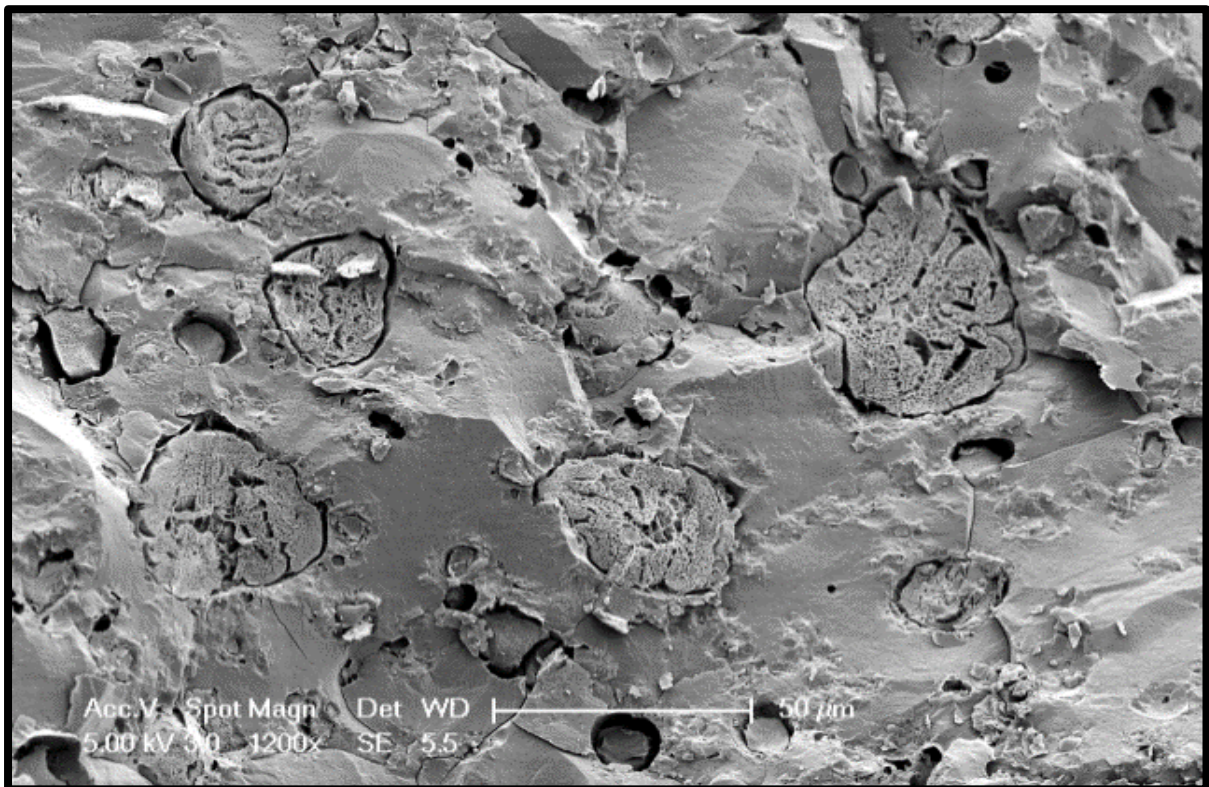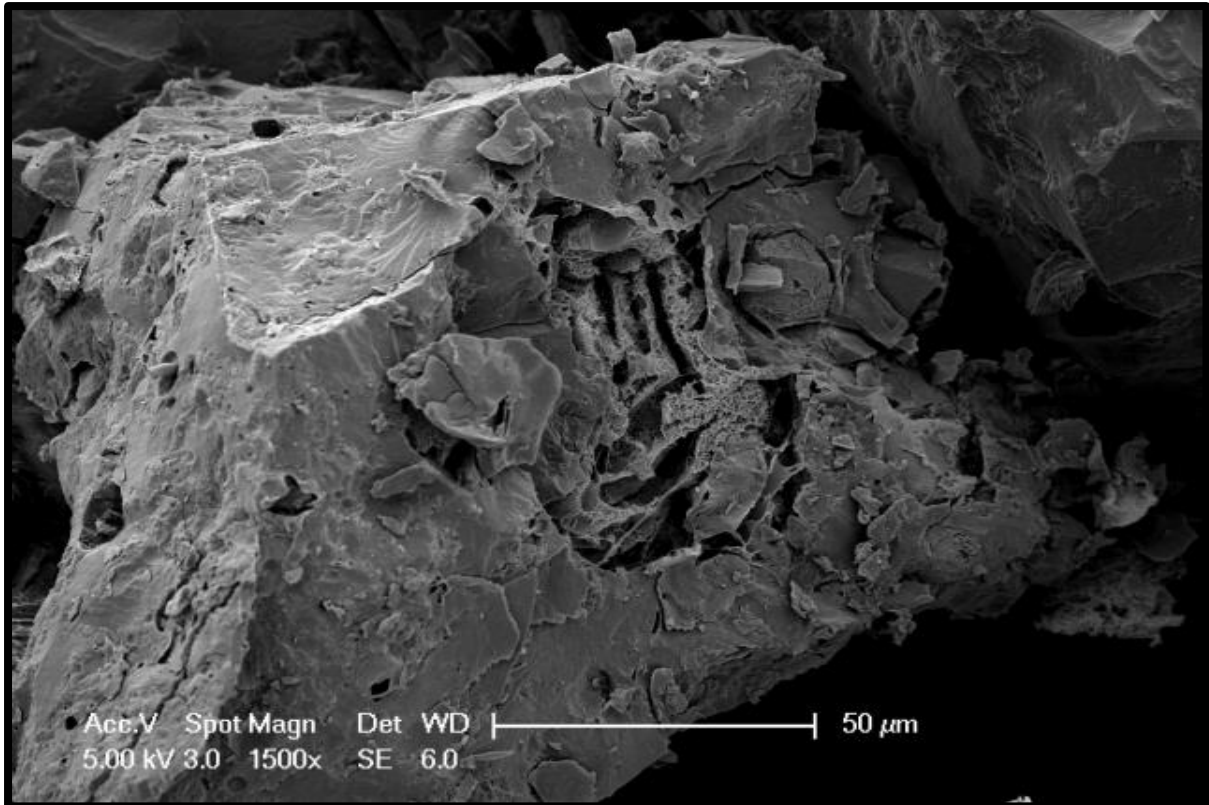
Appendix 7: Cryo SEM images of (a) 2% HMMG, and (b) 2% LMMG PO emulsions with 30% aqueous phase containing 0.4% κ-carrageenan with 0.0135M K(sorbate) and 2% XLWM Starch. Scaling indicated individually.

Appendix 8: Cryo SEM images of (a) 2% HMMG, and (b) 2% LMMG PO emulsions with 30% aqueous phase containing 0.4% κ-carrageenan with 0.0135M K(sorbate) and 2% XLWM Starch, with 3% DFPO added. Scaling indicated individually.

"Studying a PhD is like eating an elephant. You're not going to be managing it all in one sitting. You've got to tackle it one bite at a time."

I.T.Norton